SAPIENZA
Università di Roma
Dipartimento di Scienze Medico-Chirurgiche
e Medicina Traslazionale

PH. D. IN ONCOLOGY
Curriculum digestive oncology

Cycle: **XXXII**
(A.Y.: **2019/2020**)

TITLE

Targeting RNA metabolism to sensitize Pancreatic Ductal Adenocarcinoma to therapeutic treatments.

Ph.D. Student
Valentina Panzeri

Tutor Prof. Emanuela Pilozzi
Co-tutor Prof. Claudio Sette
Coordinator Prof. Bruno Annibale

SUMMARY

Chapter I. Pancreatic Ductal Adenocarcinoma (PDAC)

I. 1 Incidence and risk factors

Pancreatic ductal adenocarcinoma (PDAC) is the third most common cause of cancer-related death, with a 5 years survival rate of <5% (Jemal et al. 2011)(Miller et al. 2016). Despite advances in surgery and chemotherapy, the overall prognosis has remained practically unchanged for many decades. Due to lack of early symptoms and accurate diagnostic markers, most patients are diagnosed with disease at late stages and primary metastases in liver, abdomen and lungs. Only the 10-15% of patients have up-front resectable disease (Winter et al. 2012), the only potentially curative therapy for PDAC to date. However, even after radical resection, many patients develop recurrence and die of their disease.

The incidence rate of PDAC varies significantly between countries: in 2018 the highest age-standardized rate (ASR) incidence was registered in Europe (7.7 per 100.000 people) and North America (7.6 per 100,000 people), the lowest in Africa (2.2 per 100.000 people)(Fig.1). (McGuigan et al. 2018)(Bray et al. 2018). The incidence of PDAC is increasing in developed countries and, in this regard, Saad and colleagues have recently reported that, between 1973 and 2014, the incidence rates has a increase od 1% per year (Saad et al. 2018).

Since the PDAC incidence is very different between countries suggest that environmental factors have a important role in this pathology. Cigarette smoking is most important modifiable risk factor in PDAC and several studies have demonstrated this positive association (Bosetti et al. 2012). Alcohol consumption has been investigated through many studies, but results have been discordant so far. However, abuse alcohol consumption cause of chronic pancreatitis, which is a known risk factor for PDAC. Thus, alcohol consumption can be regarded as a risk factor for this cancer (Samokhvalov, Rehm, and Roerecke 2015).

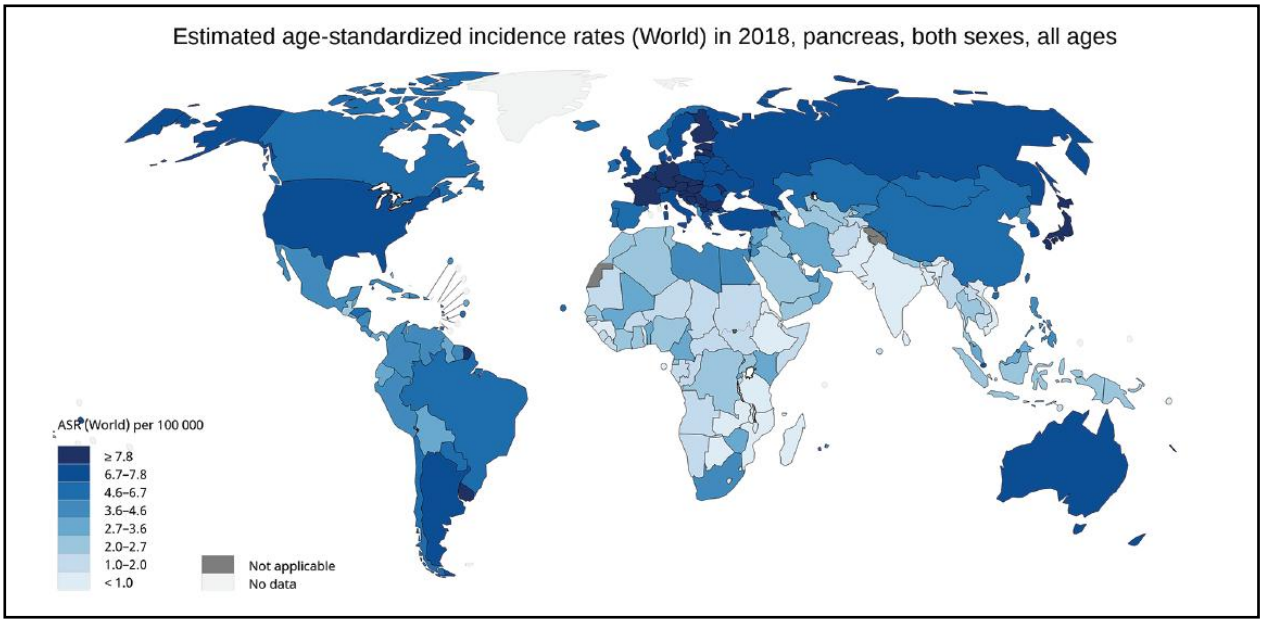

Figure 1. Map shows estimated age-standardized incidence rates (ASR) for pancreatic cancer worldwide in 2018, including bothsexes and all ages(Rawla, Sunkara, and Gaduputi 2019).

Chronic pancreatitis is a long-standing inflammation of the pancreas, about 5% of patients with this disease will develop PDAC throughout their life (Raimondi et al. 2010). An additional risk factor for PDAC is obesity; a study by the World Cancer Research Fund has reported an association between increased body mass index (BMI) and PDAC: a meta-analysis of 19 studies revealed a 10% increased risk of PDAC for every 5 BMI units, without difference between males and females (McGuigan et al. 2018).

Diabetes is another well-established risk factor for PDAC; a meta-analysis showed a double risk in patients with type one diabetes with respect to control patients (Stevens, Roddam, and Beral 2007). Notably, PDAC can also cause diabetes, raising the interest for Glycated Hemoglobin 1c (HbA1c) as a potential biomarker of early detection of the disease (Grote et al. 2011) .

I. 2 Pathogenesis and molecular characterization of PDAC.

Most PDACs arise in the region of the head of the pancreas and exhibits a glandular pattern. Clinical and histological studies identified three different types of precursor lesions leading to PDAC: pancreatic intra epithelial neoplasia (PanIN), mucinous cystic neoplasm (MCN), and intraductal papillary mucinous neoplasm (IPMN). PanIN, whose precursor lesions can be microscopic, is graded into stages 1 to 3. PanIN stage 1 is characterized by columnar mucinous epithelium with soft nuclear atypia, while PanIN stage 2 and 3 have more disorganized

structural and nuclear atypia (Fig. 2). MCN and IPMN are macroscopic cystic precursor lesions and they are less common. MCNs are large mucin producing columnar epithelial cystic lesions, supported by ovarian type stroma, while the IPMN derive in the main pancreatic duct or its major branches and grows into large cystic structures (Distler et al. 2014).

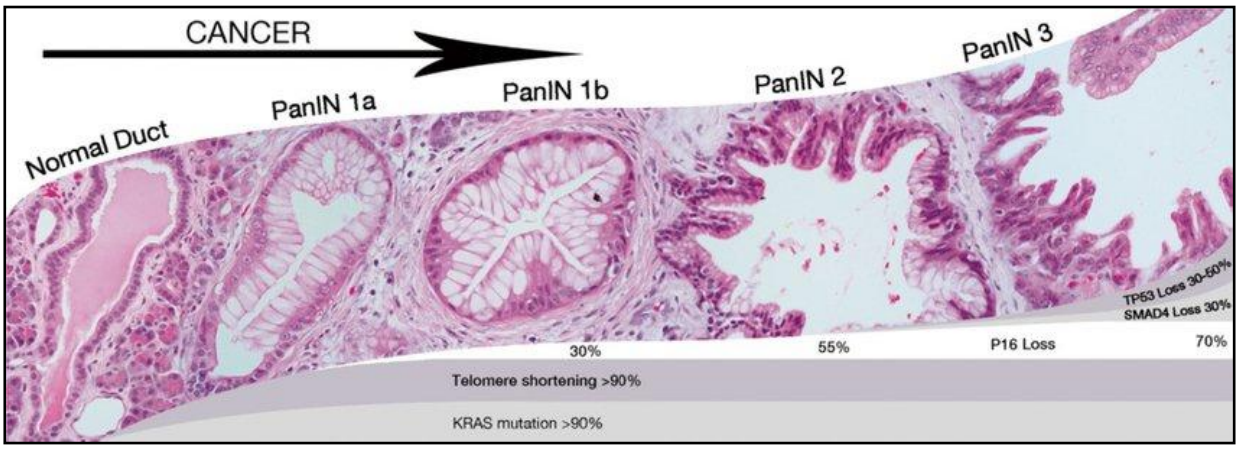

Figure 2. The PanIN progression model (Hackeng et al. 2016)

Molecular pathology studies and extensive genomic analyses have identified a model of the progression of pancreatic adenocarcinoma. More than 90% of cases of PanIN of all grades have KRAS mutations (Kanda et al. 2012). The mutational inactivation of the tumor suppressors CDKN2A, p53, and SMAD family member 4 (SMAD4) is detected with increasing frequency in type 2 - 3 lesions of PanIN, suggesting that KRAS mutations contribute to their initiation and that subsequent mutations are important for tumor progression (Roberts et al. 2016). The IPMS have GNAS (~40/80%), RNF42 (~50%) and KRAS (~40/65%) mutation (Fig.3) (Ryan, Hong, and Bardeesy 2014).

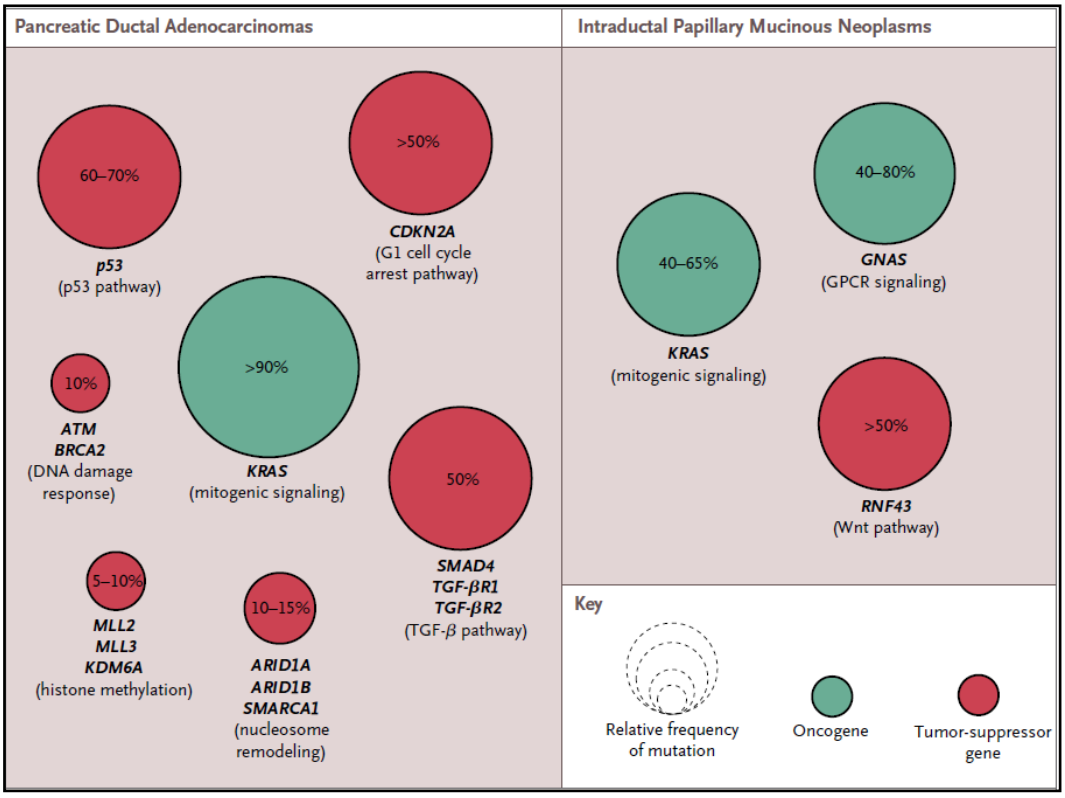

Figure 3. Approximate Frequencies of Mutations in Patients with Pancreatic Ductal Adenocarcinomas and Intraductal Papillary Mucinous Neoplasms(Ryan, Hong, and Bardeesy 2014).

Interestingly, a recent genomic analysis in PDAC identified 32 recurrently mutated genes that can be attribute into 10 pathways: KRAS, TGF-β, WNT, NOTCH, ROBO/SLIT signaling, G1/S transition, chromatin modification, SWI-SNF, DNA repair and RNA processing (Bailey et al. 2016). Interestingly, four PDAC sub-types are defined by expression analysis: squamous, pancreatic progenitor, immunogenic and aberrantly differentiated endocrine exocrine, each of which has a characteristic transcriptional signature (Bailey et al. 2016).

The recent evidence of genetic alteration in PDAC underline a large heterogeneity, which may be the basis of differences in progression and response to chemotherapeutic treatment.

I. 3 Diagnosis

Pancreatic cancer is mostly diagnosed in an advanced stage; usually early-stage pancreatic cancer is clinically silent and present symptoms that are non-specific like anorexia, abdominal pain, jaundice, weight loss, early satiety, dyspepsia and nausea (Krech and Walsh 1991). Thus, in the majority of cases the diagnosis occurs too late, when patients have already metastatic disease (Michl and Gress 2013). Almost all patients who of patients who have receive this

diagnosis die from the disease: ~70% of these die from extensive metastatic disease and ~30% have bulky primary tumors.

To date, the diagnostic modalities for suspected pancreatic cancer and high-risk screening include computed tomography (CT), magnetic resonance imaging (MRI), and endoscopic ultrasound-guided fine-needle aspiration for cytological diagnosis (EUS). The test of serum cancer antigen 19-9 (CA 19-9) is the only additional marker approved by the United States Food and Drug Administration for PDAC (McGuigan et al. 2018)(Kim et al. 2004).

To standardize clinical classification it was necessary to introduce standard criteria to to assess the severity of the disease. The Eastern Cooperative Oncology Group (ECOG) Performance Status, published in 1982, determines the quality of life of the patient. The scale goes from 0 to 5, with 0 denoting person fully active, without limitation, and 5 death (Oken et al. 1982).

Another method of staging is TNM (tumor/node/metastasis) classification, which is largely used for PDAC: it describes tumors for size, presence of lymph nodes invasion, metastases and the resectability of primarytumor(Cong et al. 2018). On this basis, PDAC is classified in four stages:

- Stage I: tumor is localized in pancreas end resectable.
- Stage II: tumor is spread locally without invasion of other organism or lymphonodes and it is resectable.
- Stage III: tumor spread to lymph nodes and invaded the pancreatic duct, only a fraction of cancers is resectable.
- Stage IV: tumor is spread to distal organs and the disease at this stage is defined as metastatic.

I. 4 Therapy

Pancreatic cancer therapy remains a challenge; surgical resection is currently the only potential cure for PDAC. Unfortunately, ~60% of patients are diagnosed when they display metastases and are not eligible to surgery ("unresectable"). Of the remaining 30-40% of PDAC cases that do not present with metastases, 15-20% is amenable to surgery ("resectable"), while the majority presents with locally advanced disease and undergoes non-surgical treatments ("borderline resectabale").

An emerging strategy for pancreatic cancer, especially for borderline resectable, is neoadjuvant or preoperative therapy. The use of FOLFIRINOX, that is a combination of fluorouracil, irinotecan, oxaliplatin and leucovorin, followed by accelerated short course radiation therapy is

currently under clinical trial (NCT01591733, *ClinicalTrials.gov*) and now it is in phase 3 trial (Murphy et al. 2018). At the moment, studies for use of gemcitabine plus albumin bound paclitaxel particles (nab-paclitaxel) like neoadjuvant therapy are in progress (NCT01560949, *ClinicalTrials.gov*.) The purpose is to increase patients who may benefit of surgery, that is the only potential cure for this pathology (Fig. 4)(Neoptolemos et al. 2018).

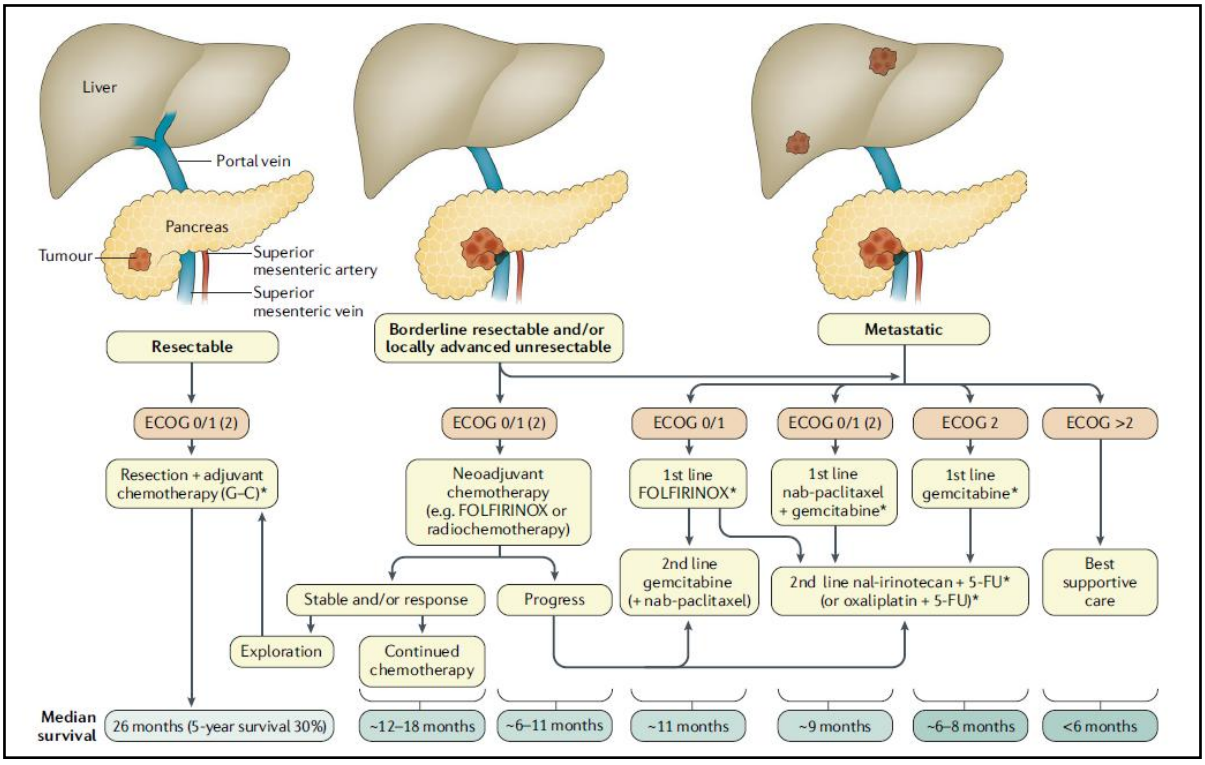

Figure 4. Suggested treatment algorithm for patients with pancreatic cancer (Neoptolemos et al. 2018).

The palliative chemotherapy is usually reserved for patients with distant metastases and/or local irresectability. Until 2011, monotherapy with gemcitabine was the first line chemotherapy ultil 2011, when the PRODIGE 4/ACCORD 11 trial demonstrated that the use of FOLFIRINOX is more benefical than in patients with metastatic pancreatic cancer (11.1 vs 6.8 months median overall survival)(Conroy et al. 2011). In 2013, the phase III MPACT trial reporting good results for another combination therapy: nab paclitaxel with gemcitabine in patients with metastatic pancreatic cancer (Von Hoff et al. 2011). Nowadays, both therapies are available for metastatic pancreatic cancer first line therapy: FOLFIRINOX is mainly used for patients with an ECOG status of 0 or 1, while the combination of Nab paclitaxel–Gemcitabine is reserved for patients with ECOG 2.

Local therapies for the unresectable tumours are considered an option for tumor control and/or symptom relief. Some methods for loco-regional therapy are: irreversible electroporation (IRE), stereotactic body radiation (SBRT), radiofrequency ablation (RFA), high intensity focused ultrasound (HIFU) and others. Studies analyzing local therapies have reported good results with tumour regression and prolonged survival in a number of patients. However, conclusive data are scarce, owing to the lack of RCTs (Neoptolemos et al. 2018).

Since many patients develop resistance or do not show benefits at first-line palliative chemotherapy, performing a second line chemotherapy acquires clinical importance for many patients. At the moment, nanoliposomal irinotecan (or oxaliplatin) and/or 5-FU–FA seems to be the best option in patients treated with first-line gemcitabine based therapy, while for patients who have used FOLFIRINOX in first line is recommended a gemcitabine treatment; but unfortunately today there are still no trials that confirm this (Neoptolemos et al. 2018).

I. 5 New approaches of therapy

Numerous targeted agents have been evaluated alone or in combination with chemotherapy in metastatic pancreatic cancer, unfortunately, most agents have so far failed to improve patient survival. Thus, finding of new therapies represents a clinical priority.

The PDAC is characterized by plentiful fibrotic stroma, causing stiffness and a poorly vascularization in tumor, which creates a barrier to drug uptake. Several approaches have been tested to reduce this stromal barrier and enhance drug delivery. Systemic administration of the modified hyaluronidase (HA) molecule PEGPH20 established decreased intratumoral HA and remodels the stroma, increasing the number of functioning tumor blood vessels. Now clinical trials to study PEGPH20 in combination with nab- paclitaxel and gemcitabine or with FOLFIRINOX are underway (Hingorani et al. 2018). Another drug used to act against the stroma is the IPI-926 inhibitor, it inhibits sonic hedgehog pathway signaling; but further studies are needed to characterize the action of this inhibitor (Olive et al. 2009) (Rhim et al. 2014). Moreover, the stroma creates an environment that impairs drug delivery to the tumor, but at the same time, seems to protect against tumor progression; more research is thus required to understand the role of stroma in PDAC.

A key mechanism by which cancer cells survive and establish tumours is suppression of the immune response, either directly or via other cells in the tumor microenvironment.

Mechanisms of immune-suppresion operated by cancer cells include activation of regulatory T cells (Treg cells) or myeloid- derived suppressor cells (MDSCs), inhibition of effectors T cells (Teff cells) or antigen presenting cells (APCs) and modulation of macrophage populations within the tumor.

T cell response is controlled by receptors with inhibitory functions, now known as immune checkpoints, which include CTLA-4, PD-1 and BTLA. Agents blocking these molecules are able to promotes endogenous anti-tumor T cell responses, in order to limit tumor growth and they are showing enormous promise in a number of cancer types (Seidel, Otsuka, and Kabashima 2018). However, to date, pancreatic cancer has proved refractory to such therapeutic approaches, probably reflecting the immunosuppressive nature of the pancreatic cancer microenvironment. An example is an anti-CTLA-4 antibody (Ipilimumab), which has been previously effective in the treatment of melanoma, renal cell carcinoma, and prostate cancer, but has shown poor results in PDAC treatment (Silva and Long 2017)(Paniccia et al. 2015). Another immunotherapeutic approach is a cancer vaccine using a tumour- specific antigen. Cancer vaccines are designed to augment antigen presentation and activate antigen-specific effectors and memory T cells, which are then primed to kill tumor cells expressing these antigens (Soares et al. 2012). The most common cellular targets utilized in recent clinical trials of PDAC cancer vaccines, including: telomerase, Wilms tumor gene, KIF20A, alpha-galactosyl (α-Gal), survivin, mutated Ras protein, human mucin MUC1 protein, and vascular endothelial growth factor receptor 2 (VEGFR2). Despite the positive immune response of patientes and good tolerability to this type of therapy, the impact on overall survival (OS) is minimal in PDAC (Paniccia et al. 2015).

The typical tumor microenviroment of PDAC that inhibits a good influx of T cells might justify the failure of immunotherapy. Moreover, the progression time of the PDAC is rapid and prevents a good response of the immune system, which requires months to develop (Paniccia et al. 2015).

Another goal of research in oncologyis the development of precision medicine, whose main purpose is to select the best therapy or combination therapy for a single patient. The diversity of genetic mutations and the tumor heterogeneity are some of obstacles that can be found in PDAC for the precision medicine. Ongoing clinical trials that investigate by genome sequencing (WGS) and RNA sequencing (RNASeq) to detect actionable drug target (NCT02750657, *ClinicalTrials.gov*)(Aung et al. 2018) or immunohistochemistry analysis before and after treatment to identify biomarkers that characterize patients who respond to a specific

treatment compared to another (Torres and Grippo 2018). Further studies are needed to discover the key molecules that characterize the drug response of each patient. The personal medicine may potentially demonstrate higher efficacy compared to a single regimen for all subtypes of PDAC.

Chapter II. Resistance tochemotherapy treatment in PDAC: looking for new targets and novel combination therapies

II.1 Resistance tochemotherapy treatment

Gemcitabine (2,2-difluoro 2-deoxycytidine, dFdC) has been thestandard of care for PDAC from 1997 to 2011, until the introduction of FOLFIRINOX (combination of 5-fluorouracil, folinic acid, irinotecan plus oxaliplatin). Emerging of drug resistance unfortunately limits the efficacy of these chemotherapeutic. Chemoresistance can be classified into two categories: intrinsic resistance (de novo or innate) and acquired resistance. Intrinsic resistance refers to a condition of chemotherapy inefficacy since the beginning of the treatment, probably due to genetic factors. On the other hand, acquired resistance develops only after the chemotherapy treatment, probably in this period the cancer cells undergo a series of alterations that cause the ultimately refractoriness to chemotherapy. Most patients develop resistance within weeks of treatment initiation, leading to poor survival (Amrutkar and Gladhaug 2017). For this reason, finding a new combination of drugs or other possible targets is a clinical urgency.

Pancreatic tumor chemosensitivity can be modulated by different signaling pathways regulating growth, proliferation, differentiation, apoptosis, invasion and angiogenesis, such as Akt, epidermal growthfactor receptor (EGFR), Notch, mitogen-activated protein kinases (MAPK). Furthermore, also epithelial-mesenchymal transition (EMT) is implicated in chemoresistance in pancreatic cancer (Z. Wang et al. 2011).

An example of the involvement of the MNK pathway in drug-resistance acquisition by PDAC was described by Adesso L. and collaborators. In their study they showed that gemcitabine induces activation of the MNK pathway and up-regulation of splicing factor SRSF1, that promotes splicing of the MNK2b transcript variant, which is able to bypass up stream regulatory pathways, thus confering increased resistance to gemcitabine. Suppression of this process enhanced the cytotoxic effects of gemcitabine, suggesting that this pathway might represent a promising therapeutic target for PDAC (Adesso et al. 2013). Another splice-variant promoting drug-resistance in PDAC cells is the PKM2 isoform of the pyruvate kinase gene (PKM), that is involved in cellular metabolism promoting the Warburg Effect (Warburg 1956). Chronic exposure to gemcitabine was found to promote PKM2 isoform and promoting PKM1 isoform rescues PDAC sensitivity to gemcitabine, this suggest the role of PKM2 in this process (Calabretta et al. 2016).

Considering the pathology of PDAC, studies are underway to look for more effective treatments able to bypass the problem of chemoresistance. Promising treatment modalities include targeting of pathways that induce chemoresistance, reshaping the desmoplastic stroma, enhancing immune checkpoint therapies and finding new combinations of chemotherapy coupled also to radiotherapy (Chandana, Babiker, and Mahadevan 2019). To conclude, the drug resistance in pancreatic cancer is multifaceted aspect and future studies targeting different pathways are required to understand and successfully treat pancreatic cancer.

II.2 *"Co-treatment with gemcitabine and nab-paclitaxel exerts additive effects on pancreatic cancer cell death"*

Since PDAC patients develop early Gemcitabine resistance, we have investigate on the effect of combined treatment of Gemcitabine with Nab-Paclitaxel. We have analyzed the cell proliferation, death, apoptosis and cell cycle distribution in PDAC cell lines. We found that the combined treatment exerted additive effects on cell death, even at lower doses of the drugs. Here I report the relative paper, in which I have collaborated.

II.3 Paper *"Co-treatment with gemcitabine and nab-paclitaxel exerts additive effects on pancreatic cancer cell death"* published on *Oncology Reports* 2018 Apr;39(4):1984-1990

Ilaria Passacantilli, **Valentina Panzeri**, Francesca Terracciano, Gianfranco Delle Fave, Claudio Sette and Gabriele Capurso

Co-treatment with gemcitabine and nab-paclitaxel exerts additive effects on pancreatic cancer cell death

ILARIA PASSACANTILLI[2,3], VALENTINA PANZERI[1,2], FRANCESCA TERRACCIANO[1,2], GIANFRANCO DELLE FAVE[1], CLAUDIO SETTE[2,3] and GABRIELE CAPURSO[1]

[1]Medical and Surgical Department of Clinical Sciences and Translational Medicine, Digestive and Liver Disease Unit, Sant'Andrea Hospital, 'Sapienza' University, I-00199 Rome; [2]Department of Biomedicine and Prevention, University of Rome 'Tor Vergata', I-00133 Rome; [3]Laboratory of Neuroembriology, Fondazione Santa Lucia, I-00142 Rome, Italy

Received July 31, 2017; Accepted January 19, 2018

DOI: 10.3892/or.2018.6233

Abstract. Pancreatic ductal adenocarcinoma (PDAC) is a highly aggressive cancer and current treatments exert small effects on life expectancy. The most common adjuvant treatment for PDAC is gemcitabine. However, relapse almost invariably occurs and most patients develop metastatic, incurable disease. The aim of the present study was to assess the activity of nanoparticle albumin-bound paclitaxel (nab-paclitaxel) alone or in combination with gemcitabine in PDAC cell lines displaying different degrees of sensitivity to gemcitabine treatment. We evaluated the effects of gemcitabine and nab-paclitaxel and their combination on cell proliferation, death, apoptosis and cell cycle distribution in PDAC cell lines either sensitive to gemcitabine, or with primary or secondary resistance to gemcitabine. Our results indicated that the dose-response of PDAC cell lines to nab-paclitaxel was similar, regardless of their sensitivity to gemcitabine. In addition, nab-paclitaxel elicited similar cytotoxic effects on a PDAC cell line highly resistant to gemcitabine that was selected after prolonged exposure to the drug. Notably, we found that combined treatment with gemcitabine and nab-paclitaxel exerted additive effects on cell death, even at lower doses of the drugs. The combined treatment caused an increase in cell death by apoptosis and in cell cycle blockage in S phase, as assessed by flow cytometry and western blot analysis of the PARP-1 cleavage. These results revealed that a combined treatment with nab-paclitaxel may overcome resistance to gemcitabine and may represent a valuable therapeutic approach for PDAC.

Correspondence to: Dr Gabriele Capurso, Digestive and Liver Disease Unit, Sant'Andrea Hospital, Via di Grottarossa 1035, I-00189 Rome, Italy
E-mail: gabriele.capurso@gmail.com

Key words: nab-paclitaxel, gemcitabine, drug resistance, pancreatic adenocarcinoma, cell cycle, cell death

Introduction

Pancreatic ductal adenocarcinoma (PDAC) is the fourth leading cause of cancer-related mortality (1) and it is estimated to become the second by 2030 (2). Less than 20% of PDAC patients are eligible for surgical resection (3) and, since chemotherapy and radiotherapy only marginally improve survival (4), the 5-year survival rate for patients is approximately 5% (1).

Since its approval by the FDA in 1996, the standard treatment for advanced PDAC in the past two decades has been chemotherapy with gemcitabine, a nucleoside analogue of deoxycytidine that has been also extensively used for the treatment of other solid tumors. Gemcitabine, however, offers only a small improvement of survival to patients with advanced PDAC compared to 5-fluorouracil (5-FU) (5). The relative lack of response to gemcitabine treatments is attributed to mechanisms of either primary or acquired resistance, many of which have been investigated extensively (6). For instance, resistance to gemcitabine can be acquired through mechanisms related to its transport, cellular uptake and metabolism within tumor cells. Furthermore, the activation of pro-survival signaling pathways and the expression of specific microRNAs can also influence the response to this drug (6). Recently, we have highlighted the impact of alternative splicing on both short-term and long-term resistance to gemcitabine. Upon brief exposure to the drug, upregulation of the oncogenic splicing factor SRSF1 induces splicing of the MNK2b protein kinase variant and phosphorylation of the translation factor eIF4E, which promote PDAC cell survival under genotoxic stress (7). Conversely, selection of gemcitabine-resistant PDAC clones after chronic exposure to the drug, correlated with increased expression of the polypyrimidine-tract binding protein (PTBP1) and alternative splicing of the pyruvate kinase gene (PKM) resulting in the promotion of the PKM2 isoform (8). The expression of PKM2 was required for the maintenance of gemcitabine-resistance in PDAC cell lines and correlated with worse recurrence-free survival in operated patients treated with adjuvant gemcitabine (8).

Recently, the standard treatment for patients with advanced PDAC has improved due to the positive results of trials with the

combination of fluorouracil-leucovorin-irinotecan-oxaliplatin (FOLFIRINOX) (9) and the addition of nanoparticle albumin-bound paclitaxel (nab-paclitaxel) to gemcitabine (10,11). These combined regimens are now considered the standard care for patients with advanced PDAC. However, toxicity limits FOLFIRINOX use to patients with a good performance status, while the combination of gemcitabine and nab-paclitaxel is usually more tolerable. Single-agent gemcitabine therapy is still an acceptable treatment in patients with advanced disease and reduced performance status, as well as in the adjuvant setting after surgical resection (12).

Nab-paclitaxel (Abraxane®; Celgene Inc., Odenton, MD, USA) is a specific formulation of paclitaxel that was developed to improve its solubility and to overcome resistance due to the desmoplastic stroma surrounding PDAC cells (13). Paclitaxel is a taxane and acts by reversibly binding to tubulin, causing defects in mitotic functions that lead to blockage of the cell cycle and eventually to apoptosis, with mechanisms that differ from those of gemcitabine. While the clinical use of nab-paclitaxel and gemcitabine has been investigated extensively (14), the available data on the activity of nab-paclitaxel as a single-agent therapy in PDAC both in clinical trials and preclinical models are poor. Therefore, the aim of the present study was to assess the activity of nab-paclitaxel alone or in combination with gemcitabine in PDAC cell lines displaying different degrees of sensitivity to gemcitabine treatment.

Materials and methods

Cell cultures and drugs. All cell lines were obtained from the Centre for Molecular Oncology, Barts Cancer Institute (London, UK) in 2004 and authenticated in 2012. The HPAF-II, Pt45P1, PANC-1 and PANC-1 DR cell lines were cultured in RPMI-1640 (Lonza, Basel, Switzerland) and MiaPaCa-2 cell line was cultured in Dulbecco's modified Eagle's medium (DMEM; Lonza). All media were supplemented with 10% fetal bovine serum (FBS; Gibco, Gaithersburg, MD, USA), gentamycin, penicillin, streptomycin and non-essential amino acids and the cells were maintained at 37˚C with 5% CO_2.

Nab-paclitaxel (Abraxane®; kindly provided by Celgene Inc.) was dissolved in physiological solution. Gemcitabine (Eli Lilly and Company, Clinton, IN, USA) was dissolved in water. The cells were plated at 50% confluency. Twenty-four hours after plating, the cells were treated with nab-paclitaxel and/or gemcitabine at the indicated concentrations for 24, 48 and 72 h before being collected for further analyses.

Cell viability assays. The cells were plated at 50% confluency in 96 wells and, after 24 h, treated with nab-paclitaxel at the concentrations indicated in Fig. 1. After 72 h of treatment, the cell viability was evaluated by MTS assay (Promega, Madison, WI, USA) following the manufacturer's instructions and by assessing the optical density (OD) at 490 nm. The results are represented as the mean ± standard deviation (SD) of three experiments.

For cell death, the cells were plated at 70% confluency and, after 24 h, treated with gemcitabine and/or nab-paclitaxel at the indicated doses. After an additional 48 h, the cells were washed in phosphate-buffered saline (PBS), trypsinized and incubated with 0.4% Trypan Blue stain (Sigma-Aldrich, St. Louis, MO, USA). Blue positive cells were then counted using the Countess II Automated Cell Counter (Invitrogen Life Technologies, Carlsbad, CA, USA) and the percentage of cell death was determined. The results are represented as the mean ± SD of three experiments.

BrdU-PI staining and cell cycle analysis. For the cell cycle analysis, the cells were treated with 10 μM BrdU (Sigma-Aldrich) in the final 30 min of treatments. Subsequently, the cells were trypsinized, washed in chilled PBS and resuspended in PBS/ethanol 70%. The samples were incubated at -20˚C until use. The cells were then centrifuged at 2,000 rpm for 5 min, washed with PBS and incubated with 2 N HCl/0.5% Triton X-100 at room temperature (RT) for 30 min. The cells were centrifuged at 2,000 rpm for 5 min and then resuspended with 0.1 M NaB_4O. After incubation for 2 min at RT, the cells were washed with PBS/1% BSA and incubated for 1 h at RT in a solution of 0.5% Tween-20/1% BSA in PBS containing 10 μl of anti-BrdU 1 mM (Becton-Dickinson and Company, Franklin Lakes, NJ, USA). Subsequently, the cells were washed with PBS/1% BSA and incubated in a solution of PBS/0.5% Tween-20/1% BSA containing 5 μl of Alexa Flour 488 anti-mouse IgG-FITC (polyclonal; cat. no. A-11001; Thermo Fisher Scientific, Waltham, MA, USA) for 30 min at RT. The cells were washed with PBS/1% BSA and incubated with PBS containing 1 mg/ml RNAse A (Roche, Basel, Switzerland) and 20 μg/ml propidium iodide (PI; Sigma-Aldrich) for 30 min at 37˚C. Subsequently the cells stained with BrDU-PI were analyzed by FACS.

Cell extracts and western blot analysis. MiaPaCa-2 cells were resuspended in lysis buffer (50 mM HEPES pH 7,4, 10% glycerol, 15 mM $MgCl_2$, 150 mM NaCl; 15 mM EGTA; 20 mM β-glycerophosphate; 1 mM dithiothreitol, 0.5 mM $NaVO_4$, 1 mM NaF and protease inhibitor cocktail) supplemented with 1% Triton X-100, sonicated for 5 sec and centrifuged for 10 min at 13,000 rpm at 4˚C. Supernatants were collected, diluted in sodium dodecyl sulphate (SDS) sample buffer and boiled for 5 min. The proteins were separated on 8 or 12% SDS-PAGE gel and transferred onto PVDF blotting membranes (Amersham Hybond; GE Healthcare, Little Chalfont, UK). The membranes were saturated in 5% non-fat dry milk in PBS plus 0.1% Tween-20 for 1 h at RT and incubated overnight at 4˚C with the following primary antibodies: Rabbit anti-PARP1 (1:500; Cell Signaling Technology, Inc., Danvers, MA, USA), mouse anti-actin (1:1,000; Santa Cruz Biotechnology, Dallas, TX, USA), rabbit anti-cyclin E2 (1:1,000; Cell Signaling Technology), rabbit anti-cyclin A2 (1:1,000), rabbit anti-cyclin B1 (1:1,000), mouse anti-cyclin D1 (1,000; cat. no. A-12) (all from Santa Cruz Biotechnology).

Results

Nab-paclitaxel exerts cytotoxic effects in PDAC cells displaying different primary sensitivity to gemcitabine. In order to assess the efficacy of nab-paclitaxel on cell proliferation and viability, we analyzed the dose-response to nab-paclitaxel of the PDAC cells displaying different sensitivity to gemcitabine, with the MiaPaCa-2 and Panc-1 cells demonstrating the highest resistance to gemcitabine, thus offering *in vitro* models of primary resistance to this drug (7,8,15).

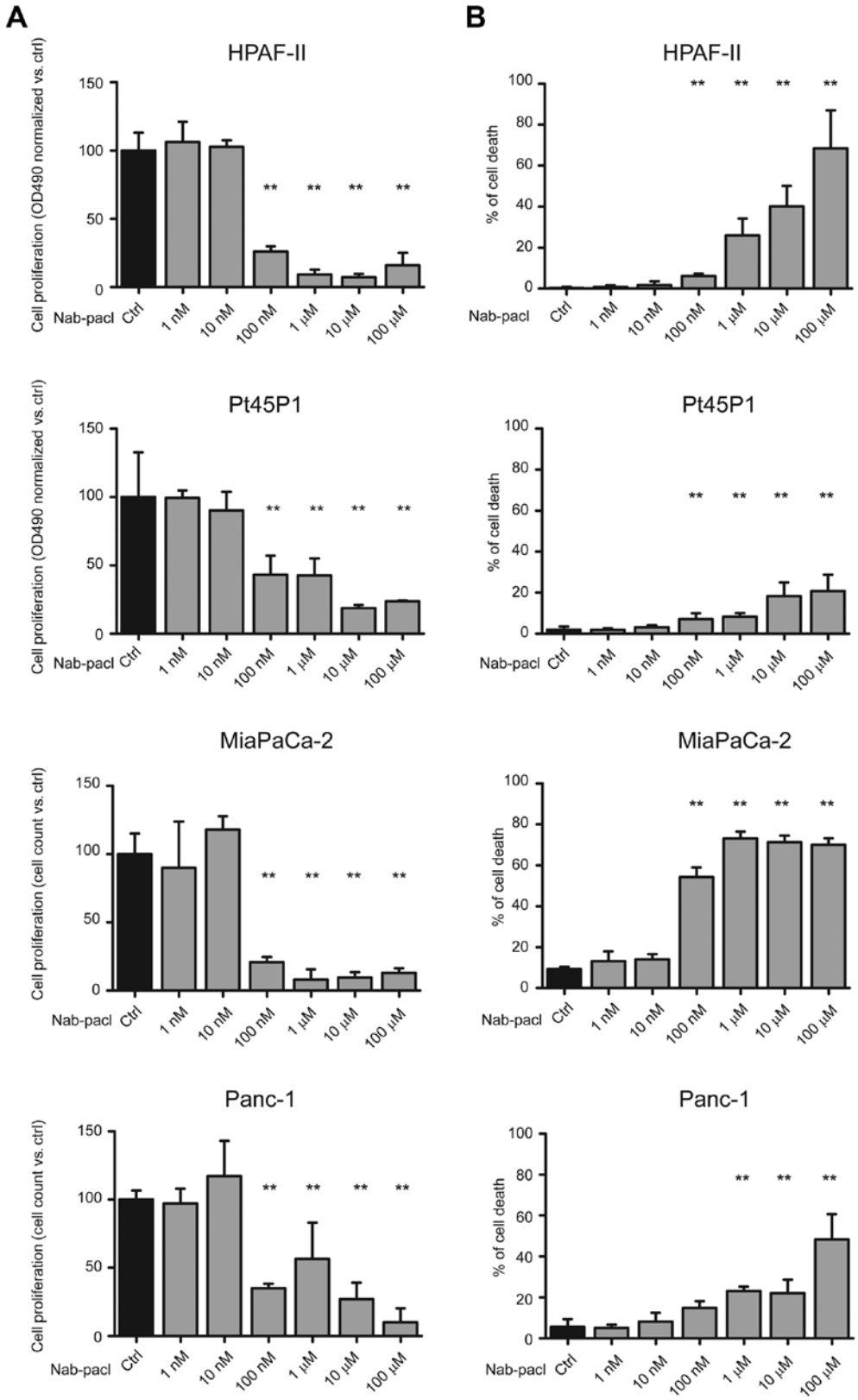

Figure 1. Nab-paclitaxel exerts a similar cytotoxic effect in PDAC cells with different sensitivity to gemcitabine. Histograms display the analysis of (A) cell proliferation performed by an MTS assay (HPAF-II and PT45P1) or by cell count (MiaPaCa-2 and Panc-1) and (B) cell death performed by Trypan blue after 72 h of treatment with the indicated doses of nab-paclitaxel. The results represent the mean ± SD of three experiments. Significance vs. control, was determined by Student's t-test: $^{**}P<0.01$.

Nab-paclitaxel induced a significant reduction of cell proliferation (60-65%) starting from the dose of 100 nM compared to controls in all PDAC cells (Fig. 1A). Furthermore, at this dose, nab-paclitaxel induced a significant increase of cell death in all cell lines with the exception of Panc-1 cells (Fig. 1B). Notably, the increase of cell death at 100 nM was modest in

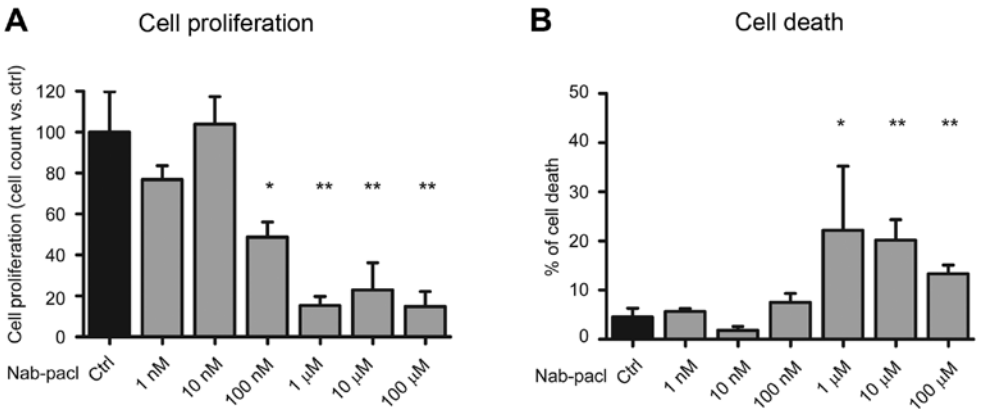

Figure 2. Nab-paclitaxel exerts cytotoxic effect in PANC-1 DR cell line with secondary resistance to gemcitabine. Histograms reveal the analysis of (A) cell proliferation performed by cell count and (B) cell death performed by Trypan blue cell count after 72 h of treatment with the indicated doses of nab-paclitaxel. The results represent the mean ± SD of three experiments. Significance vs. control was determined by Student's t-test: *P<0.05 and **P<0.01.

HPAF-II (6%) and Pt45P1 (7%) cells, whereas it was very high in MiaPaCa-2 cells (54%) (Fig. 1B), which displayed higher resistance to gemcitabine (15). Conversely, nab-paclitaxel significantly reduced Panc-1 cell proliferation at this dose without inducing cell death, whereas cell viability was affected only at micromolar doses of the drug (Fig. 1A and B). At these higher doses (1-100 μM), nab-paclitaxel led to substantial induction of cell death in the HPAF-II, MiaPaCa-2 and Panc-1 cell lines, while cell death remained at 20% in Pt45P1 even at the highest dose (Fig. 1B).

These results revealed that, regardless of their sensitivity to gemcitabine, the PDAC cells demonstrated similar sensitivity to nab-paclitaxel in terms of inhibition of cell proliferation, however, different response in terms of cell death.

Nab-paclitaxel exerts a cytotoxic effect in PDAC cells with secondary gemcitabine resistance. As aforementioned we selected PDAC cells which acquired resistance to gemcitabine after chronic exposure to the drug (8). Notably, these cells were also more resistant to cisplatin (8), another drug exerting genotoxic stress. To examine whether these drug-resistant (DR) cells were still sensitive to nab-paclitaxel, a dose-response study was performed. We found that DR-Panc-1 cells maintained the same sensitivity to nab-paclitaxel as the parental cell line, with significant inhibition of cell proliferation starting at the dose of 100 nM, while cell death increased significantly at the dose of 1 μM (Fig. 2A and B). These results confirmed that nab-paclitaxel sensitivity did not correlate with gemcitabine sensitivity and suggested that nab-paclitaxel may overcome acquired resistance to gemcitabine in PDAC cells.

Combined treatment with Nab-paclitaxel and gemcitabine exerts additive effects on the inhibition of cell proliferation. In order to understand whether nab-paclitaxel in combination with gemcitabine enhances the cytostatic and cytotoxic effects of the chemotherapeutic treatment, we tested their combined action on cell proliferation and death in MiaPaCa-2 cells, a cell line demonstrating relatively high resistance to gemcitabine (15). The combination of gemcitabine (100 nM) and nab-paclitaxel (10 nM) exerted a significant increase in cell death compared to gemcitabine alone (56 vs. 37%) (Fig. 3A). Notably, the effect of the combined treatment was similar to that exerted by gemcitabine alone at a dose 100 times higher (i.e. 10 μM; Fig. 3A). The combination of gemcitabine (30 nM) and nab-paclitaxel (10 nM) elicited a significant additive effect even when used at a suboptimal dosage (Fig. 3B). Furthermore, similar effects were also obtained with the highly resistant DR-Panc-1 cells, albeit at considerably higher doses (Fig. 3C). These data indicated that combined treatment with nab-paclitaxel and gemcitabine enhanced the cytotoxic effects of both drugs, allowing to lower their doses, thus possibly limiting adverse effects.

Combination of suboptimal doses of nab-paclitaxel and gemcitabine induces a significant increase in apoptosis. To investigate the nature of the additive effect of gemcitabine and nab-paclitaxel on PDAC cell death, we analyzed cell cycle progression and cell death in more detail in MiaPaCa-2 cells. Flow cytometry analysis with propidium iodide (PI) of cells treated with suboptimal doses of gemcitabine (30 nM) and nab-paclitaxel (10 nM) for 48 h indicated that gemcitabine strongly affected the cell cycle progression, leading to cell accumulation in S phase, whereas nab-paclitaxel elicited very mild effects. Notably, however, the addition of nab-paclitaxel to gemcitabine led to the appearance of a defined peak in the sub-G1 population of MiaPaCa-2 cells (Fig. 4A), indicating cell death by apoptosis. To confirm the effect of the combined treatment on cell apoptosis, we monitored cleavage of poly(ADP-ribose) polymerase (PARP1) by western blot analysis. Consistent with the appearance of the sub-G1 peak, PARP1 cleavage was noticeably increased in MiaPaCa-2 cells treated with the combination of the two drugs (Fig. 4B).

Addition of nab-paclitaxel to gemcitabine induces a stronger cell cycle blockage in S phase. The PI profile indicated that co-treatment with nab-paclitaxel enhanced the accumulation of cells in the S phase of the cycle compared to gemcitabine alone (Fig. 4A). To further investigate this possibility, we analyzed the incorporation of BrdU as a precise marker of DNA duplication in S phase. A short pulse of BrdU was administered to MiaPaCa-2 cells 30 min before harvesting, following 24 h of incubation with the drugs. We observed that both gemcitabine and nab-paclitaxel, used as single agents, caused an accumulation of cells in the S phase (from 45,93

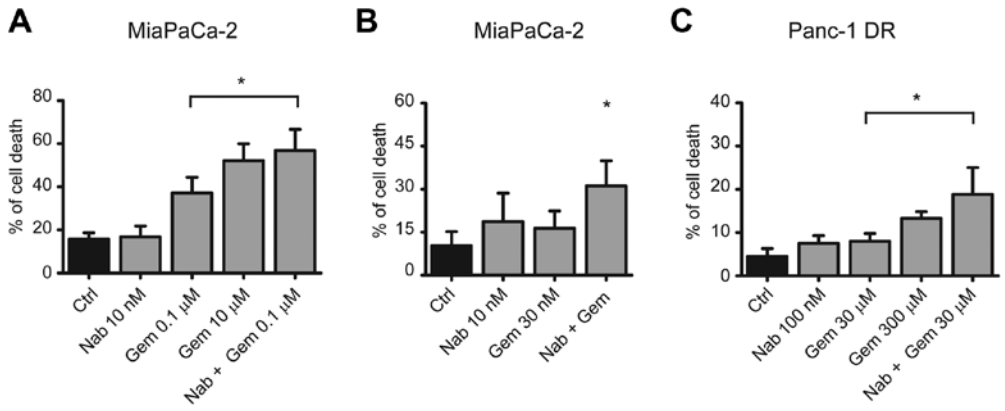

Figure 3. Combined treatment of gemcitabine and nab-paclitaxel exert an additive effect on the inhibition of cell proliferation. Histograms display the analysis of cell death performed by Trypan blue on MiaPaCa-2 cells after (A) 72 h of treatments with the indicated doses of nab-paclitaxel and gemcitabine. Significance vs. control, was determined by Student's t-test: *P<0.05. (B) Analysis of cell death after 48 h of treatments with the indicated suboptimal doses of nab-paclitaxel and gemcitabine. Statistical analysis was performed by one-way analysis of variance by ANOVA test followed by Tukey's Multiple Comparison post-test (*P<0.05). (C) Analysis of cell death performed by Trypan blue on Panc-1 DR cells after 72 h of treatments with the indicated doses of nab-paclitaxel and gemcitabine. Significance vs. control, was determined by Student's t-test: *P<0.05. All results represent the mean ± SD of three experiments.

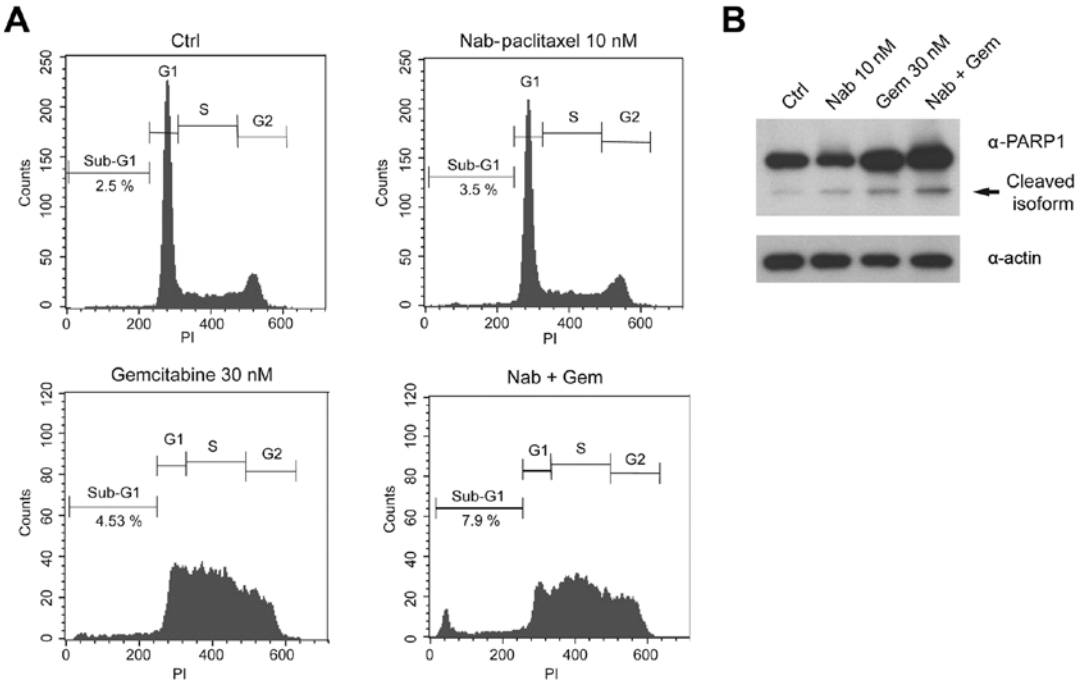

Figure 4. Combination of suboptimal dose of nab-paclitaxel and gemcitabine induces a significant increase of cell death. (A) Panels display the percentage of cells stained for propidium iodide (PI) in Sub-G1, G1, S and G2 phases in MiaPaCa-2 cells treated with nab-paclitaxel, gemcitabine or both drugs for 48 h. (B) Western blot analysis of cleaved protein PARP-1 in MiaPaCa-2 cells treated with nab-paclitaxel, gemcitabine or both drugs for 48 h.

to 78,30 and 74,37%) (Fig. 5A). Notably, the combination of both drugs resulted in an additive effect on the accumulation of cells in S phase, which reached 84.84%. As a consequence of this blockage in cell cycle progression, co-treatment with gemcitabine and nab-paclitaxel resulted in a sharp reduction of cells transiting in the G2 phase (Fig. 5A).

In addition, we checked the changes in cell cycle progression by monitoring the expression levels of phase-specific cyclins. As dislplayed in Fig. 5B, cyclin D1 levels were not affected by treatments, whereas cyclin A2 and E2 levels increased after gemcitabine administration either alone or in combination with nab-Paclitaxel, confirming that the cells are mainly blocked in the S phase. Treatment with nab-paclitaxel alone did not cause accumulation of S phase cyclins (Fig. 5B), even though the cells were blocked at this stage of the cycle. Since we noticed that nab-paclitaxel caused accumulation of cells in the left-most region of S phase (Fig. 5A), indicating very little duplication of DNA, it is probable that this drug blocks cells before the accumulation of cyclins E2 and A2. Additionally, we observed that the combined treatment with both drugs reduced the expression of cyclin B1 compared to gemcitabine alone. Since this cyclin is involved in the S-G2 cell cycle transition, its levels reflect the reduction of cells in G2 phase, which was observed in flow cytometric analyses (Figs. 4A and 5A).

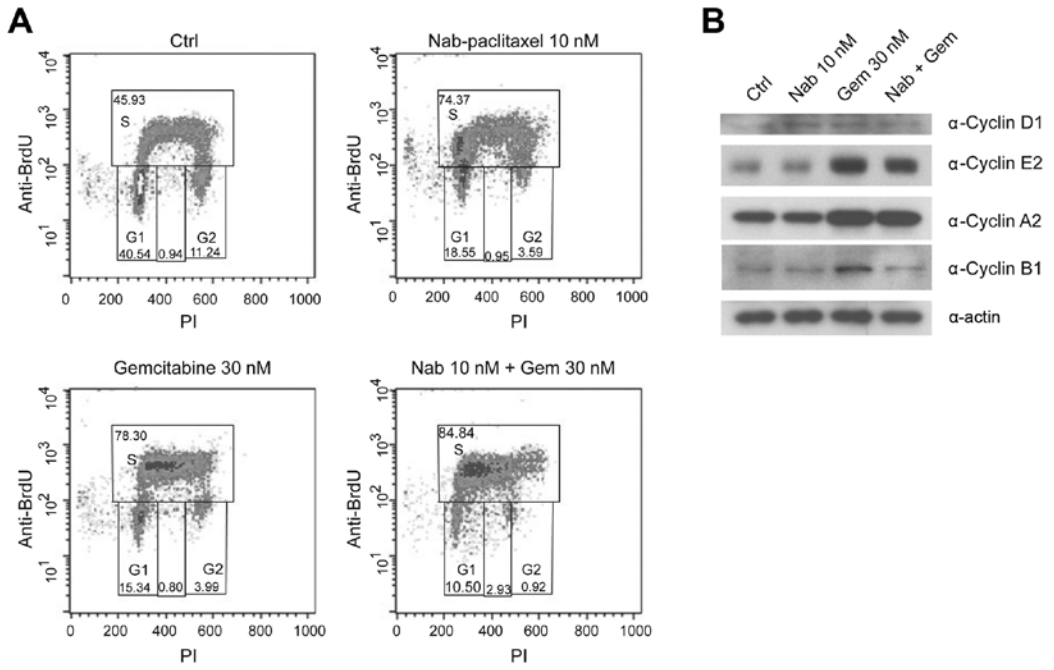

Figure 5. Combination of suboptimal dose of nab-paclitaxel and gemcitabine induces a significant increase of cell death. (A) Panels display the percentage of cells stained for propidium iodide (PI) and anti-BrdU FITC antibody. They are detected in G1, S and G2 phases in MiaPaCa-2 cells treated with nab-paclitaxel, gemcitabine or both drugs for 24 h. (B) Western blot analysis of cyclin D1, A, E and B1 in MiaPaCa-2 cells treated with nab-paclitaxel, gemcitabine or both drugs for 24 h.

Discussion

The aim of the present study was to examine the activity of nab-paclitaxel alone or in combination with gemcitabine in PDAC cell lines displaying different degree of primary resistance to gemcitabine and in a previously described model of secondary resistance to the drug (7,8).

The results of the present study revealed that nab-paclitaxel is effective in PDAC cells irrespective of their sensitivity to gemcitabine and to the status of primary or secondary (acquired) resistance (Figs. 1 and 2). Notably, both drugs demonstrated an addictive effect at suboptimal doses in cell lines with primary or secondary resistance to gemcitabine (Fig. 3).

To investigate the underlying mechanisms of the observed efficacy of nab-paclitaxel, we explored the changes occurring in the cell cycle (Figs. 4 and 5). Our results indicated that nab-paclitaxel blocked cell proliferation in a different manner compared to gemcitabine. Although both drugs caused an arrest in S phase, the cells treated with gemcitabine exhibited a different extent of DNA duplication, whereas the peak of cells treated with nab-paclitaxel is present in the left region of the graph, indicating that cells arrest as soon as they start duplicating their DNA. This difference is also illustrated by the accumulation of S phase cyclins, which is evident in gemcitabine- but not in nab-paclitaxel-treated cells. While the blockage in S phase is expected after gemcitabine exposure, due to depletion of the nucleotide pool required for DNA duplication, cells treated with nab-paclitaxel were expected to arrest in mitosis or late G2 phase due to defects in spindle elongation. However, recent data have revealed that cells treated with paclitaxel often proceeded through mitosis into the next interphase, where the majority of cell deaths occurred (16). In particular, nab-paclitaxel seemed to interfere with the very early stages of the S phase in PDAC cells (Fig. 5A). This may explain why it was previously found that the interference with the DNA replication origin activity enhanced the response of cells to paclitaxel (16).

The different mechanism of S phase blockage by the two drugs may explain the additive affect observed in the combined treatment. Markedly, such additive effect was observed both at the cell cycle and the cell death level, indicating a causal relationship between the two events. Although the molecular mechanisms involved in such effect need further investigation, our results indicated that nab-paclitaxel strongly enhances the cytotoxicity of gemcitabine and may help to overcome both primary and acquired resistance to this drug.

The *in vitro* results of the present study revealed that nab-paclitaxel, alone or in combination with gemcitabine, is an active drug in preclinical models of gemcitabine-resistant PDAC. Hence, our observations indicated that, in certain clinical scenarios, nab-paclitaxel could be active in patients with PDAC that are not responding to gemcitabine, even in monotherapy. However, clinical data on the use of nab-paclitaxel as a single agent in patients with PDAC that were previously treated with gemcitabine, are limited. In a small phase II trial, 19 patients received nab-paclitaxel after progression under gemcitabine-based therapy (17). One of them (5.3%) had a confirmed partial response and 6 (32%) exhibited stable disease as the best response. Another single-center retrospective study evaluated the use of nab-paclitaxel in 20 patients with advanced PDAC who previously exhibited progression under gemcitabine, 40% of whom also received FOLFIRINOX. Notably, about two thirds of patients had stable disease as best response, although the median OS was

only of 5.2 months (18). Further studies are needed to elucidate whether this approach may be beneficial, possibly in patients with less advanced disease.

The present study is one of the few that aimed to evaluate the efficacy of nab-paclitaxel in preclinical settings, using cell lines that are models of both primary and secondary resistance to gemcitabine. As the investigation is limited to *in vitro* models, the results should be interpreted with caution and the mechanisms of the activity observed in the present study need further experiments to be elucidated. In particular, our data are useful to generate hypotheses that need to be confirmed in other models, such as animal ones, that may better recapitulate the human pathology. Conversely, the additive effect of nab-paclitaxel and gemcitabine observed in these experiments cannot be due to factors that have been extensively investigated in animal models and that are related with tumor stroma and penetration of drugs. Another limitation of the present study concerns the lack of a defined mechanism for the observed effects. Following the revision process, we tested some common signal transduction pathways that could be involved in the response to these chemotherapeutic agents, such as the PI3K-mTOR and ERK pathways (data not shown). However, we did not find a direct correlation with the cytotoxic effect. Thus, further studies are needed to analyze the mechanisms underlying the observed effects. Considering the above-mentioned limitations, our results revealed that treatment with nab-paclitaxel may overcome resistance to gemcitabine and may represent a potentially valuable therapeutic approach for advanced PDAC.

Acknowledgements

The present study was supported by grants from the Associazione Italiana per la Ricerca sul Cancro (AIRC; IG18790 for C.S. and IG 17177 for G.C.).

Competing interests

The authors declare that they have no competing interests.

References

1. Siegel RL, Miller KD and Jemal A: Cancer Statistics, 2017. CA Cancer J Clin 67: 7-30, 2017.
2. Rahib L, Smith BD, Aizenberg R, Rosenzweig AB, Fleshman JM and Matrisian LM: Projecting cancer incidence and deaths to 2030: The unexpected burden of thyroid, liver, and pancreas cancers in the United States. Cancer Res 74: 2913-2921, 2014.
3. Fogel EL, Shahda S, Sandrasegaran K, DeWitt J, Easler JJ, Agarwal DM, Eagleson M, Zyromski NJ, House MG, Ellsworth S, *et al*: A multidisciplinary approach to pancreas cancer in 2016: A review. Am J Gastroenterol 112: 537-554, 2017.
4. Neuzillet C, Tijeras-Raballand A, Bourget P, Cros J, Couvelard A, Sauvanet A, Vullierme MP, Tournigand C and Hammel P: State of the art and future directions of pancreatic ductal adenocarcinoma therapy. Pharmacol Ther 155: 80-104, 2015.
5. Burris HA III, Moore MJ, Andersen J, Green MR, Rothenberg ML, Modiano MR, Cripps MC, Portenoy RK, Storniolo AM, Tarassoff P, *et al*: Improvements in survival and clinical benefit with gemcitabine as first-line therapy for patients with advanced pancreas cancer: A randomized trial. J Clin Oncol 15: 2403-2413, 1997.
6. Binenbaum Y, Na'ara S and Gil Z: Gemcitabine resistance in pancreatic ductal adenocarcinoma. Drug Resist Updat 23: 55-68, 2015.
7. Adesso L, Calabretta S, Barbagallo F, Capurso G, Pilozzi E, Geremia R, Delle Fave G and Sette C: Gemcitabine triggers a pro-survival response in pancreatic cancer cells through activation of the MNK2/eIF4E pathway. Oncogene 32: 2848-2857, 2013.
8. Calabretta S, Bielli P, Passacantilli I, Pilozzi E, Fendrich V, Capurso G, Fave GD and Sette C: Modulation of PKM alternative splicing by PTBP1 promotes gemcitabine resistance in pancreatic cancer cells. Oncogene 35: 2031-2039, 2016.
9. Conroy T, Desseigne F, Ychou M, Bouché O, Guimbaud R, Bécouarn Y, Adenis A, Raoul JL, Gourgou-Bourgade S, de la Fouchardière C, *et al*: FOLFIRINOX versus gemcitabine for metastatic pancreatic cancer. N Engl J Med 364: 1817-1825, 2011.
10. Von Hoff DD, Ramanathan RK, Borad MJ, Laheru DA, Smith LS, Wood TE, Korn RL, Desai N, Trieu V, Iglesias JL, *et al*: Gemcitabine plus nab-paclitaxel is an active regimen in patients with advanced pancreatic cancer: A phase I/II trial. J Clin Oncol 29: 4548-4554, 2011.
11. Von Hoff DD, Ervin T, Arena FP, Chiorean EG, Infante J, Moore M, Seay T, Tjulandin SA, Ma WW, Saleh MN, *et al*: Increased survival in pancreatic cancer with nab-paclitaxel plus gemcitabine. N Engl J Med 369: 1691-1703, 2013.
12. Vaccaro V, Sperduti I, Vari S, Bria E, Melisi D, Garufi C, Nuzzo C, Scarpa A, Tortora G, Cognetti F, *et al*: Metastatic pancreatic cancer: Is there a light at the end of the tunnel? World J Gastroenterol 21: 4788-4801, 2015.
13. Lemstrova R, Melichar B and Mohelnikova-Duchonova B: Therapeutic potential of taxanes in the treatment of metastatic pancreatic cancer. Cancer Chemother Pharmacol 78: 1101-1111, 2016.
14. Neesse A, Algül H, Tuveson DA and Gress TM: Stromal biology and therapy in pancreatic cancer: A changing paradigm. Gut 64: 1476-1484, 2015.
15. Arumugam T, Ramachandran V, Fournier KF, Wang H, Marquis L, Abbruzzese JL, Gallick GE, Logsdon CD, McConkey DJ and Choi W: Epithelial to mesenchymal transition contributes to drug resistance in pancreatic cancer. Cancer Res 69: 5820-5828, 2009.
16. Koh SB, Mascalchi P, Rodriguez E, Lin Y, Jodrell DI, Richards FM and Lyons SK: A quantitative FastFUCCI assay defines cell cycle dynamics at a single-cell level. J Cell Sci 130: 512-520, 2017.
17. Hosein PJ, de Lima Lopes G Jr, Pastorini VH, Gomez C, Macintyre J, Zayas G, Reis I, Montero AJ, Merchan JR and Rocha Lima CM: A phase II trial of nab-Paclitaxel as second-line therapy in patients with advanced pancreatic cancer. Am J Clin Oncol 36: 151-156, 2013.
18. Peddi PF, Cho M, Wang J, Gao F and Wang-Gillam A: Nab-paclitaxel monotherapy in refractory pancreatic adenocarcinoma. J Gastrointest Oncol 4: 370-373, 2013.

Chapter III. RNA metabolism in cancer

III.1 RNA metabolism

A majority of eukaryotic genes are regulated at transcriptional and post-transcriptional levels (Fig. 5). Cancer evolves through perturbations in these processesthat in turn modulate to the advantage of tumor cells cellular processes such as proliferation, differentiation, cell-cycle control, metabolism, apoptosis, motility, invasion, and angiogenesis.

The main steps of RNA processing occur co-transcriptionally and include:

- capping: the addition of a to 7- methylguanosine cap the 5' end of the pre- mRNA soon after Pol II initiates transcription, important for the RNA stability, involve in RNA quality control mechanism and contributes to nuclear export of mRNA.
- splicing: process that mediates removal of introns and the joining of exons and occur while Pol II transcribes DNA into RNA.
- polyadenylation: the addition of a poly(A) tail to the 3' end of the pre- mRNA before Pol II completes transcription.

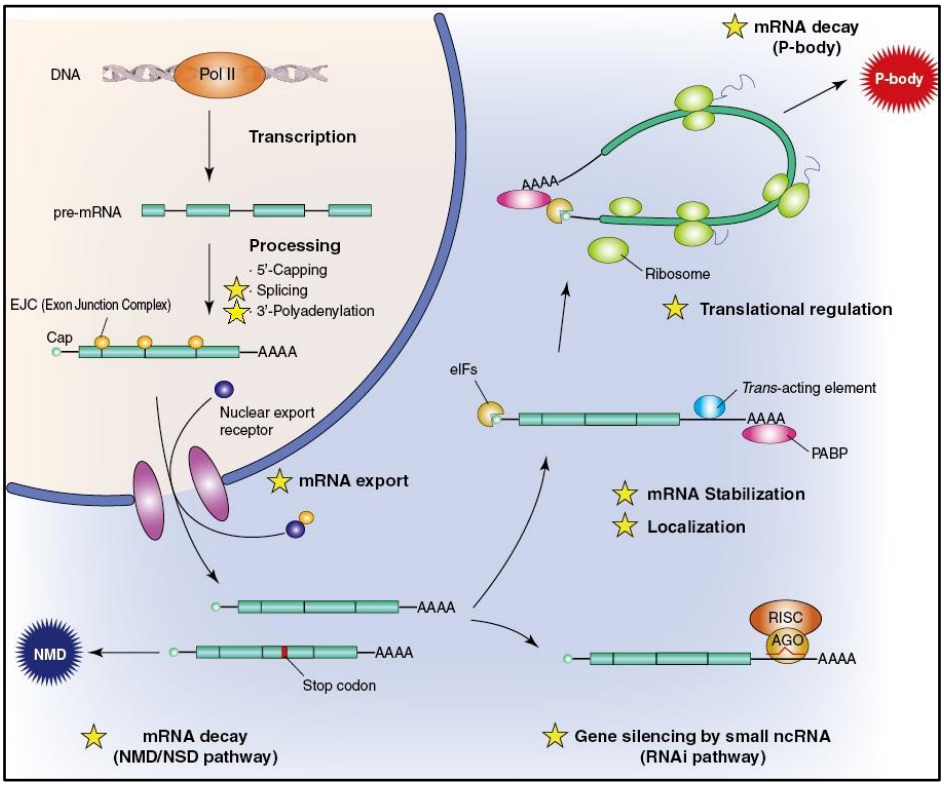

Figure 5. Overview of RNA metabolism (readapted from *https://www.mblbio.com/bio/g/product/epigenetics/RNAworld.html*)

Other steps of RNA processing take place at the post-transcriptional level, the most important are:

- mRNA export: process that occur through the Nuclear Pore Complexes (NPC) by binding to the cap-binding proteins CBP20 and CBP80 and transcription/export complex (TREX).
- mRNA stability regulation: it can happen through different process: decapping Dcp1/2 factors, deadenylase Ccr4/Pop2/Not complex, nonsense mediated decay (NMD), microRNA, long non coding RNA.
- translational regulation: mRNAs also can be sequestered in stress granules or P-bodies.

The investigation of molecular mechanisms underlying abnormal RNA processing in cancer cells is providing new opportunities of development of cancer therapeutics

III.2 RNA stability or RNA decay

The regulation of mRNA stability is a fine process for cell physiology because it permits transient expression of proteins and increases the flexibility of gene expression together with regulation rate of mRNA synthesis. Since mRNA stability is essential to determine the proteins that are produced, many factors control this event.

The addition of 7-methylguanosine-cap structure at 5' of transcript (5’ cap) and the tail of polyA at 3' protect mRNAs from decay by impeding the processing of exonucleases. Furthermore, the interaction between proteins that binds the cap (eIF4E) and the poly(A)-binding protein (PABP) promove the mRNA circularizes in the cytoplasm, this conformation lends mRNA more stable sequestering the 5’ and 3’ ends. The deadenylation induces the destabilization of transcript by releasing PABP from the 3’ and exposing mRNA to attack by exosome complex that is responsible for 3’→5’ decay. Another process is the deccaping by DCP1 and DCP2 enzymes that remove the 5'cap, thus making RNA susceptible to the decay through 5’→3’ exonuclease, XRN1 and XRN2 (Fig. 6)(Garneau, Wilusz, and Wilusz 2007)

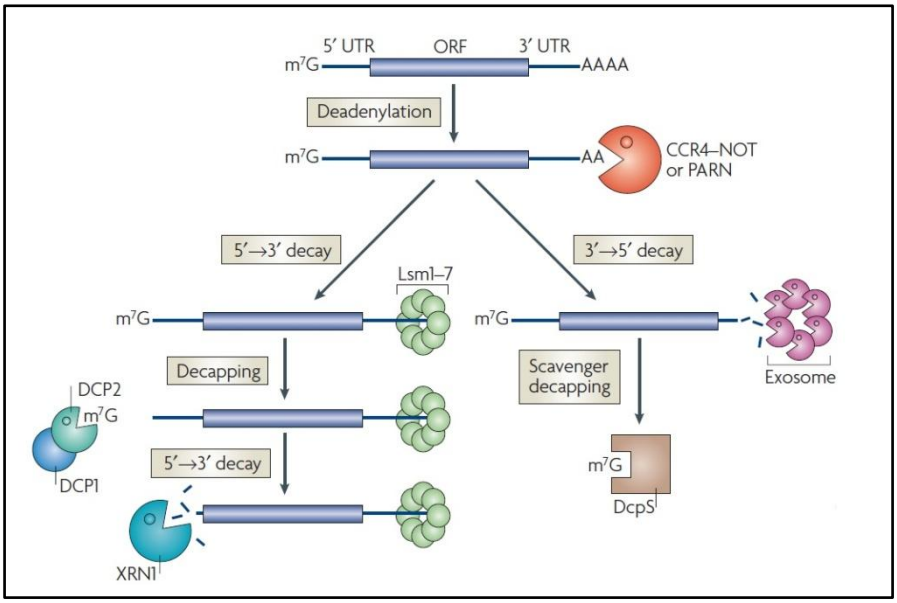

Figure 6. Mechanisms of mRNA decay (Garneau, Wilusz, and Wilusz 2007)

Non sense-mediated decay (NMD) is an evolutionarily conserved mechanism that recognizes mRNAs with a premature termination codons (PTCs) and degrades them. The identification of these transcipts occur by a complex proteins called the exon complex (EJC) that is deposited approximately 20–25 bp upstream of every intron after RNA splicing processing. The presence of an EJC after a stop codon triggers NMD, whereas EJCs before the stop codon do not, thus this system selects the mRNA that undergoRNA decay(Kurosaki and Maquat 2016).

One of the locations where the RNA decay takes place are the P-bodies, cytoplasmic ribonucleoprotein (RNP) granules primarily composed of non translating mRNA and a core of proteins involved in mRNA decay and translation repression (decapping enzyme complex, 5′ to 3′ exonuclease, deadenylase complex) (Eulalio, Behm-Ansmant, and Izaurralde 2007). Moreover P-bodies contain proteins and microRNAs involved in the miRNA repression pathway; microRNAs are hairpin-derived RNAs 20–24 nucleotides long, that post-transcriptionally repress the expression of target genes by binding to the 3' UTR of mRNA. The repressed mRNAs remain in the P body in a "standby state", thus they are ready to be transcript; this system provides a way to transiently arrest translation, so the cell has developed a faster regulation mechanism than the de novo transcription of the target gene. (Decker and Parker 2012)(Di Leva, Garofalo, and Croce 2014).

III.3 The splicing mechanism and its role in cancer

The splicing mechanism is required for the maturation of almost all human transcripts. Notably, pre-mRNAs can be processed into different mature mRNAs through alternative splicing of multiple exons, thus enabling multiple potential protein products to be generated from a single gene. This process is guided by the spliceosome, a dynamic complex consisting of small nuclear RNAs (snRNAsU1, U2, U4, U5 and U6) and many other protein factors. During the splicing reaction this complex undergoes different conformational and compositional changes (Dvinge et al. 2016).

U1 snRNP recognizes and binds to the 5’ splice site, which is located at the start of the intron, whereas U2 snRNP pairs with the branch site region adjacent to the 3’ splice site, assisted by interactions with U2 auxiliary factors (U2AFs, which form the U2AF complex) that bind to the 3’ splice site, located at the end of the intron. Interactions between U1 and U2 snRNPs bring the 5’ss and 3’ss into close proximity. Following recruitment of the U4/U6-U5 tri-snRNP, the assembled spliceosome is in active conformation; U2 and U6 interact, causing dissociation of U4 from U6 snRNA and exposition of the 5’ of U6, which binds the 5’ss displacing U1 snRNA. The splicing process proceeds via two sequential trans-esterification reactions that join the exons and release an intron lariat that is subsequently degraded. Finally, the spliceosome components are recycled for subsequent reation of splicing (Fig.7 A)(Shi 2017)(Dvinge et al. 2016).

Alternative spling events can be classified based on how the mature transcript is formed; we can found events of constitutive spliced exon, exon cassette, alternative 5'/3' splice site, retained intron and mutualy exclusive exons (Fig. 7 B).

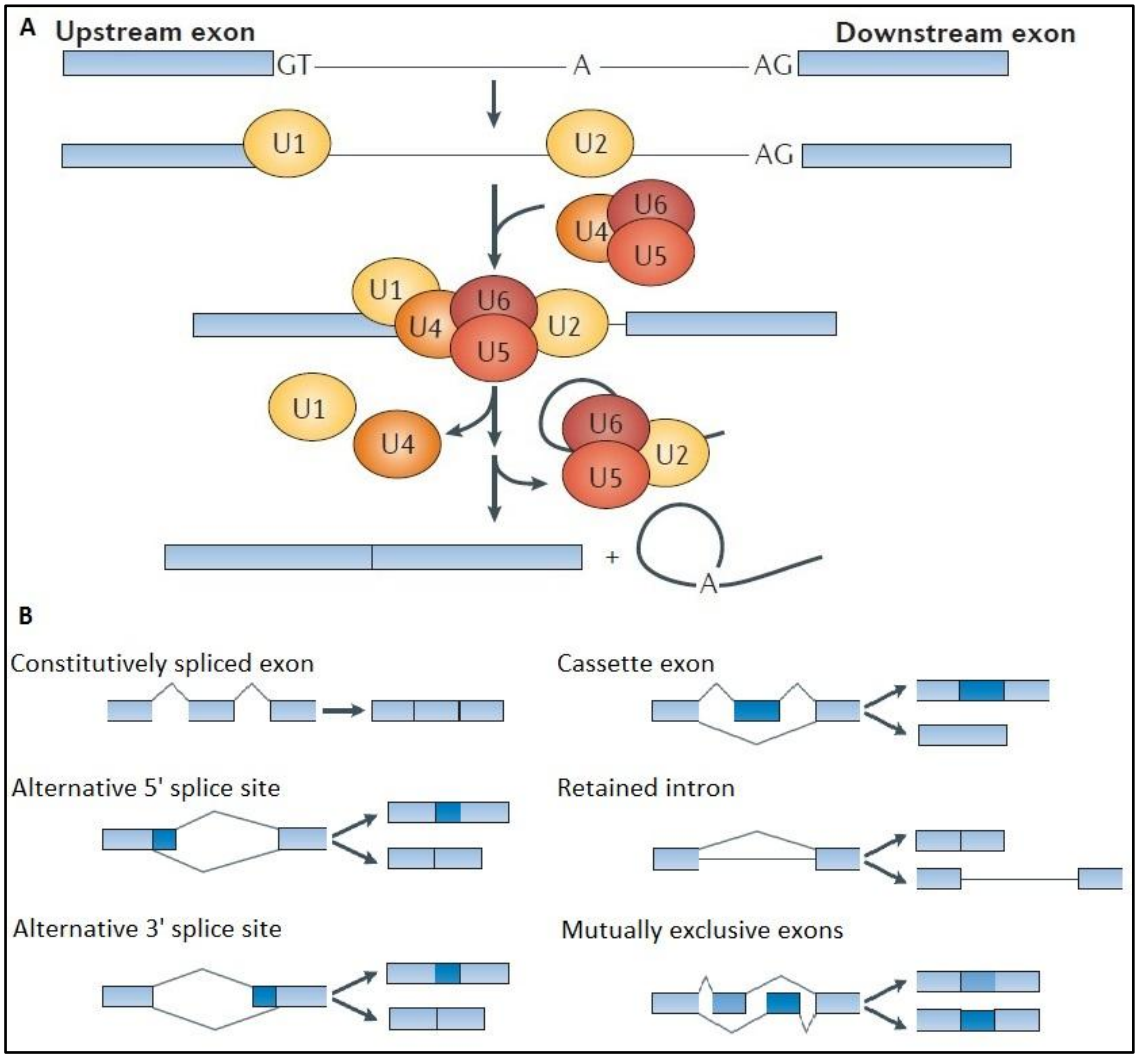

Figure 7. Schematic representation of splicing mechanism and model of constitutive and alternative splicing (Dvinge et al. 2016).

The activity of the spliceosome is regulated by both *cis* acting sequences on the pre-mRNA and *trans* acting factors,which may enhance or inhibit both recognition of the splice sites and splicing catalysis. The *cis*-acting regulatory elements are classified according to their location and activity: exonic and intronic splicing enhancers (ESEs and ISEs) or silencers (ESSs and ISSs). The *trans* acting RNA binding proteins (RBPs) recognize these elements and in turn promote or inhibit spliceosome assembly and activity. Two main classes of RBPs regulates this process: the Ser/Arg rich (SR) proteins, which mainly exert a positive regulation on the spliceosome, and the heterogeneous nuclear ribo nucleoproteins (hnRNPs), which often act antagonistically (Fig. 8). SR and hnRNPs regulate splicing in diverse ways, including facilitating recruitment of snRNP or RBPs, mask a splice site, 'looping out' an exon and other mechanisms (Dvinge et al. 2016).

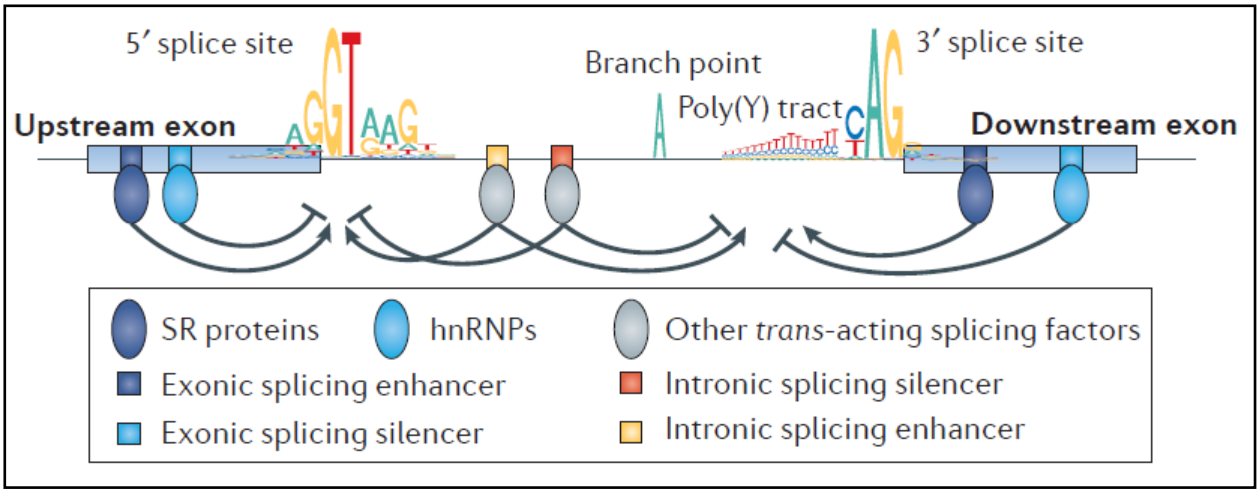

Figure 8. Spliceosome regulatory elements (Dvinge et al. 2016).

Interestingly, the activities of RBPs often depend on their relative locations within pre-mRNAs. For example hnRNPI, primarily known as polypyrimidine tract binding protein 1 (PTBP1), modulates splicing in a context-dependent manner: it promotes exon inclusion when it binds in the downstream intron and exon skipping when it binds in the upstream intron (Llorian et al. 2010). In addition to the SR proteins and hnRNPs, many other RBPs regulate splicing, including CELF, MBNL, RBFOX, STAR, NOVA and ESRP proteins. Thus, alteration of the expression of these RBPs can impact alternative splicing (Dvinge et al. 2016).

Regulation of alternative splicing has essential roles in cancer cell biology, including proliferation, differentiation, cell-cycle control, metabolism, apoptosis, motility, invasion and angiogenesis. Deregulated splicing can lead to generate oncogenic isoform that contribute to tumor establishment, progression and resistance to therapy. Analysis of data from 8,705 patients with one of 32 types of cancer revealed that tumors have up to 30% more alternative splicing events than normal tissues (Kahles et al. 2018). Many studies have found links between the altered expression and/or activity of splicing factors and cancer (Pagliarini, Naro, and Sette 2015)(J. Zhang and Manley 2013). Below I report some examples of peculiar cancer isoforms (Fig. 9).

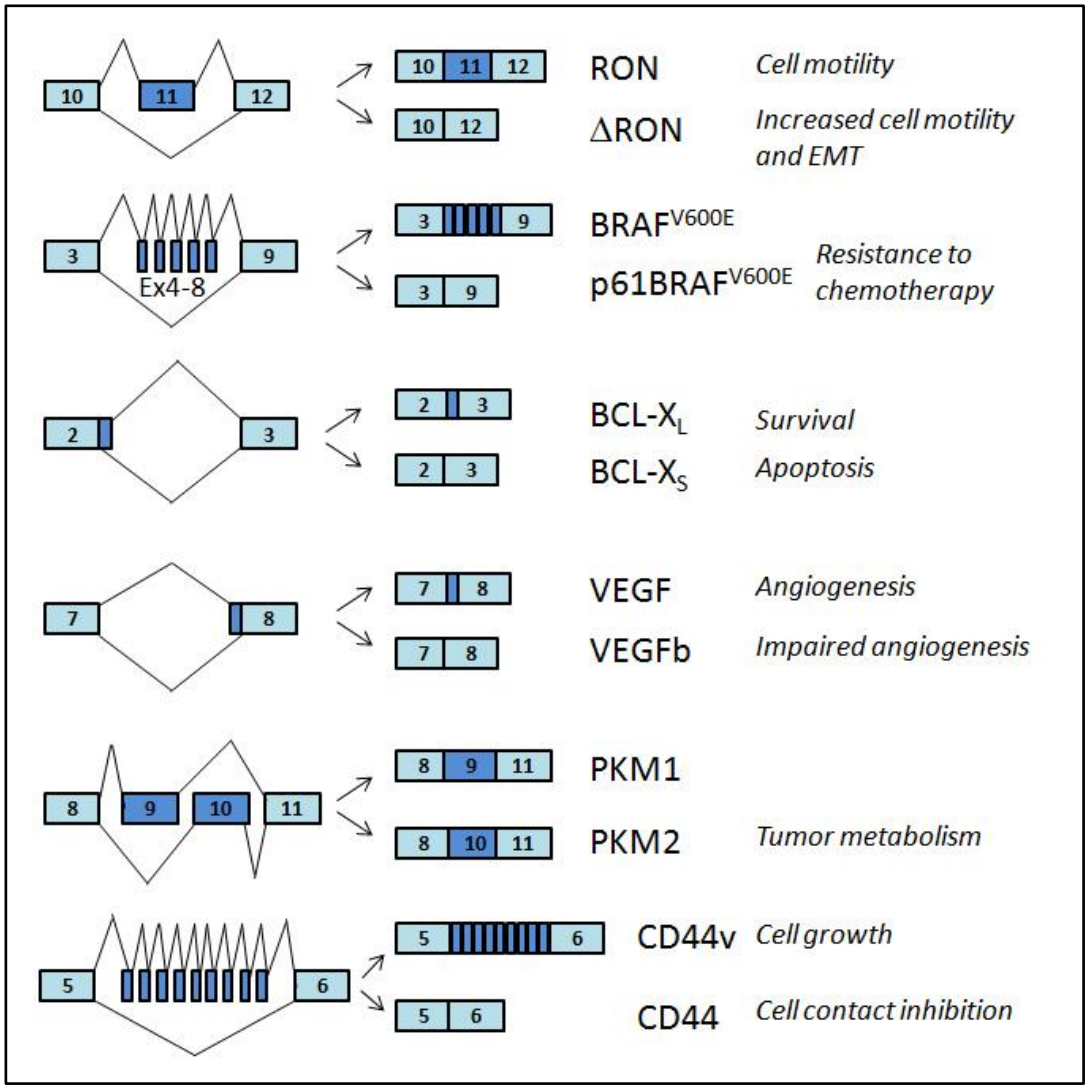

Figure 9. Examples of alternative splicing patterns in cancer.

The *RON* gene encodes a tyrosine kinase receptor involved in cell mobility and invasion in response to MSP binding. The isoform ΔRON, which lacks exon 11, is over-expressed in a number of cancers, this exon encoding for an extracellular domain, that remains constitutively active in the truncated ΔRON promoting cancer invasiveness (Collesi et al. 1996).

BRAF is a proto-oncogene encoding the serine/threonine protein kinase BRAF, which regulates the MAPK/ERK signaling pathway. The skipping of exons 4–8 cause a the truncated enzyme (*BRAF*^{V600E}) that is insensitive to the BRAF inhibitors (vemurafenib), often is utilized in cancer, and confers melanoma cell resistance to the drugs (Poulikakos et al. 2011).

BCL-X belongs to the BCL-2 protein family, that is involved in anti- or pro- apoptotic regulators. *BCL2L1* produces two splice isoforms by the alternative use of two competing 5' splice sites in exon 2. The longer isoform BCL-X_L has antiapoptotic effects and is over-expressed in various

cancer types, while the shorter isoform BCL-X_S is proapoptotic and is downregulated in cancer (Olopade et al. 1997)(Trisciuoglio et al. 2017).

VEGF stimulates angiogenesis required for tumor growth. Selection of the proximal 3'splice sites produces isoforms VEGF, that has a pro-angiogenic role and are over-expressed in a number of tumors. Instead the VEGFb isoform is formed when the distal 3'splice sites are used, it has a anti-angiogenic role and it is down-regulated in tumors. These opposing functions are caused by the different C-terminal produced, VEGFb fails to bind to its receptor, the neurophilin 1, which is required for activation of VEGF signal transduction (Nowak et al. 2008).

In tumor the isorform PKM2 is predominant and performs a critical role for tumor metabolism, like previus descripts (Dayton, Jacks, and Vander Heiden 2016).

CD44 is a trans-membrane glycoprotein that mediates the response of cells to their cellular microenvironment: lymphocyte homing, adhesion, migration, and regulation of cell growth. This variety of roles is favoured by the existence of multiple CD44 splice variants, the CD44 gene is composed of 10 constitutively spliced exons and 9 variable exons, residing between constitutive exons 5 and 6 (Ponta, Sherman, and Herrlich 2003). For example, CD44 molecules contain v6–7 were expressed specifically in a metastasizing pancreatic carcinoma cell line, but not in the parental tumor, suggesting that these variants was sufficient to render parental tumor cells metastatic (David and Manley 2010).

These cancer isoforms are due, largely, to alteration of growth pathway, that are able to influence splicing through their control of RBP and/or splicing factor. For example C-Myc regulates up-regulation of PTB, hnRNPA1 and hnRNPA2; ERK controls Sam68 activity and AKT mediates phosphorylation of SR proteins (J. Zhang and Manley 2013).

III.4 Cleavage and polyadenylation mechanism and alternative polyadenylation

The 3' end of majority of eukaryotic mRNAs and some long non-coding RNAs is cleaved and polyadenylated. It is a post-transcriptional process that involve endonucleolytic cleavage of the transcript followed by the addition of the poly(A) tail. This process, in which they are involved *cis* and *trans* elements, occurs a relevant role in stability, nuclear export and translation regulation of mRNAs. The key cis-element is located 15–30 nt upstream of the cleavage site and it is a hexameric consensus motif called the poly(A) signal (PAS), the canonical form is AAUAAA, but it can assume different variants and are mostly. Moreover, U- or GU-rich downstream

sequence elements (DSEs) and less well-defined upstream sequence elements (USEs) are nearby of PAS and they enhance cleavage efficiency. The PAS hexamer is recognized by cleavage and polyadenylation specification factor (CPSF), which is recruited co-transcriptionally and it composed of six polypeptides, named CPSF4, CPSF2, CPSF3, FIP1L1, WDR33 and CPSF1, although only the latter is the subunit that recognizes the PAS. Cleavage stimulation factor (CSTF), which is composed of three subunits (CSTF1,CSTF2, CSTF3), binds the DSE, while the cleavage factor Im (CFIm) and CFIIm interact with the USE. The poly(A) polymerase (PAP), the scaffold protein simplekin and polyadenylated-binding nuclear protein 1 (PABPN1) are additional factors that were required for conclusion of process (Fig. 10) (Elkon, Ugalde, and Agami 2013)(Gruber and Zavolan 2019).

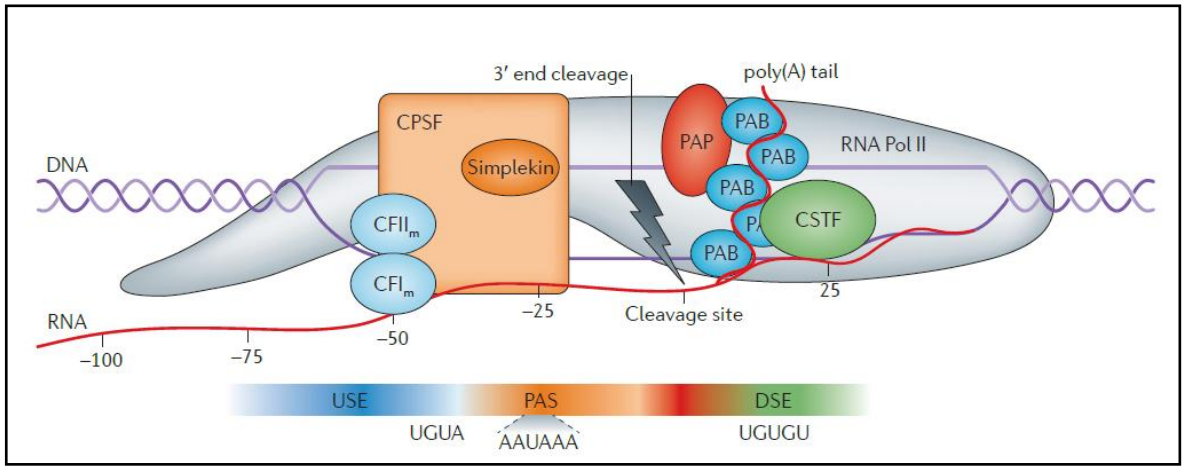

Figure 10. Core players involved in cleavage and polyadenylation mechanism (Elkon, Ugalde, and Agami 2013).

By transcriptome-wide sequencing emerges that most human genes have more than one poly (A) site, indicating the existence of alternative polyadenylation (APA). APA events can be classified into four general classes: tandem 3'UTR APA which are the most frequent APA forms and generates different isoforms changing only in the length of their 3'UTR; alternative terminal exon APA, in which the transcript ends in another exon; alternative intronic polyadenylation (IPA), in which results from the recognition of cleavage sites within introns (Fig. 11).

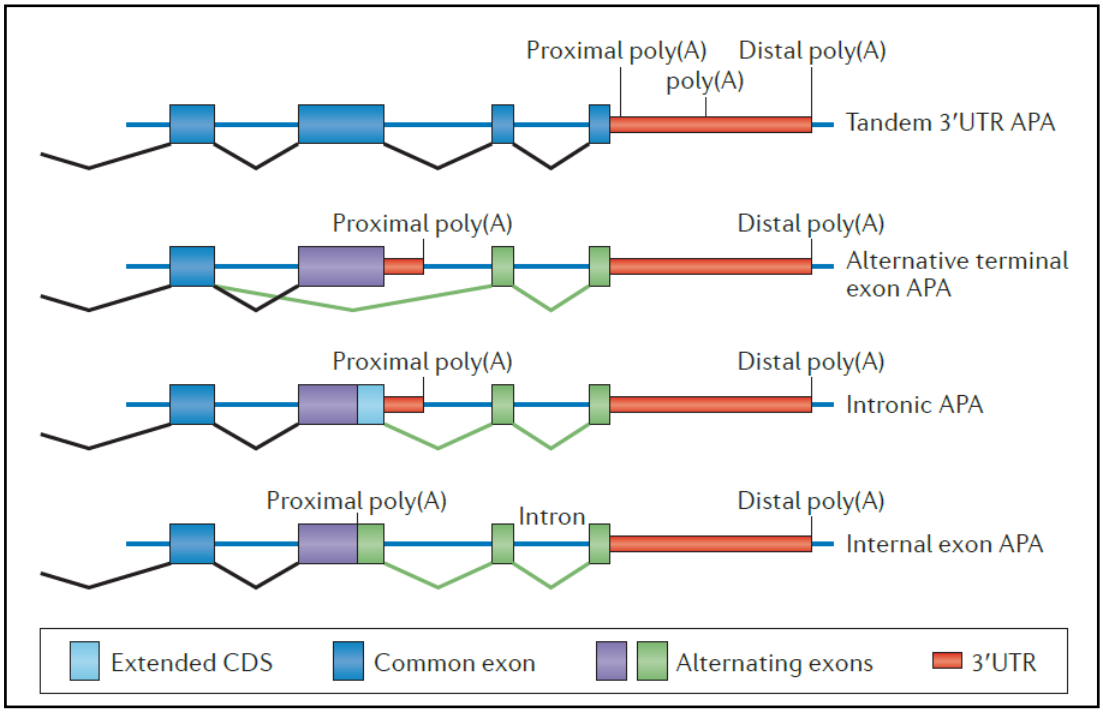

Figure 11. The four different APA types (Elkon, Ugalde, and Agami 2013)

3'UTR is a important regulative region of transcripts, it interacts with microRNAs(miRNAs) and RNA-binding proteins (RBPs). For example, in some cases oncogene activation in cancer cells is led by the generation of more stable isoforms with shorter 3'UTR, that compared to their counterparts with long 3'UTRs escape from repressive effect of miRNAs (Mayr and Bartel 2009).

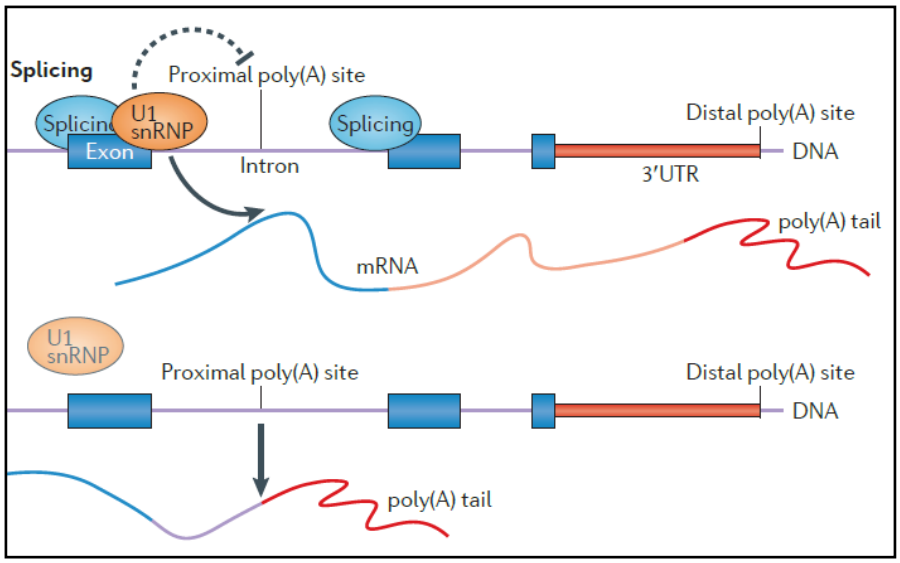

Figure 12. U1 in regulation of APA (Elkon, Ugalde, and Agami 2013)

Various multifunctional proteins that regulate splicing also participate in poly(A) site selection: PTBP1, ELAVL1, hnRNPC, PCBP1 and PABN1 (Gruber and Zavolan 2019). For example it was demonstrated that U1snRNP protects pre-mRNAs from premature cleavage (Fig.12) and its knock down promove induction of intronic poly(A) sites usage, independently of the role of U1 in splicing (Kaida et al. 2010). Physiologically, the level of U1 is not known to be regulated, thus suggest that its transient knowdown occurs in conditions in which overall transcription is upregulated. This decrease of U1 should cause a global 3'UTR shortening, similarly to the phenomenon observed in proliferation and cancer cells (Elkon, Ugalde, and Agami 2013)(Mayr and Bartel 2009).

III.5 Role of ZEB1 in PDAC and genotoxic stress response

III.5.1 Structure and function

ZEB1 is a protein encoded by the ZEB1 gene which is located on chromosome 10p11.2 in humans. It is a key factor of Epithelial–mesenchymal transition (EMT), a reversible cellular program that transiently places epithelial cells into mesenchymal cell states, involved in specific steps of embryogenesis, such as gastrulation and tissue morphogenesis during development. Moreover, it has a relevant role also in cancer progression, cancer stem cell maintenance, metastasis settlement and resistance to chemotherapy (Dongre and Weinberg 2019). ZEB1 is a transciptional factor and regulates the transcription by binding to E-promoter DNA sequences (5'-CANNTG-3') of its targets. In humans ZEB1 contains more two zinc-finger clusters at N- and C-terminal ends of the protein. The middle region consists of a homeodomain, a Smad interaction domain and a C-terminal binding protein (CtBP) domain (Fig. 13). CtBP cannot directly bind to DNA and participates in the regulation of ZEB1 function by interacting with other regulatory factors.

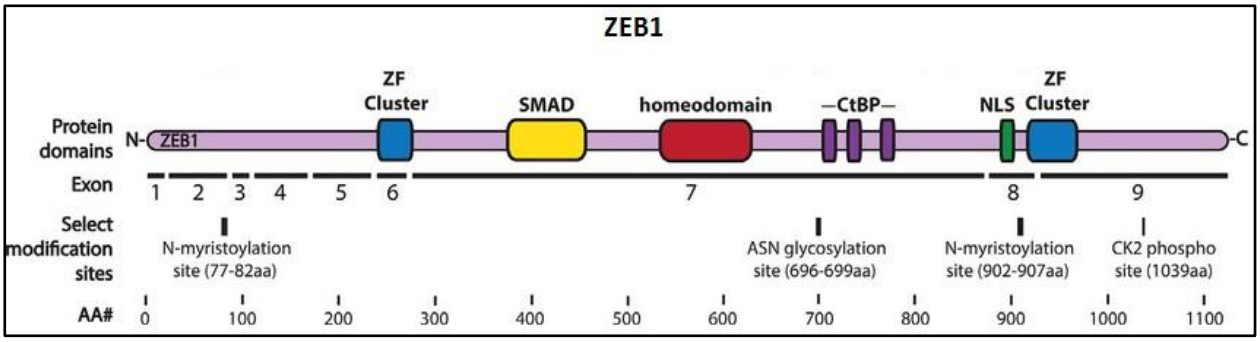

Figure 13. Schematic representation of ZEB1 structure and domain (Chung et al. 2014).

ZEB1 activates the expression of its target genes, for example Vimentin and N-cadherin by recruiting histone acetyltransferase (HATs) p300, Tip60 and PCAF; while when acting as repressor of the E-cadherin gene, ZEB1interacts with CtBP and facilitates epigenetic silencing its targetsby recruiting on its promoter histone deacetylases (HDACs), DNA methyltransferase (DNMT) and ubiquitin ligase (Y. Zhang et al. 2019).

Notably, ZEB1 also represses genes of miR-200 family members (miR-200a-b-c, miR-141 and miR-429), which in turn inhibit the synthesis of the ZEB proteins. Thus this feedback loop controls EMT/MET process by balancing the levels of expression of miR-200 family and ZEB1 (Brabletz and Brabletz 2010).

III.5.2 Role of ZEB1 in response to chemotherapy treatment

Several evidence has highlighted a correlation between mesenchymal features and chemoresistance and suggest a specific role for ZEB1.

The removed inhibition of ZEB1 expression by MiR-200c leads to resistance to trastuzumab and metastasis of HER2-positive breast cancer. Moreover, in breast cancer ZEB1 actives ataxia-telangiectasia mutated (ATM) kinase expression increasing DNA damage repair and thus promove the resistance to chemotherapy (Y. Zhang et al. 2019)(Caramel, Ligier, and Puisieux 2018).

In pancreatic cancer, ZEB1 expression could favor the selection of resistant cells population during stress condition, such as chemotherapy treatment. Indeed the depletion of ZEB1 promoted re-differentiation and re-sensitization to gemcitabine in PANC1 cell line (Z. Wang et al. 2009). Moreover, ZEB1 controls the expression of numerous oncogenic and tumor-

suppressive miRNAs, including miR-34a. ZEB1 down-regulates miR-34a expression to drive pro-actin cytoskeletal remodeling, favoring invasive and metastatic capabilities (Ahn et al. 2012).
These data support the concept that ZEB1 and EMT are relevant for transformation and progression tumor, promoting the acquisition of cellular features, such as chemoresistance and invasiveness, which are implicated in poor prognosis of patients.

III.5.3 *"Alternative polyadenylation of ZEB1 promotes its translation during genotoxic stress in pancreatic cancer cells"*

Since the acquisition of resistance to chemotherapy is a clinical problem for PDAC, knowing the mechanism that cause this phenomenon can be useful to finding new therapeutic targets. Recent evidence indicates that epithelial-to-mesenchymal transition (EMT) of PDAC cells is strictly associated to early metastasization and resistance to chemotherapy. Here, we report that ZEB1 is up-regulated after Gemcitabine treatment through post transcriptional mechanism. In particular by alternative polyadenylation of the ZEB1 transcript, leading to shortening of the 3' untranslated region (UTR) and deletion of binding sites for repressive microRNAs. Here I report the relative paper, in which I have collaborated.

III.5.4 Paper *"Alternative polyadenylation of ZEB1 promotes its translation during genotoxic stress in pancreatic cancer cells"* published on *Cell Death and Disease* (2017) 8, e3168.

Ilaria Passacantilli, **Valentina Panzeri**, Pamela Bielli, Donatella Farini, Emanuela Pilozzi, Gianfranco Delle Fave, Gabriele Capurso and Claudio Sette.

OPEN

Citation: Cell Death and Disease (2017) 8, e3168; doi:10.1038/cddis.2017.562
Official journal of the Cell Death Differentiation Association

www.nature.com/cddis

Alternative polyadenylation of ZEB1 promotes its translation during genotoxic stress in pancreatic cancer cells

Ilaria Passacantilli[1,2], Valentina Panzeri[1,2], Pamela Bielli[1,3], Donatella Farini[1], Emanuela Pilozzi[2], Gianfranco Delle Fave[2], Gabriele Capurso[2] and Claudio Sette*[,1,3]

Pancreatic ductal adenocarcinoma (PDAC) is characterized by extremely poor prognosis. The standard chemotherapeutic drug, gemcitabine, does not offer significant improvements for PDAC management due to the rapid acquisition of drug resistance by patients. Recent evidence indicates that epithelial-to-mesenchymal transition (EMT) of PDAC cells is strictly associated to early metastasization and resistance to chemotherapy. However, it is not exactly clear how EMT is related to drug resistance or how chemotherapy influences EMT. Herein, we found that ZEB1 is the only EMT-related transcription factor that clearly segregates mesenchymal and epithelial PDAC cell lines. Gemcitabine treatment caused upregulation of ZEB1 protein through post-transcriptional mechanisms in mesenchymal PDAC cells within a context of global inhibition of protein synthesis. The increase in ZEB1 protein correlates with alternative polyadenylation of the transcript, leading to shortening of the 3' untranslated region (UTR) and deletion of binding sites for repressive microRNAs. Polysome profiling indicated that shorter ZEB1 transcripts are specifically retained on the polysomes of PDAC cells during genotoxic stress, while most mRNAs, including longer ZEB1 transcripts, are depleted. Thus, our findings uncover a novel layer of ZEB1 regulation through 3'-end shortening of its transcript and selective association with polysomes under genotoxic stress, strongly suggesting that PDAC cells rely on upregulation of ZEB1 protein expression to withstand hostile environments.

Cell Death and Disease (2017) **8,** e3168; doi:10.1038/cddis.2017.562; published online 9 November 2017

Pancreatic ductal adenocarcinoma (PDAC) is among the deadliest human cancers, with rate of overall survival at 5 years from diagnosis being less than 5%.[1] Late diagnosis and the highly metastatic behavior of PDAC cells substantially contribute to such poor prognosis.[2] Moreover, despite improvement in surgical techniques and introduction of novel chemotherapeutic approaches, PDAC patients rapidly develop resistance to therapies and progress to advanced, incurable stages.

Epithelial-to-mesenchymal transition (EMT), namely the ability of an epithelial cell to acquire a fibroblast-like shape, is among the biological processes promoting metastatic dissemination of epithelial cancers, including PDAC.[3,4] EMT is a physiological process that underlies cell migration and organ colonization in the developing embryo. However, it can be re-activated upon neoplastic transformation of epithelial cells, permitting them to reach distal tissues and to give rise to metastasis.[5,6] In PDAC mouse models, EMT allows dissemination of cancer cells even before the primary tumor is fully visualized.[7] Furthermore, acquisition of the mesenchymal phenotype seems to be related to drug resistance of PDAC cells,[8-11,] in particular to gemcitabine, the standard first-line treatment for PDAC. However, the specific molecular mechanisms by which the mesenchymal phenotype contributes to chemoresistance are not fully understood.

EMT is driven by global gene expression re-programming operated by transcription factors (TFs), such as ZEB1, ZEB2, SNAIL, SLUG and TWIST.[12] All these TFs activate transcription of mesenchymal genes while repressing epithelial genes. However, emerging evidence strongly suggests that not all EMT programs are equal *in vivo*. Indeed, studies using PDAC mouse models clearly showed that EMT triggered by ZEB1 promotes cell plasticity and metastasis,[13]whereas SNAIL and TWIST had no effect on invasion or metastasis while they favored resistance to chemotherapy.[11] Furthermore, ZEB1 was shown to play a key role in early dissemination of PDAC cells.[7] Thus, regulation of ZEB1 expression is highly relevant for PDAC onset and progression.

Genotoxic stress elicited by most chemotherapeutic drugs often turns on pro-survival pathways that result in selection of resistant cells. Modulation of post-transcriptional pre-mRNA processing is a key step in the fine-tuned regulation of gene expression programs during both EMT and acquisition of drug resistance.[6,14] In the present work, we found that gemcitabine induces an increase in ZEB1 protein expression in mesenchymal PDAC cell lines, which occurred concomitantly with global inhibition of protein synthesis. Cell fractionation experiments showed that while most mRNAs are released from the polysomes following the translational block, ZEB1 mRNA remains associated with them. Mechanistically, gemcitabine

[1]Department of Biomedicine and Prevention, Section of Anatomy, University of Rome 'Tor Vergata', Rome, Italy; [2]Department of science medical/chirurgic and translational medicine, University of Rome 'Sapienza', Rome, Italy and [3]Laboratory of Neuroembryology, Fondazione Santa Lucia IRCCS, Rome, Italy
*Corresponding author: C Sette, Department Biomedicine and Prevention, Section of Anatomy, University of Rome 'Tor Vergata', Via Montpellier, 1, Rome 00133 Italy. Tel: +39 6 72596260; Fax: +39 6 72596268; E-mail: claudio.sette@uniroma2.it
Received 09.8.17; revised 15.9.17; accepted 19.9.17; Edited by GM Fimia

treatment promoted alternative polyadenylation of ZEB1 mRNA, leading to shortening of its 3' untranslated region (UTR). This shorter ZEB1 transcript variant was more efficiently associated with polysomes than longer ZEB1 transcripts in cells exposed to the drug. Our findings highlight a novel mechanism involved in ZEB1 regulation in response to genotoxic stress and suggest that its enhanced expression offers an opportunity to PDAC cells to survive to the insult while priming them for metastatic spread.

Results

Gemcitabine treatment enhances ZEB1 expression in mesenchymal PDAC cell lines. Mesenchymal phenotype has been associated with resistance to chemotherapy in PDAC.[8–11] Accordingly, colony formation assays indicated thatPt45P1 and MiaPaCa-2 PDAC cells, which express the mesenchymal marker Vimentin (Supplementary Figures S1A, B), were significantly more resistant to low dosage (0.01 μM) of gemcitabine than the HPDE immortalized epithelial ductal cells and HPAF-II PDAC cells (Supplementary Figure S1C), which both display an epithelial phenotype and express E-cadherin (Supplementary Figures S1A,B). At increasing doses (0.03–0.1 μM), Pt45P1 cells showed higher sensitivity than MiaPaCa-2 (Supplementary Figure S1C). Likewise, cleavage of full length PARP-1 also showed higher sensitivity to apoptosis of epithelial HPAF-II cells with respect toPt45P1 and MiaPaCa-2cells (Supplementary Figure S1D), confirming the correlation between drug resistance and the mesenchymal phenotype in PDAC cell lines.

To investigate which EMT-related TF was differentially expressed in PDAC cell lines, we performed conventional (cPCR) and quantitative real-time PCR (qPCR) analyses. Notably, only ZEB1 clearly segregated the mesenchymal Pt45P1 and MiaPaCa-2 from the epithelial HPAF-II cells, whereas SLUG and SNAIL were expressed at variable levels regardless of the phenotype and TWIST levels were not detectable (Figures 1a and b). Differential ZEB1 expression between epithelial and mesenchymal PDAC cells was also observed at the protein level (Figure 1c), confirming the correlation with the gemcitabine-resistant phenotype of these cells.

Poor prognosis in PDAC is mainly due to unresponsiveness of patients to chemotherapy with gemcitabine, either as single agent or in combination with other drugs.[15] Given the role of ZEB1 in PDAC cells drug resistance,[9,13] we asked whether genotoxic stress associated with chemotherapy affected its expression. Treatment with gemcitabine for 48 h elicited a significant upregulation of ZEB1 protein expression in both Pt45P1 and MiaPaCa-2 cells (Figure 1d). Notably, such increase was sustained over at least 72 h (Supplementary Figure S1E) and not accompanied by significant upregulation of ZEB1 mRNA (Figure 1e), nor by stabilization of the pre-existing ZEB1 protein, as tested by incubation of cells with the proteasome inhibitor MG132 (Figure 1f). These results suggest that gemcitabine induces upregulation of ZEB1 expression by post-transcriptional mechanism(s).

Gemcitabine induces a global inhibition of protein synthesis in PDAC cell lines. Acute chemotherapeutic treatments often activate responses that facilitate survival of cancer cells to genotoxic stress.[16–19] To investigate the post-transcriptional mechanism(s) underlying the increase in ZEB1 protein levels, we first monitored the impact of gemcitabine treatment on the mTORC1 pathway, a regulatory route of protein synthesis with strong relevance for human cancers.[20] A key target of the mTORC1 kinase is the inhibitory protein 4EBP1, which binds the translation initiation factor eIF4E and prevents its assembly with eIF4G and the RNA helicase eIF4A to form the translation initiation complex eIF4F.[20] Phosphorylation of 4EBP1 by mTORC1 causes its release from eIF4E and stimulates eIF4F assembly and cap-dependent translation. Treatment with gemcitabine caused progressive inhibition of 4EBP1 phosphorylation in Pt45P1 and MiaPaCa-2cells by 24–72 h, with increasing prevalence of the non-phosphorylated form (γ) of 4EBP1 (Figure 2a). To confirm the effect of genotoxic stress on the inhibition of cap-dependent translation, we performed methyl-cap pulldown assays to isolate the eIF4F complex.[21] Drug treatment impaired association of eIF4A and eIF4Gwith eIF4E on methyl-cap in both cell lines, whereas binding of hypo-phosphorylated 4EBP1 was increased (Figure 2b). In line with this effect, gemcitabine caused a global decrease of mRNA loaded on polysome fractions while it increased the peaks associated with monosomes (80S) and free ribonucleoproteinparticles (RNPs), which are not engaged in translation (Figure 2c). Thus, genotoxic stress triggered by gemcitabine inhibits cap-dependent translation and generally stalls protein synthesis in PDAC cells.

ZEB1mRNAis selectively maintained on polysomes during genotoxic stress. Since upregulation of ZEB1 in PDAC cells occurred in a context of global protein synthesis inhibition, we specifically analyzed the profile of ZEB1 mRNA distribution in polysome fractionation experiments.ZEB1 transcript, like those of the housekeeping genes HPRT and GAPDH, was almost equally distributed between polysome and RNP fractions in control cells, and this pattern was not substantially affected by 12 h treatment with gemcitabine (Figures 3a and b). However, while prolonged exposure to the drug (48 h) caused a drastic decrease in polysomal loading of the HPRT and GAPDH mRNAs, ZEB1 mRNA was actively retained on polysomes with respect to the free RNP fraction (Figures 3a and b). Notably, this regulation was specific for ZEB1, as transcripts of other EMT-related TFs (SLUG and SNAIL) behaved like HPRT and GAPDH mRNAs and in line with the global decrease of mRNA translation (Figures 3a and b). Quantitative analyses by qPCR confirmed that treatment with gemcitabine significantly increased the polysome/RNP ratio for ZEB1 mRNA (Figure 3c) while decreasing that of HPRT and GAPDH mRNAs.

Polysomal recruitment of mRNAs upon inhibition of cap-dependent translation can be mediated by internal ribosome entry segments (IRES)-mediated translation.[22] IRES are structured sequences located in the 5′UTR of mRNAs and promote ribosome recruitment. Search in the Ensemble database (http://www.ensembl.org/index.html) revealed annotation of two classes of 5′ UTR for ZEB1 transcripts encoded by alternative first exons. Exon 1-containing transcripts encode for short 5′ UTRs with unstructured nucleotide sequence (ENST00000320985.14, 100 bp; ENST00000560721.6,

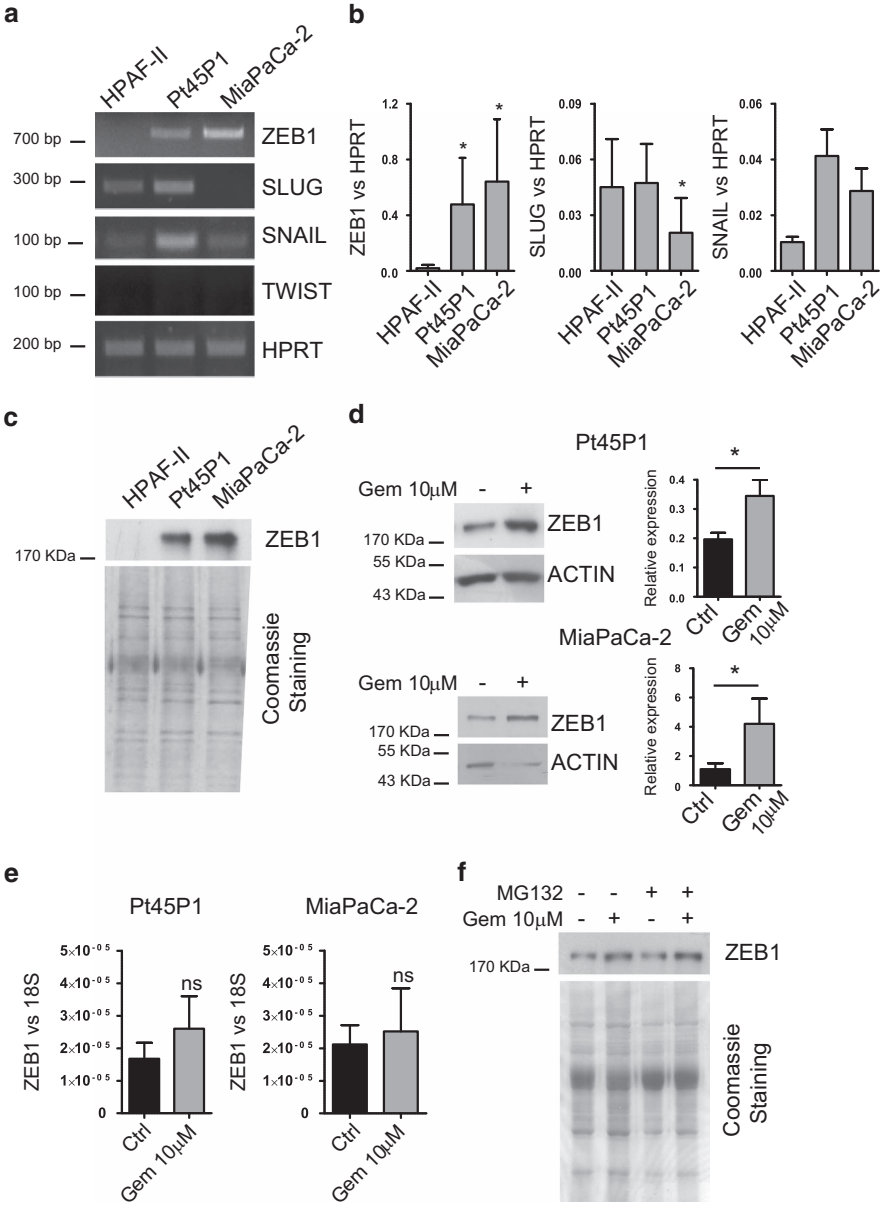

Figure 1 Gemcitabine induces upregulation of ZEB1 protein in mesenchymal PDAC cells. Conventional (**a**) and quantitative (**b**) RT-PCR analysis of ZEB1, SLUG, SNAIL and TWIST mRNA expression in the indicated PDAC cell lines. *HPRT* was used as housekeeping gene for normalization. (**c**) Western blot analysis of ZEB1 protein expression in the indicated PDAC cell lines. Coomassie blue staining was performed as sample loading control. (**d**) Western blot and (**e**) quantitative RT-PCR of ZEB1 expression in Pt45P1 and MiaPaCa-2 cells treated or not with gemcitabine (10 μM) for 48 h. (**f**) Western blot analysis of ZEB1 protein expression in MiaPaCa-2 cells treated or not with gemcitabine (10 μM) for 48 h. MG132 was added to cells in the last 8 h of treatment. Bar graphs in (**b**), (**d**) and (**e**) represent the mean ± S.D. of three experiments. * $P<0.05$; n.s. = not significant

22 bp; ENST00000542815.7, 71 bp; ENST00000361642.9, 63 bp), whereas exon 1C encodes a longer, structured 5′ UTR of 392 nucleotides (ENST00000446923.6) that resembles an IRES sequence (Supplementary Figure S2A). To test whether this sequence acted as IRES, we inserted it into the intercistronic region of the pRF construct, which contains the Renilla and Firefly luciferase genes as upstream and downstream cistrons, respectively (Supplementary Figure S2B).[23] Transfection of this construct into MiaPaCa-2 cells indicated that, unlike the Myc IRES element, the exon 1C-encoded sequence was unable to induce expression of the downstream cistron regardless of gemcitabine treatment (Supplementary Figure S2B), suggesting that it does not possess IRES activity. Accordingly, we found that ZEB1 transcripts containing this longer 5′ UTR were not selectively retained on polysomes upon treatment with gemcitabine (Supplementary Figure S2C). Thus, alternative 5′ UTR usage and/or IRES-dependent translation are unlikely responsible for the increased translation of ZEB1 upon gemcitabine-induced stress.

Alternative polyadenylation of ZEB1 supports its translation upon genotoxic stress. Translation regulation can be also modulated by changes in the 3′ UTR of target mRNAs, which result from alternative polyadenylation (APA)

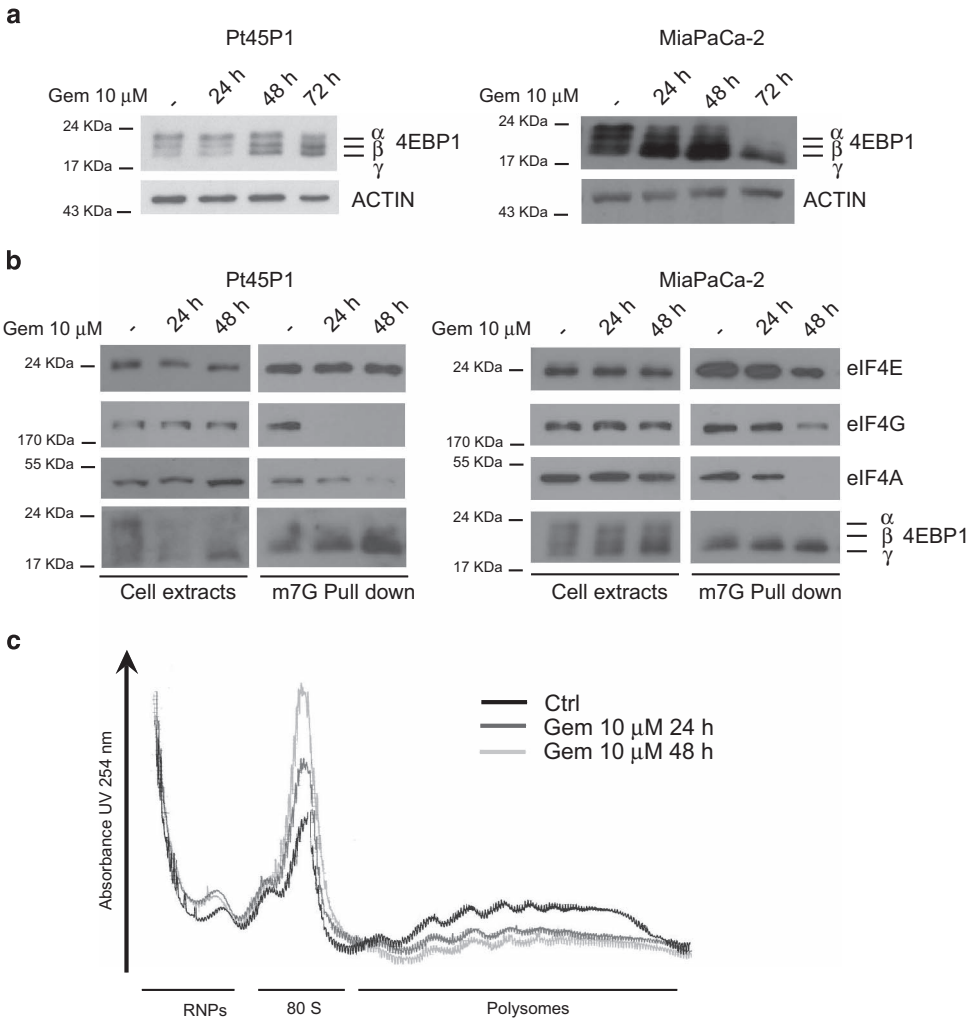

Figure 2 Gemcitabine causes global inhibition of cap-dependent translation in PDAC cells.(**a**) Western blot analysis of 4EBP1 in the indicated PDAC cell lines treated for increasing time with 10 μM gemcitabine. Hyper- (α,β), and hypophosphorylated (γ) 4EBP1 are indicated. (**b**) Western blot analyses of cell extracts (left panels) and methyl-7-cap pulldown assays (right panels) using the indicated PDAC cells treated or not with 10 μM gemcitabine for increasing time. Components of the eIF4F complex (eIF4E, eIF4G and eIF4A) and 4EBP1 are indicated. (**c**) Plot of the absorbance profile of fractions obtained on sucrose gradients to isolate polysomes from monosome (80S) and free RNPs in MiaPaCa-2 cells treated or not with 10 μM gemcitabine for the indicated time

regulation.[24] Three main alternative polyadenylation signals (PAS) are present in the ZEB1 last exon (indicated as p1–p3 from proximal to distal in Figure 4a). Notably, binding sites for microRNAs that repress ZEB1 expression by targeting its 3′ UTR (miR-200 family and miR-205)[9,25] are located between the p1 and p2 PAS (Figure 4a).By using reverse primers located upstream of the p1, p2 or p3 PAS, we observed that treatment of MiaPaCa-2 cells with gemcitabine caused shortening of the 3'UTR of ZEB1, with selective decrease of transcripts terminating at the p2 and p3 PAS (Figure 4b). To verify that shortening was due to APA regulation, we performed 3'-RACE experiments in MiaPaCa-2 cells treated or not with gemcitabine. Drug treatment caused reduced termination of the ZEB1 transcript at the p2 PAS, without affecting termination at the p1 PAS (Figure 4c). Sequencing of the PCR product verified the presence of a PAS at the p2 region and polyadenylation (Figure 4d), thus confirming that ZEB1 APA regulation is sensitive to stress.

Next, we asked whether APA resulted in differential polysomal loading of ZEB1 alternative transcripts. Polysome fractionation experiments in control and gemcitabine-treated samples revealed that the p1/p2 ratio and p1/p3 ratio were significantly increased in the polysome fraction and reduced in the RNP fraction obtained from MiaPaCa-2 cells treated with gemcitabine (Figure 4e). These experiments indicate that gemcitabine causes a general shortening of the 3'UTR of ZEB1, and that transcripts containing the shorter 3'UTR are more efficiently retained on polysomes than longer transcripts during genotoxic stress in PDAC cells.

Discussion

Cancer cells display remarkable adaptability to adverse environments, which likely contributes to acquisition of resistance to therapeutic treatments.[18] This is particularly true for PDAC cells and manifests in the failure of efficacious therapies for patients after years of efforts and research in the

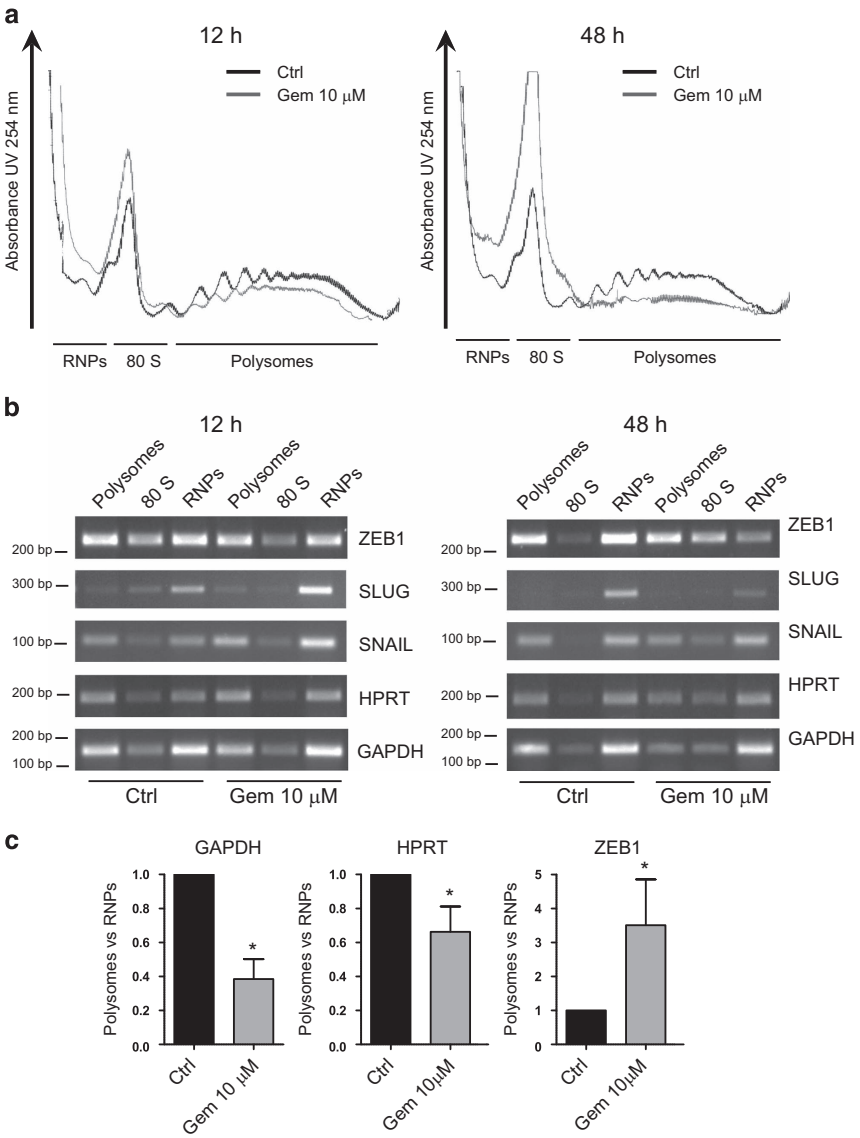

Figure 3 ZEB1mRNAis selectively maintained on polysomes during genotoxic stress. (**a**) Absorbance profiles of fractions obtained on sucrose gradients to isolate polysomes from monosome (80S) and free RNPs in MiaPaCa-2 cells treated or not with 10 μM gemcitabine for 12 h (left panel) or 48 h (right panel). (**b**) Conventional RT-PCR analysis of the distribution of the indicated mRNAs in polysome, 80S and RNP fractions from cells shown in (**a**).(**c**) Quantitative RT-PCR of the ratio of distribution between polysome and RNP fractions of the indicated mRNA. Data are normalized for the ratio in control cells and represent the mean $\pm$ S.D. of three experiments. * $P < 0.05$

field.[2,15] One feature that is related to the refractoriness of PDAC cells to treatments is their plasticity. Indeed, acquisition of a mesenchymal phenotype by epithelial PDAC cells is thought to be responsible for both metastatic behavior and resistance to chemotherapy.[7-11,13,] Although EMT can be set in motion by several TFs,[12] ZEB1 plays a unique and prominent role in PDAC metastasization and resistance to treatments.[13] Nevertheless, how and when ZEB1 expression is altered in response to chemotherapy is still largely unknown. Herein, we found that upregulation of ZEB1 expression is an early event in such response, which occurs within 24–48 h from exposure of PDAC cells to gemcitabine. Importantly, ZEB1 upregulation is driven by a post-transcriptional mechanism that occurs in the absence of changes in ZEB1 transcript levels and in a general context of translational inhibition. In this scenario, while most mRNAs are depleted from the polysomes, ZEB1 transcripts remain associated with the translational machinery and likely insure continuous translation of this key TF under gemcitabine-elicited genotoxic stress. Thus, our findings suggest that the peculiar post-transcriptional regulation of ZEB1 expression represents a feedback mechanism set in motion by mesenchymal PDAC cells to withstand adverse conditions caused by chemotherapy.

Protein synthesis is an energy-consuming process and cells tune it down under various types of stress, including genotoxic stress elicited by most chemotherapeutic drugs.[22]Nevertheless, some proteins are instrumental to survive under stress conditions and need to be translated. In most cases, regulation of translation under stress is conferred by the 5' and 3'UTR of target transcripts. In our study, we provide evidence that changes in the 3'UTR of ZEB1 contribute to its

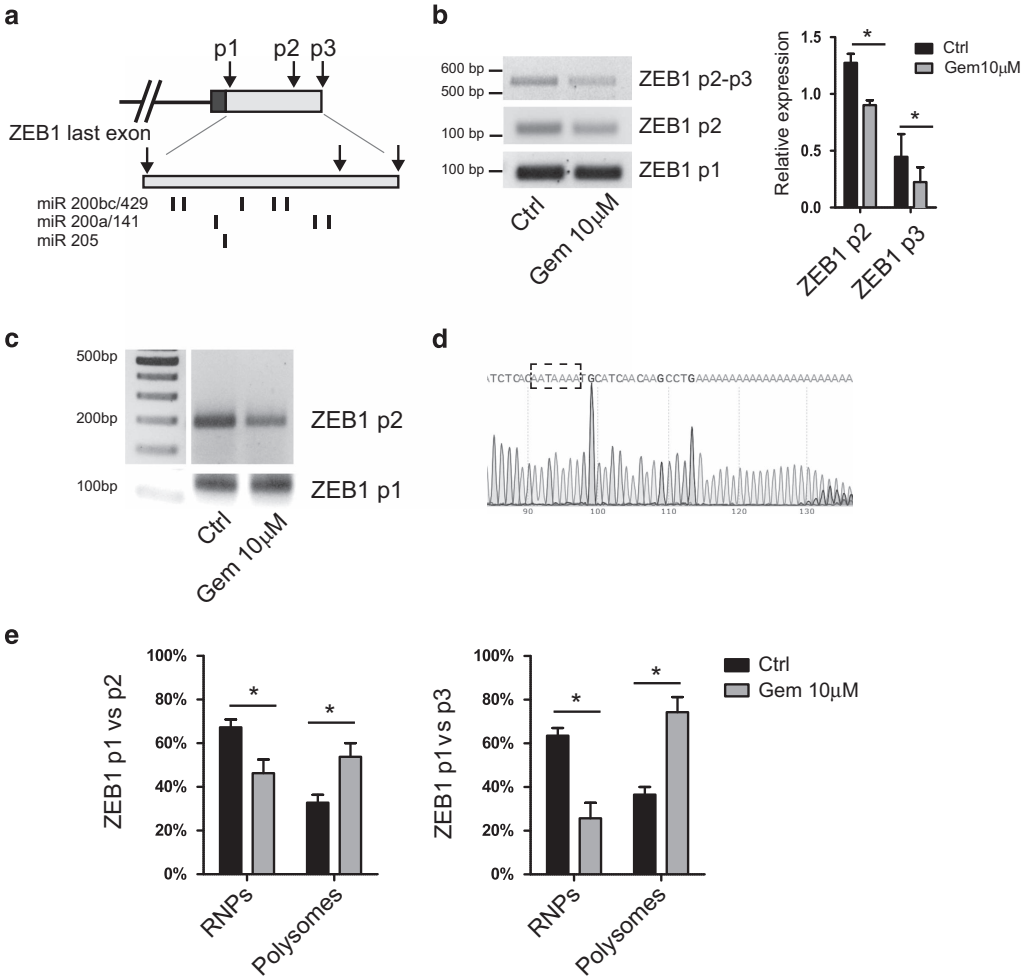

Figure 4 ZEB1 mRNA 3′-end shortening supports its translation upon genotoxic stress. (**a**) Schematic representation of the 3′ UTR region of ZEB1. Arrows indicate position of the three PASs present in the last exon of ZEB1. Inset shows magnification of the 3′ UTR region with the position of the binding sites for microRNAs known to exert repression of ZEB1 expression in MiaPaCa-2 cells located between p1 and p2 (arrows). (**b**) RT-PCR analyses of the expression of the last exon-encoded portion of the ZEB1 mRNA in cells treated or not with 10 μM gemcitabine for 48 h. Primers p2–p3 were used to amplify transcripts terminating at p3, primers p2 to amplify transcripts terminating at p2 or p3, primers p1 for all transcripts. Bar graph shows quantitative densitometric analyses (mean ± S.D. of three experiments; *$P<0.05$). (**c**) 3′-end RACE analyses of cells described in (**b**) using forward primers located upstream of p2 or p1, as indicated. (**d**) Sequence analysis of the band amplified by 3′-end RACE using the p2 primer confirming the PAS and polyadenylation of the transcript. (**e**) Quantitative RT-PCR of the ratio of distribution between RNP and polysome fractions of mRNAs. Data represent the ratio between p1 and p2 or p3 amplified signals to highlight shortening of the transcript and its relative distribution between polysomes and RNPs (mean ± S.D. of three experiments; * $P<0.05$)

sustained expression upon genotoxic stress. It is well established that many microRNAs elicit translational repression by binding to complementary sequences in the 3'UTR of target transcripts. Recent evidence suggests that most human 3'UTR sequences contain more than one PAS and that alternative PAS selection leads to expression of multiple transcript variants through APA.[24] In general, progressive shortening of the 3'UTR through selection of proximal PASs should relieve repression by microRNAs and promote translation. Accordingly, it has been observed that global 3'UTR shortening correlates with high proliferative rates whereas lengthening occurs during cell differentiation.[24]The 3'UTR of ZEB1 is particularly long (~2500 nucleotides) and contains putative binding sites for many microRNAs, including members of the miR-200 family that repress its expression in cancer epithelial cells.[25] Genotoxic stress caused shortening of the 3'UTR, with selective depletion of transcripts terminating at the distal PASs (p2 and p3) in cells treated with gemcitabine. Notably, most of the microRNA binding sites, including all the sites for the repressive miR-200 members, map between p1 and p2. APA leading to shortening of the 3'UTR should relieve translational repression of ZEB1 by these microRNAs. In line with this hypothesis, treatment with gemcitabine differentially affected the association of ZEB1 transcript variants with polysomes, with proportional increase in those terminating at p1 and corresponding depletion of transcripts terminating at p2 and p3. Thus, progressive shortening of the ZEB1 transcript may promote its translation by removing inhibition by microRNAs and favoring its recruitment onto polysomes. Since ZEB1 and miR-200 members are under mutual control in a negative feedback loop,[9]we suggest that this mechanism may rapidly shift the balance in favor of ZEB1 and mesenchymal features in PDAC cells exposed to gemcitabine.

APA is regulated by changes in the activity and/or expression of key components of the cleavage and polyadenylation complex, which often cooperate with accessory RNA binding proteins (RBPs) that bind elements located near the regulated PAS.[24] Some of these RBPs, like Sam68 and hnRNPH, are often upregulated in human cancers and can suppress or enhance recognition of cryptic PASs depending on the context.[26,27]Notably, localization and function of Sam68,[28] as well as many other RBPs,[18,29] is regulated upon genotoxic stress. Thus, it is possible that gemcitabine-induced stress promotes the recruitment of specific RBPs to the ZEB1 transcript, thereby affecting the choice of the proximal PAS and enhancing translational efficiency. Alternatively, APA is also modulated by the rate of transcription.[24] Changes in the phosphorylation status of the RNA polymerase II (RNAPII) affect its elongation rate within the transcription unit and its pausing at PAS. This modulation of RNAPII dynamics can alter the time window for PAS recognition and usage.[24] More recently, it has also been shown that reduced expression of RNAPII upon several stresses, including DNA damage, switches APA regulation from the preferred PAS to alternative ones in selected transcripts.[30] In this regard, gemcitabine is known to reduce the transcriptional activity of PDAC cells[16] and might contribute to the switch in ZEB1 APA by concomitantly regulating RNAPII expression or function and depleting endogenous nucleotides due to interference with their biosynthesis. These observations suggest that further mechanistic studies will be required to dissect the exact mechanism(s) involved in ZEB1 APA regulation during genotoxic stress. Furthermore, since ZEB1-driven EMT is particularly efficient to confer the highly aggressive and resistant phenotype typifying PDAC cells,[13] our findings also suggest that development of tools to alter APA in ZEB1 may help sensitizing PDAC cells to genotoxic stress.

Materials and Methods

Cell culture, treatments and tranfections. HPDE, HPAF-II and Pt45P1 were cultured in RPMI 1640 medium (Lonza, Switzerland) supplemented with 10% fetal bovine serum (Gibco Thermo Fisher, Waltham, MA, USA), MiaPaCa-2 cells were cultured in DMEM medium (Lonza) supplemented with 10% fetal bovine serum (Gibco). Cells were grown in a 37 °C humidified atmosphere of 5% CO_2. Gemcitabine (Eli Lilly & Company, Indianapolis, IN, USA) was dissolved in water and stored at − 20 °C.

RT-PCR and qPCR analysis. Total RNA was extracted from cells using Trizol reagent (Invitrogen Thermo Fisher, Waltham, MA, USA) according to the manufacturer's instructions. After digestion with RNase free DNase (Ambion Thermo Fisher, Waltham, MA, USA), RNA was resuspended in RNase free water (Sigma-Aldrich, St. Louis, MO, USA); 1 μg of total RNA was retrotranscribed using M-MLV reverse transcriptase (Promega, Madison, WI, USA). Five percent of the reaction was used as template for RT-PCR analysis (GoTaq, Promega) or qPCR analysis (SYBR Green method, Roche, Germany). Primers used are listed in Supplementary Table S1.

Protein extraction and western blot analysis. Cells were resuspended in lysis buffer (100 mM NaCl, 15 mM $MgCl_2$, 2 mM EDTA, 20 mM Hepes, 10% Glycerol, 1 mM dithiothreitol, 2 mM Na-ortovanadate, Protease-Inhibitor Cocktail (Sigma-Aldrich) and 1% Triton X-100). After10 min of incubation in ice, extracts were centrifuged for 10 min at 12 000 rpm at 4 °C, supernatants were resuspended in SDS-page sample buffer and boiled for 5 min. Western blot analysis was performed as previously described.[31] The following primary antibodies (overnight at4 °C) were used: rabbit anti-Actin (1 : 1000, Sigma-Aldrich), mouse anti-GAPDH (1 : 1000, Santa Cruz Biotechnology, Santa Cruz, CA, USA), rabbit anti-E-cadherin (1 : 1000, Santa Cruz Biotechnology), mouse anti-Vimentin (1 : 1000, Santa Cruz Biotechnology), rabbit anti-ZEB1 (1 : 1000, Sigma-Aldrich), rabbit anti-eiF4E (1 : 1000, Cell Signalling Technology, Danvers, MA, USA), rabbit 4EBP1 (1 : 1000, Cell Signalling Technology), rabbit anti PARP-1 (1 : 1000, Cell Signalling Technology), rabbit anti eiF4A (1 : 1000, Abcam, UK), rabbit anti-eIF4G (1 : 1000, Cell Signalling Technology). Secondary anti-mouse or anti-rabbit IgGs conjugated to horseradish peroxidase (Amersham, UK) were incubated for 1 h at RT (1 : 10 000). Immunostained bands were detected by chemiluminescence method (Santa Cruz Biotechnology).

Colony formation assay. Single-cell suspensions were plated in 35 mm plates (500 cells/plate for Pt45P1 andMiaPaCa-2; 700 cells/plate for HPDE and HPAF-II). After 1 day, cells were treated for 24 h with gemcitabine at the dose indicated. At the end of the incubation, the medium was replaced every 48 h. After 10 days, cells were fixed in methanol for 10 min, stained overnight with 5% Giemsa (Sigma-Aldrich), washed twice in PBS and dried. Pictures were taken using a digital camera to count and measure the colonies. Results represent the mean of at least three experiments $\pm$ s.d.

Polysomes-RNPs fractionation by sucrose gradients. Polysomes fractionation was performed as indicated previously.[21,32] Briefly, MiaPaCa-2 cells were homogenized in lysis buffer (100 mM NaCl, 10 mM $MgCl_2$, 30 mM Tris-HCl [pH 7.5], 1 mM DTT, 30 U/ml RNasin) supplemented with 1% Triton X-100. After 5 min of incubation on ice, the lysates were centrifuged for 10 min at 12 000 × *g* at 4 °C. The supernatants (1.5 mg of protein extracts) were loaded on a 15–50% (wt/vol) sucrose gradients and sedimented by centrifugation for 110 min at 37 000 r.p.m. in a Beckman SW41 rotor (Fullerton, CA, USA). Each gradient was collected in 10 fractions, RNA was extracted by phenol/chloroform method. Fractions 1–5 (Polysomes) and 8–10 (RNPs) were pulled and analyzed by RT-PCR and qPCR methods.

3′ RACE PCR. Total RNA (1 μg) was used for retrotranscription with 0.5 μg of oligo oligo-dT tail followed by an anchor sequence.[26] PolyA enriched/anchor tagged cDNA was subsequently used in RT-PCR experiments using gene-specific forward primers in presence of anchor reverse primer.

Conflict of Interest

The authors declare no conflict of interest.

Acknowledgements. We wish to thank Dr Chiara Naro for helpful discussion and advice. This work was supported by grants from the Associazione Italiana Ricerca sul Cancro (AIRC, IG 18790 to CS and IG 17177 to GC).

Publisher's Note

1. Torre LA, Bray F, Siegel RL, Ferlay J, Lortet-Tieulent J, Jemal A. Global cancer statistics, 2012. *CA Cancer J Clin* 2015; **65**: 87–108.
2. Giovannetti E, van derBorden CL, Frampton AE, Ali A, Firuzi O, Peters GJ. Never let it go: stopping key mechanisms underlying metastasis to fight pancreatic cancer. *Semin Cancer Biol* 2017; **44**: 43–59.
3. Lambert AW, Pattabiraman DR, Weinberg RA. Emerging biological principles of metastasis. *Cell* 2017; **168**: 670–691.
4. Zhou P, Li B, Liu F, Zhang M, Wang Q, Liu Y *et al*. The epithelial to mesenchymal transition (EMT) and cancer stem cells: implication for treatment resistance in pancreatic cancer. *Mol Cancer* 2017; **16**: 52.
5. De Craene B, Berx G. Regulatory networks defining EMT during cancer initiation and progression. *Nat Rev Cancer* 2013; **13**: 97–110.
6. Pradella D, Naro C, Sette C, Ghigna C. EMT and stemness: flexible processes tuned by alternative splicing in development and cancer progression. *Mol Cancer* 2017; **16**: 8.
7. Rhim AD, Mirek ET, Aiello NM, Maitra A, Bailey JM. McAllister *et al*. EMT and dissemination precede pancreatic tumor formation. *Cell* 2012; **148**: 349–361.
8. Arumugam T, Ramachandran V, Fournier KF, Wang H, Marquis L, Abbruzzese JL *et al*. Epithelial to mesenchymal transition contributes to drug resistance in pancreatic cancer. *Cancer Res* 2009; **69**: 5820–5828.

9. Wellner U, Schubert J, Burk UC, Schmalhofer O, Zhu F, Sonntag A *et al.* The EMT-activator ZEB1 promotes tumorigenicity by repressing stemness-inhibiting microRNAs. *Nat Cell Biol* 2009; **11**: 1487–1495.
10. Wang Z, Li Y, Kong D, Banerjee S, Ahmad A, Azmi AS *et al.* Acquisition of epithelial-mesenchymal transition phenotype of gemcitabine-resistant pancreatic cancer cells is linked with activation of the notch signaling pathway. *Cancer Res* 2009; **69**: 2400–2407.
11. Zheng X, Carstens JL, Kim J, Scheible M, Kaye J, Sugimoto H *et al.* Epithelial-to-mesenchymal transition is dispensable for metastasis but induces chemoresistance in pancreatic cancer. *Nature* 2015; **527**: 525–530.
12. Puisieux A, Brabletz T, Caramel J. Oncogenic roles of EMT-inducing transcription factors. *Nat Cell Biol* 2014; **16**: 488–494.
13. Krebs AM, Mitschke J, Lasierra Losada M, Schmalhofer O, Boerries M, Busch H *et al.* The EMT-activator Zeb1 is a key factor for cell plasticity and promotes metastasis in pancreatic cancer. *Nat Cell Biol* 2017; **19**: 518–529.
14. Paronetto MP, Passacantilli I, Sette C. Alternative splicing and cell survival: from tissue homeostasis to disease. *Cell Death Differ* 2016; **23**: 1919–1929.
15. Vaccaro V, Sperduti I, Vari S, Bria E, Melisi D, Garufi C, Nuzzo C *et al.* Metastatic pancreatic cancer: is there a light at the end of the tunnel? *World J Gastroenterol* 2015; **21**: 4788–4801.
16. Adesso L, Calabretta S, Barbagallo F, Capurso G, Pilozzi E, Geremia R *et al.* Gemcitabine triggers a pro-survival response in pancreatic cancer cells through activation of the MNK2/eIF4E pathway. *Oncogene* 2013; **32**: 2848–2857.
17. Calabretta S, Bielli P, Passacantilli I, Pilozzi E, Fendrich V, Capurso G *et al.* Modulation of PKM alternative splicing by PTBP1 promotes gemcitabine resistance in pancreatic cancer cells. *Oncogene* 2016; **35**: 2031–2039.
18. Pagliarini V, Naro C, Sette C. Splicing regulation: a molecular device to enhance cancer cell adaptation. *Biomed Res Int* 2015; **2015**: 543067.
19. Palam LR, Gore J, Craven KE, Wilson JL, Korc M. Integrated stress response is critical for gemcitabine resistance in pancreatic ductal adenocarcinoma. *Cell Death Dis* 2015; **6**: e1913.
20. Laplante M, Sabatini DM. mTORsignaling in growth control and disease. *Cell* 2012; **149**: 274–293.
21. Bianchini A, Loiarro M, Bielli P, Busà R, Paronetto MP, Loreni F *et al.* Phosphorylation of eIF4E by MNKs supports protein synthesis, cell cycle progression and proliferation in prostate cancer cells. *Carcinogenesis* 2008; **29**: 2279–2288.
22. Spriggs KA, Bushell M, Willis AE. Translational regulation of gene expression during conditions of cell stress. *Mol Cell* 2010; **40**: 228–237.
23. Coldwell MJ, Mitchell SA, Stoneley M, MacFarlane M, Willis AE. Initiation of Apaf-1 translation by internal ribosome entry. *Oncogene* 2000; **19**: 899–905.
24. Tian B, Manley JL. Alternative polyadenylation of mRNA precursors. *Nat Rev Mol Cell Biol* 2017; **18**: 18–30.
25. Gregory PA, Bert AG, Paterson EL, Barry SC, Tsykin A, Farshid G *et al.* The miR-200 family and miR-205 regulate epithelial to mesenchymal transition by targeting ZEB1 and SIP1. *Nat Cell Biol* 2008; **10**: 593–601.
26. La Rosa P, Bielli P, Compagnucci C, Cesari E, Volpe E, Farioli Vecchioli S *et al.* Sam68 promotes self-renewal and glycolytic metabolism in mouse neural progenitor cells by modulating Aldh1a3 pre-mRNA 3'-end processing. *Elife* 2016; **5**: e20750.
27. Nazim M, Masuda A, Rahman MA, Nasrin F, Takeda JI, Ohe K *et al.* Competitive regulation of alternative splicing and alternative polyadenylation by hnRNP H and CstF64 determines acetylcholinesterase isoforms. *Nucleic Acids Res* 2017; **45**: 1455–1468.
28. Busà R, Geremia R, Sette C. Genotoxic stress causes the accumulation of the splicing regulator Sam68 in nuclear foci of transcriptionally active chromatin. *Nucleic Acids Res* 2010; **38**: 3005–3018.
29. Shkreta L, Chabot B. The RNA splicing response to DNA damage. *Biomolecules* 2015; **5**: 2935–2977.
30. Yu L, Rege M, Peterson CL, Volkert MR. RNA polymerase II depletion promotes transcription of alternative mRNA species. *BMC Mol Biol* 2016; **17**: 20.
31. Di Florio A, Capurso G, Milione M, Panzuto F, Geremia R, Delle Fave G *et al.* Src family kinase activity regulates adhesion, spreading and migration of pancreatic endocrine tumour cells. *Endocr Relat Cancer* 2007; **14**: 111–124.
32. Paronetto MP, Zalfa F, Botti F, Geremia R, Bagni C, Sette C. The nuclear RNA-binding protein Sam68 translocates to the cytoplasm and associates with the polysomes in mouse spermatocytes. *Mol Biol Cell* 2006; **17**: 14–24.

Supplementary Information accompanies this paper on *Cell Death and Disease* website (http://www.nature.com/cddis)

Chapter IV. RNA Binding Proteins: structure and functions

IV.1 Role of RNA Binding Proteins: structure and functions

RNA-binding proteins (RBPs) represent a large family of proteins, able to to bind various types of RNAs through an RNA-binding domain (RBD). Some of the classical RBD by which RBP bind their target RNAs are:

- RNA recognition motif (RRM)

  Each RRM is made up of about 90 amino acids and consists of two conserved sub-motifs (RNP1 and RNP2). Structurally, it is composed of four anti-parallel β sheets stacked against two α-helices(βαββαβ); each RRM domain can recognize between 4 and 8 nucleotides by using ß-sheet surface extensions or by using exposed loops connecting ß-sheet to a ß-sheet or α-helix. To intensify specificity and affinity for an mRNA, RBPs generally contain more than one RRM and bind RNA cooperatively.

- hnRNP-K-Homology domain (KH domain)

  It is approximately 70 amino acids long and it is formed by three α-helices and three anti-parallel ß-sheet. Each KH domain can recognize 4 nucleotides through hydrogen bonds, electrostatic interaction and shape complementarity. Structural analyses indicate that KH domains are versatile in recognizing a large panel of sequences; however, its affinity and specificity of interaction is low. To bypass this problem the strategies are extend the surface of interaction and the repetition of multiple KH domains, so several copies of KH domains can act in synergy and efficiently.

- Zinc-finger domain

  Each zinc finger consists of about 25–30 amino acids and forms a ββα topology that is held together by the central Zn^{2+}ion.

- Double-stranded RNA binding domain(dsRBD)

  dsRBD consists of70-90 amino acids and it has αβββα protein folder. Most dsRBD recognize the dsRNA rather than the RNA sequence and it controls many RNA related functions such as RNA interference, localization, editing and translocation.

- Piwi/Argonaute/Zwille (PAZ) and Piwi domain

  The PAZ domain structure contain two sub-domains with a notable cleft between them.

PAZ domains are commonly found in proteins involved in miRNA biogenesis, such as Dicer and Ago. The piwi domain is only present in argonaute and its principal function is to hydrolize single strand RNA guided by double strand RNA.

- DEAD-box domain

  DEAD box proteins form the largest RNA helicase family and are characterized by the presence of an Asp-Glu-Ala-Asp (DEAD) motif. DEAD box helicases play a central role in cellular RNA metabolism and in assembly of larger multicomponent, such as the spliceosome or the translation initiation machinery.

Although RBPs bind to various classes of RNAs such as ribosomal RNAs, mRNAs, snRNA, snoRNA, tRNAs and non-coding RNAs, about half of the RBPs conducts their function by binding to mRNAs and regulating their fate (Fig. 14). RBPs coordinately bind to each mRNA and form ribonucleoprotein (RNP) complexes, which are dynamic and specifically modulated during the different steps of post-transcriptional RNA processing, such as splicing, nuclear export, stability control and translation.

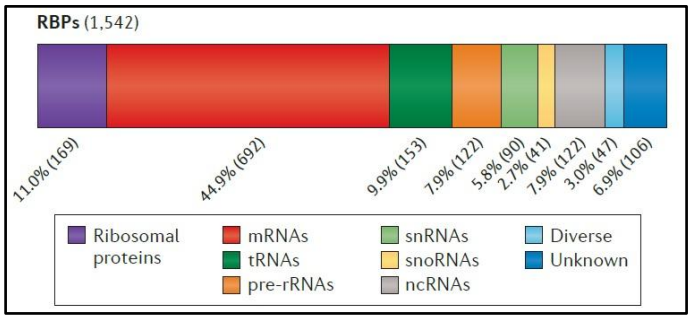

Figure 14. Target RNA classification of RBPs (Gerstberger, Hafner, and Tuschl 2014).

Dynamic RNP complexes can act to mature, process, regulate or transport RNAs. The RBPs can remodel of RNA structures to promove the interaction of other RBPs and enzymatic RNA-processing complexes to RNA; prevent aggregation, misfolding and incomplete processing; facilitate the movement of RNA targets in various cellular compartments (Hentze et al. 2018).

IV.2. The role of RBPs in cancer and novel therapeutic strategies targeting their activity.

Alterations in the RNA metabolism pathway can lead to genome-wide changes in the cellular transcriptome and proteome that subsequently affect cell growth, proliferation, invasion and death. An important contribution to this deregulation is given by the activity and the aberrant

expression of the RBPs. Somatic mutations in gene encoding splicing factors were identified in the last decade in myelodysplastic syndrome (Yoshida et al. 2011) and later found also in solid tumors like mucosal melanoma, bladder cancer and pancreatic cancer. A study that analyzes 404 splicing factors genes from 33 cancer typers in TCGA database, identified 119 SF with significant mutations and by RNA sequencing analysis they reveals that altered splicing events are correlated with selected splicing factor mutations (Seiler et al. 2018). The splicing factors most frequently mutated are SF3B1, U2AF1, SRSF2 and ZRSR2. They can confer cellular advantage at cancer cells promoting oncogenic isoform, transcription alterations and non sense mediated decay (NMD) (Obeng, Stewart, and Abdel-Wahab 2019). Furthermore, altered expression of RBPs contribute to development and progression of human cancer promoting oncogenic isoforms. For example, SR splicing factor 1 (SRSF1) is upregulatedin many types of tumors promotes inclusion of exon 13b of the kinase Mnk2 to generate the MNK2B isoform, which induces eIF4E phosphorylation independently of MAPK signalling and promotes cap-dependent translation (Karni et al. 2007). Importantly, exposure of PDAC cells to gemcitabine causes an increase in SRSF1 expression and in MNK2B splicing, thus supporting cell survival to the drug (Adesso et al. 2013). In the context of breast cancer, SRSF1 over-expression also promotes alternative splicing of BIM and BIN1 to facilitate the expression of isoforms that lack pro-apoptotic functions(Anczuków et al. 2012). SRSF3 is over-expressed in many cancers and its downregulation promots the expression of the p53β isoform that favours p53-mediated senescence (Dvinge et al. 2016). The oncogene c-MYC mediates the up-regulation of several hnRNPs (hnRNPA1, hnRNP A2 and PTBP1). Over-expression of PTBP1 in cancer cells contributes to aerobic glycolysis by promoting the expression of a specific isoform of pyruvate kinase (PKM2) (David et al., Nature 2010) and contributing to acquisition of chemotherapy resistance in PDAC cells (Calabretta et al. 2016). PTBP1 is also up-regulated in bladder cancer and correlates with poor prognosis in patients. Mechanistically, it was shown that expression of PTBP1 promotes cell cycle progression and expression of several pro-oncogenic variants involved in many biological processes, like cell survival (FAS), proliferation (NUMB, PKM), cytoskeleton organization (ACTN1, MACF1, TPM1, and CTNND1) and interaction with the extracellular matrix (CD44) (Bielli et al. 2018). Another oncogenic splicing factor induced by MYC at the transcriptional level is the STAR protein Sam68. In cancer cells, Sam68 modulates several steps of mRNA metabolism, such as alternative splicing, nuclear export and mRNA translation (Bielli et al., 2011a). In particular Sam68 promotes: the inclusion of variable exons in

the CD44 pre-mRNA, which correlates with invasive phenotypes; the short isoform of CYCLIN D1 (CYCLIN D1b), which promotes cell proliferation; the pro-apoptoticBCL-$X_S$isoform (Bielli et al., 2011a). Accordingly, knockdown of the endogenous Sam68 in different types of human cancer cell lines reduced proliferation and tumorigenicity (Bielli et al. 2011a).

Thus, these examples bring out a central role of the RBPs ininitiation and progression of cancer. Targeting RBPs for cancer therapy has gained more relevant in the last years using different approaches: small-molecule inhibitors, anti-sense oligonucleotides (ASO), siRNA, peptides and aptamers (Fig.15).

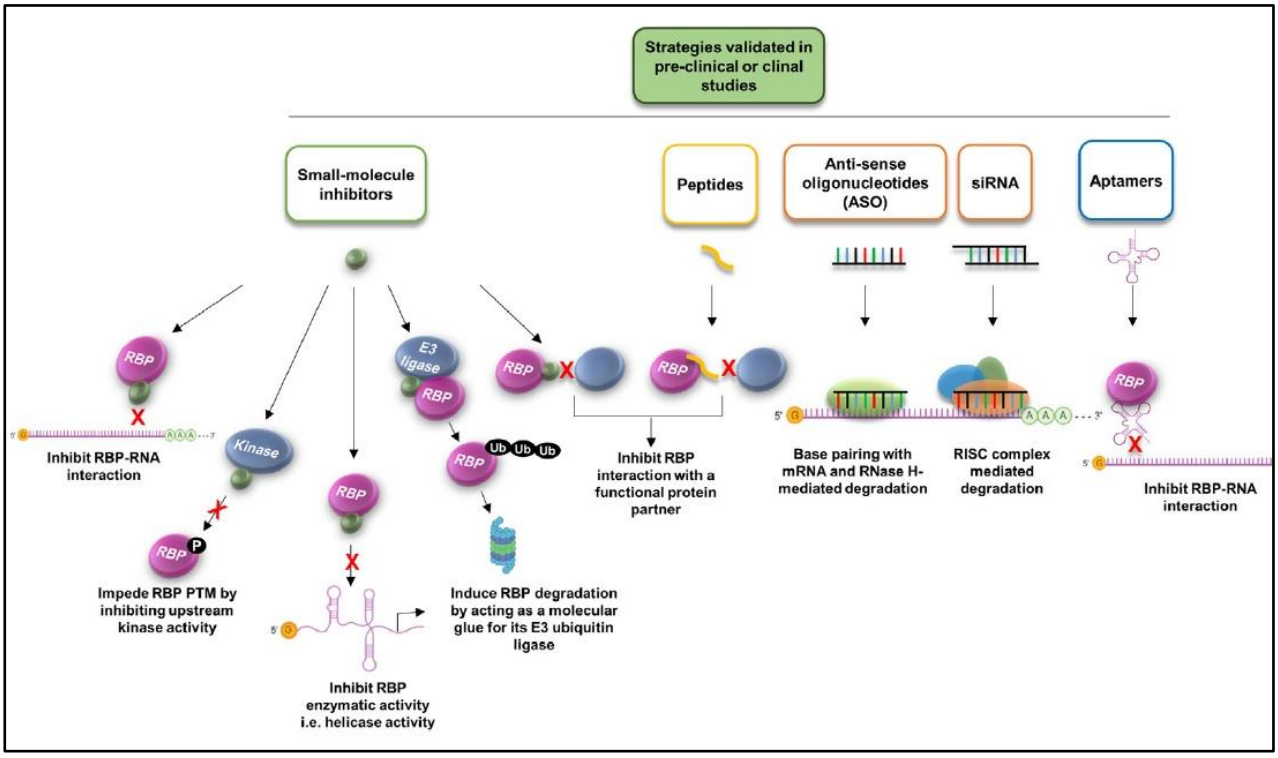

Figure 15. Strategies that are being applied to target RBPs for cancer therapeutics (Mohibi, Chen, and Zhang 2019).

RBP functions can be inhibited by using small molecules that act in different ways:

- by binding to the RBD and, subsequently, inhibiting RBP-RNA interaction
- by inhibiting the activity of the enzymes involved
- by inhibiting enzymatic activity of an RBP towards its target mRNA
- by inducing RBP degradation through targeting its E3 ubiquitin ligase
- by disrupting interaction between RBP and its protein partner essential for its function in cancer.

For example the eukaryotic translation initiator factor 4E (eIF4E) play an instrumental role in tumorigenesis and cancer progression, thus several strategies have been applied to design small molecules that target eIF4E directly or indirectly. One method is using the cap-binding agonists (4Ei-1 and Bn7-GMP), a synthetic nucleotide derivative that blocks the binding of eIF4E to the mRNA cap. Another approach is inhibit the interaction between eIF4E andeIF4G by several small molecules (4EGI-1, 4E1RCat, 4E2RCat). Another approach is to sequester eIF4E by modulating the activity of 4E-BP; since 4E-BPs are direct substrates of the mTOR kinase, targeting the mTOR signaling pathway is a therapeutically option for inhibiting translation, for this ragion several inhibitors with anti-cancer activity have been developed in the last decades (Rapamycin, RAD001, and CCI-779) (Mohibi, Chen, and Zhang 2019).

Antisense oligonucleotides (ASOs) are short (15-30 bp) single stranded DNA moleculaes complementary to the RNA target. Upon binding to their target mRNAs, ASOs alter protein production either by modulating the splicing mechanism or by enhancing degradation of target RNA through the action of RNaseH. To date, six ASO drugs have been approved for the treatment of diseases such as viral infections and neurological diseases. For example Nusinersen, an ASO that corrects SMN2 splicing (Rigo et al. 2012), in 2016 was approved by the FDA as the first drug specific forthe treatment of spinal muscular atrophy (SMA), a neurodegenerative disorder characterized by progressive loss of motorneurons and caused by loss or mutation of SMN1, an RBP involvedin spliceosome. Nusinersen ameliorates the phenotype and survival of SMA patients and is having notable success in the clinical setting (Mercuri et al. 2018). Although there are currently no approved ASOs for cancer treatment, many studies are in progress. For example, ASO that block the expression of eIF4E [LY2275796] has been developedand has completed a phase I clinical trial (Hong et al. 2011).

Small interfering RNA (siRNA)-nanoparticles were introduced in 2010 and FDA approved the first siRNA-based drugin 2018: Onpattrois a siRNA-based treatment for symptoms of peripheral nerve disease(polyneuropathy)(Yin and Rogge 2019). Studies focusing on the optimization for these therapies are underway, in particular concerning attempts to conjugate siRNAs with another molecule: antibody fragment, receptor ligand, or sugar to guide the siRNA to the target cell and that do not interfere with healthy cells (Mohibi, Chen, and Zhang 2019).

Aptamers can be either nucleic acid or peptide-based and fold into sequence specific three-dimensional structures that can recognize unique targets. The advantage over antibodies is that they are smaller, have better stability and are not immunogenic. For instance, the aptamer

AS1411 targets the RBP nucleolin, which regulates RNA polymerase I transcription, and is being tested as anti-cancer therapy (Morita et al. 2018).

Anti-cancer peptides also represent promising opportunities in targeting oncogenic functions, due to their high specificity, selectivity, small dimension and high biocompatibility. For example, peptides that target eIF4E interfere with its interaction with eIF4G, leading to inhibition of cap-dependent translation (Mohibi, Chen, and Zhang 2019).

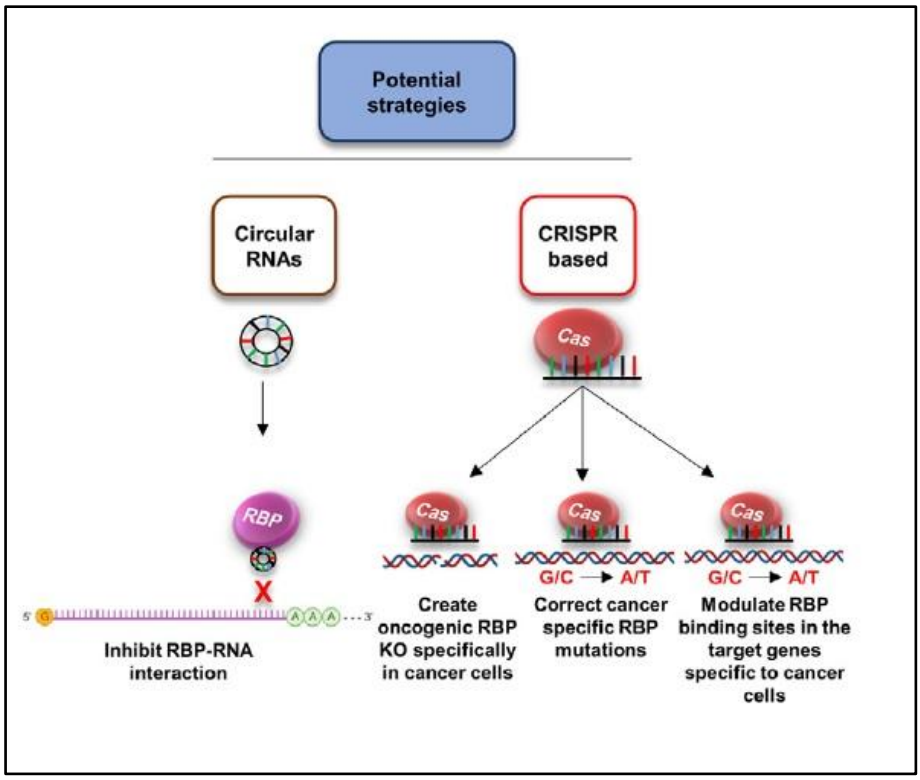

Figure 16. Potential strategies that are being applied to target RBPs(Mohibi, Chen, and Zhang 2019).

Circular RNAs (circRNAs) and the CRISP/Cas9 system offer additional potential strategies to target RBPs in cancer (Fig. 16). CircRNAs are closed circle RNAs formed by back-splicing and can act as sponges for both miRNAs and RBPs, preventing their binding to targetmRNAs. In this way, circRNAs have been shown to regulate both transcription and splicing processes. Moreover, circRNA are very stable and have a long half-life in cells. These properties make the circRNAs promising therapeutic toolsfor targeting RBP functions. However, to date there is no clinical application of circRNAs in cancer, but it could represent a promising path to pursue in the future (Kristensen et al. 2018)(Mohibi, Chen, and Zhang 2019).

The CRISPR/Cas9 system is based on the use of the Cas9 protein, a molecular scissor capable of cutting a target DNA, which can be programmed to make specific modifications to the genome

of cells. It can be used to knockout specific genes, including those encoding oncogenic RBPs in cancer cells, thus correcting cancer-specific RBP mutations or modulating RBP binding sites in mRNAs that cause aberrant splicing of oncogenes (Mohibi, Chen, and Zhang 2019).

IV.3. "*Identification of the RNA binding protein MEX3A as a prognostic factor and chemosensitivity regulator in Pancreatic Ductal Adenocarcinoma(PDAC)"*

Since the importance that RBPs have acquired over the last few decades in tumorcells, we have investigated the involvement of RBPs in PDAC patients by unbiased bioinformatics screeningusing “The Cancer Genome Atlas (TCGA)” database. Thus, we have identify MEX3A, RBP whose high expression is related to poor prognosis and we have caratherizated its role in PDAC cell lines and in pancreatic mouse model. Below I report the sperimental work that I conduct during my PhD student.

IV.4. Paper: "*Identification of the RNA binding protein MEX3A as a prognostic factor and chemosensitivity regulator in Pancreatic Ductal Adenocarcinoma (PDAC)"*

Valentina Panzeri[1,2], Isabella Manni[3], Alessia Capone[2], Emanuela Pilozzi[4], Giulia Piaggio[3], Gabriele Capurso[5], Claudio Sette[2,6].

1.Department of Science Medical/Chirurgic and Translational Medicine, University of Rome "Sapienza", Rome, Italy
2.Santa Lucia Foundation IRCCS, Rome, Italy
3.Department of Research, Advanced Diagnostics and Technological Innovation, UOSD SAFU, Regina Elena National Cancer Institute, Rome, Italy.
4. Department of Clinical and Molecular Medicine, University of Rome "Sapienza", Rome, Italy
5.PancreatoBiliary Endoscopy and EUS Division, Pancreas Translational and Clinical Research Center, San Raffaele Scientific Institute IRCCS, Milan, Italy.
6.Institute of Human Anatomy and Cell Biology, Catholic University of the Sacred Heart, Rome, Italy.

IV.4.1 Abstract

Pancreatic ductal adenocarcinoma (PDAC) is a highly aggressive cancer. Most patients present with advanced disease at diagnosis, which only permits palliative chemotherapeutic treatments. Both innovative chemotherapeutic treatments and targeted therapies have shown little efficacy so far. Thus, improvement in PDAC management represents a clinical priority.

Dysregulation of RNA processing pathways in cancer cells is emerging as a distinct feature, which can be exploited to precisely stratify patients and as therapeutic vulnerability. To identify novel biomarkers that are capable to distinguish between tumors with potentially different responses to treatments and to test the potential of targeting RNA processing dysregulation as novel therapeutic approach for PDAC, we performed a bioinformatics screening for splicing factors associated with PDAC prognosis in “The Cancer Genome Atlas (TCGA)” database. We selected 202 genes among those encoding RNA binding proteins (RBPs) and other proteins (i.e. kinases) that are involved in nuclear RNA processing and found 12 genes that displayed a significant correlation with progression free survival (PFS) in surgically resected PDAC patients. Out of these candidates, we focused our attention on MEX3A because it was previously shown to mark intestinal stem cells that are refractory to chemotherapeutic treatments.

Increased expression of MEX3A correlated with higher disease stage in PDAC patients. Knockdown of MEX3A in PDAC cells enhanced sensitivity to chemotherapeutic treatment and impaired cell cycle progression. RNA sequencing analyses of MEX3A-depleted cells highlighted hundreds of genes whose expression is sensitive to MEX3A, with significant enrichment in cell cycle genes and regulation of transcription. Our findings uncover a new pathway possibly

involved in the acquisition of chemoresistance by PDAC cells, which may be suitable for therapeutic targeting in PDAC patients.

IV.4.2 Introduction

Late diagnosis and/or presence of metastases in pancreatic ductal adenocarcinoma (PDAC) strongly limit therapeutic options and patients show a 5 years survival rate of <5% (Miller et al. 2016). Despite advances in surgery and chemotherapy, the prognosis of patients has remained practically unchanged, thus finding new early biomarkers and novel therapies represent a clinical priority for PDAC (Neoptolemos et al. 2018).

In the last decade, several genome-wide analyses of cancer transcriptomes have shown that tumor cells can modulate gene expression at the level of alternative splicing (AS) or other steps of RNA processing (Eswaran et al. 2013). AS is guided by the spliceosome, a dynamic complex consisting of small nuclear RNAs (snRNAs U1, U2, U4, U5 and U6) and a wide repertoire of associated protein factors, which removes introns and ligates exons to produce the mature mRNA. Alternative recognition of exonsis regulated by both *cis* acting sequences on the pre-mRNA and *trans* acting factors, which enhance or inhibit recognition of the splice sites and splicing catalysis. Thus, changes in the expression of some of these *trans*-acting RNA binding proteins (RBPs) have been directly linked to the expression of oncogenic isoforms that confer several advantages to tumor cells (Dvinge et al. 2016). For instance, up-regulation of PTBP1 in bladder cancer promotes cell cycle progression and expression of pro-oncogenic splice variants related to cell survival (FAS), proliferation (NUMB, PKM), cytoskeleton organization (ACTN1, MACF1, TPM1, and CTNND1), and interaction with the extracellular matrix (CD44) (Bielli et al. 2018). Sam68 is also overexpressed in many human cancers and its promotes cell-cycle progression and survival to genotoxic stress, likely through induction of oncogenic splice variants like BCL-XL, cyclin D1b, CD44 variants (Bielli et al. 2011b). Moreover, splicing factors can be modulated by chemotherapeutic treatments. For instance, SRSF1 is up-regulated in PDAC upon exposure to gemcitabine and it inducesthe oncogenic MNK2b splice variant (Adesso et al. 2013). Moreover, chronic treatment with the drug selected clones of PDAC cells that overexpressed PTBP1, which contributes to aerobic glycolysis by promoting the expression of a specific isoform of pyruvatekinase (PKM2 isoform) (Calabretta et al. 2016).

Herein, we have investigated the involvement of RBPs in PDAC by unbiased bioinformatics screening. We found that 12 genes are significantly correlated with progression free survival

(PFS) in surgically resected PDAC patients. We focus our study on MEX3A because it was recently demonstrated that its expression marks intestinal stem cells that are refractory to chemotherapeutic treatments (Barriga et al. 2017).

In *Caenorhabditis elegans*, MEX-3 regulates blastomere identity during early embryogenesis and germline totipotency in the adult worm. Mutations of the *mex-3* locus are embryonic lethal in the worm (Draper et al. 1996). In human, MEX3A belongs to a family that includes four members: MEX3A, MEX3B, MEX3C and MEX3D. MEX3 proteins have two K homology (KH) domains and one RING finger domain with E3 ubiquitin ligase activity at the C-terminal. MEX3A function is still rather unknown. All MEX3 proteins are nucleocytoplasmic shuttling proteins containing anuclear export signal (NES) consensus sequence in their N-terminal region. MEX3A and MEX3B are component of P bodies, structures involved in mRNA degradation and translational repression (Buchet-Poyau et al. 2007)(Pereira et al. 2013). MEX3A regulates the intestinal differentiation, polarity and stemness features, partially through binding to the 3' untranslated region (UTR) of CDX2 and repressing its expression (Pereira et al. 2013). Regarding cancer, MEX3A knock-down was shown to suppress cell proliferation and migration in human gastric cancer cells (Jiang et al. 2012), but the mechanism involved is completely unknown.

Our studies now correlate MEX3A expression with a more malignant PDAC phenotype and show that its knock-down sensitizes PDAC cells to chemotherapy. RNA-seq analysis idenfied functional clusters of MEX3A-regulated genes that are involved in transcription and cell cycle progression. MEX3A positively regulated expression of cyclin D1 and CDK6, proteins required for the G1-S transition, and MEX3A knock-down significantly reduced PDAC cell proliferation through a block in this transition of the cell cycle. Our work suggests that MEX3A may representa valuable new therapeutic target for PDAC treatment.

IV.4.3 Material and methods

Cell culture, tranfectionsand treatments

MiaPaCa-2, ASPC1, C5M2 cells were cultured in DMEM medium (Sigma D5796) supplemented with 10% fetal bovine serum (Gibco), Non Essential Amino Acids 100X (Thermo Fischer 11140035) and gentamicin 200X (Thermo Fischer 15710-049). HPAF-II was cultured in RPMI 1640 medium (Euroclone ECM2001L) supplemented with 10% fetal bovine serum, Non Essential Amino Acids 100X and gentamicin 200X. Cells were grown in a 37°C humidified atmosphere of 5% CO2.

To generated clones drug resistant MiaPaCa-DR, we espoused MiaPaCa-2 cells to chronic treatment with Gemcitabine (1uM) for 7 days, at the end the clones were amplified and treated recurring with the drug to maintain the selection.

MiaPaCa-2 cells were transfected with FLAG or MEX3A-FLAG plasmids using Lipofectamine 2000 (Invitrogen). For RNAi, cells were transfected with 100nM siRNAs using Lipofectamine RNAi Max (Invitrogen) and Opti-MEM medium (Invitrogen) following the instructions provided. siRNA for MEX3A are sense 5'-GUGUUUCCCUUCACUCUCUdTdT-3' and antisense, 5'-AGAGAGUGAAGGG AAACACdTdT-3 (Sigma), whose sequences are taken from paper of Jiang H. (Jiang et al. 2012), smartpool of MEX3A were bought from Dharmacon (On target plus smartpoll siRNA).

The cells were synchronized through 0,5mM mimosine drug (Sigma) for 18 hours, then le cells were washed 3 times with PBS and were recuperated after 6 hours for the S phase of cell cycle.

Gemcitabine (Eli Lilly & Company, Indianapolis, IN, USA) was dissolved in water and stored at − 20 °C for one month.

Bioinformatics analysis

Bioinformatics screening to search RBP associated with PDAC prognosis are performed by “The Cancer Genome Atlas (TCGA)” database.R2 genomics platform (http://r2.amc.nl) was used to evaluate the associationof splicing factors with pancreatic adenocarcinoma cancer stage.

RT-PCR and qPCR analysis

RNA was extracted from cells usingTrizol reagent (Invitrogen Thermo Fisher) according to the manufacturer’s instructions. After digestion with RNase free DNase (Thermo Fisher), RNA was resuspended in RNase free water (Sigma-Aldrich); 1µg of total RNA was retrotranscribed using M-MLV reverse transcriptase (Promega). 20ng of cDNAwas used as template for RT-PCR analysis (GoTaq, Promega) or qPCRanalysis (SYBR Green method, Roche). Primers used are listed in Supplementary Table S1.

Protein extraction and western blot

The pellet of cells were resuspended in lysis buffer (150 mMNaCl, 15 mM MgCl2, 15 mM EDTA, 50mM Hepes, 10% Glycero, 20mM β-glicerophosphate, 1% Triton X-100). The tissue extract were extracted by RIPA buffer (TrisHCl 50mM, NP40 1%, NaCl 150mM, NaDeoxycholate 0,5%, EDTA 2mM, SDS 0,1%). Both buffers were completed with 1mMdithiothreitol, 2 mM Na-ortovanadate and Protease-Inhibitor Cocktail (Sigma). After 10 min of incubation in ice, extracts

were sonicated at maximum intensity for 5", then they were centrifuged for 10 min at 13 000 rpm at 4 °C, supernatants were resuspended in SDS-page sample buffer and boiled for 10 min. The following primary antibodies (over night at 4 °C) were used: rabbit-MEX3A (1:1000, Sigma), rabbit anti-Actin (1:1000, Sigma-Aldrich), mouse anti-GAPDH(1:1000, Santa Cruz Biotechnology), rabbit anti-E-cadherin (1:2000, Cell Signaling), mouse anti-Vimentin (1:1000, Santa Cruz Biotechnology), rabbit anti PARP-1 (1:1000, Cell Signalling Technology). Secondary anti-mouse or anti-rabbit IgGs conjugated tohorseradish peroxidase (Amersham, UK) were incubated for 1h at RT (1:10000). Immunostained bands were detected by chemiluminescence method (Bio-rad).

Cell viability assays

MTS assay: cells were plated at 50% confluence in 96 wells, after 72 h of treatment, the cell viability was evaluated by MTS assay (Promega) following the manufacturer's instructions and by assessing the optical density (OD) at 490 nm.

Clonogenic assay: single-cell suspensions were plated in multiwell-6 (2000cells/well). The next day the cells are treated and after10 days, cells were fixed in methanol 100% for 10 min at room temperature, stained overnight with crystal violet 0.05% (Sigma-Aldrich), washed with H_2O and dried. Pictures were taken using a digital camera to count and measure the colonies.

Cell cycle

Cells were pulse-labeled with 10 uM thymidine analog bromodeoxyuridine(BrdU) for 30 minutes, thus BrdUis incorporated into newly synthesized DNA in cells entering and progressing through the S phase of the cell cycle. After the cells are fixed with a 30% PBS/70% ethanol solution over night at -20°C. Cell cycle were evaluated by flowcytometry using double staining with propidium iodide (PI) (20 mg/mL) and anti-BrdUantibody (0.125ug x sample) in the presence of ribonuclease A (1ug/ml). A total of 10.000 events were counted with FACSCalibur flow cytometer (BectonDickinson) and analyzed using FlowJo program (BectonDickinson).

UV-crosslinked RNA immunoprecipitation (CLIP) assay

CLIP assays were performed following the protocol of Bielli P. (Bielli and Sette 2017) and RNA associated with FLAG-MEX3A was represented as percentage of input.

RNA seq

For RNA-seq analysis, total RNA was extracted using Qiagen RNeasy micro/mini plus Kit from MiaPaCa-2 cells transfected with Ctrl (n=4), MEX3A (n=4), MEX3A (n=4) siRNA for 48 hours,.

The libraries were constructed by QuantSeq 3'mRNA. The sequencing results obtained, for differential gene expression, were filtered by discarding the genes whose expression levels didn't exceed 25 reads.

Analysis for enriched GO functional clusters was performed using g:Profilertool.

IV.4.4 Results

1. Identification of RNA processing regulators associated with PDAC prognosis.

To search for RNA processing regulatory factors that potentially impact on PDAC biology, we performed an unbiased bioinformatic screening by querying "The Cancer Genome Atlas (TCGA)" database. We selected 202 genes among those encoding RNA binding proteins (RBPs) and other proteins (i.e. kinases) that are involved in nuclear RNA processing (i.e. splicing and/or cleavage and polyadenylation). We found 12 genes that displayed a significant correlation with progression free survival (PFS) in surgically resected PDAC patients. In some cases, high expression of the RBP correlated with worse PFS (i.e. MEX3A and SRRM1), whereas high expression of other RBPs correlated with better prognosis (i.e. CELF3; onco-suppressor-like factors)(Fig.1A,B). Most of these genes also correlated with overall survival (OS) of patients in the same dataset (Supplementary Fig.1). Moreover, bioinfomatic analysis of another PDAC dataset (R2; https://r2.amc.nl) indicated that "oncogenic-like factors"(i.e. MEX3A and SRRM1) show significant positive correlation with higher disease stage in PDAC patients, whereas decreased expression of "oncosuppressor-like" factors (CELF3 and ELAVL3) correlated with higher disease stage (Fig. 1C). These observations suggest that PDAC progression and outcome correlates with, and may be affected by, a different repertoire of RNA processing factors.

2. MEX3A expression correlates with more malignant PDAC phenotype and its knock down sensitizes at chemotherapy treatment.

We focused our study on MEX3A because this gene was recently shown to mark an intestinal stem cell population that is particularly refractory to chemotherapeutic treatments (Barriga et al. 2017). Poor prognosis in PDAC mainly relies on rapid acquisition of chemoresistance (Neoptolemos et al. 2018). Thus, to test the predictive value of our bioinformatic analysis, we evaluated if expression of MEX3A correlates with drug resistance in PDAC cell lines. We used two PDAC cell lines (HPAF and ASPC1) that express epithelial markers and display a less aggressive phenotype, and two mesenchymal-likeand more malignant cell lines (C5M2 and MiaPaCa-2). We found that MEX3A is expressed at higher RNA and protein levels in vimentin-positive C5M2 and MiaPaCa-2 cells with respect to HPAF-II and ASPC1 cells (Fig.2A,B). Moreover, MTS assay with two doses of Gemcitabine, the most used first-line chemotherapeutic drug for PDAC (Neoptolemos et al. 2018), showed that cells expressing higher levels of MEX3A are more resistant to treatments than low-MEX3A expressing cells

(Fig.2C). More importantly, depletion of MEX3A using two different siRNAs (Fig.2D-E) reverted chemoresistance in both MiaPaCa2 (Fig. 2F) and C5M2 (Supplementary Fig. 2A) cells and enhanced cell death, as indicated by the concomitant increase in cleaved PARP1 expression (Fig. 2G, Supplementary Fig. 2B).

Next, we generated MiaPaCa-2 drug-resistant clones (MiaPaCa-2-DR) by chronic exposure of cells to treatment with Gemcitabine (1uM) for 7 days. At the end of the selection, surviving clones were isolated and amplified under recurring monthly treatments with the drug to maintain the selection. To confirmthe drug-resistant phenotype of MiaPaCa-2-DR cells, we analyzed cell survival by clonogenic assays. While treatment with Gemcitabine reduced the number of colonies in a dose dependent-manner in parental MiaPaCa-2 cells, DR cells were insensitive to treatments (Fig. 2H). Notably, we found that MEX3 expression was increased in MiaPaCa-2-DR cells with respect to parental cells (Fig. 2I). These results support a functional role for MEX3A in the acquisition and maintenance of adrug-resistant phenotype in PDAC cells.

3. MEX3A regulates genes involved in cell cycle progression and RNA processing.

To investigate the role of MEX3A in PDAC cells, we performed RNA-seq analysis of MiaPaCa-2 cells silenced or not for this RBP. Bioinformatics analysis revealed 164 MEX3A-regulated genes in cells transfected with two independent siRNAs, of which 45 were up-regulated and 119 down-regulated (Fig.3A). Functional clustering of MEX3A-regulated genes identified “transcription”, “signal transduction”, “RNA metabolism”, “apoptotis” and “cell cycle” as principal pathways (Fig.3B). Direct analysis of four down-regulated genes (*CCND1*, *TCF7*, *TEAD2* and *CDK6*) by quantitative real time PCR (qPCR) validated the results of the RNA-seq and bioinformatic analyses (Fig.5C). To test whether MEX3A directly interacts with the mRNAs of these regulated genes, we performed UV-crosslink and RNA immunoprecipitation (CLIP) assay in MiaPaCa-2cells over-expressing FLAG-MEX3A or transfected with empty vector. Notably, we detected a strong enrichment of CLIP signals for Cyclin D1 and CDK6 mRNAs in the MEX3A immunoprecipitates with respect to control immunoprecipitates (Fig. 3D). These results suggest that MEX3A regulates gene expression by directly binding to target mRNAs.

4. MEX3A affects cell cycle progression in PDAC cells.

Since "cell cycle" emerged among the principal pathways potentially regulated by MEX3A in PDAC cells, we investigated the impact of MEX3A expression on cell cycle progression. Silencing

of MEX3A in MiaPaCa-2 cells caused a significant reduction in proliferation, as measured by colony formation assay, cell counting and MTS assay (Fig. 4A-C). FACS analyses showed that MEX3A depletion causes a significant enrichment in G1 and reduction of S phase already after 24 hours, a phenotype that was more dramatic after 48 hours from silencing (Fig. 4D). This result suggests that MEX3A expression is important for completion of the G1 phase of the cycle and transition into the S phase. In line with this hypothesis, we also found that MEX3A expression is regulated during the cell cycle and is higher in G1 than in S phase in MiaPaCa-2 cells released from a block induced by treatment with Mimosine for 16 hours (Fig. 4E-G).

5. MEX3A is up-regulated at pre-syntimatic stage in MKC mice.

To analyse the expression of MEX3A in an in vivo model of PDAC, we employed the mouse LSL-$Kras^{G12D/+}$ Pdx-1-Cre PDAC mouse model, characterized by pancreas-specific expression of an oncogenic Kras mutant allele. In particular we used a mouse model crossed with the MITO-Luc mouse, which expresses luciferase under the control of a mitotic promoter (NFYA). In the resulting MKC mouse model, itis possible to measure physiologicalas well as aberrant proliferation in any body tissue by non-invasive bioluminescence imaging (BLI) (de Latouliere et al. 2016). We collected pancreas from MKC mice at differente stage of PDAC progression. Importantly, we found that MEX3A is upregulated already at a pre-symptomatic stage, before the tumor mass is detected, with respect to control healthymice (Fig. 5). On the other hand, other splicing factors (SRSF1 and PTBP1) involved in PDAC chemoresistant phenotype were up-regulated at later symptomatic stages. This observation suggests that MEX3A is involved in the early events of PDAC tumorigenesis.

IV.4.5 Discussion

PDAC is one of the most aggressive tumors; due to its extremely poor prognosis and lack of clear benefits obtained by new therapies in the last decades, PDAC is emerging as a clinical priority in oncology (Miller et al. 2016). One of the features that contributes to such poor outcome is acquisition of early resistance to chemotherapeutic treatments in PDAC patients, thus limiting their effectiveness (Neoptolemos et al. 2018). Therefore, improving the knowledge

of PDAC biology may help identify new therapeutic targets and develop tools to counteract chemoresistance.

Altered expression of RBPs is a common phenomen on during development and progression of cancers. Dysregulated RBPs often promote oncogenic isoforms that interfere with cell cycle, cell proliferation and invasion (Z.-L. Wang et al. 2018). To identify RBPs altered in PDAC and possibly contributing to its malignancy, we performed a bioinformatics screen for RBPs correlated with PDAC prognosis using patients data deposited in “The Cancer Genome Atlas (TCGA)” database. Out of more than 200 candidates screened, we found only 12 genes that displayed a significant correlation with progression free survival (PFS) in surgically resected PDAC patients. We focused our attention on MEX3A because it was previously shown to mark intestinal stem cells that are refractory to chemotherapeutic treatments (Barriga et al. 2017). This observation attracted our attention because subpopulation of cancer cells particularly resistant to chemotherapeutic treatments are thought to guide relapse of disease in many cancers (Z.-L. Wang et al. 2018). Moreover, other authors recently found that MEX3A is up regulated also in multiple cancers by screening of 1,542 human RBPs across 15 cancer types present in TCGA datasets (Z.-L. Wang et al. 2018). Furthermore, MEX3A was significantly up-regulated in gastric tumor tissues in comparison with adjacent non-tumors tissues (Jiang et al. 2012). These findings suggest a role of MEX3A in the pathogenesis of human cancers. However, in spite of these emerging correlations, MEX3A function is still rather unknown. Here, we show that MEX3A is involved in the regulation of cell cycle progression and cell proliferationin PDAC. MEX3A depletion caused a significant enrichment in cells in G1 and the consequent reduction of cells in S phase, thus suggesting that a delay or a block on the G1/S transition underlies the negative effect observed on cell proliferation.

Interestingly, MEX3A know-down also sensitized PDAC cells totreatment with gemcitabine, one of the drugsused in first line chemotherapy for this pathology. Moreover, MEX3A was up-regulated in MiaPaCa-2 cells selected after chronic exposure to gemcitabine. These results indicate a functional role of MEX3A in acquisition of drug-resistance and it can acquire clinical relevance, as most PDAC patients rapidly develop resistance to chemotherapy. Notably, we also observed that in a mouse PDAC model MKC that recapitulate human PDAC histopathological and clinical features, MEX3A is upregulated already at pre-symptomatic stage. This suggest that MEX3A represents an early event during PDAC tumorigenesis, whereas other splicing factors (SRSF1 and PTBP1), which contribute to PDAC chemoresistance (Calabretta et al. 2016)(Adesso

et al. 2013), were up-regulatedat later stages. Thus, MEX3A could also represent a prognostic biomarker of PDAC at pre-symptomatic stage, which may be of relevance at least for screenings directed at categories at risk for PDAC.

MEX3A is able to regulate the stability of CDX2 mRNA by interaction with a putative MEX-3 recognition element (MRE). This motif consists of a bipartite sequence characterized by AGAG and UUUA motifs separated by two Uracil bases (Pagano et al. 2009), which is located in the 3'UTR of the CDX2 transcript (Pereira et al. 2013). Furthermore, MEX3B, a member of the MEX3 family with high structural homology to MEX3A, is also implicated in RNA stability. In particular, MEX3B was shown to bind to the 3' UTR of the HLA-A mRNA and destablize this transcript (Huang et al. 2018). We speculated that MEX3A may also have an effect on target RNA stability in PDAC cells. Our RNA sequencing experiments in MEX3A-depleted cells identified 165 potential targets for this RBP, which were enriched in functional categories of relevance for PDAC biology. So far, we have shown that MEX3A binds directly to two of these potential targets, the CYCLIN D1 and CDK6 mRNAs. Further experiments are underway to confirm the hypothesis that direct binding of MEX3A to its target mRNAs affects their stability in PDAC cells.

In conclusion, our study identifies MEX3A asa novel RBP involved in PDAC, whose high expression correlates with poor prognosis and advanced stage of PDAC tumor. MEX3A acts in cell cycle regulation targeting the mRNAs encoding for proteins involved in the G1/S transition of the cell cycle (CDK6 and CYCLIND1) and sensitizes PDAC cells to gemcitabine treatment. Moreover, MEX3A is upregulated at pre-symptomatic stage in PDAC mouse models, suggesting that MEX3A represents an early event during PDAC tumorigenesis.

IV.4.6 Figures

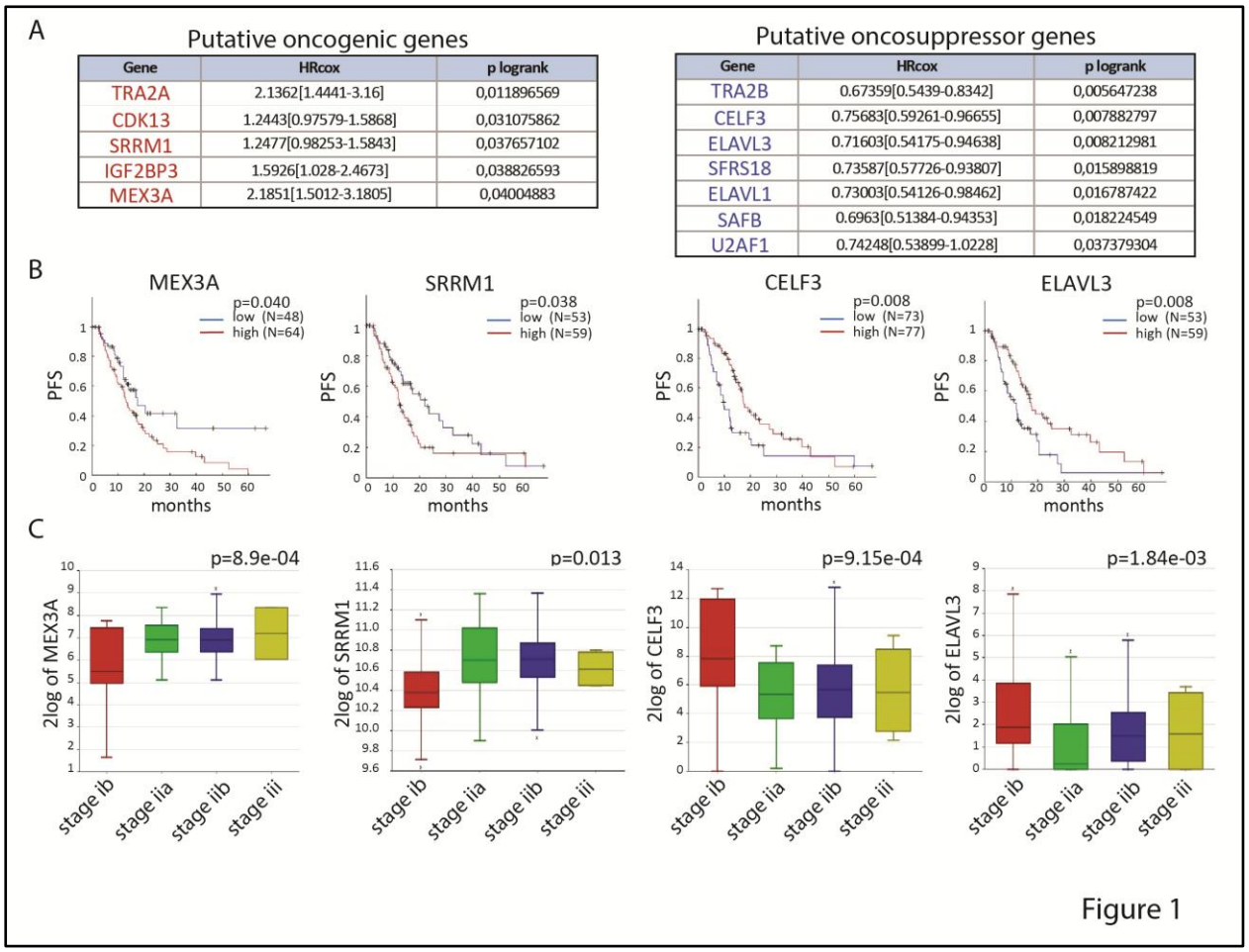

Figure 1

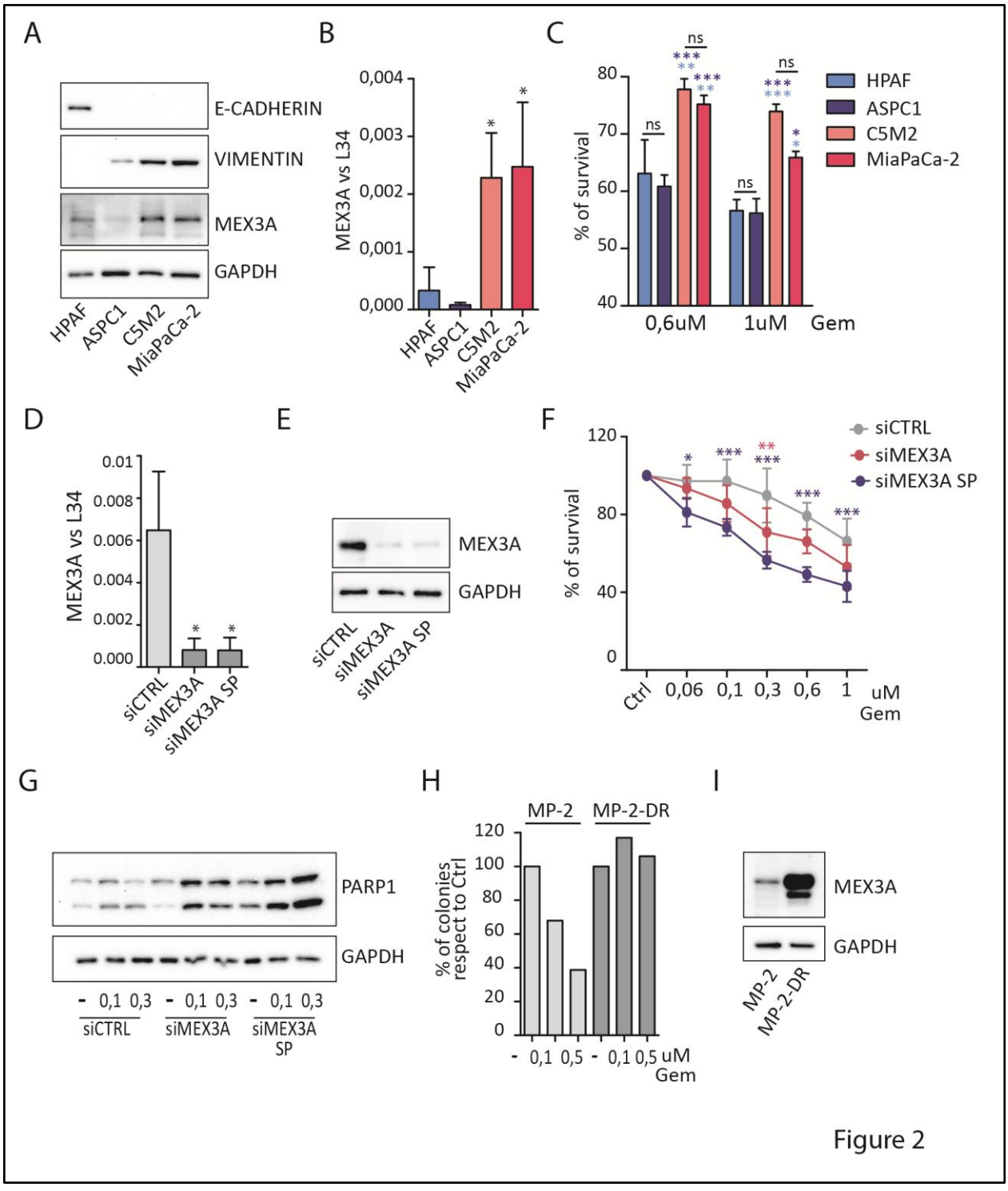
A
E-CADHERIN
VIMENTIN
MEX3A
GAPDH
HPAF
ASPC1
C5M2
MiaPaCa-2
B
MEX3A vs L34
0,004
0,003
0,002
0,001
0,000
C
% of survival
HPAF
ASPC1
C5M2
MiaPaCa-2
ns
0,6uM
1uM
Gem
D
MEX3A vs L34
0.01
0.008
0.006
0.004
0.002
0.000
siCTRL
siMEX3A
siMEX3A SP
E
MEX3A
GAPDH
F
siCTRL
siMEX3A
siMEX3A SP
% of survival
Ctrl
0,06
0,1
0,3
0,6
1
uM
Gem
G
PARP1
GAPDH
siCTRL
siMEX3A
siMEX3A SP
H
MP-2
MP-2-DR
% of colonies respect to Ctrl
uM
Gem
I
MEX3A
GAPDH
MP-2
MP-2-DR

Figure 2

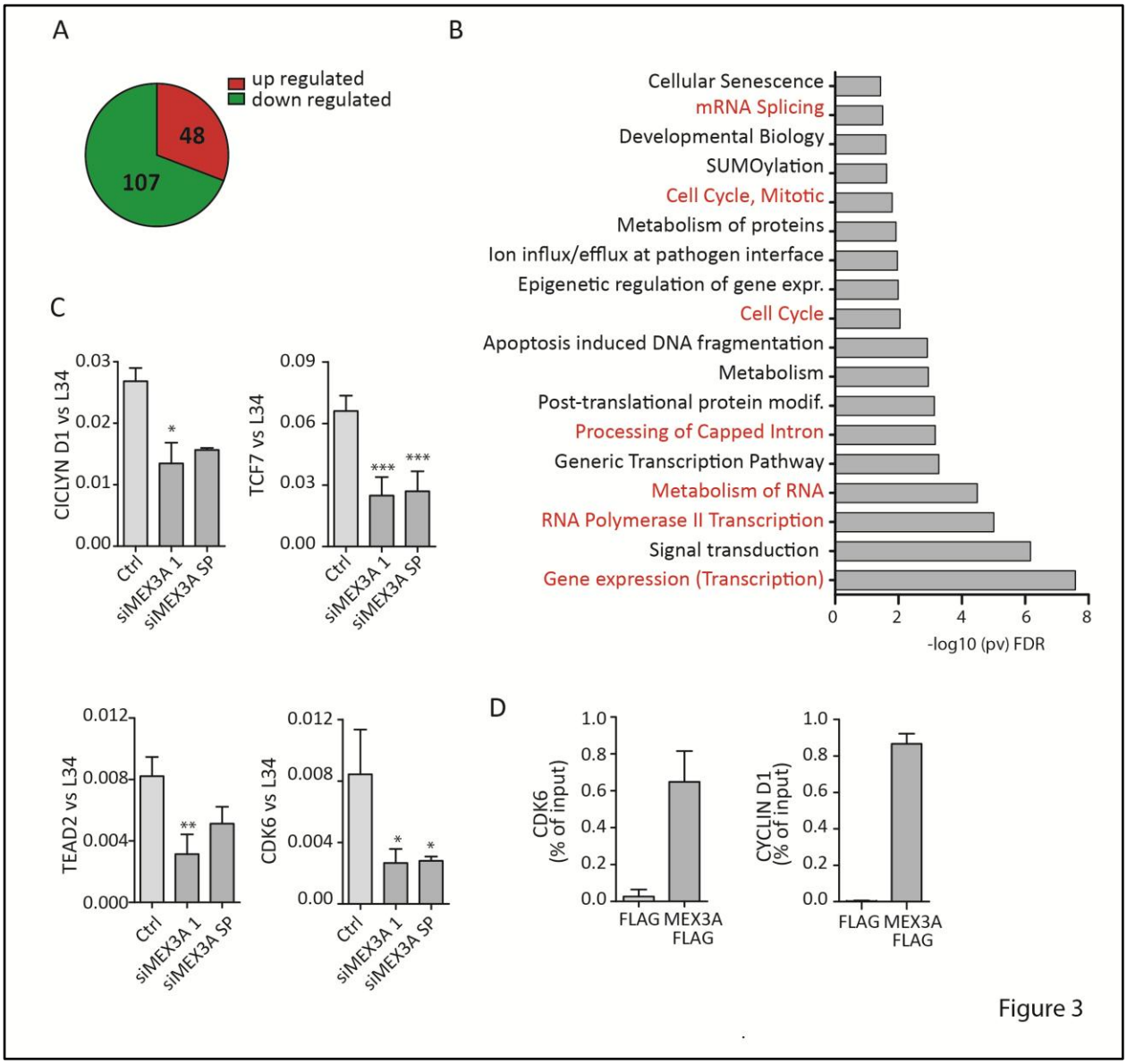
A
up regulated
down regulated
48
107
B
Cellular Senescence
mRNA Splicing
Developmental Biology
SUMOylation
Cell Cycle, Mitotic
Metabolism of proteins
Ion influx/efflux at pathogen interface
Epigenetic regulation of gene expr.
Cell Cycle
Apoptosis induced DNA fragmentation
Metabolism
Post-translational protein modif.
Processing of Capped Intron
Generic Transcription Pathway
Metabolism of RNA
RNA Polymerase II Transcription
Signal transduction
Gene expression (Transcription)
0
2
4
6
8
-log10 (pv) FDR
C
CICLYN D1 vs L34
0.03
0.02
0.01
0.00
*
Ctrl
siMEX3A 1
siMEX3A SP
TCF7 vs L34
0.09
0.06
0.03
0.00
***
***
Ctrl
siMEX3A 1
siMEX3A SP
TEAD2 vs L34
0.012
0.008
0.004
0.000
**
Ctrl
siMEX3A 1
siMEX3A SP
CDK6 vs L34
0.012
0.008
0.004
0.00
*
*
Ctrl
siMEX3A 1
siMEX3A SP
D
CDK6
(% of input)
1.0
0.8
0.6
0.4
0.2
0.0
FLAG
MEX3A
FLAG
CYCLIN D1
(% of input)
1.0
0.8
0.6
0.4
0.2
0.0
FLAG
MEX3A
FLAG

Figure 3

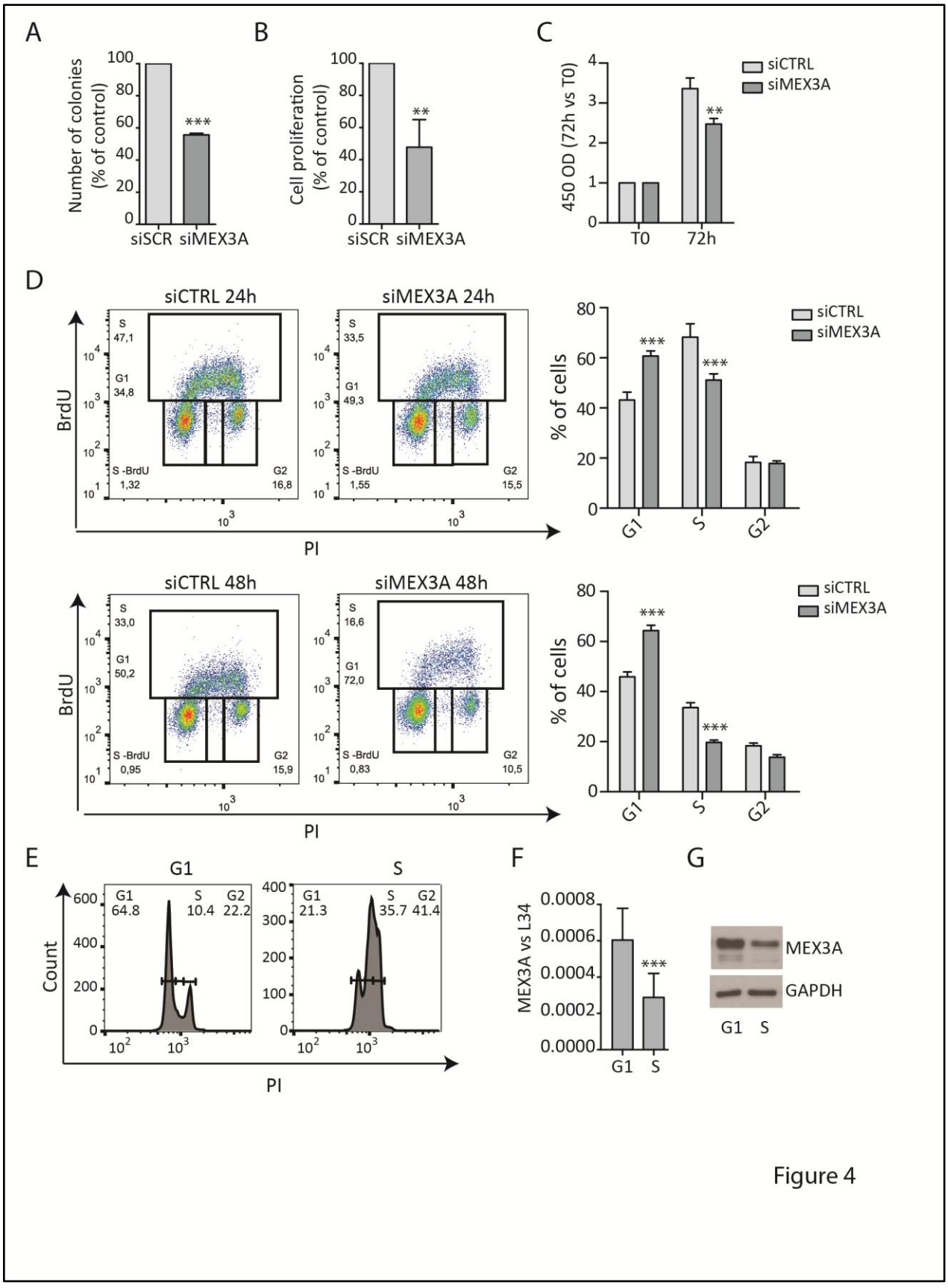
A
Number of colonies (% of control)
100
80
60
40
20
0
***
siSCR siMEX3A
B
Cell proliferation (% of control)
100
80
60
40
20
0
**
siSCR siMEX3A
C
450 OD (72h vs T0)
4
3
2
1
0
**
T0 72h
siCTRL
siMEX3A
D
siCTRL 24h
siMEX3A 24h
BrdU
PI
S 47,1
G1 34,8
S -BrdU 1,32
G2 16,8
S 33,5
G1 49,3
S -BrdU 1,55
G2 15,5
% of cells
80
60
40
20
0
***
***
G1 S G2
siCTRL
siMEX3A
siCTRL 48h
siMEX3A 48h
S 33,0
G1 50,2
S -BrdU 0,95
G2 15,9
S 16,6
G1 72,0
S -BrdU 0,83
G2 10,5
E
G1
S
Count
PI
G1 64.8
S 10.4
G2 22.2
G1 21.3
S 35.7
G2 41.4
F
MEX3A vs L34
0.0008
0.0006
0.0004
0.0002
0.0000
***
G1 S
G
MEX3A
GAPDH
G1 S

Figure 4

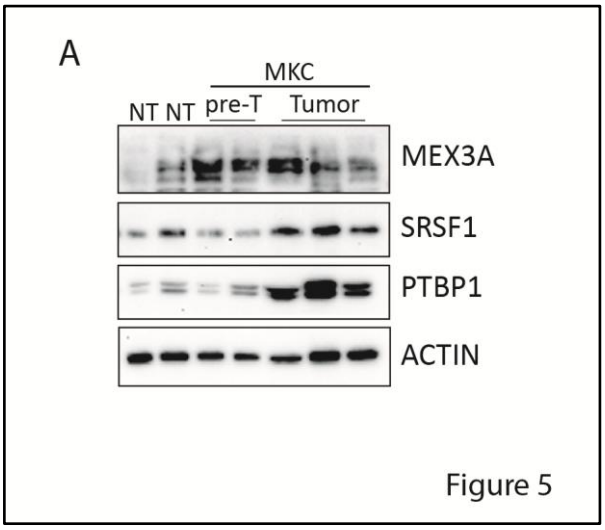

Figure 5

A

Overall Survival			
Gene	**HRcox**	**pcox**	**p logrank**
CELF3	0.74831[0.61125-0.9161]	0,004970851	0,000080396
ELAVL3	0.69452[0.53236-0.90608]	0,007210177	0,000269333
HNRNPD	1.2671[1.0284-1.5612]	0,026207424	0,003652443
PNISR	0.77367[0.62555-0.95685]	0,01794108	0,004655789
TRA2A	1.9192[1.3638-2.7007]	0,00018388	0,006346791
RBM7	0.77475[0.62416-0.96166]	0,020639616	0,007529469
TRA2B	0.74636[0.61389-0.90741]	0,003339019	0,010267264
MEX3A	2.0702[1.4894-2.8775]	1,4837E-05	0,01161216
RBPMS	0.76056[0.58768-0.9843]	0,037502598	0,016805663
SUGP2	0.70964[0.55212-0.91211]	0,007399118	0,01694985
DAZAP1	Inf[Inf-Inf]	0,999999997	0,0177347
ESRP2	1.5671[1.1158-2.201]	0,009529791	0,023725765
HNRNPH2	0.74314[0.58472-0.94449]	0,01523029	0,035022603
ELAVL1	0.75323[0.5652-1.0038]	0,053100857	0,036395975

Figure supplementary 1

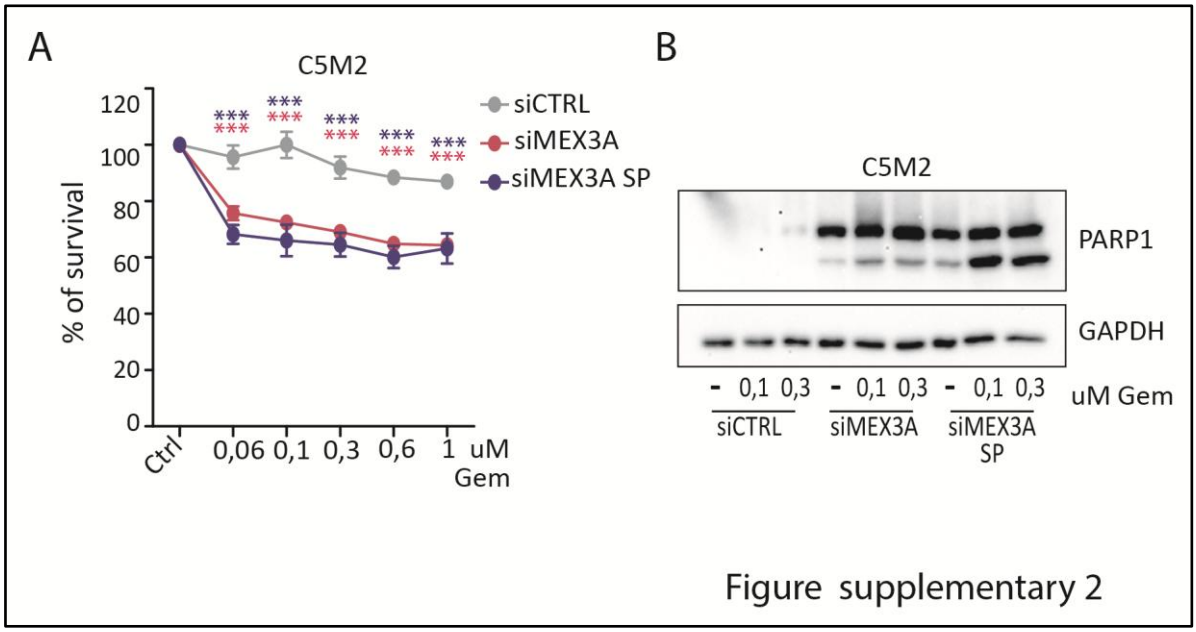

Figure supplementary 2

IV.4.7 Figure legends

Figure 1. **RNA processing regulators associated with PDAC prognosis**. **A)** RBPs and kinases whose expression is significantly correlated with PFS in PDAC patients in TGCA database. Blue indicates putative onco-suppressor genes, red indicates putative oncogenic genes. **B)** Kaplan-Meier curve of PFS for MEX3A and SRRM1 (oncogenic-like factors) and CELF3 and ELAVL3 (onco-suppressor-like factors) in PDAC patients.

Figure 2. MEX3A expression correlates with more malignant PDAC phenotype and its knock down sensitizes at chemotherapy treatment. A) Western blot of indicated proteins in PDAC cells. **B)** Level of expression of MEX3A vs L34 in PDAC cells**. C**) % of survival evaluated by MTS assay after 72h of treatment with increasing doses of gemcitabine (0,6uM and 1uM) in PDAC cells. Statistical analysis are reported in light blu when is refered at HPAF cell line, while in blu when is refered at ASPC1 cell line. qRT-PCR **D)** and western blot **E)** to check the silencing of MEX3a with siMEX3A or siRNA smartpool (SP) Dharmacon. **F)** % of survival evaluated by MTS assay after 72h of treatment with different doses of gemcitabine in MiaPaCa-2 cells transfected with CTRL, MEX3A or MEX3A SP siRNAs**. G)** Western blot of PARP1 and GAPDH in samples treated with gemcitabine after knockdown of MEX3A. **H)** Clonogenic assay to evaluate survival of thedrug resistant MiaPaCa-2 (MP-DR) clone. **I)** Western blot of MEX3A expression in MP-DR. Statistical analyses were performed by two way Anova (C-F) and one way Anova (B-D) (*P ≤ 0.05,** P≤0.01, ***P ≤ 0.001).

Figure 3. MEX3A controls genes involved in cell cycle, transcription and RNA metabolism. A) Schematic representation of genes up/down regulated after depletion of MEX3A revealed by RNA-seq analysis common in both silencing. **B)** Gene ontology (Reactome) of all regulated genes using the g-profiler web server. **C)** qRT-PCR validation of genes down-regulated involved in cell proliferation. **D)** Bar graphs showing results of qPCR analyses of CDK6 and CYCLIN D1 genes co-precipitated by FLAG antibody in CLIP experiments, the samples are normalized respect to input. Statistical analyses were performed by one way Anova (C) (*P ≤ 0.05,** P≤0.01, ***P ≤ 0.001).

Figure 4.MEX3A affects cell cycle progression in PDAC cells. **A)** Clonogenic assay performed in MiaPaCa-2 cells transfected with CTRL or MEX3A siRNAs. **B)** % of cell proliferation, relative to controll, of live cells MiaPaCa-2 cells transfected with CTRL or MEX3A siRNAs after 72h. **C)** MTS assay after 72h from silencing of MEX3A in MiaPaCa-2 cells. **D)** FACS analysis showing DNA content (propidium iodide, PI) and bromodeoxyuridine (BrdU) incorporation of MiaPaCa-2 cells transfected with CTRL or MEX3A targeting siRNAs at 24h or 48h. The percentage of cells in G1, S and G2 phase are indicated. **E)** FACS analysis showing DNA content (PI) of MiaPaCa-2 cells after release from mimosine synchronization. Times were chosen for enrichment of cells in the G1 and S phases of the cycle. qPCR **F)** and Westernblot **G)** analyses of MEX3A expression in G1 and S phase cells. Statistical analyses were performed by the paired Student's t-test (A-F), One way Anova (B) or Two wayAnova (D) (*P ≤ 0.05,** P≤0.01, ***P ≤ 0.001).

Figure 5.Expression analysis of RNA Binding Proteins in pancreatic tissue of MKC mice. A) Western blot analysis of MEX3A, SRSF1 and PTBP1 expression in pancreas tissue of control (NT) and MKC mice at pre-symptomatic (pre-T) and symptomatic (T) stage.

Figure supplementary 1. RNA processing regulators associated with PDAC prognosis. **A)** RBPs and kinases whose expression is significantly correlated with overall survival (OV) in PDAC patients in TGCA database. Blue indicates putative onco-suppressor genes, red indicates putative oncogenic genes.

Figure supplementary 2. A)% of survival evaluated by MTS assay after 72h of treatment with different doses of gemcitabine in C5M2 cells transfected with CTRL, MEX3A or MEX3A SP siRNAs**. B)** Western blot of PARP1 and GAPDH in samples treated with gemcitabine after knockdown of MEX3A in C5M2 cells.Statistical analyses were performed by Two way Anova (A) (***P ≤ 0.001).

IV.4.8 Supplementary data

Primers	
CDK6 fw	TGACCAGCAGCGGACAAATA
CDK6 rv	CAAGACTTCGGGTGCTCTGT
CYCLIN D1 fw	CCTACTTCAAATGTGTGGAGAAG
CYCLIN D1 rv	GGGGATGGTCTCCTTCATCTTA
L34 fw	GTCCCGAACCCCTGGTAATAGA
L34 rv	GGCCCTGCTGACATGTTTCTT
MEX3A fw	TCTACAAAGAGGCCGAGCTG
MEX3A rv	CCCTCACCGGTGTCTTGATG
TEAD2 FW	ACCGCCAGATGCAGTTGATT
TEAD2 RV	GTCGTAGATCTGCCGGACG
TCF7 fw	CCCCCAACTCTCTCTCTACGA
TCF7 rv	AGGTCAGGGAGTAGAAGCCA

IV.4.9 References

Adesso, L., S. Calabretta, F. Barbagallo, G. Capurso, E. Pilozzi, R. Geremia, G. Delle Fave, and C. Sette. 'Gemcitabine Triggers a Pro-Survival Response in Pancreatic Cancer Cells through Activation of the MNK2/EIF4E Pathway'. *Oncogene* 2013. 32 (23): 2848–57. https://doi.org/10.1038/onc.2012.306.

Barriga, Francisco M., Elisa Montagni, Miyeko Mana, Maria Mendez-Lago, Xavier Hernando-Momblona, Marta Sevillano, AmyGuillaumet-Adkins, et al. 'Mex3a Marks a Slowly Dividing Subpopulation of Lgr5+ Intestinal Stem Cells'. *Cell Stem Cell* 2017. 20 (6): 801-816.e7. https://doi.org/10.1016/j.stem.2017.02.007.

Bielli, Pamela, Roberta Busà, Maria Paola Paronetto, and Claudio Sette. 'The RNA-Binding Protein Sam68 Is a Multifunctional Player in Human Cancer'. *Endocrine-Related Cancer* 2011. 18 (4): R91–102. https://doi.org/10.1530/ERC-11-0041.

Bielli, Pamela, and Claudio Sette. 'Analysis of in Vivo Interaction between RNA Binding Proteins and Their RNA Targets by UV Cross-Linking and Immunoprecipitation (CLIP) Method'. *Bio-Protocol* 2017. 7 (10). https://doi.org/10.21769/BioProtoc.2274.

Buchet-Poyau, Karine, Julien Courchet, Hervé Le Hir, Bertrand Séraphin, Jean-Yves Scoazec, Laurent Duret, Claire Domon-Dell, Jean-Noël Freund, and Marc Billaud. 'Identification and Characterization of Human Mex-3 Proteins, a Novel Family of Evolutionarily Conserved RNA-Binding Proteins Differentially Localized to Processing Bodies'. *Nucleic Acids Research* 2007. 35 (4): 1289–1300. https://doi.org/10.1093/nar/gkm016.

Calabretta, S., P. Bielli, I. Passacantilli, E. Pilozzi, V. Fendrich, G. Capurso, G. DelleFave, and C. Sette. 'Modulation of PKM Alternative Splicing by PTBP1 Promotes Gemcitabine Resistance in Pancreatic Cancer Cells'. *Oncogene* 2016. 35 (16): 2031–39. https://doi.org/10.1038/onc.2015.270.

Draper, B. W., C. C. Mello, B. Bowerman, J. Hardin, and J. R. Priess. 'MEX-3 Is a KH Domain Protein That Regulates Blastomere Identity in Early C. Elegans Embryos'. *Cell* 1996. 87 (2): 205–16. https://doi.org/10.1016/s0092-8674(00)81339-2.

Dvinge, Heidi, Eunhee Kim, Omar Abdel-Wahab, and Robert K. Bradley. 'RNA Splicing Factors as Oncoproteins and Tumour Suppressors'. *Nature Reviews Cancer* 2016. 16 (7): 413–30. https://doi.org/10.1038/nrc.2016.51.

Eswaran, Jeyanthy, Anelia Horvath, SuchetaGodbole, SirigiriDivijendra Reddy, PrakritiMudvari, KazufumiOhshiro, Dinesh Cyanam, et al. 'RNA Sequencing of Cancer Reveals Novel Splicing Alterations'. *Scientific Reports* 2013. 3: 1689. https://doi.org/10.1038/srep01689.

Jiang, Hong, Xuemei Zhang, Jinhong Luo, Chunyan Dong, JunliXue, Wei Wei, Jingde Chen, Jun Zhou, Yong Gao, and Changqing Yang. 'Knockdown of HMex-3A by Small RNA Interference Suppresses Cell Proliferation and Migration in Human Gastric Cancer Cells'. *Molecular Medicine Reports* 2012. 6 (3): 575–80. https://doi.org/10.3892/mmr.2012.943.

Latouliere, Luisa de, Isabella Manni, Carla Iacobini, Giuseppe Pugliese, Gian Luca Grazi, Pasquale Perri, Paola Cappello, Franco Novelli, Stefano Menini, and Giulia Piaggio. 2016. 'A Bioluminescent Mouse Model of Proliferation to Highlight Early Stages of Pancreatic Cancer: A Suitable Tool for Preclinical Studies'. Annals of Anatomy = Anatomischer Anzeiger: Official Organ of the Anatomische Gesellschaft 207 (September): 2–8. https://doi.org/10.1016/j.aanat.2015.11.010.

Miller, Kimberly D., Rebecca L. Siegel, Chun Chieh Lin, Angela B. Mariotto, Joan L. Kramer, Julia H. Rowland, Kevin D. Stein, Rick Alteri, and AhmedinJemal. 'Cancer Treatment and Survivorship Statistics, 2016'. *CA: A Cancer Journal for Clinicians* 2016. 66 (4): 271–89. https://doi.org/10.3322/caac.21349.

Neoptolemos, John P., JörgKleeff, Patrick Michl, Eithne Costello, William Greenhalf, and Daniel H. Palmer. 'Therapeutic Developments in Pancreatic Cancer: Current and Future Perspectives'. Nature Reviews. *Gastroenterology& Hepatology* 2018.15 (6): 333–48. https://doi.org/10.1038/s41575-018-0005-x.

Pereira, Bruno, Sofia Sousa, Rita Barros, Laura Carreto, Patrícia Oliveira, Carla Oliveira, Nicolas T. Chartier, et al. 'CDX2 Regulation by the RNA-Binding Protein MEX3A: Impact on Intestinal Differentiation and Stemness'. *Nucleic Acids Research* 2013. 41 (7): 3986–99. https://doi.org/10.1093/nar/gkt087.

Wang, Ze-Lin, Bin Li, Yu-Xia Luo, Qiao Lin, Shu-Rong Liu, Xiao-Qin Zhang, Hui Zhou, Jian-Hua Yang, and Liang-Hu Qu. 'Comprehensive Genomic Characterization of RNA-Binding Proteins across Human Cancers'. *Cell Reports* 2018. 22 (1): 286–98. https://doi.org/10.1016/j.celrep.2017. 12.035.

Chapter V. Role of cyclin-dipendent kinase (CDK) in RNA processing dysregulation

V.1 Role of cyclin-dipendent kinase (CDK) in RNA metabolism

Cyclin-dependent kinases (CDKs) are a family of serine-threonine kinases, whose activity depends on the expression of the cyclins, identified in the 1970s-1980s as proteini nvolved in cell cycle regulation. Beyond their function in cell cycle control, CKIs play also indispensable roles in a variety of biological processes, including transcriptional regulation, epigenetics, DNA damage response and repair (DDR), stemness, metabolism and angiogenesis (Hydbring, Malumbres, and Sicinski 2016)(Liang et al. 2015).

Cell cycle progression is driven by heterodimeric complexes formed by cyclin with cyclin-dependent kinase (CDK 4, 6, 2, 1). Cell cycle entry is driven by the formation of cyclin D–CDK4/6 complexes that phosphorylate and inactivate the retinoblastoma protein, pRB, thus E2F is activated and promotes the expression of multiple cell cycle genes. The activation of CDK2, by cyclin E, leads to the phosphorylation of multiple transcription factors, like NF-Y and MYC, contributing to regulation of cell cycle. Conversely the Cyclin D1 – CDK4 complex inhibits the anti-proliferative genes following inactivation of transcription factors such as SMAD3 (Otto and Sicinski 2017).

At transcriptional level the CDKs act phosphorylating the serine of carboxyl-terminal domain (CTD) of the RNA polymerase II (RNAPII), consisting of 52 heptad repeats of the YSPTSPS. The transcription process is divided into accurate phases of initiation, pausing, elongation, termination and the CDKs occur their action in each specific phase. CDK8 is required to activate the transcription machinery at the promoter level and it modulates CDK7 activity by phosphorylation cyclin H, its partner. CDK7 phosphorylates Ser5 and Ser7 duringin itiation and phosphorylates CDK9, that together whit CDK12/CDK13 phosphorylate Ser2 promoting elongation of RNAPII (Fig.17) (Sánchez-Martínez et al. 2019).

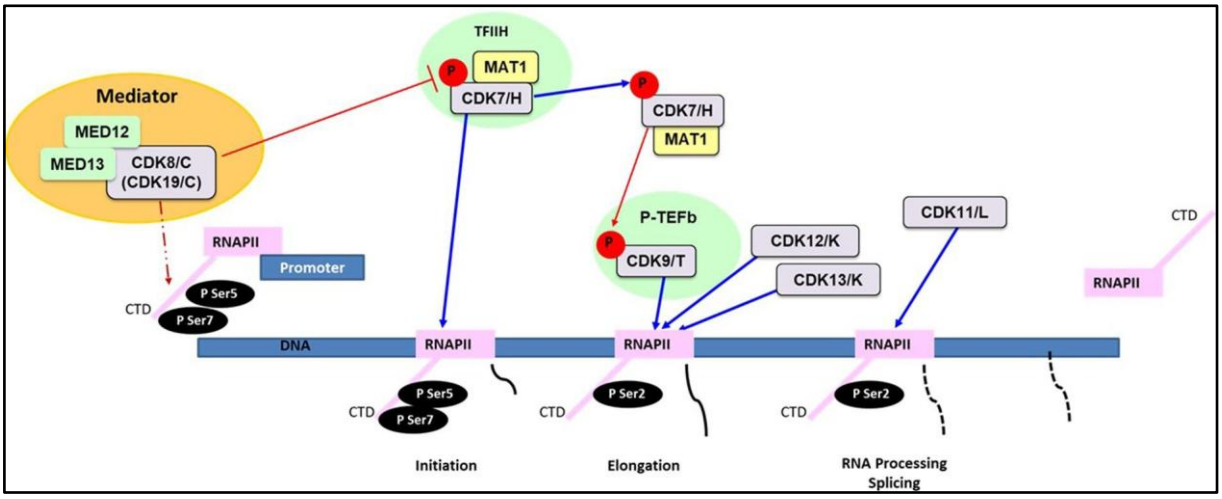

Figure 17. Regulation of RNA PolII by CDKs (Sánchez-Martínez et al. 2019)

CDK12 and CDK13 regulate both constitutive and alternative RNA splicing by virtue of their RS motifs. By this activity, CDK12 and 13 contribute to the maintaining of self-renewal in mouse embryonic stem cells (Dai et al. 2012) and to the regulation of axonal elongation (Chen et al. 2014). Despite their similarity, CDK12 and CDK13 do not have identical functions and recent studies indicate that CDK13 regulates distinct subsets of genes and biological processes from CDK12, including snRNA and snoRNA gene expression, and extracellular/growth signalling pathways (Liang et al. 2015). CDK12 controls alternative polyadenylation (APA), specifically regulating the expression of genes involved in response to DNA damage, stress, and heat shock (Dubbury, Boutz, and Sharp 2018)(Li et al. 2017). Since the CDKs are often deregulated in cancer, in the last decades many CDK inhibitor were developed and there are several ongoing clinical trials. The first CDK inhibitors developed clinically lacked potency and selectivity, and had limited therapeutic effect; an example is Flavopiridol, that has been investigated as a single agent and in combinations, but with low levels of activity and high toxicity seen. Dinaciclib, a multi-CDK-inhibitor (CDK 1, 2, 5, 9), first described in 2010, shows abetter tolerance over longer times pans, especially in refractory patients (Parry et al. 2010). The action of dinaciclib in combination with MK-2206, an inhibitor pf AKT, limits pancreatic tumor growth and metastases in patient-derived xenograft models (Hu et al. 2015). Abemaciclib and palbociclib are CDK4/6 inhibitors FDA-approved for certain advanced breast cancers (Lee, Shepherd, and Johnston 2019)(J. Lu 2015). Studies investigate the effects of combinatory treatments with palbociclib on pancreatic cancer are on going: Cisplatin, Carboplatin (NCT02897375, *ClinicalTrials.gov*),ERK1/2 Inhibitor (NCT03454035, *ClinicalTrials.gov*) and PI3K/mTOR (NCT03065062*, ClinicalTrials.gov*).

V.2 RNA processing dysregulation as tool to sensitize PDAC cells to therapeutic treatments.

V.2.1 Background

The most frequent mutation in PDAC affects the KRAS oncogene, with >90% incidence (Waters and Der 2018) and the most aggressive subtypes of PDAC are characterized by expression of genes involved in inflammation, hypoxia, metabolic reprogramming, TGF-β and MYC pathways. Interestingly, KRAS stabilizes MYC protein and dictates dependency on this pathway in PDAC cells (Vaseva et al. 2018). MYC up-regulation frequently occurs in cancer cells, leading to global transcription activation. This condition generates a transcriptional overload, causing a stress on the splicing machinery (Dang 2012)(Bradner, Hnisz, and Young 2017) and rendering MYC-overexpressing cells particularly sensitive to splicing inhibition(Hsu et al. 2015).

Regarding PDAC, it was previously shown that both acute and chronic treatment with chemotherapeutic agents causes up-regulation of splicing factors, such as SRSF1 and PTBP1, which in turn enhance the ability of PDAC cells to withstand genotoxic treatments through splicing modulation (Adesso et al. 2013)(Calabretta et al. 2016). Furthermore, a recent study has highlighted global splicing dysregulation in PDAC (J. Wang et al. 2017), even though the splicing factors and/or the mechanisms responsible for such alteration were not characterized.

Splicing dysregulation in cancer is often due to aberrant expression of splicing regulatory proteins (Paronetto, Passacantilli, and Sette 2016)(Diederichs et al. 2016). For instance, MYC drives the expression of multiple core spliceosome proteins and of accessory splicing factors in cancer cells, including the oncogenic SRSF1 (Das et al. 2012), PTBP1 (David et al. 2010) and Sam68 (Caggiano et al. 2019). These observations suggest that elucidation of the RNA processing mechanisms and of the splicing signatures altered in PDAC cells may reveal new biomarkers for this disease.

V.2.2 Results

MYC-overexpressing tumors are particularly sensitive to inhibition of transcription and/or splicing (Bradner, Hnisz, and Young 2017). Recent data have shown that PDAC cells with high MYC levels are strongly sensitive to THZ1, a cyclin dependent kinase inhibitor (CDKi) for CDK7, CDK12 and CDK13, which all regulate the elongation rate of the RNA polymerase (RNAPII)(Lu et al. 2019). THZ1 also represses MYC expressionand was proposed as valuable drug for the MYC

overexpressing triple-negative breast cancer (TNBC)(Li et al. 2017). We found that MiaPaCa-2 cells are much more sensitive to THZ1 than the TNBC cell line MDA-MB-231 (Fig.18 A). Moreover, MiaPaCa-2 cells were also highly sensitive to other CDKi with wider (dinaciclib: pan-CDKi) or narrower (THZ531: inh. of CDK12 and CDK13) spectrum of action (Fig.18B). All CDKi exerted much stronger effects on cell viability than JQ1 (Fig.18C), a BRD4 inhibitor that impacts on transcription and MYC function that is in clinical trials for PDAC.

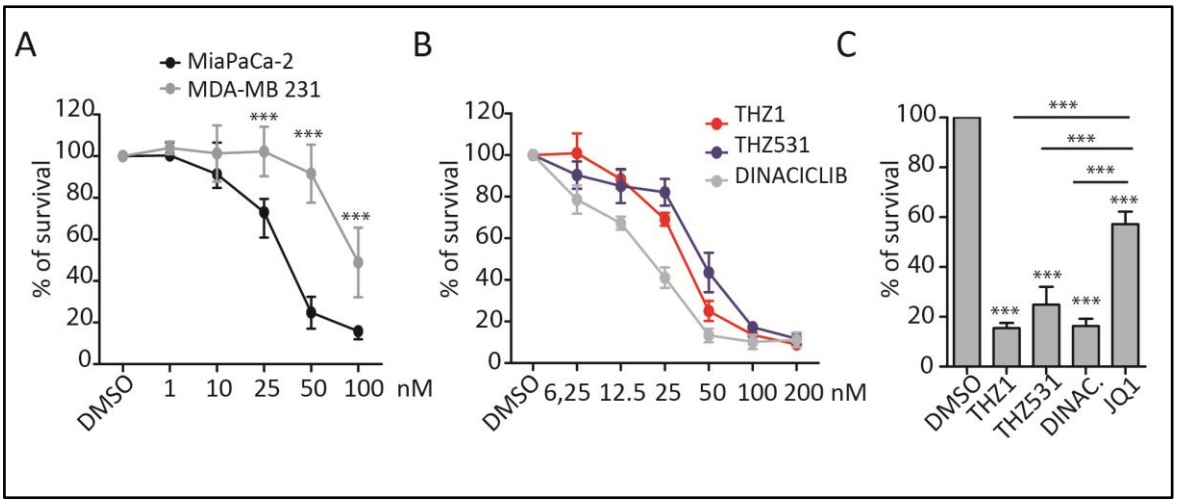

Figure 18. MiaPaCa2 cells are sensitive to CDKi THZ1 and THZ531. A) MTS assay of MiaPaCa-2 and MDA-MB 231 cells treated for 72h with THZ1. **B)** MTS assay of MiaPaCa-2 cells treated for 72h with indicated doses of THZ1, THZ531 and DINACICLIB. **C)** MTS assay of MiaPaCa-2 cells treated with THZ1 (100nM), THZ531 (100nM), DINACICLIB (100nM) and JQ1 (800nM) for 72h.(***P ≤ 0.001, according to one-way Anova).

Since THZ531 displayed comparable activity with the other CDKi, our analysis suggests that inhibition of CDK12 and CDK13 alone might represent a valuable therapeutic approach to limit PDAC cell proliferation/survival. Notably CDK13 expression correlated with poor PFS in PDAC patients from our bioinformatics screening of "The Cancer Genome Atlas (TCGA)" database (Fig. 19) (Panzeri V. at al. *paper in preparation*, see paragraph IV.4 of thesis).

Putative oncogenic genes

Gene	HRcox	p logrank
TRA2A	2.1362[1.4441-3.16]	0,011896569
CDK13	1.2443[0.97579-1.5868]	0,031075862
SRRM1	1.2477[0.98253-1.5843]	0,037657102
IGF2BP3	1.5926[1.028-2.4673]	0,038826593
MEX3A	2.1851[1.5012-3.1805]	0,04004883

Figure 19. Kinases expression is significantly correlated with PFS in PDAC patients in TGCA database. Kinases whose expression is significantly correlated with PFS inPDAC patients in TGCA database.

Since MYC promotes expression of several RBPs, we also checked whether CDKi affected expression of RBPs in PDAC cells (Hsu et al. 2015). Western blot analyses showed that expression of some oncogenic RBPs was selectively inhibited by either THZ1 (hnRNPA1 and PTBP1) or THZ531 (MEX3A), whereas others (SRSF1, hnRNPH) were targeted by both drugs (Fig. 20A). Moreover, mass spectrometry analyses demonstrated that CDK12/13 are associate with numerous RNA processing factor (e.g. SRSF1, Sam68, TRA2A, ect.)(Liang et al. 2015b). This result suggests that CDKi may exert widespread effects on transcriptome regulation in PDAC also through regulation of RBP expression or activity. In support of this hypothesis, the reduced MEX3A levels caused by THZ531 treatment correlated with reduced expression of its target mRNAs (Cyclin D1; Fig.20 B) (Panzeri V. at al. *paper in preparation*, see paragraph IV.4 of thesis).

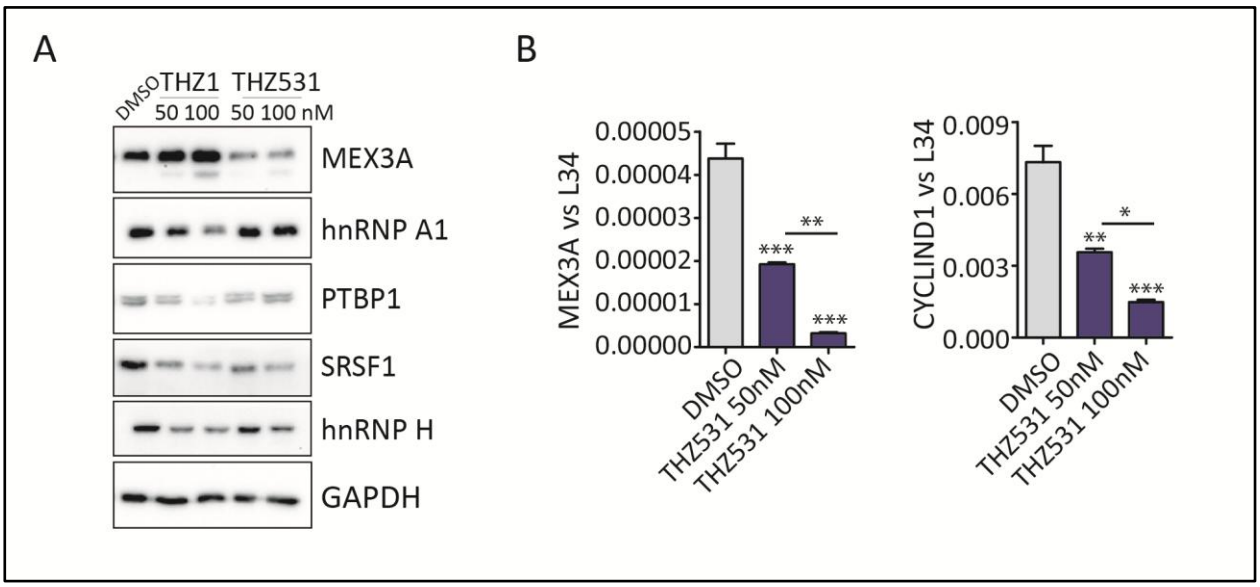

Figure 20. CDKi modulate RBP expression and its target mRNA. A)Western blot analysis of RBPs after 48h of treatment with THZ1 (50nM) and THZ531 (100nM). B) qRTPCR analysis of MEX3A and CYCLIN D1 mRNA levels after treatment withTHZ531. Statistical analyses were performed by One way Anova (C,E) (*P≤0.05, **P ≤ 0.01, ***P ≤ 0.001).

CDK12 depletion represses DNA damage response (DDR) genes due to defective RNA processing and premature cleavage at internal polyadenylation sites (IPA) of their pre-mRNAs(Dubbury, Boutz, and Sharp 2018). THZ531, and to a lesser extent THZ1, caused IPA selection in PDAC cells (Fig.21 A) and this affect is attributed to action of CDK12, because only the depletion of CDK12, and not of CDK13, increase the IPA level of ATM and FANCD2 (Fig. 21 B). These results indicate a crucial role of the CDK12/13 pathways in PDAC and suggest that of CDK12/13-dependent RNA processing in PDAC may enhance therapeutic treatments in PDAC.

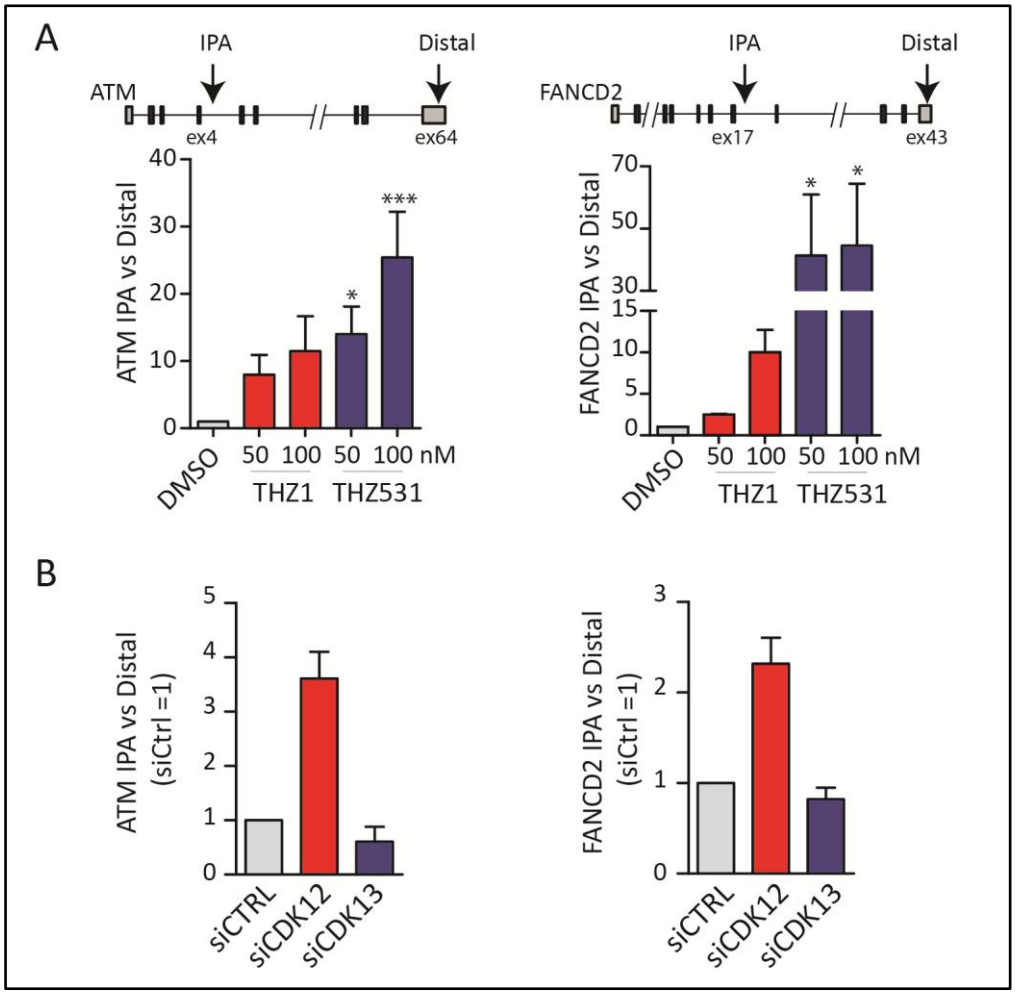

Figure 21. DKi modulate DDR genes. A) qRT-PCR analysis to evaluate the increased of IPA events in ATM and FANCD2 genes after 24h of treatment with THZ1 and THZ531 (50-100nM).

These results indicate a crucial role of CDK pathways involved in RNA processing in PDAC and combined treatment of chemotherapy and CDKi may represent a valuable therapeutic approach for PDAC.

Appendix

Here I report twopaperspublished to which I contributed during my PhD. These studies have been performed in bladder cancer and prostate cancer, but may also have implications in PDAC. polypyrimidine-tract binding protein PTBP1 is up-regulated in drug resistant (DR) PDAC cells and it promotesPKM2 splicing, favouring the acquisition of chemotherapy resistance in pancreatic cancer(Calabretta et al. 2016). Moreover, by bioinformatic analysis with R2 database (https://r2.amc.nl) emerges that PTBP1 is upregulated in patients with poor prognosis in PDAC-TCGA dataset (Fig. 22).

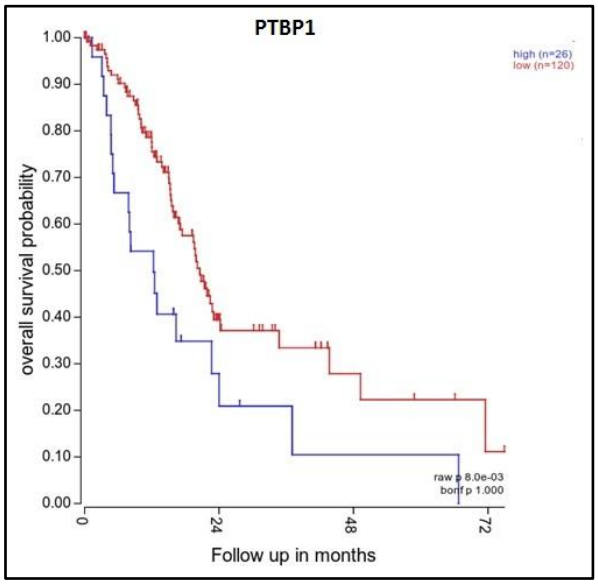

Figure 22. Kaplam Maier curve of Overall Survival for PTBP1 in PDAC patients, p value= $8x10^{-3}$.

The oncogene c-MYC is a transcription factor involed in tumor growth, proliferation, transcription and metabolism of cancer cell, moreover it orchestrates changes in the tumor microenvironment, including suppression of the host immune response and activation of angiogenesis. It is altered in many type of cancer including in PDAC, understanding mechanisms of action of c-MYC can help to detect potential to therapeutic target also in PDAC (Hessmann et al. 2016).

1. Paper "The Splicing Factor PTBP1 Promotes Expression of Oncogenic Splice Variants and Predicts Poor Prognosis in Patients with Non-muscle-Invasive Bladder Cancer"

Bielli P, **Panzeri V**, Lattanzio R, Mutascio S, Pieraccioli M, Volpe E, Pagliarulo V, Piantelli M, Giannantoni A, Di Stasi SM, Sette C.

Clin Cancer Res. 2018 Nov 1;24(21):5422-5432.

Published OnlineFirst July 16, 2018; DOI: 10.1158/1078-0432.CCR-17-3850

Translational Cancer Mechanisms and Therapy

Clinical Cancer Research

The Splicing Factor PTBP1 Promotes Expression of Oncogenic Splice Variants and Predicts Poor Prognosis in Patients with Non–muscle-Invasive Bladder Cancer

Pamela Bielli[1,2], Valentina Panzeri[2,3,4], Rossano Lattanzio[5,6], Simona Mutascio[1,2], Marco Pieraccioli, [1,2], Elisabetta Volpe[2], Vincenzo Pagliarulo[7], Mauro Piantelli[5], Antonella Giannantoni[8], Savino M. Di Stasi[9], and Claudio Sette[2,4]

Abstract

Purpose: Non–muscle-invasive bladder cancer (NMIBC) is a malignant disease characterized by high heterogeneity, which corresponds to dysregulated gene expression and alternative splicing (AS) profiles. Bioinformatics analyses of splicing factors potentially linked to bladder cancer progression identified the heterogeneous nuclear ribonucleoprotein I (i.e., PTBP1) as candidate. This study aimed at investigating whether PTBP1 expression associates with clinical outcome in patients with NMIBC.

Experimental Design: A cohort of 152 patients presenting with primary NMIBC (pTa-pT1) was enrolled. Primary NMIBCs were assessed for PTBP1 expression by IHC, and the results were correlated with clinical data using Kaplan–Meier curves and Cox regression analyses. Cell proliferation and survival assays were performed to assess the function of PTBP1. Furthermore, the impact of PTBP1 on the AS pattern of specific bladder cancer–related genes was investigated in cancer cell lines and in patients' specimens.

Results: Public datasets querying highlighted a positive correlation between PTBP1 expression and NMIBC progression, which was then confirmed by IHC analysis. High PTBP1 expression was associated with worse clinical outcome in terms of incidence of tumor relapse and survival in patients with NMIBC. Interestingly, downregulation of PTBP1 in bladder cancer cell lines affected prosurvival features. Accordingly, PTBP1 modulated AS of bladder cancer–related genes in cell lines and patient's specimens.

Conclusions: PTBP1 expression correlates with disease progression, poor prognosis, and worse survival in patients with NMIBC. Downregulation of PTBP1 expression affects prosurvival features of bladder cancer cells and modulates AS of genes with relevance for bladder cancer, suggesting its role as an outcome-predictor in this disease. *Clin Cancer Res; 24(21); 5422–32. ©2018 AACR.*

Introduction

Bladder cancer is the sixth most common cancer in men, with an estimated 429,800 cases diagnosed in 2012 and 165,100 deaths for the disease worldwide (1). It is typically subdivided in three main categories on the basis of management goals and prognosis: non—muscle-invasive bladder cancer (NMIBC), muscle-invasive bladder cancer, and metastatic bladder cancer. NMIBC represents the most frequent form and includes carcinoma *in situ* (stage Tis), papillary lesions confined to the urothelium (stage Ta), or invading the lamina propria (stage T1; ref. 2). Complete transurethral resection of bladder tumors (TURBT) is the routine initial diagnostic and therapeutic step in management. However, over 50% NMIBCs will recur and up to 25% will progress to muscle-invasive disease (3). Because of the probability of recurrence and progression, NMIBC requires repeated surveillance and intervention and is among the most expensive cancers to treat from diagnosis to death (4).

Criteria assessing patient and tumor characteristics provide valuable information about disease recurrence, progression, and

[1]Department of Biomedicine and Prevention, University of Rome Tor Vergata, Rome, Italy. [2]Fondazione Santa Lucia IRCCS, Rome, Italy. [3]Department of Science Medical/Chirurgic and Translational Medicine, University of Rome "Sapienza", Rome, Italy. [4]Institute of Human Anatomy and Cell Biology, Università Cattolica del Sacro Cuore, Rome, Italy. [5]Department of Medical, Oral & Biotechnological Sciences, G. d'Annunzio University, Chieti, Italy. [6]Center of Excellence on Aging and Translational Medicine (CeSi-Met), G. d'Annunzio University, Chieti, Italy. [7]Department of Emergency and Organ Transplantation, University Aldo Moro, Bari, Italy. [8]Department of Surgical and Biomedical Sciences, University of Perugia, Perugia, Italy. [9]Department of Experimental Medicine and Surgery, University of Rome Tor Vergata, Rome, Italy.

Note: Supplementary data for this article are available at Clinical Cancer Research Online (http://clincancerres.aacrjournals.org/).

S.M. Di Stasi and C. Sette contributed equally to this article.

Corresponding Authors: Claudio Sette, Catholic University of the Sacred Heart, Largo Francesco Vito 1, Rome 00168, Italy. Phone: 3906-5017-03264; Fax: 3906-5017-03338; E-mail: claudio.sette@unicatt.it; and Savino M. Di Stasi, Department of Experimental Medicine and Surgery, University of Rome Tor Vergata, Via Montpellier 1, Rome 00133, Italy. E-mail: sdistas@tin.it

doi: 10.1158/1078-0432.CCR-17-3850

Published OnlineFirst July 16, 2018; DOI: 10.1158/1078-0432.CCR-17-3850

Translational Relevance

PTBP1 expression positively correlates with NMIBC progression and with worse clinical outcome of patients. Mechanistically, PTBP1 regulates prosurvival features and modulates alternative splicing of bladder cancer–related genes in NMIBC cell lines and patient specimens. Thus, PTBP1 expression and its splicing signature can represent novel outcome-predictor markers for NMIBC.

proposed treatments. The European Organisation for Research and Treatment of Cancer (EORTC) electronic risk calculator (http://www.eortc.be/tools/bladdercalculator) is commonly used to assess recurrence and progression potential of newly diagnosed cancers. The parameters used are tumor size and number, pathologic stage and grade, presence of carcinoma *in situ* (CIS), and prior recurrence rate (5). Ease of use and absence of expensive molecular tests represent the main advantages of this and other scoring models (6, 7). However, reproducibility of pathologic stage and grade is modest and remains a critical clinical concern.

Strong efforts are currently aimed at identifying molecular markers with robust diagnostic and prognostic value for NMIBC (8). Although several molecular markers are currently approved by the FDA and its European counterpart (9), their value in predicting NMIBC recurrence and progression is limited and none of them is recommended by clinical guidelines (10). Thus, identification of valuable markers or therapeutic targets that reduce the likelihood of recurrence and/or progression is a clinical priority for NMIBC management.

Dysregulation of splicing is emerging as a key feature of human cancers with therapeutic perspective (11). Splicing leads to excision of introns and ligation of exons from the precursor mRNA (pre-mRNA) and is orchestrated by the spliceosome, a macromolecular machinery composed of five small nuclear ribonucleoprotein particles and hundreds of auxiliary proteins (12). When the exon–intron boundaries (splice sites) display high levels of conservation, exons are almost always included in the mRNA (constitutive exons), whereas exons lacking strong consensus sequences are subjected to regulation (alternative exons). In this case, exon recognition is tuned by *trans*-acting splicing factors (SF) that bind to *cis*-regulatory sequences. The interplay between antagonistic SFs determines whether a target exon is included or skipped through a process named alternative splicing (AS; ref. 12). Because most splice isoforms engage specific interactions and behave as distinct proteins (13), AS increases the coding potential of genomes and represents an evolutionary advantage (14). However, its flexible regulation is prone to errors and defective splicing contributes to neoplastic transformation (11, 13). In this regard, splicing inhibition is envisioned as an effective anticancer therapy, as many tumors are very sensitive to this approach (11).

The main classes of SFs are the serine-arginine (SR) proteins and the heterogeneous nuclear ribonucleoproteins (hnRNP), which often act antagonistically in AS regulation (12). Members of both classes, like SRSF1 (15, 16) and hnRNPA1, A2 and I (also known as PTBP1; refs. 17, 18), were shown to play oncogenic functions. Notably, although AS dysregulation has been reported also in bladder cancer (19), limited information is available regarding the SFs responsible for this process and their possible association with prognosis. Herein, we have performed bioinformatics search for SR and hnRNP proteins associated with bladder cancer progression. Our study identified hnRNPI/PTBP1 as a factor linked to disease progression and suggest PTBP1 as a new prognostic factor and possible therapeutic target for NMIBC progression.

Materials and Methods

Bioinformatics analysis

R2 genomics platform (http://r2.amc.nl) and Oncomine database (www.oncomine.org) were used to evaluate the association of splicing factors with bladder cancer grade using Hoglund, Dyrskjot, and Sanchez-Carbayo datasets (20–22).

Study population and ethics statement

Patients with histologically proven primary pTa and pT1 bladder urothelial carcinoma were enrolled in the study. Inclusion criteria were as follows: age $\geq$18 years, adequate bone marrow reserve, normal renal and liver function and Eastern Cooperative Oncology Group performance status between 0 and 2 (23). Exclusion criteria were as follows: previous bladder cancer; non-urothelial carcinomas; previous or concomitant urinary tract carcinoma *in situ* and urothelial carcinoma of the upper urinary tract and urethra; bladder capacity less than 200 mL; untreated urinary tract infection; severe systemic infection; urethral strictures preventing endoscopic catheterization; previous radiotherapy to the pelvis; other concurrent chemotherapy, radiotherapy, treatment with biological response modifiers; other malignant diseases within 5 years of trial registration (except for adequately treated basal cell or squamous cell skin cancer, and *in situ* cervical cancer); pregnancy; other factors precluding study participation.

All patients underwent TURBT of endoscopically detected tumors, ensuring that muscle was included in resected samples, as specified by European Association of Urology guidelines (2). Before TURBT, a cold-cup biopsy of apparently nontumor-bearing and tumor were taken and stored at -80°C until analysis. Tumors were staged in accordance with the TNM classification (24) and biopsies were graded according to WHO classifications (25). Risk categories for recurrence and progression were assessed in accordance with EORTC risk tables for NMIBC (5). Within 6 hours of TURBT, patients received a single intravesical instillation of 40 mg mitomycin. Four to 6 weeks after TURBT, patients without muscle in resected samples, positive or suspect cytology, carcinoma *in situ*, stage T1, or grade 3 tumors underwent restaging transurethral resection, random cold-cup bladder and prostatic urethra biopsies, and upper urinary tract imaging. No adjuvant intravesical therapy was given to patients with low-risk NMIBC. Patients with intermediate-risk and high-risk NMIBC were scheduled to receive adjuvant long-term intravesical chemotherapy with mitomycin, or immunotherapy with bacillus Calmette-Guerin, starting approximately 3 weeks after TURBT procedures. Patients were followed up with abdominal ultrasonography, urinary cytology, and cystoscopy every 3 months for 2 years, twice during the third year, and yearly thereafter.

All procedures performed in studies involving human participants were in accordance with the ethical standards and with the Declaration of Helsinki. The Institutional Review Board approved the study design, and all enrolled patients signed an informed consent form providing details of treatments.

Published OnlineFirst July 16, 2018; DOI: 10.1158/1078-0432.CCR-17-3850

IHC and statistical analysis

PTBP1 IHC was performed on formalin-fixed, paraffin-embedded tissues obtained from 152 patients with primary pTa-pT1 NMIBC. Antigen was retrieved by microwave treatment at 750 W for 10 minutes in 10 mmol/L sodium citrate buffer (pH 6.0). Sections were incubated for 60 minutes at room temperature with 1:500 anti-PTBP1 antibody (sc-16547, Santa Cruz Biotechnology), or nonimmune serum as control, using the LSAB Signal Amplification Kit (K0690, Dako). PTBP1 expression was defined by the presence of nuclear staining in tumor cells. IHC analysis was done in blind by two pathologists (M. Pieraccioli and R. Lattanzio) unaware of clinicopathologic information, with 80% concordance in evaluation. Thirty cases (19.7%) in which evaluation of PTBP1 expression differed by >10% between the two observers were reevaluated. After consensus was achieved, the absolute interobserver variability (mean difference % ± SD) recorded was 3.95% ± 3.14%.

The relationship between PTBP1 expression and clinicopathologic parameters was investigated by Pearson χ^2 test or Fisher exact test. All clinical analyses were performed on an intent-to-treat basis. Primary endpoint was disease-free interval (DFS), defined as time from initial TURBT randomization to first cystoscopy noting recurrence. Secondary endpoints were progression-free (PFS), overall (OS), and disease-specific survival (DSS). Starting from initial TURBT, PFS was defined as time until onset of muscle-invasive disease as recorded by pathologic assessment of transurethral resection samples or biopsy samples, OS as time until death from any cause, and DSS as time until death from bladder cancer. Patients without recurrence or progression were censored at the last cystoscopy, and those lost to follow-up were censored at the last known day of survival. Endpoints were studied by the Kaplan–Meier method and comparisons were made by the log-rank test. Association of PTBP1 expression with outcome, adjusted for other prognostic factors, was tested by Cox proportional hazards model. Appropriateness of the proportional hazard assumption was assessed by plotting the log cumulative hazard functions over time and checking for parallelism. SPSS Version 15.0 (SPSS) was used throughout and $P < 0.05$ was considered statistically significant.

Cell cultures and manipulations

Bladder cancer cell lines, RT4, RT112, and EJ (26), were purchased and kindly provided by Dr. Francesca Velotti (La Tuscia University, Viterbo, Italy), and further authentication has not been performed. Bladder cancer cell lines were cultured in RPMI1640 medium (LONZA) supplemented with 10% FBS (Gibco) at 37°C with 5% CO_2. *Mycoplasma* contamination of cell cultures was routinely tested by Hoechst 33258 stain (27), every 2 to 3 weeks. Upon thawing, bladder cancer cell lines have been subcultured for not more than 15 passages. RNAi experiments, protein extractions, and immunofluorescence analyses were performed as described previously (28, 29).

For clonogenic, cell cycle, proliferation, and adhesion assays, cells were silenced twice with CTRL or PTBP1 siRNAi (80 nmol/L). Colony-forming assay was performed as described previously (30). Briefly, 24 hours after transfection, 400 cells were plated in 60-mm dishes and cultured for one week. After fixation-staining for 30 minutes with glutaraldehyde 6.0% (v/v)/crystal violet 0.5% (w/v) solution, colonies with n >50 cells were counted.

For cell cycle/sub-G_1 analyses, cells were pulse-labeled with 10 μmol/L BrdU for 45 minutes before harvesting and fixed with a 30% PBS/70% ethanol solution for 30 minutes in ice. Hypodiploid events and cell cycle were evaluated by flow cytometry using propidium iodide (PI) staining (20 μg/mL) and anti-BrdU antibody in the presence of 13 Kunitz U/mL ribonuclease A as described previously (31). A total of 15×10^3 events were counted with FACSCalibur flow cytometer (Becton Dickinson) and analyzed using FlowJo program (Becton Dickinson).

Cell death was evaluated by staining for Annexin V (1 μg/mL) and PI (1 μg/mL; eBioscience) and analyzed by flow cytometry (FACSCanto; BD Biosciences). The combination of Annexin V and PI staining discriminates live cells (Annexin V/PI double negative) from apoptotic cells (Annexin V/PI double positive).

Splicing assay, UV-crosslinked RNA immunoprecipitation (CLIP), and qRT-PCR analyses

RNA was extracted from cells using TRIzol reagent (Invitrogen), and PCR analyses were performed as described previously (28, 29). Primers are listed in Supplementary Information. Quantitative expression level of CD44 variable exons was calculated by ΔC_t method relative to total CD44. CLIP assays were performed as extensively described and RNA associated with PTBP1 was represented as percentage of input (32).

Results

PTBP1 expression correlates with poor prognosis in tumor bladder patients

Public datasets (R2 genomics analysis and visualization platform, http://r2.amc.nl) were queried for correlation between expression of SR proteins and hnRNPs and bladder cancer progression. Expression of PTBP1 (i.e., hnRNPI) was found to significantly correlate with disease progression in the Hoglund cohort including 308 patients (Fig. 1A; Supplementary Fig. S1A). PTBP1 expression also resulted significantly higher in invasive T1 stage compared with noninvasive Ta stage cancers (Fig. 1B). Analysis of two other datasets (https://www.oncomine.org: Dyrskjot and Sanchez-Carbayo datasets) confirmed that PTBP1 expression is increased in infiltrating and superficial bladder cancers compared with normal tissue (Supplementary Fig. S1B–S1D). More importantly, Kaplan–Meier analysis highlighted significant association between high PTBP1 mRNA expression and low OS probability ($P < 0.001$; Fig. 1C). In contrast, expression of other SFs was either unchanged or slightly affected, or associated only with G3 tumors (i.e., hnRNPA2B1, hnRNPC, hnRNPL, SRSF7, and SRSF10; Fig. 1A; Supplementary Fig. S1A).

To determine whether the bioinformatics analysis of mRNA expression levels in public databases represents a valuable tool to identify proteins with oncogenic potential, PTBP1 upregulation was also tested at the protein level by Western blot analysis using a cohort of surgical tumor (T) and nontumor (NT) specimens from 50 patients with NMIBC. PTBP1 protein was significantly increased in the neoplastic lesions compared with the adjacent nonneoplastic urothelium ($P = 0.003$; Fig. 2A). To extend this analysis, we enrolled a cohort of 178 patients. After initial TURBT, we excluded 13 patients because of concomitant urothelial carcinoma of the upper urinary tract ($n = 3$) and prostatic urethra

Published OnlineFirst July 16, 2018; DOI: 10.1158/1078-0432.CCR-17-3850

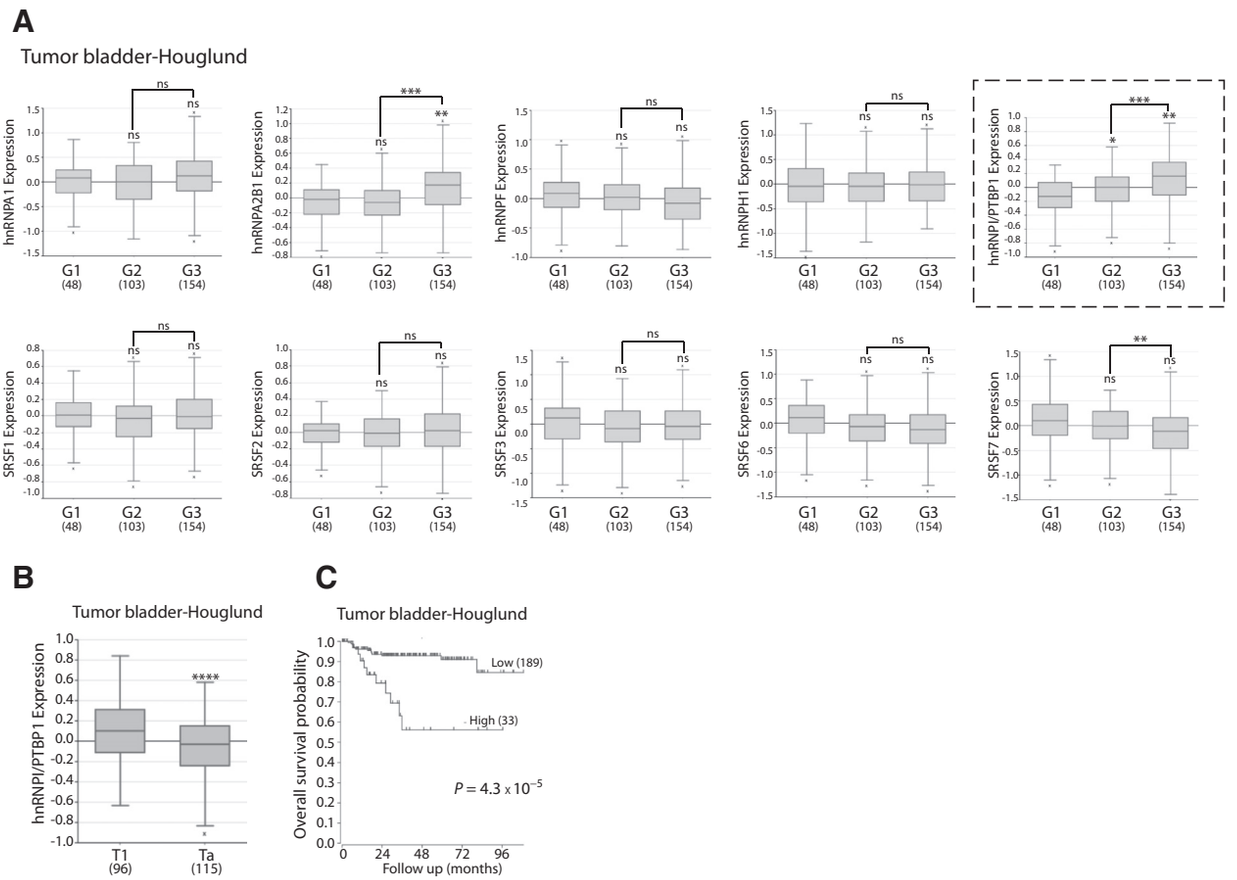

Figure 1.

mRNA expression level of the splicing factor PTBP1 is increased in bladder tumor. Analysis of the expression of splicing factors in tumor bladder patients at stage G1 versus stage G2 and stage G3 (**A**) and at stage Ta (noninvasive papillary carcinoma) versus stage T1 (invasive carcinoma); **B**. Boxes, median (horizontal line); whiskers, distances from the largest and smallest value to each end of the box; dots, outliers. Mean values were compared with the two-tailed unpaired *t* test. Data used for the analysis are from GSE 32894 Tumor Bladder-Hoglund-dataset (308 patients) deposited in R2 genomics analysis and visualization platform (http://r2.amc.nl). ns, no significance; *, $P \leq 0.05$; **, $P \leq 0.01$; ***, $P \leq 0.001$. **C,** Kaplan–Meier overall survival analysis of the total Hoglund cohort based on the cut-off value of PTBP1 expression levels calculated by the R2 system. The difference between the curves for PTBP1-high and PTBP1-low groups were compared by log-rank test.

($n = 4$), histology other than pure urothelial carcinoma ($n = 4$), and consent refusal ($n = 2$). Restaging TURBT was performed in 69 patients (54 with high-risk disease and 15 with multifocal intermediate-risk disease) and histologic findings showed that 10 patients with residual stage pTa or pT1 tumor were eligible, whereas 9 with concomitant carcinoma *in situ* (pTis) and 4 with muscle-invasive disease (stage pT2) were ineligible. Of the remaining 152 patients (see clinical features and tumor characteristics in Table 1), 74 cases (48.7%) were noninvasive papillary carcinoma (pTa) and 78 (51.3%) were tumors invading subepithelial connective tissue (pT1). According to EORTC risk tables classification for NMIBC (5), the cancer progression risk was low in 27 cases (17.7%), intermediate in 70 cases (46.1%), and high in 54 cases (36.2%; Table 1).

Percentage of PTBP1-positive cells was significantly higher in tumor specimens with respect to the nonneoplastic urothelium (Supplementary Fig. S2A), and it ranged from 3% to 98% (mean ± SE = 40.7 ± 2.9) in tumor tissues. Examples of PTBP1 expression in patients with low-, intermediate-, and high-risk of cancer progression are shown in Fig. 2B. Notably, significant increase in PTBP1 expression was associated with risk of cancer progression (Fig. 2C).

To dichotomize PTBP1 expression, a cutoff of 6% positive cells was chosen according to the ROC curve analysis (AUC = 0.779, $P < 0.001$; Supplementary Fig. S2B and S2C). Tumors with >6% positive cells ($n = 105$) were considered PTBP1^{High} and those with ≤6% positive cells ($n = 47$) were PTBP1^{Low}. PTBP1 expression directly correlated with pT1 tumors ($P < 0.001$), grade 3 tumors ($P < 0.001$), and tumors with high risk of progression ($P < 0.001$; Table 1). We also found direct correlation between PTBP1^{High} and the number of patients experiencing tumor recurrence ($P = 0.001$), cancer progression ($P = 0.021$), overall mortality ($P = 0.047$), and cancer mortality ($P = 0.029$; Table 1). Furthermore, Kaplan–Meier analysis indicated that PTBP1^{High} expression was significantly associated with lower DFS, PFS, OS, and DSS rates (Fig. 2D). In particular, survival rates for patients with PTBP1^{High} and PTBP1^{Low} tumors were 39.0% versus 68.1% (DFS; $P < 0.001$), 89.5% versus 100.0% (PFS; $P = 0.023$), 57.1% versus 74.5% (OS; $P = 0.006$), and 90.5% versus 100.0% (DSS; $P = 0.024$).

Published OnlineFirst July 16, 2018; DOI: 10.1158/1078-0432.CCR-17-3850

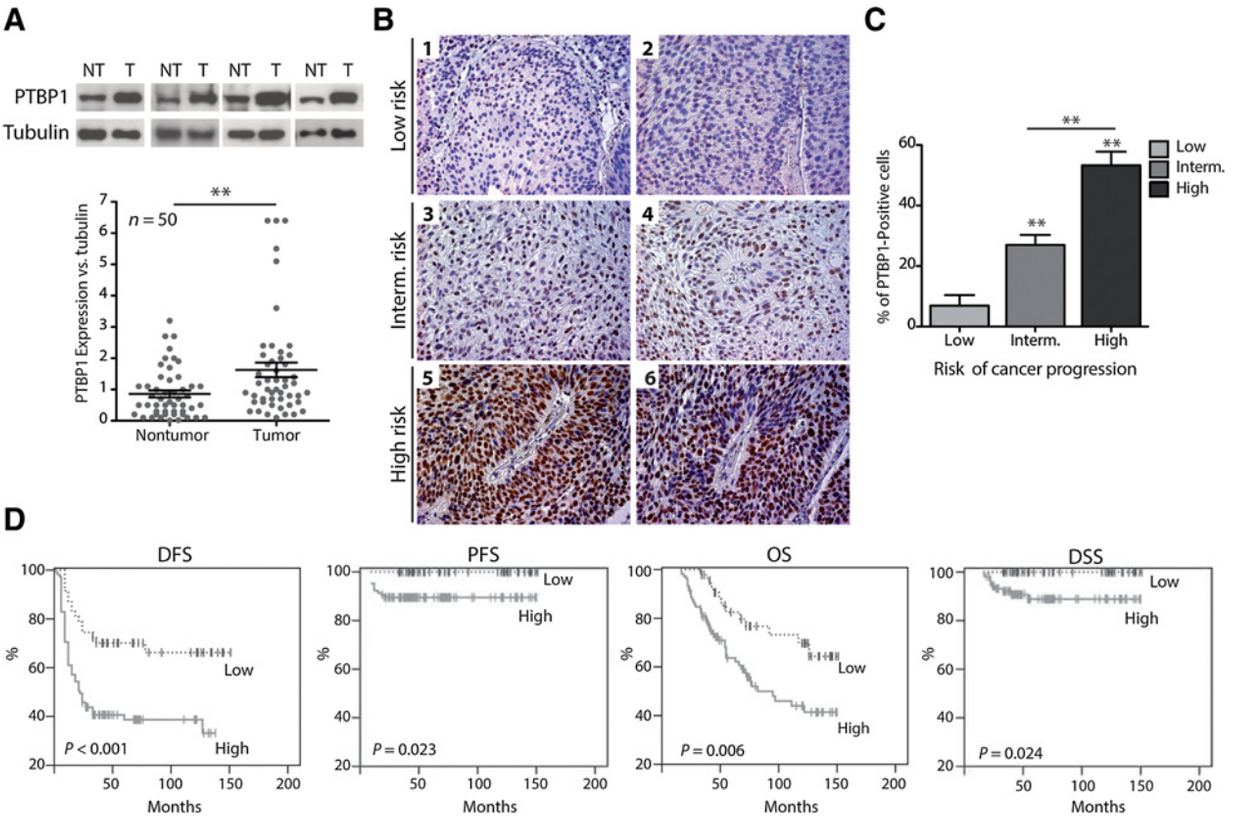

Figure 2.

PTBP1 expression correlates with bladder cancer patient outcome. **A,** Representative Western blot analysis of PTBP1 expression in tumor (T) and adjacent nontumor (NT) surgical specimens from 4 of the 50 patients with NMIBC examined (top). Tubulin was used as loading control. Densitometric analysis of PTBP1 expression relative to tubulin in nontumor and tumor specimens is shown in the dots graph below ($n = 50$; **, $P < 0.001$, independent-sample t test). **B,** Representative images of IHC analysis of PTBP1 expression in two patients with low- (1, 2), intermediate- (3, 4), and high- (5, 6) risk of progression. **C,** Expression of PTBP1 in patients with NMIBC according to risk of cancer progression. The expression of PTBP1 was assessed by IHC analysis of paraffin-embedded sections (mean percent of positive tumor cells ± SE; **, $P < 0.001$, independent-sample t test). **D,** Kaplan–Meier DFS, PFS, OS, and DSS analyses of 152 patients with NMIBC stratified in high (solid gray line) and low (dashed black line) PTBP1 expression levels in tumor tissue. Statistical analysis was performed by the log-rank test.

Finally, univariate analysis showed that PTBP1^{High} was significantly associated with poor DFS [HR = 2.6; 95% confidence interval (CI), 1.5–4.6; $P = 0.001$) and OS (HR = 2.4; 95% CI, 1.3–4.5; $P = 0.008$; Supplementary Table S1). Multivariate analysis demonstrated that the only factors negatively impacting on survival were tumor grade (DFS; $P = 0.018$), and age of patients at diagnosis (OS; $P < 0.001$; Supplementary Table S2).

These observations confirm the predictive value of our bioinformatics analysis of deposited mRNA expression levels and highlight PTBP1 as a novel marker of poor prognosis and disease progression, thus suggesting its oncogenic role in bladder cancer.

PTBP1 depletion affects prosurvival features of bladder cancer cells

To investigate whether PTBP1 was functionally relevant for bladder cancer cells, we knocked down its expression by two rounds of transfection with siRNAs (siPTBP1) and obtained an almost complete depletion in three bladder cancer cell lines (RT4, RT112, and EJ; Supplementary Fig. S3A). Silencing of PTBP1 expression significantly reduced growth of all cell lines as measured by clonogenic assays (Fig. 3A; Supplementary Fig. S3B). Cytofluorimetric analysis of the cell cycle indicated that PTBP1 knockdown resulted in the reduction of cells engaged in active S-phase (BrdU-positive cells) and in the concomitant increase of cells in inactive S-phase (not incorporating BrdU but stalled with DNA content between 2N and 4N; Fig. 3B; Supplementary Fig. S3C). Moreover, depletion of PTBP1 dramatically increased the population of cells with a sub-G_1 DNA content (Fig. 3C; Supplementary Fig. S3D), suggesting that stalling in the S-phase was followed by cell death. Indeed, double staining with Annexin V and PI (Fig. 3D; Supplementary Fig. S3E) and immunofluorescence analysis of caspase-3 cleavage (Supplementary Fig. S3F) confirmed the significant increase in apoptotic cells after depletion of PTBP1 in all three cell lines.

To test whether depletion of PTBP1 affects the response of bladder cancer cells to chemotherapeutic treatment with mitomycin C, we used a suboptimal concentration of the drug (0.03 μmol/L) and set out conditions to reduce PTBP1 without strongly affecting cell survival (lower siRNA concentration and single round of transfection). Under these conditions, silencing of PTBP1 enhanced the cytotoxic effect of mitomycin C on bladder cancer cells death, as indicated by double staining with

Published OnlineFirst July 16, 2018; DOI: 10.1158/1078-0432.CCR-17-3850

Table 1. PTBP1 status according to clinical and pathologic features and to clinical outcome of patients ($N = 152$)

Variable	PTBP1 Low: *n* (%)	PTBP1 High: *n* (%)	*P*[a]
Age			
≤65	17 (36.2)	33 (31.4)	0.580
>65	30 (63.8)	72 (68.6)	
Gender			
Male	36 (76.6)	84 (80.0)	
Female	11 (23.4)	21 (20.0)	0.670
pT classification			
pTa	42 (89.4)	32 (30.5)	<0.001[b]
pT1	5 (10.6)	73 (69.5)	
Tumor grade			
1–2	43 (91.5)	55 (52.4)	<0.001[b]
3	4 (8.5)	50 (47.6)	
Risk of cancer progression			
Low	21 (44.7)	6 (5.7)	
Intermediate	22 (46.8)	48 (45.7)	<0.001[b]
High	4 (8.5)	51 (48.6)	
Recurrence			
No	32 (68.1)	41 (39.0)	0.001[b]
Yes	15 (31.9)	64 (61.0)	
Progression			
No	47 (100.0)	94 (89.5)	0.021[b]
Yes	0 (0.0)	11 (10.5)	
Overall survival			
Death free	35 (74.5)	60 (57.1)	0.047[b]
Death from any cause	12 (25.5)	45 (42.9)	
Disease-specific survival			
Death free	47 (100.0)	95 (90.5)	0.029[b]
Death from bladder cancer	0 (0.0)	10 (9.5)	

[a]Pearson χ^2 test.
[b]Statistically significant.

Annexin V and PI (Fig. 3E; Supplementary Fig. S3G) and analysis of caspase-3 cleavage (Supplementary Fig. S3H).

These results demonstrate that PTBP1 favors bladder cancer cell proliferation and survival and that it protects them from chemotherapeutic treatment.

PTBP1 regulates bladder cancer–relevant splice variants

PTBP1 is best known for its role in AS (33) and expression of oncogenic splice variants has been positively associated with disease progression in patients with bladder cancer (19, 34). We noted that some of these AS events are potential PTBP1 targets (Supplementary Table S3; refs. 35, 36). To test whether PTBP1 promotes the expression of these prooncogenic variants in bladder cancer cells, we examined its impact on the splicing pattern of eight genes. The oncogenic splice variants of seven of these genes were expressed in all three cell lines, whereas *CD44* alternative variants were detected only in RT112 cells (Supplementary Fig. S4A and S4B). Notably, knockdown of PTBP1 reverted splicing of the prooncogenic variant of all its potential bladder cancer–related target genes (Fig. 4A and B; refs. 35, 36). On the other hand, exon 3 in *PIK4CB* and exon 5–6 in *LRRFIP2*, which are not its predicted target exons (Supplementary Table S3), were unaffected by PTBP1 depletion.

In addition to being involved in cell proliferation (*PKM* and *NUMB*) or cell death (*FAS*), which are affected by PTBP1 depletion (Fig. 3), several of the PTBP1 target genes encode for proteins that regulate the cell cytoskeleton and adhesion (*ACTN1*, *MACF1*, *TPM1*, *CD44*, and *CTNND1*). Accordingly, we found that knockdown of PTBP1 impaired cell adhesion in bladder cancer cell lines (Supplementary Fig. S4C), indicating that changes in the splicing pattern of these genes may be functionally relevant. In this regard, *CD44* is a prototypic example of AS-regulated gene. It contains 19 exons, nine of which (V2-V10) are alternatively spliced to yield multiple variants (CD44v) that encode for variable extracellular ligand-binding domains of this transmembrane glycoprotein and whose inclusion correlates with tumor progression and metastasis (37). To investigate which of the variable CD44 exons is regulated by PTBP1, we performed semiquantitative PCR (sqPCR) analyses in RT112 cells. Interestingly, inclusion of variable exons between v2 and v7 was reduced in cells depleted of PTBP1, whereas that of other variable exons (v8 to v10) was not (Supplementary Fig. S5A). Quantitative PCR (qPCR) confirmed this exon-specific regulation in PTBP1-depleted cell (Supplementary Fig. S5B).

PTBP1 directly binds in proximity of regulated exons in bladder cancer cells

To test whether PTBP1 plays a direct role in the regulation of its target exons, we investigated PTBP1 recruitment on pre-mRNAs *in vivo* by performing UV-crosslink and RNA immunoprecipitation (CLIP) assays (32). PTBP1 exerts a position-dependent effect on AS by promoting exon inclusion when it binds in the downstream intron and exon skipping when it binds in the upstream intron (Supplementary Fig. S5C and S5D, top; refs. 35, 36). Thus, CLIP experiments were performed in the presence of RNase I (fragment size ~200 bp; ref. 32) and we analyzed PTBP1 recruitment near the downstream intron of the positively regulated exon v7 of *CD44* and exon 99 of *MACF1* (Supplementary Fig. S5C) and the upstream intron of the negatively regulated exon 6a of *TPM1* and exon 2 of *CTNND1* (Supplementary Fig. S5D). In both cases, we detected a significant enrichment of PTBP1 binding in the target regions with respect to nonregulated exons (Supplementary Fig. S5C and S5D). These results demonstrate that PTBP1 specifically binds target exons *in vivo* and highlight its direct role in AS regulation of genes with strong relevance for bladder cancer.

PTBP1 expression associates with CD44 splicing regulation in patients with bladder cancer

To evaluate whether regulation of splicing by PTBP1 was also detected in NMIBC specimens, we performed qPCR analysis of CD44 variable exons that are regulated (v5 and v7) or not (v9) by PTBP1. We selected 18 patients with variable PTBP1 levels (0%–95% positive cells in IHC) from the cohort (Fig. 5A). Strikingly, PTBP1 expression was positively correlated with inclusion of its target exons v5 and v7, whereas the PTBP1-insensitive v9 exon was not significantly associated (Fig. 5B). These results strongly indicate that PTBP1 expression influences splicing outcome in patients with bladder cancer.

Discussion

NMIBC mortality rate and management costs are strikingly high, underlining the need for valuable prognostic markers and therapeutic targets. In this regard, the splicing signature of human cancers is recently emerging as a sophisticated marker to distinguish tumor subtypes and precisely stratify patients (38). Herein, an unbiased approach to identify SFs with prognostic value in NMIBC undertaken by querying public databases has highlighted PTBP1 as a key predictive factor. We report that PTBP1 expression levels positively associate with disease progression and worse

Published OnlineFirst July 16, 2018; DOI: 10.1158/1078-0432.CCR-17-3850

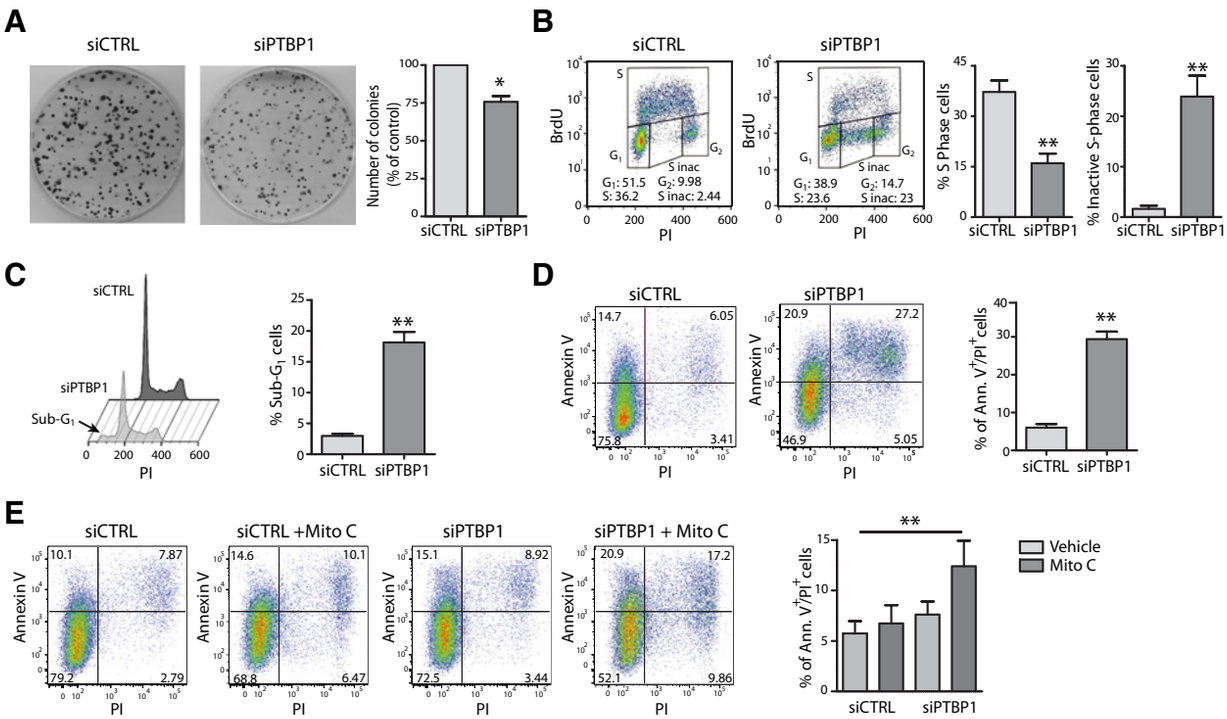

Figure 3.

Modulation of PTBP1 expression affects prosurvival features in bladder cancer cells. **A,** Representative images of clonogenic assay performed with RT4 bladder cancer cells transfected twice with CTRL (siCTRL) or PTBP1 (siPTBP1) siRNAs. Bar graph represents the percentage of colonies formation with respect to siCTRL cells (set as 100%; mean ± SD of three independent experiments). **B** and **C,** Representative bivariate plot profiles of cytometric analysis showing DNA content (PI) versus BrdU incorporation (**B**) and plot profiles of PI incorporation (**C**). RT4 cells were pulse labeled with BrdU for 45 minutes and successively stained with BrdU antibody and PI. G_1, S, G_2, and inactive S (S inac) phase gates (square boxes) and the percentage of cells at each phase is indicated (**B**). Bar graphs show the percentage of cells in S and inactive S (**B**) and sub-G_1 (**C**) phases. **D** and **E,** Representative plot profiles of Annexin V/PI cytometric analysis of RT4 cells transfected twice (**D**) or once (**E**) with the indicated siRNAs and treated (**E**) or not (**D**) with suboptimal amount of mitomycin C (0.03 μmol/L) for 24 hours. Bar graphs represent the percentage of double positive Annexin V and PI cells (mean ± SD of three independent experiments). Statistical analyses were performed by the paired Student *t* test (**A–D**) or one-way ANOVA (**E**; *, $P \leq 0.05$; **, $P \leq 0.01$).

prognosis in patients. Accordingly, PTBP1 promotes prosurvival features of bladder cancer cells and favors splicing of oncogenic variants in both cell lines and patients. Thus, our study shows the predictive value of bioinformatics analysis of deposited gene expression datasets. Furthermore, it uncovers an oncogenic role for PTBP1 in NMIBC and identifies new potential prognostic and therapeutic targets for this disease.

Aberrant splicing regulation often confers selective advantage to tumor cells by favoring oncogenic splice variants of cancer-related genes (13, 39, 40). For instance, upregulation of PTBP1 in human cancer cells affected glycolytic metabolism by promoting splicing of the PKM2 variant (17), leading to acquisition of chemotherapy resistance in pancreatic cancer (18). Likewise, we found that knockdown of PTBP1 in bladder cancer cells augmented the cytotoxic effects of mitomycin C. More importantly, PTBP1 expression level exhibits a strong prognostic value in bladder cancer, as we found a significant correlation between PTBP1 expression, disease progression and worse outcome in a relatively large cohort of patients. Indeed, although, multivariate analysis did not identify PTBP1 expression as an independent predictor of outcome, its expression level is included among the variables that impact on disease progression and outcome, while Kaplan–Meier curves revealed that high expression of PTBP1 correlates with poor DFS, PFS, OS, and DSS. These observations reveal that PTBP1 can be considered a valuable marker to stratify patients with NMIBC in term of risk prediction and evaluation of its expression levels could support the current histologic classification and improve clinical evaluation of patients. This information may also help guiding clinical decisions regarding the follow-up, such as choosing between conservative adjuvant therapy or more aggressive treatment strategies.

We observed a 2- to 3-fold increase of PTBP1 expression in bladder cancer through public datasets analysis. Although this change in expression might appear limited, comparable small changes in expression of other splicing factors were previously shown to trigger oncogenic transformation, like in the case of SRSF1 (15, 16). On the contrary, strong upregulation of splicing factors can be toxic for the cell (15, 41). Thus, the reported increase in expression of PTBP1 in bladder cancer might be sufficient for its oncogenic function. Nevertheless, we cannot rule out the possibility that posttranscriptional regulation of PTBP1 also contributes to its oncogenic potential. For instance, alternative usage of exon 9 generates PTBP1 isoforms showing different target specificity and splicing activity (42). This regulation might impact on the oncogenic role of PTBP1 in bladder cancer and might also influence the multivariate analysis. However, because antibodies specific for these PTBP1 isoforms are not available and no data regarding isoform-specific expression were deposited in the

Published OnlineFirst July 16, 2018; DOI: 10.1158/1078-0432.CCR-17-3850

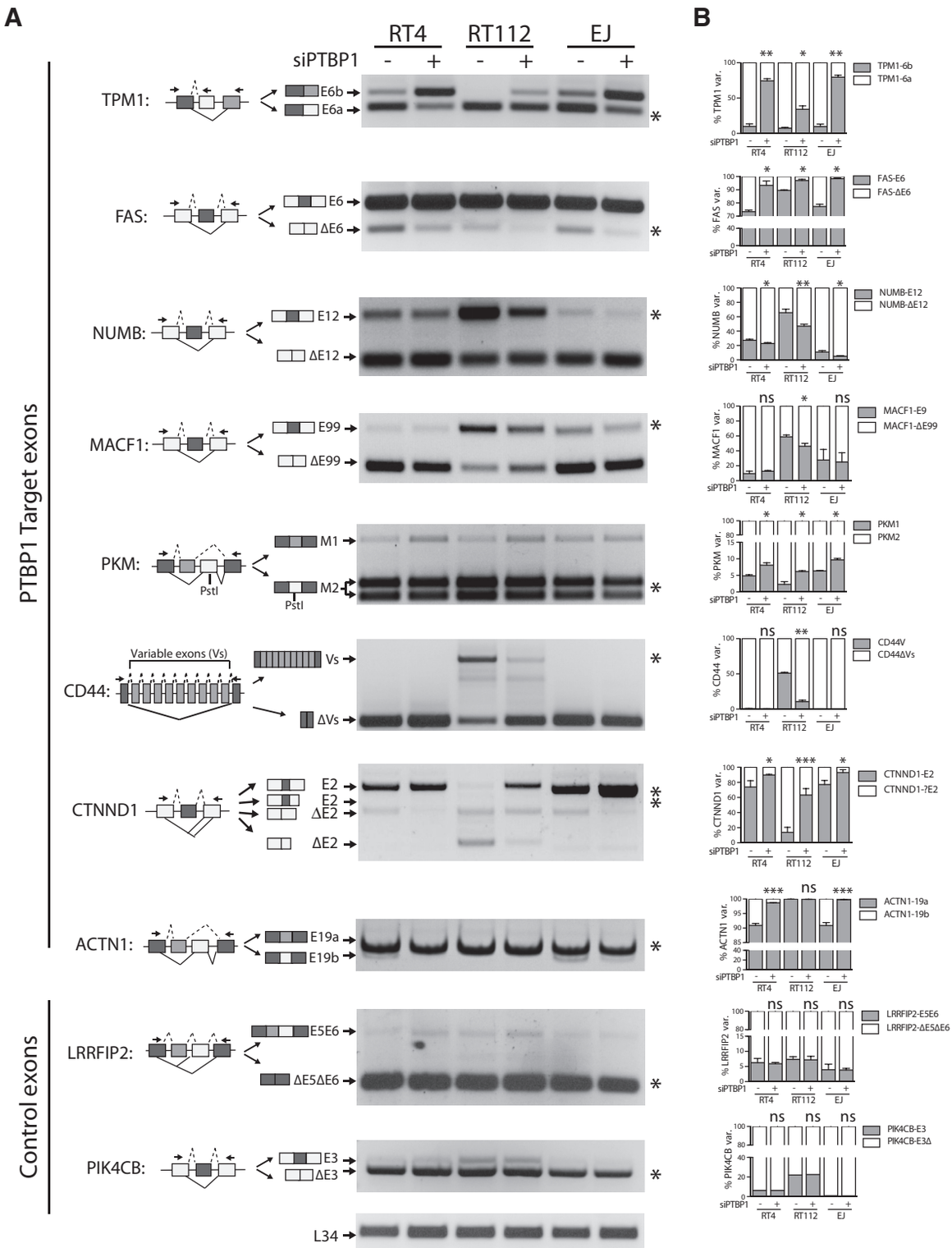

Figure 4.

PTBP1 modulates alternative splicing of bladder cancer-related gene. **A,** sqPCR of *in vivo* splicing assays performed in bladder cancer cell lines silenced with control (−) or PTBP1 (+) siRNAs of specific bladder cancer gene targets. Schematic representation of alternative splicing events (left) analyzed is shown on the left. Exons (boxes) and introns (lines) are indicated on the left. The oncogenic splice variant is indicated (*) to the right of the agarose gel. **B,** Densitometric analysis (right graphs) of the splicing assays shown in **A** (mean ± SD, $n = 3$). Statistical analyses were performed by the paired Student *t* test (*, $P \leq 0.05$; **, $P \leq 0.01$; ***, $P \leq 0.001$; ns, not significant).

Published OnlineFirst July 16, 2018; DOI: 10.1158/1078-0432.CCR-17-3850

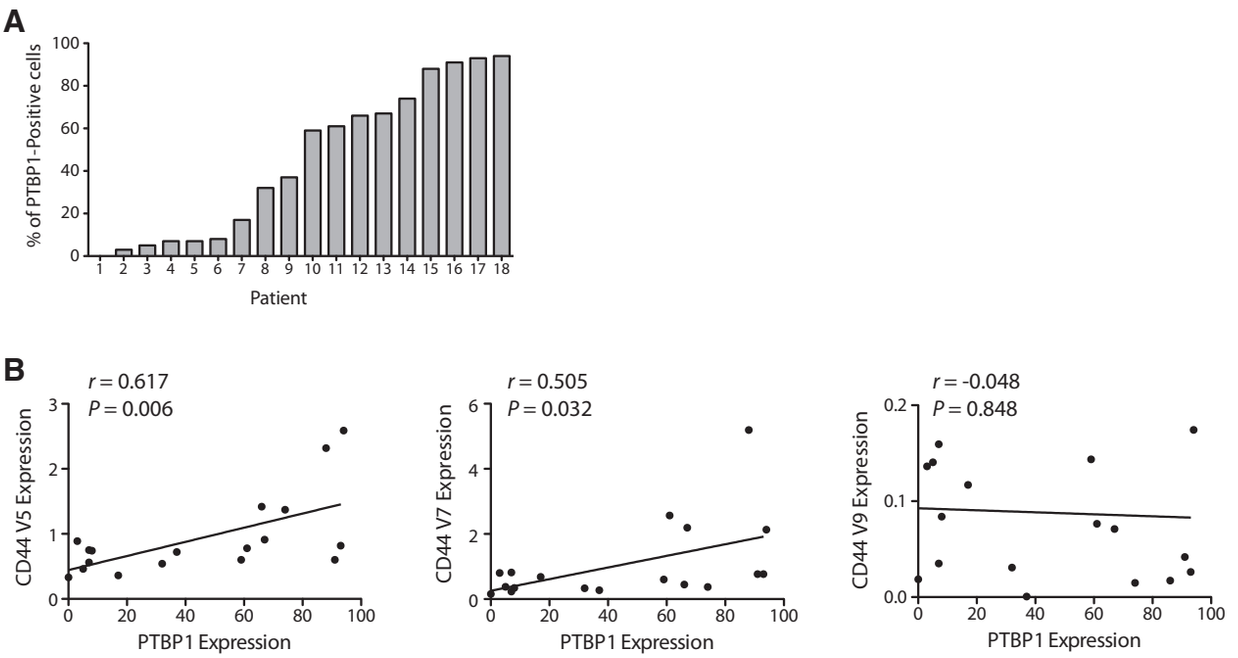

Figure 5.

Inclusion of CD44 variable exons v5 and v7 correlates with PTBP1 expression in patients with bladder cancer. **A,** PTBP1 expression assessed by IHC analysis is expressed as percentage of positive cells. **B,** Pearson correlations between PTBP1 and variable exons V5, V7, and V9 expression, assessed by qPCR analysis, in 18 patients with NMIBC.

public datasets, we could not investigate this aspect in our cohort of patients.

Expression of prooncogenic splice variants is associated with bladder cancer progression (19). We noted that several of these bladder cancer–regulated genes were potential target of PTBP1. Accordingly, knockdown of PTBP1 expression readily reverted splicing of these genes to the less oncogenic variant. Moreover, we report a positive correlation between the expression level of PTBP1 and the inclusion of variable exons v5 and v7 of *CD44* in NMIBC patients' specimens. On the basis of these observations, we hypothesize that the relationship between AS changes in these genes and bladder cancer progression might rely on PTBP1 expression. PTBP1 likely exerts a direct effect on these targets, as we detected its recruitment in proximity of the regulated exons in bladder cancer cells. Notably, PTBP1-regulated genes encode for proteins related to cell survival (*FAS*), proliferation (*NUMB*, *PKM*), cytoskeleton organization (*ACTN1*, *MACF1*, *TPM1*, and *CTNND1*), and interaction with the extracellular matrix (*CD44*). Furthermore, depletion of PTBP1 affected proliferation, survival, and adhesion of bladder cancer cells, suggesting a causative role for this SF in oncogenic features of NMIBC cells. For instance, the increase in apoptosis observed in absence of PTBP1 may rely on a splicing switch in favor of the proapoptotic and membrane-associated *FAS* variant (+E6). In contrast, repression of exon 6 inclusion by PTBP1 generates a soluble prosurvival isoform of FAS (sFAS; ref. 43). Likewise, PTBP1 promotes inclusion of variable exon v6 in *CD44* and this isoform promotes stemness and metastasis in colorectal cancer cells (44). Increased inclusion of *CD44* variable exons has been reported in bladder cancer (34, 45, 46). Our study now correlates inclusion of variable exons v5 and v7 with PTBP1 expression in 19 patients with NMIBC, suggesting that deregulation of *CD44* AS in bladder cancer may be directly caused by altered expression of PTBP1. Noteworthy, although we focused on PTBP1 splicing targets with direct relevance for bladder cancer, our findings do not rule out possible effects of PTBP1 on other variants of the same or other genes in this disease.

In conclusion, our study shows that upregulation of PTBP1 in bladder cancer cells alters their transcriptome in favor of prooncogenic splice variants and correlates with worse outcome in patients. Thus, we suggest that PTBP1 expression and its splicing signature represent novel outcome-predictor markers for NMIBC.

Disclosure of Potential Conflicts of Interest

A. Giannantoni is a consultant/advisory board member for Ipsen. C. Sette is an employee of Fondazione Santa Lucia. No potential conflicts of interest were disclosed by the other authors.

Authors' Contributions

Conception and design: P. Bielli, S.M. Di Stasi, C. Sette
Development of methodology: P. Bielli, V. Panzeri, R. Lattanzio, S.M. Di Stasi
Acquisition of data (provided animals, acquired and managed patients, provided facilities, etc.): V. Panzeri, M. Pieraccioli, E. Volpe, A. Giannantoni, S.M. Di Stasi, C. Sette, S. Mutascio
Analysis and interpretation of data (e.g., statistical analysis, biostatistics, computational analysis): V. Panzeri, M. Pieraccioli, E. Volpe, A. Giannantoni, S.M. Di Stasi, C. Sette
Writing, review, and/or revision of the manuscript: P. Bielli, V. Panzeri, R. Lattanzio, V. Pagliarulo, M. Piantelli, S.M. Di Stasi, C. Sette
Administrative, technical, or material support (i.e., reporting or organizing data, constructing databases): P. Bielli, R. Lattanzio, A. Giannantoni, S.M. Di Stasi
Study supervision: V. Pagliarulo, S.M. Di Stasi, C. Sette
Other: S. Mutascio

Acknowledgments

We wish to thank Dr. Christian Verri (University of Rome Tor Vergata, Italy) for help in the initial steps of this work and Dr. Francesca Velotti (La Tuscia University, Viterbo, Italy) who kindly provided bladder cancer cell lines. The research was supported by the Associazione Italiana Ricerca sul Cancro (AIRC; IG18790) and by Italian Ministry of Health "Ricerca Finalizzata 2011" (GR-2011-02348423).

The costs of publication of this article were defrayed in part by the payment of page charges. This article must therefore be hereby marked *advertisement* in accordance with 18 U.S.C. Section 1734 solely to indicate this fact.

Received December 29, 2017; revised May 2, 2018; accepted July 10, 2018; published first July 16, 2018.

References

1. Torre LA, Bray F, Siegel RL, Ferlay J, Lortet-Tieulent J, Jemal A. Global cancer statistics, 2012. CA Cancer J Clin 2015;65:87–108.
2. Babjuk M, Burger M, Zigeuner R, Shariat SF, van Rhijn BW, Compérat E, et al. EAU guidelines on non-muscle-invasive urothelial carcinoma of the bladder: update 2013. Eur Urol 2013;64:639–53.
3. Burger M, Catto JW, Dalbagni G, Grossman HB, Herr H, Karakiewicz P, et al. Epidemiology and risk factors of urothelial bladder cancer. Eur Urol 2013;63:234–41.
4. Svatek RS, Hollenbeck BK, Holmäng S, Lee R, Kim SP, Stenzl A, et al. The economics of bladder cancer: costs and considerations of caring for this disease. Eur Urol 2014;66:253–62.
5. Sylvester RJ, van der Meijden AP, Oosterlinck W, Witjes JA, Bouffioux C, Denis L, et al. Predicting recurrence and progression in individual patients with stage TaT1 bladder cancer using EORTC risk tables: a combined analysis of 2596 patients from seven EORTC trials. Eur Urol 2006;49:466–77.
6. Fernandez-Gomez J, Madero R, Solsona E, Unda M, Martinez-Piñeiro L, Gonzalez M, et al. Predicting nonmuscle invasive bladder cancer recurrence and progression in patients treated with bacillus Calmette-Guerin: the CUETO scoring model. J Urol 2009;182:2195–203.
7. Rosevear HM, Lightfoot AJ, Nepple KG, O'Donnell MA. Usefulness of the Spanish Urological Club for Oncological Treatment scoring model to predict nonmuscle invasive bladder cancer recurrence in patients treated with intravesical bacillus Calmette-Guérin plus interferon-α. J Urol 2011;185:67–71.
8. Kamat AM, Hegarty PK, Gee JR, Clark PE, Svatek RS, Hegarty N, et al. International consultation on urologic disease-european association of urology consultation on bladder cancer 2012. ICUD-EAU international consultation on bladder cancer 2012: screening, diagnosis, and molecular markers. Eur Urol 2013;63:4–15.
9. Bryan RT, Zeegers MP, James ND, Wallace DM, Cheng KK. Biomarkers in bladder cancer. BJU Int 2010;105:608–13.
10. van Rhijn BW, Catto JW, Goebell PJ, Knüchel R, Shariat SF, van der Poel HG, et al. Molecular markers for urothelial bladder cancer prognosis: toward implementation in clinical practice. Urol Oncol 2014;32:1078–87.
11. Lee SC, Abdel-Wahab O. Therapeutic targeting of splicing in cancer. Nat Med 2016;22:976–86.
12. Matera AG, Wang Z. A day in the life of the spliceosome. Nat Rev Mol Cell Biol 2014;15:108–21.
13. Paronetto MP, Passacantilli I, Sette C. Alternative splicing and cell survival: from tissue homeostasis to disease. Cell Death Differ 2016;23:1919–29.
14. Barbosa-Morais NL, Irimia M, Pan Q, Xiong HY, Gueroussov S, Lee LJ, et al. The evolutionary landscape of alternative splicing in vertebrate species. Science 2012;338:1587–93.
15. Karni R, de Stanchina E, Lowe SW, Sinha R, Mu D, Krainer AR. The gene encoding the splicing factor SF2/ASF is a proto-oncogene. Nat Struct Mol Biol 2007;14:185–93.
16. Anczuków O, Rosenberg AZ, Akerman M, Das S, Zhan L, Karni R, et al. The splicing factor SRSF1 regulates apoptosis and proliferation to promote mammary epithelial cell transformation. Nat Struct Mol Biol 2012;19:220–8.
17. David CJ, Chen M, Assanah M, Canoll P, Manley JL. HnRNP proteins controlled by c-Myc deregulate pyruvate kinase mRNA splicing in cancer. Nature 2010;463:364–8.
18. Calabretta S, Bielli P, Passacantilli I, Pilozzi E, Fendrich V, Capurso G, et al. Modulation of PKM alternative splicing by PTBP1 promotes gemcitabine resistance in pancreatic cancer cells. Oncogene 2016;35:2031–9.
19. Thorsen K, Sørensen KD, Brems-Eskildsen AS, Modin C, Gaustadnes M, Hein AM, et al. Alternative splicing in colon, bladder, and prostate cancer identified by exon array analysis. Mol Cell Proteomics 2008;7:1214–24.
20. Sjödahl G, Lauss M, Lövgren K, Chebil G, Gudjonsson S, Veerla S, et al. A molecular taxonomy for urothelial carcinoma. Clin Cancer Res 2012;18:3377–86.
21. Dyrskjøt L, Kruhøffer M, Thykjaer T, Marcussen N, Jensen JL, Møller K, et al. Gene expression in the urinary bladder: a common carcinoma in situ gene expression signature exists disregarding histopathological classification. Cancer Res 2004;64:4040–8.
22. Sanchez-Carbayo M, Socci ND, Lozano J, Saint F, Cordon-Cardo C. Defining molecular profiles of poor outcome in patients with invasive bladder cancer using oligonucleotide microarrays. J Clin Oncol 2006;24:778–89.
23. Sjödahl G, Lauss M, Lövgren K, Chebil G, Gudjonsson S, Veerla S, et al. A molecular taxonomy for urothelial carcinoma. Clin Cancer Res 2012;18:3377–86.
24. Oken MM, Creech RH, Tormey DC, Horton J, Davis TE, McFadden ET, et al. Toxicity and response criteria of the Eastern Cooperative Oncology Group. Am J Clin Oncol 1982;5:649–55.
25. Sobin LH, Wittekind CH. UICC (International Union Against Cancer): TNM classification of malignant tumours, 5th ed. New York, NY: Wiley Liss; 1997. p. 107–190.
26. Marshall CJ, Franks LM, Carbonell AW. Markers of neoplastic transformation in epithelial cell lines derived from human carcinomas. J Natl Cancer Inst 1977;58:1743–51.
27. Chen TR. In situ detection of mycoplasma contamination in cell cultures by fluorescent Hoechst 33258 stain. Exp Cell Res. 1977;104:255–62.
28. Bielli P, Bordi M, Di Biasio V, Sette C. Regulation of BCL-X splicing reveals a role for the polypyrimidine tract binding protein (PTBP1/hnRNP I) in alternative 5′ splice site selection. Nucleic Acids Res 2014;42:12070–81.
29. Bielli P, Busà R, Di Stasi SM, Munoz MJ, Botti F, Kornblihtt AR, et al. The transcription factor FBI-1 inhibits SAM68-mediated BCL-X alternative splicing and apoptosis. EMBO Rep 2014;15:419–27.
30. Franken NAP, Rodermond HM, Stap J, Haveman J, van Bree C. Clonogenic assay of cells *in vitro*. Nat Protoc 2006;1:2315–2319.
31. Zhu H. Cell proliferation assay by flow cytometry (BrdU and PI Staining). Bio Protoc 2012;Bio101:e198.
32. Bielli P, Sette C. Analysis of *in vivo* interaction between RNA binding proteins and their RNA targets by UV cross-linking and immunoprecipitation (CLIP) method. Bio Protoc 2017;7:e2274.
33. Kafasla P, Mickleburgh I, Llorian M, Coelho M, Gooding C, Cherny D, et al. Defining the roles and interactions of PTB. Biochem Soc Trans 2012;40:815–20.
34. Kobayashi K, Matsumoto H, Matsuyama H, Fujii N, Inoue R, Yamamoto Y, et al. Clinical significance of CD44 variant 9 expression as a prognostic indicator in bladder cancer. Oncol Rep 2016;36:2852–60.
35. Xue Y, Zhou Y, Wu T, Zhu T, Ji X, Kwon YS, et al. Genome-wide analysis of PTB-RNA interactions reveals a strategy used by the general splicing repressor to modulate exon inclusion or skipping. Mol Cell 2009;36:996–1006.
36. Llorian M, Schwartz S, Clark TA, Hollander D, Tan LY, Spellman R, et al. Position-dependent alternative splicing activity revealed by global profiling of alternative splicing events regulated by PTB. Nat Struct Mol Biol 2010;17:1114–23.
37. Senbanjo LT, Chellaiah MA. CD44: a multifunctional cell surface adhesion receptor is a regulator of progression and metastasis of cancer cells. Front Cell Dev Biol 2017;5:18.

Published OnlineFirst July 16, 2018; DOI: 10.1158/1078-0432.CCR-17-3850

38. Trincado JL, Sebestyén E, Pagés A, Eyras E. The prognostic potential of alternative transcript isoforms across human tumors. Genome Med 2016;8:85.
39. Zhang J, Manley JL. Misregulation of pre-mRNA alternative splicing in cancer. Cancer Discov 2013;3:1228–37.
40. Pagliarini V, Naro C, Sette C. Splicing regulation: a molecular device to enhance cancer cell adaptation. Biomed Res Int 2015;2015:543067.
41. Paronetto MP, Achsel T, Massiello A, Chalfant CE, Sette C. The RNA-binding protein Sam68 modulates the alternative splicing of Bcl-x. J Cell Biol 2007;176:929–39.
42. Wollerton MC, Gooding C, Robinson F, Brown EC, Jackson RJ, Smith CW. Differential alternative splicing activity of isoforms of polypyrimidine tract binding protein (PTB). RNA 2001;7:819–32.
43. Izquierdo JM, Majós N, Bonnal S, Martínez C, Castelo R, Guigó R, et al. Regulation of Fas alternative splicing by antagonistic effects of TIA-1 and PTB on exon definition. Mol Cell 2005;19:475–84.
44. Todaro M, Gaggianesi M, Catalano V, Benfante A, Iovino F, Biffoni M, et al. CD44v6 is a marker of constitutive and reprogrammed cancer stem cells driving colon cancer metastasis. Cell Stem Cell 2014;14:342–56.
45. Miyake H, Eto H, Arakawa S, Kamidono S, Hara I. Over expression of CD44V8–10 in urinary exfoliated cells as an independent prognostic predictor in patients with urothelial cancer. J Urol 2002;167:1282–7.
46. Omran OM, Ata HS. CD44s and CD44v6 in diagnosis and prognosis of human bladder cancer. Ultrastruct Pathol 2012;36:145–52.

2. c-MYC empowers transcription and productive splicing of the oncogenic splicing factor Sam68 in cancer

Caggiano C, Pieraccioli M, **Panzeri V**, Sette C, Bielli P.

Nucleic Acids Res. 2019 Jul 9;47(12):6160-6171.

6160–6171 *Nucleic Acids Research, 2019, Vol. 47, No. 12* *Published online 8 May 2019*
doi: 10.1093/nar/gkz344

c-MYC empowers transcription and productive splicing of the oncogenic splicing factor Sam68 in cancer

Cinzia Caggiano[1,†], Marco Pieraccioli[1,†], Valentina Panzeri[1,2], Claudio Sette[1,3,*] and Pamela Bielli[1,4,*]

[1]Laboratory of Neuroembryology, IRCCS Fondazione Santa Lucia, 00143 Rome, Italy, [2]Department of Science medical/chirurgic and translational medicine, University of Rome Sapienza,00189 Rome, Italy, [3]Institute of Human Anatomy and Cell Biology, Catholic University of the Sacred Hearth, 00168 Rome, Italy and [4]Department of Biomedicine and Prevention, University of Rome Tor Vergata, 00133 Rome, Italy

Received August 6, 2018; Revised April 19, 2019; Editorial Decision April 23, 2019; Accepted April 24, 2019

ABSTRACT

The splicing factor Sam68 is upregulated in many human cancers, including prostate cancer (PCa) where it promotes cell proliferation and survival. Nevertheless, in spite of its frequent upregulation in cancer, the mechanism(s) underlying its expression are largely unknown. Herein, bioinformatics analyses identified the promoter region of the Sam68 gene (*KHDRBS1*) and the proto-oncogenic transcription factor c-MYC as a key regulator of Sam68 expression. Upregulation of Sam68 and c-MYC correlate in PCa patients. c-MYC directly binds to and activates the Sam68 promoter. Furthermore, c-MYC affects productive splicing of the nascent Sam68 transcript by modulating the transcriptional elongation rate within the gene. Importantly, c-MYC-dependent expression of Sam68 is under the tight control of external cues, such as androgens and/or mitogens. These findings uncover an unexpected coordination of transcription and splicing of Sam68 by c-MYC, which may represent a key step in PCa tumorigenesis.

INTRODUCTION

Prostate cancer (PCa) is among the most common tumors in adult men (1). PCa onset and progression rely on androgen receptor (AR) signaling and androgen deprivation therapy (ADT) represents the most effective cure (2). However, despite significant advances in treatments, PCa almost inevitably relapses with hormone-insensitive forms (CRPC) that are currently incurable (2). Among the factors contributing to PCa pathogenesis, aberrant splicing of cancer-specific genes contributes by promoting isoforms involved in growth, metastatic progression and hormone resistance of PCa cells (3,4). For example, a constitutively active splice variant of AR (AR-V7) is overexpressed in CRPC, where it promotes cell proliferation and migration by regulating a specific subset of genes even under ADT conditions (5). Likewise, the anti-apoptotic BCL-X long splice variant (BCL-XL) confers chemotherapy resistance (6), whereas the Cyclin D1b isoform promotes AR transcriptional activity (7). In support of their pro-oncogenic features, expression of these splice variants is linked to poor prognosis in PCa patients (7–9).

Precursor messenger RNA (pre-mRNA) splicing is operated by the spliceosome, a complex ribonucleoprotein machinery that removes introns and ligates exons to yield the mature mRNA (10). Although most exons are constitutively spliced in the mRNA, others are subjected to regulation through a process named alternative splicing (AS). Alternative recognition of exons is due to the presence of *cis*-regulatory RNA elements that recruit the spliceosome and sequence-specific *trans*-acting splicing factors (10). Moreover, since splicing is tightly coupled to transcription, mechanisms impacting on the RNA polymerase II (RNAPII) elongation rate, nucleosome positioning or histone modifications also contribute to exon recognition (10). These regulatory mechanisms are kept under tight control in the cell, whereas their dysregulation contributes to the onset and progression of human cancers (11,12), including PCa (3,4).

Splicing dysregulation is often determined by the altered expression of specific splicing factors (11,12). An example is provided by Sam68 (*KHDRBS1*), which is overexpressed in PCa and other human cancers (13). Sam68 promotes cell-cycle progression and survival to genotoxic stress of PCa cells (14), likely through induction of oncogenic splice variants like BCL-XL, cyclin D1b, CD44 variants and AR-V7

*To whom correspondence should be addressed. Tel: +39 06 72596260; Fax: +39 06 72596268; Email: pamela.bielli@uniroma2.it
Correspondence may also be addressed to Claudio Sette. Tel: +39 06 30154858; Fax: +39 06 501703338; Email: claudio.sette@unicatt.it
†The authors wish it to be known that, in their opinion, the first two authors should be regarded as Joint First Authors.

(3,4). Furthermore, Sam68 interacts with both AR and AR-V7, enhancing their transcriptional activity and androgen signaling (15). However, in spite of its well described upregulation in human cancers (13), no studies have directly addressed the mechanisms underlying its transcriptional regulation.

Herein, by carrying out a bioinformatics search for transcription factors that potentially regulate Sam68 expression we have identified the proto-oncogene c-MYC (*MYC*) as strong candidate. Our study documents the direct binding of c-MYC to the Sam68 promoter region as well as its effect on the transcriptional activation of the gene and productive splicing of the nascent transcript. Furthermore, we provide evidence that c-MYC-dependent expression of Sam68 is under the tight control of external cues and linked to favorable conditions, such as androgen and/or mitogen stimulation. These findings uncover an unexpected coordination of transcription and splicing of Sam68 by c-MYC, which may represent a vulnerable target for PCa treatment.

MATERIALS AND METHODS

Bioinformatics analyses

Sam68 promoter characterization was performed utilizing bioinformatics tools present in UCSC Genome Browser (https://genome.ucsc.edu; GRCh37/h19) and analyzing ChIP-seq data for RNAPII, H3K27Ac, H3K4Me1 and H3K4Me3 tracks from ENCODE project (https://www.encodeproject.org). Chromatin State Segmentation track displays a chromatin state segmentation from nine human cell types learned by computationally integrating ChIP-seq data for nine factors plus input using a Hidden Markov Model. In UCSC Genome Browser, *in silico* analysis of Sam68 promoter was performed using 'HMR Conserved Transcription Factor Binding Site' tool that use the Transfac Matrix Database (v.7.0). c-MYC ChIP-seq analyses was performed using 'Transcription Factor ChIP-seq (161 factors) from ENCODE with Factorbook motifs' tool.

Tumor Prostate Cancer datasets analysis was carried out utilizing Jenkins (GSE46691), Sawyers (GSE21034) and Sueltman (GSE29079) published datasets (16–18). Gene expression data for correlation analyses were downloaded from R2 genomics analysis and visualization platform (http://r2.amc.nl). Pearson's correlation was used to evaluate the association between Sam68 and c-MYC expression. For gene expression analyses, the patients were divided into two groups according to the median of c-MYC gene expression. Then, *Z*-scores value of Sam68 was calculated in each sample and Mann–Whitney test was used to establish the significance level of Sam68 between the two groups (19).

Plasmid constructs and oligonucleotides

Intergenic region, human wild-type and deletion mutants of Sam68 and hnRNP A1 promoters were cloned in pGL3-basic vector (Promega). Human c-MYC and MAX expression plasmids were cloned in pCDNA3 vector (Invitrogen, Life technologies). Site-directed mutagenesis on pGL3-Sam68 promoter was performed using QuikChangeR II XL Site-Directed Mutagenesis Kit according to manufacturer's instruction (Stratagene). Sam68 minigene was cloned into the EcoRI/SalI restriction sites of pCI vector (Promega). All constructs were generated using genomic DNA or cDNA isolated from LNCaP cells as template. Inserts were amplified by the Phusion Hot Start High-Fidelity DNA polymerase (Thermo Fisher Scientific) and plasmids sequenced by Cycle Sequencing (Eurofins Genomics). Oligonucleotides used in this study are listed in the Supplementary Table S1.

Cell lines maintenance and transfection

Human prostate cancer cell lines LNCaP and 22Rv1 were cultured in RPMI 1640 medium (LONZA), while PC3 and DU145 PCa cell lines and human embryonic kidney cell line HEK293T were maintained in Dulbecco's modified Eagle's medium (LONZA). All media were supplemented with 10% Fetal Bovine Serum (FBS) (Gibco), penicillin (50 U/ml)/streptomycin (50 μg/ml) (Corning), 50 μg/ml gentamicin sulfate (Aurogene), 1% non-essential amino acids (Euroclone), 10 mM Hepes (Euroclone) and 1 mM sodium pyruvate (Aurogene). Cells were maintained in culture at 37°C under 5% CO_2 in a humidified incubator, no longer than 3 months. Cell lines utilized were tested for mycoplasma contamination using MycoAlert Mycoplasma Detection Kit (LONZA). LNCaP and HEK293T were transfected with the indicated reporter or expression vectors using Lipofectamine 2000 (Invitrogen) as previously described (20). For c-MYC (double transfection) and splicing factors (single transfection) RNAi experiments, PCa cells were transfected with 40 nM siRNAs using Lipofectamine RNAiMax (Invitrogen, Life technologies) according to manufacturer's instruction. Control and c-MYC siRNAs were purchased from Dharmacon (On target plus human c-MYC L-003282-02 and On target plus non targeting pool D-001810-10) and Qiagen (Flexi Tube siRNA MYC SI03101847 and Negative control SI03650325). Sequences of control and splicing factors siRNAs were previously described (20).

Cell treatments and proliferation analysis

Growth arrest was induced by culturing PCa cells in 0% FBS and with 1 μM Enzalutamide (MDV3100; Sigma-Aldrich), or DMSO as vehicle control. For cell proliferation assays, cells were pulsed with 30 μM BrdU (Sigma-Aldrich) for 30 min. After PBS washes, cells were collected, fixed with 70% ethanol and stained with anti-BrdU antibody (347580, BD Biosciences) and propidium iodide (Sigma-Aldrich). Cell-cycle analysis was carried out using flow cytometry (FACSCalibur, BD Biosciences) according to manufacturer's instructions.

Cell extracts and immunoblot analysis

Whole extract preparation was performed as previously described (21). Briefly, cells were resuspended in lysis buffer [50 mM Hepes, pH 7.4, 150 mM NaCl, 15 mM $MgCl_2$, 10% glycerol, 1 mM dithiothreitol, 20 mM β-glycerophosphate, 0.5 mM $NaVO_4$, protease inhibitor cocktail (Sigma-Aldrich), 0.5% Triton X-100]. After 10 min of ice incubation, cell suspension was centrifuged for

10 min at 12 000 × *g* at 4°C and supernatant fractions were collected. Samples were denatured in Laemmli Sample buffer and 3–30 μg of total extract was separated on sodium dodecyl sulphate-polyacrylamide gelelectrophoresis (SDS-PAGE) and transferred to Polyvinylidene Fluoride (PVDF) membranes. Western blot analysis was carried using the following antibodies: anti-SAM68 (A302-110A, Bethyl Laboratories); anti-β-actin (A2066, Sigma-Aldrich); anti-β-tubulin (T4026, Sigma-Aldrich); anti-c-MYC (sc764, Santa Cruz Biotechnology); anti-hnRNP A1 (sc32301, Santa Cruz Biotechnology); anti-MAX (sc2011, Santa Cruz Biotechnology); anti-hnRNP I (sc16547 Santa Cruz Biotechnology); anti-hnRNP A2/B1 (sc393674, Santa Cruz Biotechnology); anti-GFP (sc9996, Santa Cruz Biotechnology); Anti-RNA polymerase II (sc899, Santa Cruz Biotechnology); anti-RNA polymerase II subunit B1, clone 3E10 (phospho CTD Ser-2, 04-1571, Millipore); anti-RNApolymerase II subunit B1, clone 3E8 (phospho-CTD Ser5; 04-1572, Millipore); anti-Flag (F3165, Millipore); anti-hnRNP H and anti-hnRNP F (kindly provided by Prof. B. Chabot, Université de Sherbrooke, Canada).

Luciferase-based report assay

Luciferase-based report assay was performed in HEK293T cells as previously described (22). Briefly, HEK293T cells were co-transfected with internal control (Renilla) and indicated (Firefly) luciferase reporters in presence or not of c-MYC, or MAX, expressing vectors. Luciferase assays were carried out at the indicated time points using the Dual Luciferase Reporter assay (Promega). Data were normalized for transfection efficiency by ratio between Firefly and Renilla luciferase activity, and represented as fold activation with respect to the control.

RNA extraction, gene expression and splicing assay analysis

RNA was extracted from cells using the Trizol reagent according to manufacturer's instructions (Invitrogen, Life technologies) and treated with RNase-free DNase (Ambion). A total of 1 μg of RNA was retrotranscribed with M–MLV reverse transcriptase (Promega) and random primers (Roche). Gene expression and splicing patterns were evaluated by semi-quantitative (sqPCR) and quantitative (qPCR) PCR analyses using 10 ng of cDNA template. For splicing assay experiments, sqPCR analysis was performed using the following cycles: 95°C for 5 min (1 cycle) −95°C for 10 s, 56°C for 10 s, 72°C for 15 s (28 or 35 cycles for minigene-derived or endogenous isoforms, respectively)− and a final extension at 72°C for 5 min. The percentage Spliced-In Index (PSI/ψ) was calculated from densitometric analysis of PCR products as ψ = exon inclusion/ (exon inclusion + exon skipping) band intensities. qPCR analysis was carried out using PowerUp SYBR Green Master Mix (Applied Biosystems) and Applied Biosystems StepOnePlus Real-Time PCR system (Applied Biosystems) according to the manufacturer's instructions. Quantitative evaluation of gene and Sam68-ΔKH isoform expression was calculated relative to Histone 3 and Sam68-KH, respectively, by ΔΔCq method (21).

Analysis of RNA polymerase II (RNAPII) transcriptional rate on Sam68 pre-mRNA was performed as previously described (23). Briefly, LNCaP cells were grown overnight on 60-mm plates to 70–80% confluency and treated with 75 μM of 5,6-Dichlorobenzimidazole 1-β–D-ribofuranoside (DRB; Sigma-Aldrich) in culture medium for 6 h to reversibly halt transcription. After two washes in phosphate buffered saline (PBS), cells were incubated in fresh medium up to 30 min. Every 5 min cells were collected for RNA isolation. Fold change of Sam68 exon1–intron1 relative to exon8–intron8 expression was calculated by ΔΔCq method (21).

Chromatin immunoprecipitation

ChIP experiments were performed as previously described (22). Briefly, LNCaP cells were fixed by the addition of 1% (vol/vol) formaldehyde to the culture medium for 10 min at room temperature and then quenched in 125 mM glycine for 5 min. Cells were washed three times in PBS and lysed in nuclei extraction buffer (5 mM Pipes pH 8, 85 Mm KCl, 0.5% NP40) for 2 h, at 4°C under rotation. Lysate was centrifuged at 1200 × *g* for 5 min at 4°C. Nuclei pellet was resuspended in sonication buffer (10 mM ethylenediaminetetraacetic acid (EDTA) pH 8, 50 mM Tris–HCl pH 8, SDS 1%) and sonicated with Bioruptor (Dyagenode) to yield chromatin size of ∼400 bp and insoluble debris was removed by centrifugation. Cross-linked DNA was then quantified, diluted 1:10 with dilution buffer (0.01% SDS, 1.1% Triton X100, 1.2 mM EDTA, 16.7 mM Tris/HCl pH 8.0, 167 mM NaCl) and incubated with 5 μg of specific c-MYC antibody (sc-764X, Santa Cruz Biotechnologies), IgGs (Sigma-Aldrich) and no antibody, as a negative controls, under rotation at 4°C overnight. Dynabeads protein G (Invitrogen, Life technologies) were incubated with the mixture under rotation at 4°C for 2 h, then washed and heated at 65°C overnight to reverse formaldehyde cross-links. Immunoprecipitated DNA was recovered according to standard procedures and analyzed by qPCRs. DNA associated with c-MYC is represented as percentage of input, calculated by ΔCq method (21).

UV-crosslinked and RNA immunoprecipitation (CLIP) assays

UV-crosslinked and RNA immunoprecipitation (CLIP) assays were performed as previously described (24). Briefly, cells were washed once with PBS, UV-irradiated (400 mJ/cm2) and collected by scraping in lysis buffer [50 mM Tris pH 8, 100 mM NaCl, 1 mM MgCl2, 0.1 mM CaCl2, 1% NP40, 0.1% SDS, 0.5 mM Na3VO4, 1 mM dithiothreitol, protease inhibitor cocktail (Sigma-Aldrich), RNase inhibitor (Promega)]. After brief sonication, samples were incubated with DNase-RNase free (Ambion) for 3 min at 37°C and then centrifuged at 15000 × *g* for 3 min at 4°C. A total of 1 mg of supernatant (cell extract) was diluted to 1 ml with lysis buffer and immunoprecipitated with anti-hnRNP F (kindly provided by Prof. B. Chabot, Université de Sherbrooke, Canada) or IgGs (control) in the presence of Dynabeads protein G (Invitrogen, Life technologies) and 10 μl/ml of RNaseI 1:1000 (Ambion). Immunoprecipitates

(IPs) were incubated for 2 h at 4°C under rotation. After two washes with high-salt buffer (50 mM Tris–HCl, pH 7.4, 1 M NaCl, 1 mM EDTA, 1% Igepal CA-630, 0.1% SDS, 0.5% sodium deoxycholate) and Proteinase K buffer (100 mM Tris–HCl, pH 7.4, 50 mM NaCl, 10 mM EDTA), the IPs were resuspended in Proteinase K buffer supplemented with 50 μg of Proteinase K and incubated 1 h at 55°C. RNA was isolated and retrotranscribed by standard procedures. About 10% of cell extract (0.1 mg) was treated with 50 μg of Proteinase K and RNA purified (input).

RESULTS

c-MYC binds the promoter region of Sam68

To identify the promoter region of the Sam68 gene (*KHDRBS1*), we queried the UCSC Genome Browser database (http://genome.ucsc.edu; GRCh37/h19) for RNA polymerase II (RNAPII) occupancy and chromatin features of active transcription within the gene and in the upstream intergenic region (∼20 kilobases). Chromatin immunoprecipitation (ChIP) sequencing datasets from seven human cell lines revealed that RNAPII peaks are present in the region spanning approximately −400 and +300 base pairs (bp) from the transcription start site (TSS) (Figure 1A and Supplementary Figure S1A). RNAPII peaks are flanked by deposition of histone marks typically enriched in active promoters (H3K4me3) and transcriptional regulatory elements (H4K3me1 and H3K27Ac) (Figure 1A). To evaluate the promoter activity of this region, we cloned the genomic sequence located between −534 and +297 bp from the TSS upstream of the luciferase reporter gene and transfected it into HEK293T cells. The putative promoter region of Sam68 displayed higher activity to that of the human *HNRPA1* promoter, while being significantly weaker than the viral SV40 promoter (Figure 1B). No transcriptional activity was observed with an intergenic DNA region of the same length. Progressive deletion mutants indicated that the region between −130 bp and +297 bp from the TSS is required for the optimal activity of the Sam68 promoter (Figure 1C). These results suggest that a relatively small genomic region acts as promoter for Sam68 expression in human cells.

To identified transcription factors that potentially bind *cis*-regulatory DNA elements in the Sam68 promoter, we queried the HMR Conserved Transcription Factor Binding Sites, the ENCODE Transcription Factor Binding Tracks datasets and ChIP-seq experiments deposited in the UCSC Genome Browser database. Among others, we found two potential binding sites for the oncogenic transcription factor c-MYC that are located at −64 and −45 bp from the Sam68 TSS (Supplementary Figure S1B), within the region required for optimal transcriptional activity (Figure 1C). Analysis of ChIP-seq experiments in multiple cell lines (Encode Project, https://www.encodeproject.org) confirmed the binding of c-MYC to the Sam68 promoter region (Figure 1D and Supplementary Figure S1C), suggesting a direct regulation of Sam68 expression by this transcription factor in cancer cells.

Sequence analysis of the Sam68 promoter highlighted two perfect c-MYC consensus E-box binding sites (CACGTG; Supplementary Figure S2A). To directly test whether c-MYC regulates Sam68 transcription, we performed ChIP experiments in LNCaP cells, an androgen-sensitive PCa cell line expressing high levels of Sam68 (14). Semiquantitative (sqPCR) and quantitative (qPCR) PCR analyses detected a significant enrichment of c-MYC in the promoter region of Sam68 (Figure 2A and B), which was comparable to that observed for other c-MYC targets, such as cyclin B1, nucleolin (25) and hnRNP A1 (26). By contrast, no binding was observed in the intergenic (16q22) control region of chromosome 16, indicating specificity of binding (Figure 2A and B).

Next, we tested whether c-MYC modulates Sam68 expression. Co-transfection of the Sam68 promoter reporter and c-MYC resulted in significant induction (∼2-fold) of the luciferase activity (Figure 2C), which was comparable to that observed with the hnRNPA1 promoter (Figure 2C and Supplementary Figure S2B). Individual (Mut1: CACGTG→AAAGTA; Mut2: CACGTG→AAAGTT) or double mutation (Mut1-2: CACGTG/CACGTG→AAAGTA/AAAGTT) of the putative E-box binding sites significantly impaired c-MYC-dependent activation of the Sam68 promoter (Figure 2C and Supplementary Figure S2C), with Mut1 causing the greatest influence. Interestingly, the double mutant (Mut1-2) did not show additive effect (Figure 2C), suggesting that c-MYC activity primarily relies on E-Box1 and that additional regions participate to regulation.

The c-MYC transcriptional activity often relies on its functional interaction with the co-regulator MAX (27). Thus, we also tested their possible cooperation on the regulation of Sam68 expression. Under sub-optimal conditions (24 h after transfection), MAX did not affect Sam68 expression when overexpressed alone, but it significantly enhanced the transcriptional activity of c-MYC on the Sam68 promoter in co-transfected cells (Supplementary Figure S2D). Collectively, these findings identify c-MYC as a direct regulator of Sam68 transcription.

c-MYC positively regulates Sam68 expression in prostate cancer

To test whether Sam68 expression is under the control of c-MYC in PCa cells, we knocked down its expression in four PCa cell lines (LNCaP, 22RV1, PC3 and DU145) using two pools of siRNAs (siRNA#1 and #2). c-MYC depletion caused a significant reduction in Sam68 expression at both mRNA and protein levels (Figure 3A–D), which was comparable to that exerted on hnRNP A1 (26) (Supplementary Figure S3A–D). These results indicate that c-MYC promotes Sam68 expression in PCa cells.

The pro-oncogenic role of c-MYC mainly relies on regulation of gene expression programs (28), including genes encoding core spliceosome components (29) and pro-oncogenic splicing factors (19,26). Since upregulation of both c-MYC (16,30) and Sam68 (14,15) have been reported in PCa, we asked whether their expression levels correlated in patients by analyzing public datasets (R2 genomics; http://r2.amc.nl). Pearson's correlation analysis using the Jenkins PCa dataset (GSE46691) deposited in R2 genomics (16) revealed a positive correlation ($P < 0.0001$) between c-MYC and Sam68 expression (Figure 3E). Similar positive corre-

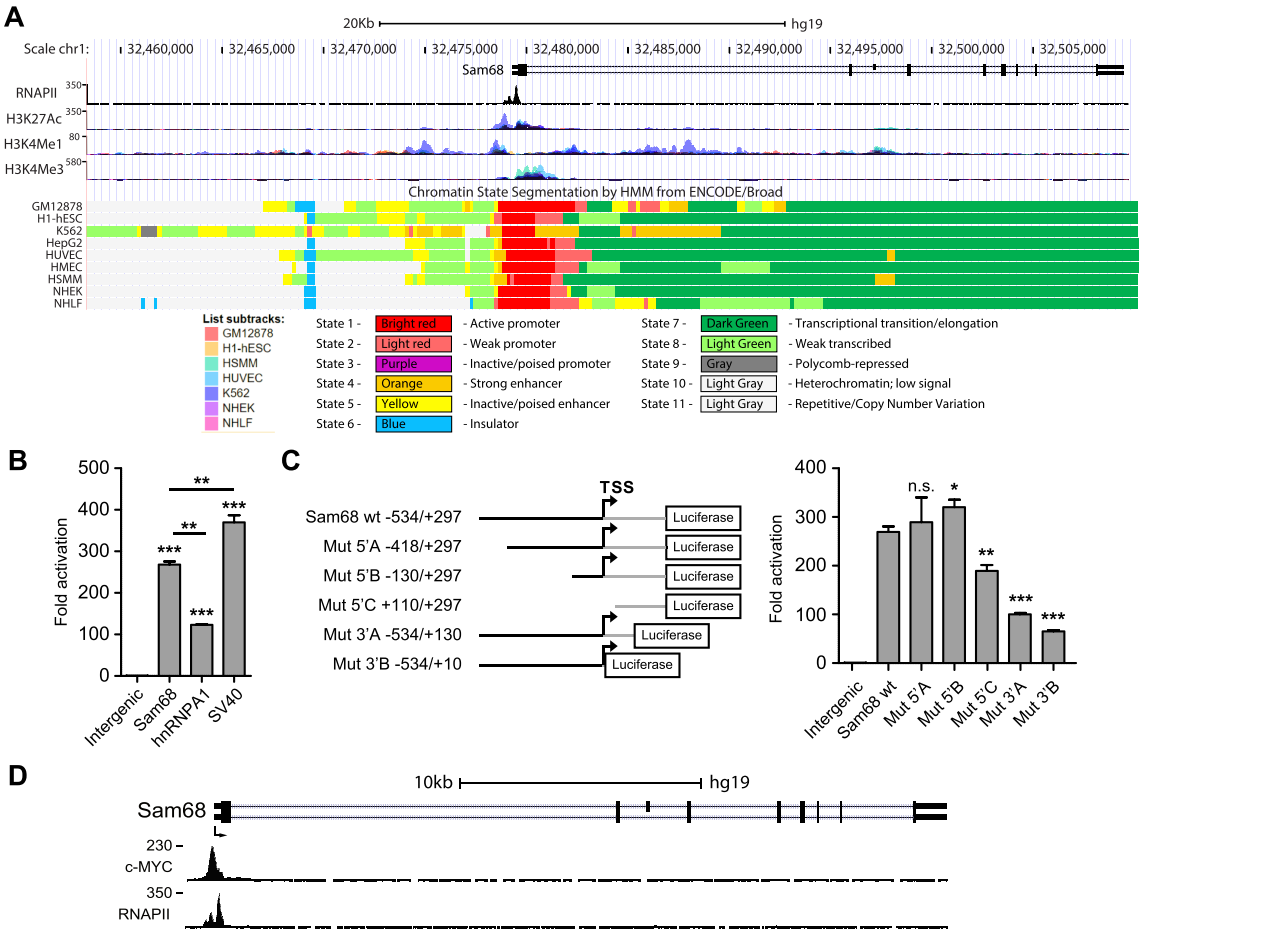

Figure 1. Identification of the Sam68 promoter region. (**A**) UCSC Genome Browser snapshot of RNAPII, H3K27Ac, H3K4Me1 and H3K4Me3 ChIP-seq profiles and Chromatin State Segmentation of the Sam68 locus, including an ∼20 Kbp upstream intergenic region. Chromatin state segmentation (colored rectangles; state 1–11) and cell lines (colored squares; List subtracks) are indicated. (**B** and **C**) Bar graphs represent luciferase activity of Sam68, hnRNP A1 and SV40 promoters compared to an upstream intergenic region (intergenic; −17753 to −16920 bp from the TSS) used as negative control (B), and of Sam68 promoter deletion mutants (Mut5′A, Mut5′B, Mut5′C, Mut3′A, Mut3′B) compared to the wild-type (wt) and interegenic reporters (C). A schematic representation of wt and mutant reporters is also shown; the upstream (black line) and downstream (gray line) regions from the Sam68 TSS are indicated (C; *left panel*). All Luciferase assays were performed in HEK293T 48 h post-transfection. Data represent mean ± SD of three biological replicates. Statistical significance was calculated by Student's *t*-test. $*P < 0.05$; $**P < 0.01$; $***P < 0.001$; n.s., not significant. (**D**) Representative ChIP-seq analysis of c-MYC and RNAPII binding to the Sam68 promoter region in NB4 cells with a schematic representation of the Sam68 gene structure showing predicted TSS (arrow), introns (horizontal lines) and exons (boxes).

lation between c-MYC and Sam68 expression was found by analyzing other datasets of PCa patients (GSE21034 and GSE29079) (17,18) (Supplementary Figure S3E and F). Furthermore, *Z*-score classification of patients for low and high expression of c-MYC confirmed that Sam68 levels are significantly higher in the MYC^{high} compared to the MYC^{low} group (Figure 3F; Supplementary Figure S3E and F). These findings suggest a direct link between upregulation of c-MYC and Sam68 transcription in PCa.

c-MYC downregulation impacts on Sam68 expression during cell growth arrest

Both c-MYC and Sam68 promote PCa cell proliferation (14,31), whereas cell growth arrest is linked to c-MYC downregulation (32). Thus, we asked whether Sam68 expression was perturbed under conditions that induce growth arrest. Serum deprivation of LNCaP cells for 6 days significantly impaired proliferation, as indicated by a reduction of BrdU positive cells (Figure 4A). Under these conditions, we also observed concomitant downregulation of both c-MYC and Sam68 mRNA and protein levels (Figure 4B and C). Serum deprivation and c-MYC silencing did not exert additive effects on Sam68 expression (Supplementary Figure A and B), suggesting that they function in the same pathway. Notably, a similar concomitant reduction of c-MYC and Sam68 expression was also observed in PC3 cells induced to growth arrest by serum deprivation (Supplementary Figure S4C–E).

Most PCas maintain dependency on androgens for cell proliferation and tumor growth. For this reason, inhibition of AR signaling represents the first-line therapy for this cancer. Thus, to impair PCa cell growth by an alternative approach, we treated the androgen-dependent LNCaP cells with Enzalutamide, a clinically approved AR inhibitor (2). Exposure of LNCaP cells to 1μM Enzalutamide for 6

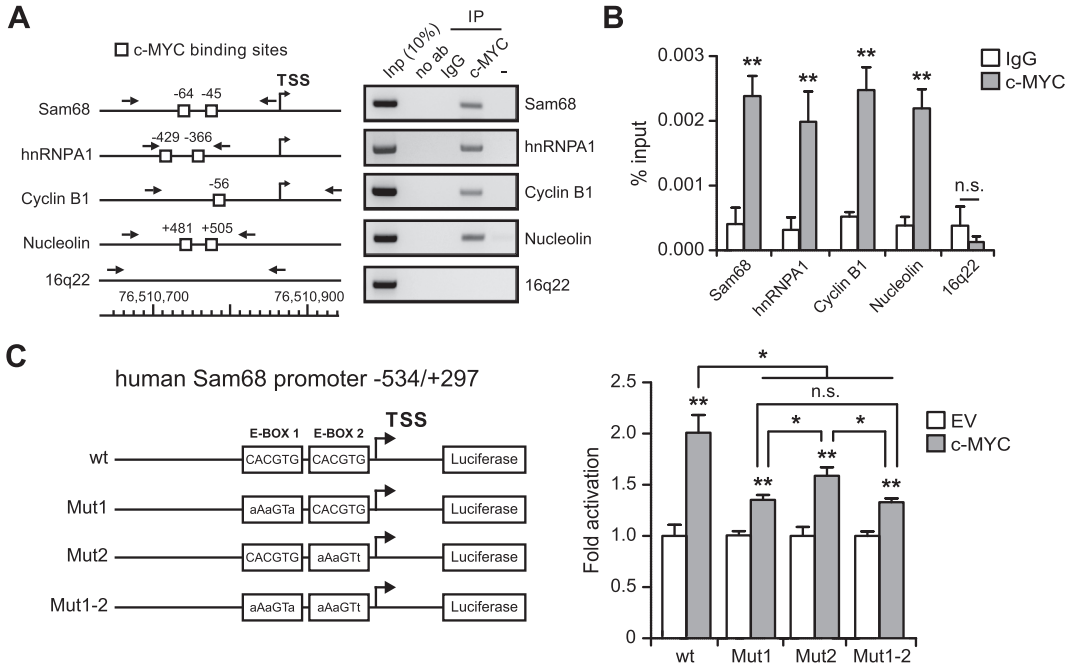

Figure 2. c-Myc binds to the Sam68 promoter region. (**A**) sqPCR and (**B**) qPCR analyses of ChIP experiments performed in LNCaP cells using c-MYC antibody and IgG (IgG), or no antibody (no ab), as negative control. Associated DNA is expressed as % of input (B). Schematic representation of the indicated gene promoters and of the 16q22 intergenic region is shown in (A) (*left panel*). c-MYC binding sites (solid box), TSS and primers position for PCR analyses (arrows) are indicated. (**C**) The bar graph represents the luciferase assay performed in HEK293T cells transfected with wt or mutated (Mut1, Mut2 and Mut1-2) Sam68 promoter reporters in combination, or not (empty vector, EV), with c-MYC-pCDNA3 vector (c-MYC). A schematic representation of wt and c-MYC binding site mutants (Mut1, Mut2 and Mut1-2) of the Sam68 promoter is also shown (*left panel*). (B and C) Data represent mean ± SD of three biological replicates. $*P < 0.05$; $**P < 0.01$; $***P < 0.001$; n.s., not significant (Student's *t*-test).

days induced a significant reduction of proliferation (Figure 4D). Strikingly, also under this condition we observed a concomitant reduction in Sam68 and c-MYC levels (Figure 4E and F), indicating that the effect was linked to ADT-mediated growth arrest. As expected, proliferation of the androgen-insensitive PC3 cells was not affected by Enzalutamide treatment (Supplementary Figure S4F) and neither c-MYC nor Sam68 expression was significantly modulated (Supplementary Figure S4G and H). These results suggest that under adverse growth conditions, PCa cells concomitantly downregulate c-MYC and Sam68 expression to halt proliferation.

c-MYC affects alternative splicing of Sam68 through modulation of the RNAPII elongation rate

Regulation of exon 3 splicing in the Sam68 transcript has been previously related to growth conditions (33). Inclusion of exon 3 generates the full-length variant with an intact KH domain for RNA binding, whereas skipping of exon 3 generates an isoform that presents a 39-amino acid deletion in this domain (Sam68-ΔKH) (Figure 5A) and is unable to bind RNA (34). Although difficult to detect in cell lines under culture conditions, the Sam68-ΔKH splice variant was shown to be induced upon growth arrest in non-transformed fibroblasts (33). We observed an ∼30–50% increase in the levels of the Sam68-ΔKH variant in LNCaP cells exposed to either serum deprivation or Enzalutamide treatment, as determined by both sqPCR (Figure 5B) and qPCR (Figure 5C). These results indicate that growth arrest impacts on Sam68 AS in PCa cells. Since under these conditions expression of c-MYC is also halted (Figure 4), we asked whether c-MYC is involved in the Sam68 splicing switch. Strikingly, c-MYC depletion recapitulated the increase in exon 3 skipping observed under growth arrest in LNCaP cells (Figure 5D and E), indicating that c-MYC promotes both expression and productive splicing of the Sam68 full length variant.

Transcription and splicing are functionally coupled, and transcription-related processes influence splicing outcome (10). For instance, changes in the RNAPII elongation rate modulate splicing of hundreds of genes (35). Fast RNAPII elongation rate correlates with its phosphorylation in Serine 2 (p-Ser2) and we observed that c-MYC depletion reduced the levels of this post-translational modification in LNCaP cells (Figure 5F). Thus, to investigate whether the transcriptional activity of c-MYC influences Sam68 AS, we first tested the effect of c-MYC on the RNAPII elongation rate within the Sam68 transcription unit. To this end, we quantified RNAPII processivity as the ratio between promoter-distal and promoter–proximal regions of the Sam68 pre-mRNA at steady state (36). qRT-PCR analysis using primers located at the exon 1/intron 1 (430 bp from TSS) and exon 8/intron 8 boundaries (25707 bp from TSS) revealed a reduction in RNAPII processivity in c-MYC-depleted LNCaP cells (Figure 5G, steady state and Supplementary Figure S5A and B). This effect was even more evident in nascent pre-mRNA analyzed 20 min after release from the transcriptional block caused by incubation with the RNAPII inhibitor 5,6-dichloro-l-b-D-

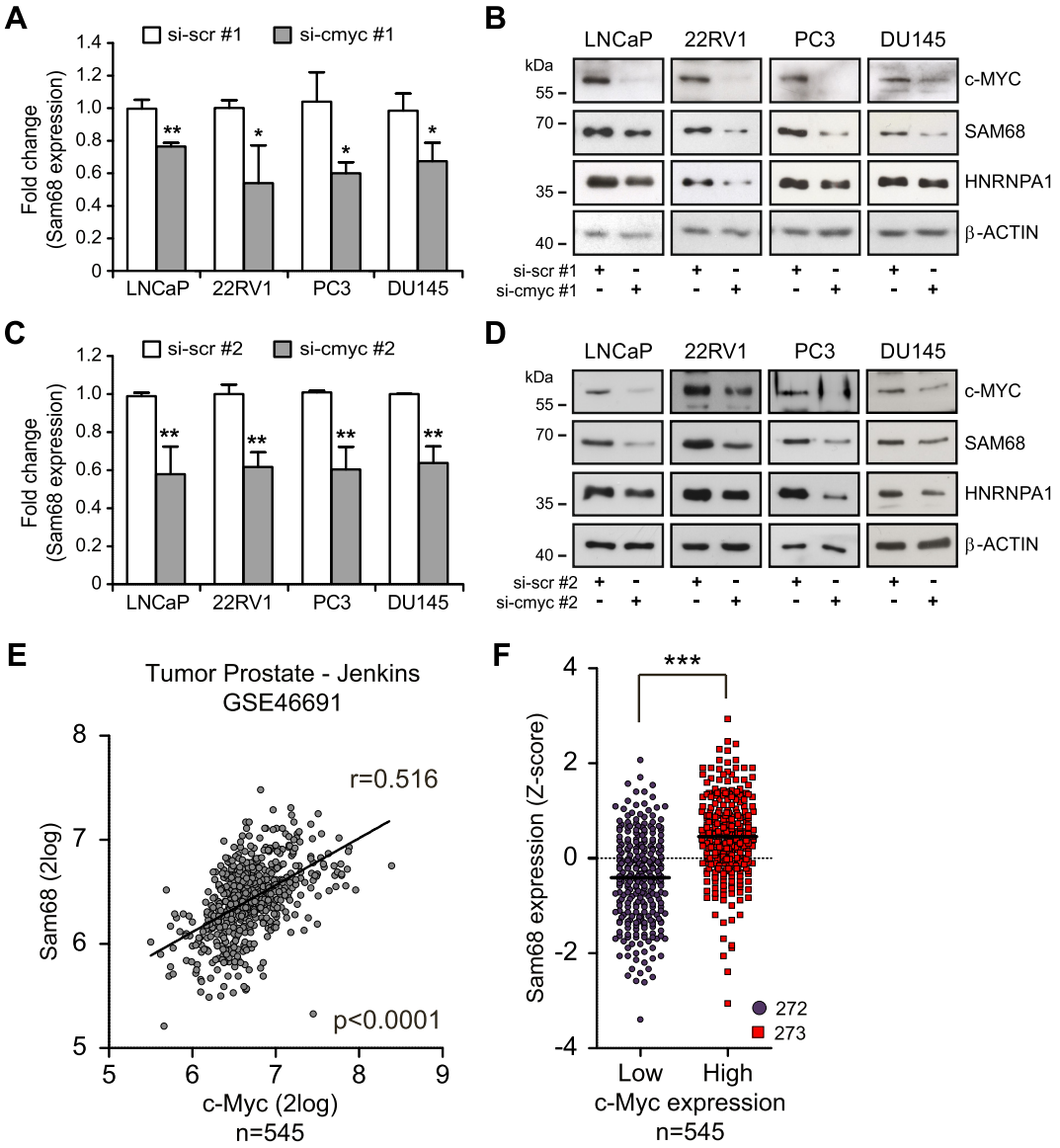

Figure 3. c-MYC regulates Sam68 expression in PCa. (**A**–**D**) qPCR (A and C) and western blot (B and D) analyses of Sam68 expression in PCa cells lines transfected with two different pools of c-Myc (si-cmyc #1 and si-cmyc #2) or control (si-scr #1 and si-scr #2) siRNAs. (A and C) Fold change of Sam68 expression relative to Histone 3 expression was calculated by the ΔΔCq method. Data represent mean ± SD of three biological replicates. *$P <$ 0.05; **$P < 0.01$ (Student's *t*-test). (**E**) Plot showing Sam68 and c-MYC expression in 545 PCa patients retrieved from the Jenkins (GSE46691) dataset. Pearson's correlation coefficient (r) and *P*-value are reported. (**F**) Sam68 expression profile in PCa patients (Jenkins-GSE46691) classified according to *Z*-score normalization in c-MYC^{low} (blue circles) and c-MYC^{high} (red squares) expressing group. The dot plot shows distribution and the median (horizontal line). Statistical significance was calculated by Mann–Whitney test, *** $P < 0.001$.

ribofuranosylbenzimidazole (DRB) (23). At this time point, when exon8/intron8 expression in the pre-mRNA reaches a plateau (Supplementary Figure S5C), depletion of c-MYC caused a two-fold reduction in RNAPII processivity within the Sam68 gene (Figure 5G, 20 min post-DRB).

These observations suggest that reduction of the RNAPII elongation rate may underlie the effect of c-MYC on Sam68 splicing. To test this possibility by an alternative approach, LNCaP cells were treated with suboptimal doses of DRB to reduce RNAPII p-Ser2 phosphorylation (Figure 5H) and its elongation rate without blocking transcription (35). Interestingly, we found that splicing of the Sam68-ΔKH isoform could be recapitulated in a dose-dependent manner in LNCaP cells treated with sub-optimal concentrations of DRB (Figure 5H and I; Supplementary Figure S5D). Similar results were obtained with two other RNAPII phosphorylation inhibitors, flavopiridol and LDC067 (Supplementary Figure S5E–H). Collectively these results suggest that the effect of c-MYC on Sam68 exon 3 splicing is mediated by a change in the RNAPII elongation rate.

A slow RNAPII elongation rate promotes recruitment of hnRNP F and skipping of Sam68 exon 3

Changes in the RNAPII elongation rate may induce inclusion or skipping of alternative exons through kinetic or re-

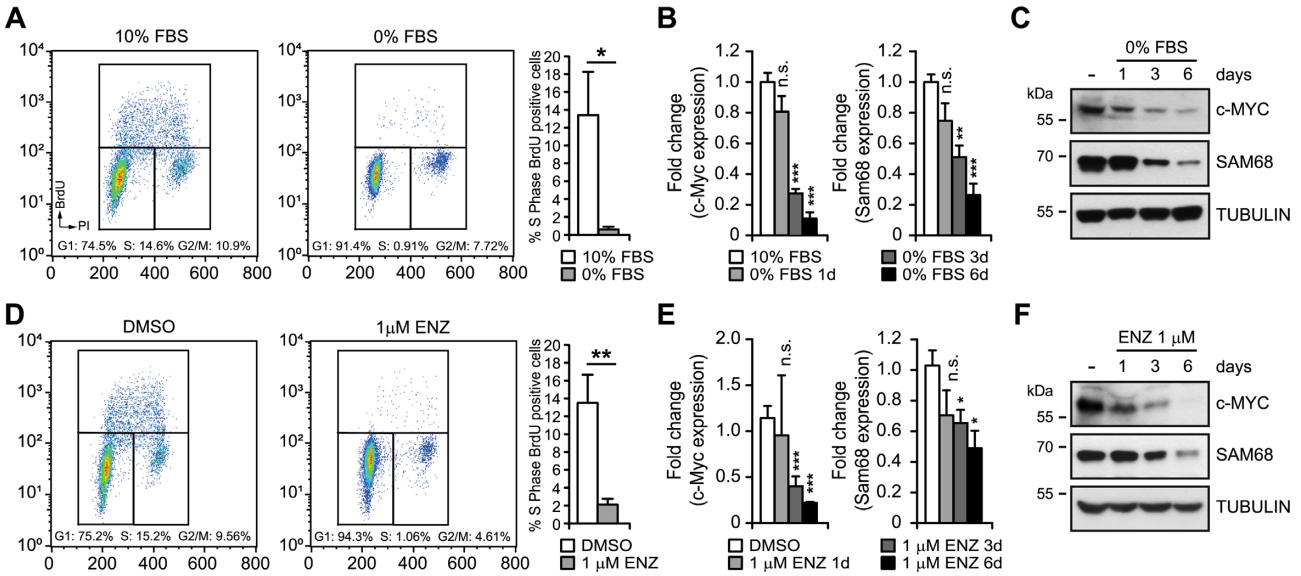

Figure 4. PCa cell growth arrest concomitantly induces c-MYC and Sam68 downregulation. (**A**–**F**) Representative dot plot profiles of cytometric analyses showing DNA content versus BrdU incorporation in LNCaP cells after 6 days of serum deprivation (A) or 1 μM Enzalutamide (D) conditions. Bar graphs (A and D) represents the percentage of S-phase BrdU positive cells after 6 days of treatment. qPCR (B and E) and western blot (C and F) time-course analyses of c-MYC and Sam68 expression (1d: 1 day; 3d: 3 days; 6d: 6 days). Fold change of Sam68 and c-MYC expression relative to Histone 3 expression was calculated by the ΔΔCq method. Data represent mean ± SD of three biological replicates. $^{*}P < 0.05$; $^{**}P < 0.01$; $^{***}P < 0.001$; n.s., not significant (Student's *t*-test).

cruitment mechanisms (37), non mutually exclusive models that can also cooperate in splicing regulation (38). In the first case, a slow elongation offers a window of opportunity to the weaker splice sites before stronger splice sites of constitutive exons are transcribed. In the recruitment model, the slower RNAPII is able to recruit splicing regulators to modulate recognition of the alternative exon splice sites. Since phosphorylation of RNAPII mediates its interaction with splicing factors (SFs) during pre-mRNA transcription and processing (39), we hypothesized that reduction of p-Ser2 phosphorylation might affect the recruitment of specific SF(s) to the Sam68 pre-mRNA in addition to its effects on the elongation rate. To test this hypothesis, we searched for binding motifs of splicing factors within exon 3 and flanking intronic sequences using the SpliceAid 2 (http://193.206.120.249/splicing_tissue.html) (40) and RBP map (http://rbpmap.technion.ac.il/) (41) prediction tools (Supplementary Figure S6A). We found several potential binding sites for Sam68 itself, for c-MYC-regulated members of the hnRNP family (Supplementary Figure S6A), which generally act as splicing repressors, and for ETR-3, a splicing repressor that was recruited by slow RNAPII (38). To test whether these splicing factors could modulate exon 3 splicing, we constructed a minigene encompassing the whole alternatively spliced region of Sam68, from exon 2 to exon 4 including intervening introns (Supplementary Figure S6B). Splicing assays in HEK293T cells indicated that Sam68 does not regulate its own AS (Supplementary Figure S6B), nor this event was regulated by hnRNP A2, hnRNP I (PTBP1) and ETR-3 (Supplementary Figure S6C). By contrast, hnRNP A1, hnRNP F and hnRNP H promoted skipping of exon 3 (Supplementary Figure S6C). More importantly, qPCR analyses revealed that overexpression of the highly homologous hnRNP F and hnRNP H promoted exon 3 skipping also in the endogenous Sam68 transcript in LNCaP cells, whereas hnRNP A1 was ineffective (Figure 6A). Accordingly, hnRNP F/H depletion significantly reduced exon 3 skipping in the endogenous Sam68 transcript, whereas hnRNP A1 knockdown did not (Figure 6B). These results suggest that hnRNP F/H are strong candidates for regulation of Sam68 splicing in PCa cells.

c-MYC is known to regulate the expression of several splicing factors (19,42). Notably, we found that c-MYC depletion in LNCaP cells caused also mild downregulation of hnRNP F/H expression, in addition to that of its known targets (Supplementary Figure S6D). Since exon 3 skipping occurred in spite of the slightly reduced levels of hnRNP F/H, we asked whether modulation RNAPII elongation rate by c-MYC promoted recruitment of these factors on the Sam68 pre-mRNA. To test this possibility, we treated LNCaP cells with DRB, which mimicked the effect of c-MYC depletion on RNAPII phosphorylation and exon 3 splicing without significantly affecting expression of hnRNP F/H or other c-MYC-regulated splicing factors (Supplementary Figure S6E). CLIP experiments showed that recruitment of hnRNP F to the exon 3 region of the Sam68 pre-mRNA was significantly increased upon DRB treatment (Figure 6C).

DISCUSSION

Sam68 is upregulated and plays key roles in several human tumors (13), including PCa (14,15). However, despite its relevance in oncogenic processes, how Sam68 transcription is dysregulated in cancer cells remains unknown. Our study now demonstrates that the oncogenic transcription factor c-MYC promotes expression and proper splicing of

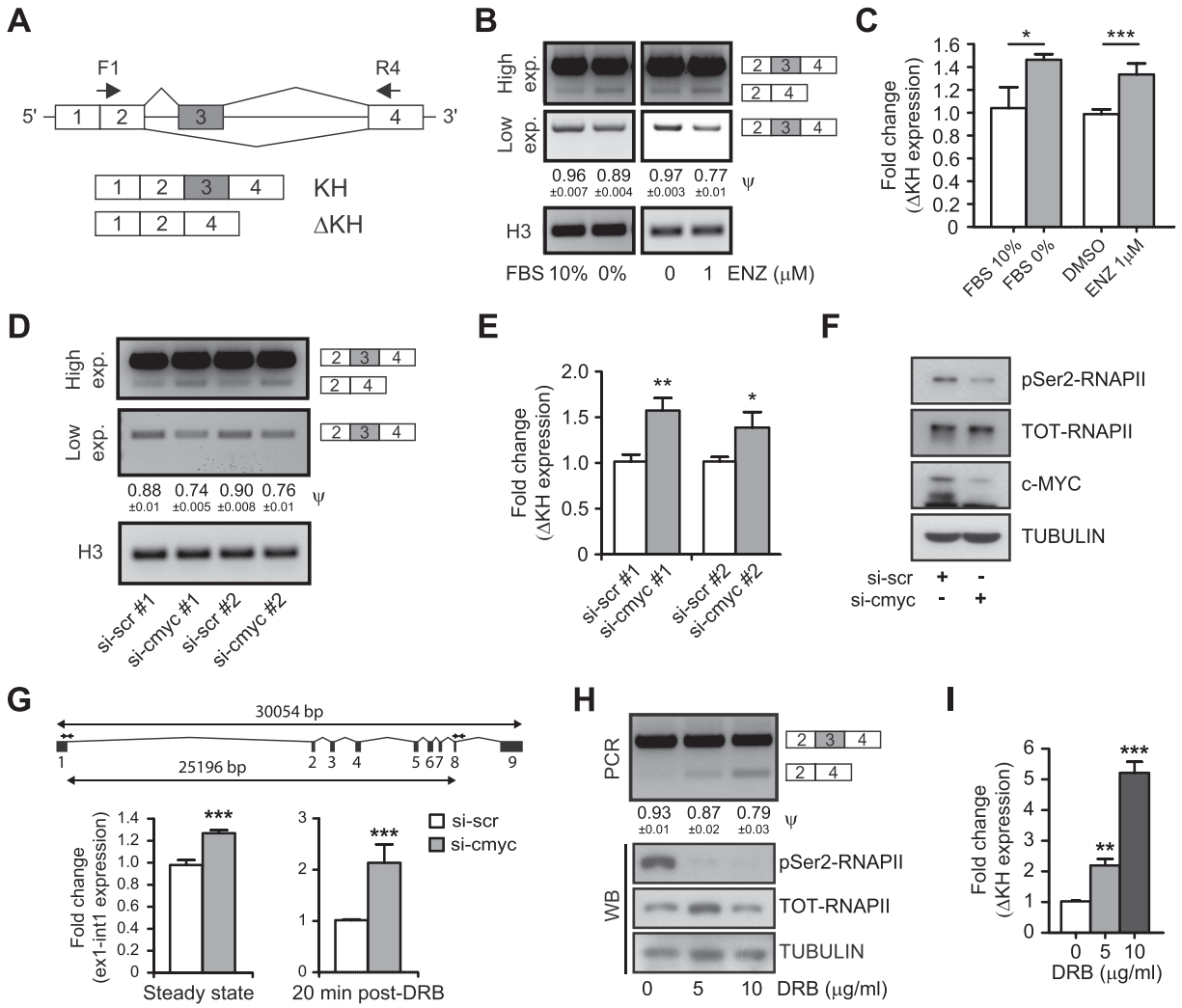

Figure 5. c-MYC modulates the AS of Sam68. (**A**) Diagram showing AS of Sam68. Exons (boxes), introns (horizontal lines) and position (arrows) of primers used for sqPCR are shown. (**B**–**E**) sqPCR (B and D) and qPCR (C and E) analyses of Sam68-ΔKH and KH splicing in LNCaP cells cultured under serum deprivation condition (0% FBS) or in presence of 1 μM Enzalutamide (Enz) (B and C), or transfected with control (si-scr #1 and #2) or c-MYC (si-myc #1 and #2) siRNAs (D and E). (**F**) Representative western blot analysis showing the expression level of c-MYC, total (TOT-RNAPII) and Serine2 (pSer2-RNAPII) RNAPII in LNCaP cells transfected with control (si-scr #1) or c-MYC (si-myc #1) siRNAs. Tubulin was used as loading control. (**G**) Bar graphs represent qPCR evaluation of Sam68 exon1-intron1 and exon8–intron8 ratio performed at steady state level (left) and 20min post-DRB release (right). LNCaP cells transfected with either control (si-scr #1) or c-MYC (si-cmyc #1) siRNAs were treated with 75 μM DRB for 6 h and RNA was extracted 20 min after DRB release. Data are reported as fold change of Sam68 exon1–intron1 relative to exon8–intron8 expression calculated by the ΔΔCq method. A scheme of Sam68 gene and primers position (arrows) used for qPCR is shown. (**H** and **I**) sqPCR (H) and qPCR (I) analyses showing Sam68-ΔKH and -KH ratio in LNCaP cells treated for 12 h with suboptimal DRB concentration. A representative western blot (WB) analysis (H) of the pSer2-RNAPII and TOT-RNAPII expression levels is also shown. Tubulin was used as loading control. (B, D and H) The Percent of Spliced-In Index (PSI; ψ) is reported below the gels. (C, E and I) Fold change of Sam68-ΔKH expression relative to Sam68-KH expression was calculated by the ΔΔCq method. (B–E, G–I) Mean ± SD of three biological replicates. *$P < 0.05$; **$P < 0.01$; ***$P < 0.001$ (Student's t-test).

Sam68 mRNA to yield high levels of this protein in PCa cells. Furthermore, we show that c-MYC and Sam68 expression are tightly linked to favorable environmental conditions, whereas downregulation of c-MYC under androgen and/or serum deprivation correlates with repression of Sam68 transcription and exon 3 splicing, yielding a variant unable to bind RNA (Figure 6D). Thus, our work uncovers the molecular mechanism underlying dysregulation of Sam68 expression in PCa, a finding that is probably extendible to other human cancers in which the c-MYC oncogene is upregulated.

To identify potential regulators of Sam68 transcription, we queried public datasets provided by the Encode project using the UCSC Genome Browser tool. This unbiased analysis identified a subset of transcription factors potentially involved in the regulation of Sam68 expression. Among them, we focused on c-MYC because of its well-established oncogenic function in human cancers (43). The activity of c-MYC profoundly alters the transcriptome of cancer cells (44). Furthermore, mounting evidence supports a key role for c-MYC also in the control of splicing, which further diversifyies the transcriptome of cancer cells. Indeed, spliceosome components (29,45) and splicing factors, including

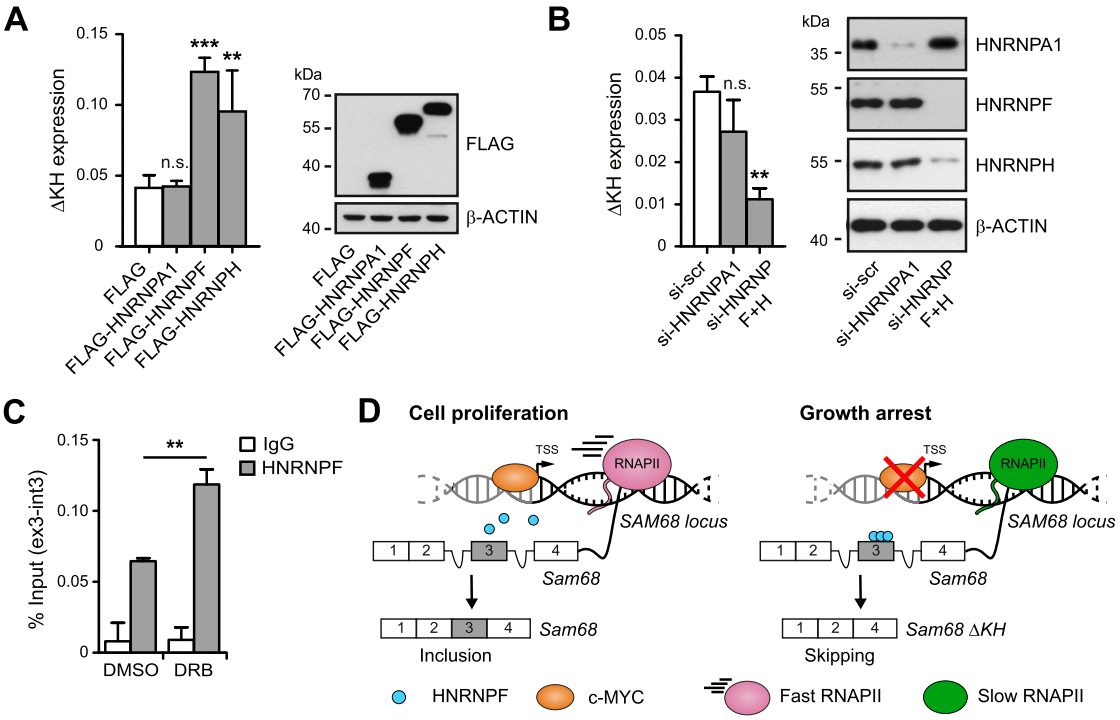

Figure 6. hnRNP F modulates the AS of Sam68 exon 3. (**A** and **B**) qPCR analyses of *in vivo* splicing assay performed in LNCaP cells transfected (A) or depleted (B) for the indicated splicing factors. Bar graphs (A and B; *left panels*) show the fold change of Sam68-ΔKH expression relative to Sam68-KH expression calculated by the ΔΔCq method. A representative western blot analysis (A and B; *right panel*) to asses the expression levels of the indicated splicing factors is shown. β-actin was used as loading control. (**C**) CLIP assays performed in LNCaP cells treated (DRB) or not (DMSO) with 5 μg/ml of DRB to detect the recruitment of hnRNP F on the endogenous Sam68 pre-mRNA. The immunoprecipitation was performed using hnRNP F antibody or IgGs, as negative control. RNA associated with hnRNP F was quantified by qPCR using primers located at the Sam68 exon 3–intron 3 boundary and represented as percentage (%) of input. (**D**) Schematic model for c-MYC-driven Sam68 gene expression and AS regulation. (**A**–**C**) Bars represent mean ± SD of three biological replicates. $^{**}P < 0.01$; $^{***}P < 0.001$; n.s., not significant (Student's *t*-test).

SRSF1, PTBP1, hnRNP A1 (19,26) are direct targets of c-MYC. Notably, SRSF1 expression promotes proliferation, cell survival and anchorage-independent growth in several tumors (19) and its phosphorylation by SRPK1 controls angiogenesis through the splicing regulation of VEGF (46), which is essential in highly vascularized cancers like PCa (47). On the other hand, the regulation of spliceosome components is required for c-MYC-driven malignant transformation (29,45), suggesting that safeguarding splicing fidelity is a key element for the pro-oncogenic function of c-MYC. Our study now identifies Sam68 as an additional splicing regulator under c-MYC control in cancer. We found a highly significant correlation between c-MYC and Sam68 expression in PCa patients, suggesting that this regulation is functional *in vivo*. Although our work was focused on PCa, it is likely that c-MYC more generally regulates Sam68 expression in cancer, as ChIP-seq peaks for this transcription factor within the Sam68 promoter region were found in cell lines of different origin.

Bioinformatics analyses revealed a relatively small region upstream of the first Sam68 coding exon that displays promoter features, such as histone marks of active transcription and RNAPII occupancy. Since the transcriptional activity of this region was confirmed in reporter assays, our study identifies a core promoter of human Sam68 that is active in multiple cell types. Our results also show that c-MYC mainly acts through binding to two E-boxes proximal to the TSS. Importantly, c-MYC expression is increased in PCa and correlates with disease severity (30,48). Since Sam68 and c-MYC upregulation is correlated in PCa patients, our findings suggest that Sam68 takes part to the oncogenic program activated by c-MYC in prostate cells.

c-MYC expression overrides growth arrest and reduces the capacity of cancer cells to differentiate (32). Sam68 appears to support the same functions, as its depletion impaired PCa cell proliferation (14) and induced neural stem cell differentiation (49). Thus, we tested the possibility that the expression of c-MYC and Sam68 responds to favorable growth conditions in PCa cells. As expected, we observed a concomitant reduction of c-MYC and Sam68 expression under conditions that cause proliferation arrest, such as serum deprivation and inhibition of AR signaling. These findings suggest the existence of a c-MYC-Sam68 functional axis in PCa and highlight a possible novel role for Sam68 as mediator of c-MYC function.

The KH domain is crucial for the RNA-binding activity of Sam68 (34). It was previously reported that a Sam68 splice variant lacking a functional KH domain (Sam68-ΔKH) is generated upon growth arrest (33) and this variant was proposed to participate to cell cycle arrest in fibroblasts. Nevertheless, whether the Sam68-ΔKH variant existed in cancer cells and the mechanisms underlying its expression had not been investigated. Sam68-ΔKH results from exon 3 skipping during pre-mRNA splicing. We observed an

increase in exon 3 skipping upon growth arrest induced by either serum or androgen deprivation and this effect was recapitulated by knockdown of c-MYC. Thus, c-MYC likely controls both transcription and productive splicing of Sam68. This regulation may have widespread impact on the transcriptome of PCa cells. Expression of Sam68-ΔKH may not only impair splicing of the direct Sam68 targets, but also affect those of SRSF1 because Sam68 is required to inhibit non-sense mediated decay (NMD) of SRSF1 transcripts (50). These observations suggest that the c-MYC- mediated oncogenic program may also rely on a widespread splicing program empowered by the network of cross-regulation between its downstream effectors. Since c-MYC lacks molecular features that can be targeted by small molecule inhibitors, identification of downstream effectors may help develop treatments for *MYC*-driven cancers. For instance, antisense oligonucleotides (ASOs) targeting splicing of Sam68 exon 3 may weaken the c-MYC oncogenic program in PCa and enhance the efficacy of other anti-cancer treatments.

Mechanistically, we linked c-MYC action to modulation of RNAPII activity. Since c-MYC influences RNAPII occupancy across the transcribed unit of its target genes, as well as phosphorylation of RNAPII at Serine 2 (51), c-MYC might alter Sam68 splicing by affecting the RNAPII elongation rate within the locus. Indeed, we found that depletion of c-MYC decreased Ser-2 phosphorylation of RNAPII in LNCaP cells and reduced the RNAPII elongation rate in the Sam68 gene, which correlated with exon 3 skipping. In our experiments RNAPII processivity was calculated as ratio of regions in the same transcript, thus it should be independent of the total amount of transcript produced by the gene. Nevertheless, since transcription efficiency and RNAPII processivity are mechanistically linked (39), they could impact on each other and we cannot completely distinguish between these two aspects affected by c-MYC. However, the effect on Sam68 splicing could be recapitulated by treatment of cells with several CDK9 inhibitors. Thus, our results suggest that reducing the RNAPII elongation rate is sufficient for exon 3 splicing regulation and that c-MYC coordinates transcription and splicing of Sam68 by affecting the RNAPII elongation rate.

Changes in RNAPII dynamics can affect splicing by affecting recruitment of specific splicing factors to the regulated exons (37). Such model was recently demonstrated for the *CFTR* gene, where reduced RNAPII processivity allowed recruitment of the splicing repressor ETR-3 and promoted exon skipping (38). Herein, by performing bioinformatics analyses and splicing assays, we identified hnRNP F as a regulator of Sam68 exon 3 splicing, whose recruitment to the pre-mRNA is favored by a slow RNAPII in PCa cells. We focused on hnRNP F because its antibody functioned better than that of hnRNP H under CLIP conditions in LNCaP cells. However, given their high homology, this antibody also partially recognizes hnRNP H and it is likely that exon 3 skipping is due to binding of both hnRNPs to the Sam68 transcript.

In conclusion, our study reveals that c-MYC contributes to regulation of Sam68 transcription and productive splicing in PCa cells through modulation of RNAPII dynamics within the gene.

SUPPLEMENTARY DATA

Supplementary Data are available at NAR Online.

FUNDING

Italian Ministry of Health 'Ricerca Finalizata 2011' [GR-2011-02348423]; Ricerca Finalizzata 2016 [RF-2016-02363460]; Associazione Italiana Ricerca sul Cancro (AIRC) [IG18790]. Funding for open access charge: Italian Ministry of Health "Ricerca Corrente".
Conflict of interest statement. None declared.

REFERENCES

1. Siegel,R.L., Miller,K.D. and Jemal,A. (2017) Cancer Statistics, 2017. *CA Cancer J. Clin.*, **67**, 7–30.
2. Pignot,G., Maillet,D., Gross,E., Barthelemy,P., Beauval,J.B., Constans-Schlurmann,F., Loriot,Y., Ploussard,G., Sargos,P., Timsit,M.O. *et al.* (2018) Systemic treatments for high-risk localized prostate cancer. *Nat. Rev. Urol.*, **15**, 498–510.
3. Munkley,J., Livermore,K., Rajan,P. and Elliott,D.J. (2017) RNA splicing and splicing regulator changes in prostate cancer pathology. *Hum. Genet.*, **136**, 1143–1154.
4. Sette,C. (2013) Alternative splicing programs in prostate cancer. *Int. J. Cell Biol.*, **2013**, 458727–458737.
5. Hu,R., Lu,C., Mostaghel,E.A., Yegnasubramanian,S., Gurel,M., Tannahill,C., Edwards,J., Isaacs,W.B., Nelson,P.S., Bluemn,E. *et al.* (2012) Distinct transcriptional programs mediated by the ligand-dependent full-length androgen receptor and its splice variants in castration-resistant prostate cancer. *Cancer Res.*, **72**, 3457–3462.
6. Mercatante,D.R., Mohler,J.L. and Kole,R. (2002) Cellular response to an antisense-mediated shift of Bcl-x pre-mRNA splicing and antineoplastic agents. *J. Biol. Chem.*, **277**, 49374–49382.
7. Burd,C.J., Petre,C.E., Morey,L.M., Wang,Y., Revelo,M.P., Haiman,C.A., Lu,S., Fenoglio-Preiser,C.M., Li,J., Knudsen,E.S. *et al.* (2006) Cyclin D1b variant influences prostate cancer growth through aberrant androgen receptor regulation. *Proc. Natl. Acad. Sci. U.S.A.*, **103**, 2190–2195.
8. Castilla,C., Congregado,B., Chinchon,D., Torrubia,F.J., Japon,M.A. and Saez,C. (2006) Bcl-xL is overexpressed in hormone-resistant prostate cancer and promotes survival of LNCaP cells via interaction with proapoptotic Bak. *Endocrinology*, **147**, 4960–4967.
9. Comstock,C.E., Augello,M.A., Benito,R.P., Karch,J., Tran,T.H., Utama,F.E., Tindall,E.A., Wang,Y., Burd,C.J., Groh,E.M. *et al.* (2009) Cyclin D1 splice variants: polymorphism, risk, and isoform-specific regulation in prostate cancer. *Clin. Cancer Res.*, **15**, 5338–5349.
10. Braunschweig,U., Gueroussov,S., Plocik,A.M., Graveley,B.R. and Blencowe,B.J. (2013) Dynamic integration of splicing within gene regulatory pathways. *Cell*, **152**, 1252–1269.
11. Anczukow,O. and Krainer,A.R. (2016) Splicing-factor alterations in cancers. *RNA*, **22**, 1285–1301.
12. Sveen,A., Kilpinen,S., Ruusulehto,A., Lothe,R.A. and Skotheim,R.I. (2016) Aberrant RNA splicing in cancer; expression changes and driver mutations of splicing factor genes. *Oncogene*, **35**, 2413–2427.
13. Bielli,P., Busa,R., Paronetto,M.P. and Sette,C. (2011) The RNA-binding protein Sam68 is a multifunctional player in human cancer. *Endocr. Relat. Cancer*, **18**, R91–R102.
14. Busa,R., Paronetto,M.P., Farini,D., Pierantozzi,E., Botti,F., Angelini,D.F., Attisani,F., Vespasiani,G. and Sette,C. (2007) The RNA-binding protein Sam68 contributes to proliferation and survival of human prostate cancer cells. *Oncogene*, **26**, 4372–4382.
15. Rajan,P., Gaughan,L., Dalgliesh,C., El-Sherif,A., Robson,C.N., Leung,H.Y. and Elliott,D.J. (2008) The RNA-binding and adaptor protein Sam68 modulates signal-dependent splicing and transcriptional activity of the androgen receptor. *J. Pathol.*, **215**, 67–77.
16. Jenkins,R.B., Qian,J., Lieber,M.M. and Bostwick,D.G. (1997) Detection of c-myc oncogene amplification and chromosomal anomalies in metastatic prostatic carcinoma by fluorescence in situ hybridization. *Cancer Res.*, **57**, 524–531.

17. Taylor,B.S., Schultz,N., Hieronymus,H., Gopalan,A., Xiao,Y., Carver,B.S., Arora,V.K., Kaushik,P., Cerami,E., Reva,B. *et al.* (2010) Integrative genomic profiling of human prostate cancer. *Cancer Cell*, **18**, 11–22.
18. Brase,J.C., Johannes,M., Mannsperger,H., Falth,M., Metzger,J., Kacprzyk,L.A., Andrasiuk,T., Gade,S., Meister,M., Sirma,H. *et al.* (2011) TMPRSS2-ERG-specific transcriptional modulation is associated with prostate cancer biomarkers and TGF-beta signaling. *BMC Cancer*, **11**, 507–515.
19. Das,S., Anczukow,O., Akerman,M. and Krainer,A.R. (2012) Oncogenic splicing factor SRSF1 is a critical transcriptional target of MYC. *Cell Rep.*, **1**, 110–117.
20. Annibalini,G., Bielli,P., De Santi,M., Agostini,D., Guescini,M., Sisti,D., Contarelli,S., Brandi,G., Villarini,A., Stocchi,V. *et al.* (2016) MIR retroposon exonization promotes evolutionary variability and generates species-specific expression of IGF-1 splice variants. *Biochim. Biophys. Acta*, **1859**, 757–768.
21. Bielli,P., Busa,R., Di Stasi,S.M., Munoz,M.J., Botti,F., Kornblihtt,A.R. and Sette,C. (2014) The transcription factor FBI-1 inhibits SAM68-mediated BCL-X alternative splicing and apoptosis. *EMBO Rep.*, **15**, 419–427.
22. Paronetto,M.P., Cappellari,M., Busa,R., Pedrotti,S., Vitali,R., Comstock,C., Hyslop,T., Knudsen,K.E. and Sette,C. (2010) Alternative splicing of the cyclin D1 proto-oncogene is regulated by the RNA-binding protein Sam68. *Cancer Res.*, **70**, 229–239.
23. Singh,J. and Padgett,R.A. (2009) Rates of in situ transcription and splicing in large human genes. *Nat. Struct. Mol. Biol.*, **16**, 1128–1133.
24. Bielli,P. and Sette,C. (2017) Analysis of in vivo Interaction between RNA binding proteins and their RNA targets by UV Cross-linking and Immunoprecipitation (CLIP) Method. *Bio Protoc.*, **7**, e2274.
25. Haggerty,T.J., Zeller,K.I., Osthus,R.C., Wonsey,D.R. and Dang,C.V. (2003) A strategy for identifying transcription factor binding sites reveals two classes of genomic c-Myc target sites. *Proc. Natl. Acad. Sci. U.S.A.*, **100**, 5313–5318.
26. David,C.J., Chen,M., Assanah,M., Canoll,P. and Manley,J.L. (2010) HnRNP proteins controlled by c-Myc deregulate pyruvate kinase mRNA splicing in cancer. *Nature*, **463**, 364–368.
27. Amati,B. and Land,H. (1994) Myc-Max-Mad: a transcription factor network controlling cell cycle progression, differentiation and death. *Curr. Opin. Genet. Dev.*, **4**, 102–108.
28. Dang,C.V., O'Donnell,K.A., Zeller,K.I., Nguyen,T., Osthus,R.C. and Li,F. (2006) The c-Myc target gene network. *Semin. Cancer Biol.*, **16**, 253–264.
29. Koh,C.M., Bezzi,M., Low,D.H., Ang,W.X., Teo,S.X., Gay,F.P., Al-Haddawi,M., Tan,S.Y., Osato,M., Sabo,A. *et al.* (2015) MYC regulates the core pre-mRNA splicing machinery as an essential step in lymphomagenesis. *Nature*, **523**, 96–100.
30. Gurel,B., Iwata,T., Koh,C.M., Jenkins,R.B., Lan,F., Van Dang,C., Hicks,J.L., Morgan,J., Cornish,T.C., Sutcliffe,S. *et al.* (2008) Nuclear MYC protein overexpression is an early alteration in human prostate carcinogenesis. *Mod. Pathol.*, **21**, 1156–1167.
31. Rebello,R.J., Pearson,R.B., Hannan,R.D. and Furic,L. (2017) Therapeutic approaches targeting MYC-Driven prostate cancer. *Genes (Basel)*, **8**, 71–87.
32. Sabo,A., Kress,T.R., Pelizzola,M., de Pretis,S., Gorski,M.M., Tesi,A., Morelli,M.J., Bora,P., Doni,M., Verrecchia,A. *et al.* (2014) Selective transcriptional regulation by Myc in cellular growth control and lymphomagenesis. *Nature*, **511**, 488–492.
33. Barlat,I., Maurier,F., Duchesne,M., Guitard,E., Tocque,B. and Schweighoffer,F. (1997) A role for Sam68 in cell cycle progression antagonized by a spliced variant within the KH domain. *J. Biol. Chem.*, **272**, 3129–3132.
34. Chen,T., Damaj,B.B., Herrera,C., Lasko,P. and Richard,S. (1997) Self-association of the single-KH-domain family members Sam68, GRP33, GLD-1, and Qk1: role of the KH domain. *Mol. Cell. Biol.*, **17**, 5707–5718.
35. Ip,J.Y., Schmidt,D., Pan,Q., Ramani,A.K., Fraser,A.G., Odom,D.T. and Blencowe,B.J. (2011) Global impact of RNA polymerase II elongation inhibition on alternative splicing regulation. *Genome Res.*, **21**, 390–401.
36. Batsche,E., Yaniv,M. and Muchardt,C. (2006) The human SWI/SNF subunit Brm is a regulator of alternative splicing. *Nat. Struct. Mol. Biol.*, **13**, 22–29.
37. Naftelberg,S., Schor,I.E., Ast,G. and Kornblihtt,A.R. (2015) Regulation of alternative splicing through coupling with transcription and chromatin structure. *Annu. Rev. Biochem.*, **84**, 165–198.
38. Dujardin,G., Lafaille,C., de la Mata,M., Marasco,L.E., Munoz,M.J., Le Jossic-Corcos,C., Corcos,L. and Kornblihtt,A.R. (2014) How slow RNA polymerase II elongation favors alternative exon skipping. *Mol. Cell*, **54**, 683–690.
39. Hsin,J.P. and Manley,J.L. (2012) The RNA polymerase II CTD coordinates transcription and RNA processing. *Genes Dev.*, **26**, 2119–2137.
40. Piva,F., Giulietti,M., Burini,A.B. and Principato,G. (2012) SpliceAid 2: a database of human splicing factors expression data and RNA target motifs. *Hum. Mutat.*, **33**, 81–85.
41. Paz,I., Kosti,I., Ares,M. Jr., Cline,M. and Mandel-Gutfreund,Y. (2014) RBPmap: a web server for mapping binding sites of RNA-binding proteins. *Nucleic Acids Res.*, **42**, W361–W367.
42. David,C.J. and Manley,J.L. (2010) Alternative pre-mRNA splicing regulation in cancer: pathways and programs unhinged. *Genes Dev.*, **24**, 2343–2364.
43. Dang,C.V. (2012) MYC on the path to cancer. *Cell*, **149**, 22–35.
44. Walz,S., Lorenzin,F., Morton,J., Wiese,K.E., von Eyss,B., Herold,S., Rycak,L., Dumay-Odelot,H., Karim,S., Bartkuhn,M. *et al.* (2014) Activation and repression by oncogenic MYC shape tumour-specific gene expression profiles. *Nature*, **511**, 483–487.
45. Hsu,T.Y., Simon,L.M., Neill,N.J., Marcotte,R., Sayad,A., Bland,C.S., Echeverria,G.V., Sun,T., Kurley,S.J., Tyagi,S. *et al.* (2015) The spliceosome is a therapeutic vulnerability in MYC-driven cancer. *Nature*, **525**, 384–388.
46. Amin,E.M., Oltean,S., Hua,J., Gammons,M.V., Hamdollah-Zadeh,M., Welsh,G.I., Cheung,M.K., Ni,L., Kase,S., Rennel,E.S. *et al.* (2011) WT1 mutants reveal SRPK1 to be a downstream angiogenesis target by altering VEGF splicing. *Cancer Cell*, **20**, 768–780.
47. Mavrou,A., Brakspear,K., Hamdollah-Zadeh,M., Damodaran,G., Babaei-Jadidi,R., Oxley,J., Gillatt,D.A., Ladomery,M.R., Harper,S.J., Bates,D.O. *et al.* (2015) Serine-arginine protein kinase 1 (SRPK1) inhibition as a potential novel targeted therapeutic strategy in prostate cancer. *Oncogene*, **34**, 4311–4319.
48. Hawksworth,D., Ravindranath,L., Chen,Y., Furusato,B., Sesterhenn,I.A., McLeod,D.G., Srivastava,S. and Petrovics,G. (2010) Overexpression of C-MYC oncogene in prostate cancer predicts biochemical recurrence. *Prostate Cancer Prostatic Dis.*, **13**, 311–315.
49. La Rosa,P., Bielli,P., Compagnucci,C., Cesari,E., Volpe,E., Farioli Vecchioli,S. and Sette,C. (2016) Sam68 promotes self-renewal and glycolytic metabolism in mouse neural progenitor cells by modulating Aldh1a3 pre-mRNA 3′-end processing. *Elife*, **5**, e20750.
50. Valacca,C., Bonomi,S., Buratti,E., Pedrotti,S., Baralle,F.E., Sette,C., Ghigna,C. and Biamonti,G. (2010) Sam68 regulates EMT through alternative splicing-activated nonsense-mediated mRNA decay of the SF2/ASF proto-oncogene. *J. Cell Biol.*, **191**, 87–99.
51. Rahl,P.B., Lin,C.Y., Seila,A.C., Flynn,R.A., McCuine,S., Burge,C.B., Sharp,P.A. and Young,R.A. (2010) c-Myc regulates transcriptional pause release. *Cell*, **141**, 432–445.

REFERENCES

Adesso, L., S. Calabretta, F. Barbagallo, G. Capurso, E. Pilozzi, R. Geremia, G. Delle Fave, and C. Sette. 2013. 'Gemcitabine Triggers a Pro-Survival Response in Pancreatic Cancer Cells through Activation of the MNK2/EIF4E Pathway'. *Oncogene* 32 (23): 2848–57. https://doi.org/10.1038/onc.2012.306.

Ahn, Young-Ho, Don L. Gibbons, Deepavali Chakravarti, Chad J. Creighton, Zain H. Rizvi, Henry P. Adams, Alexander Pertsemlidis, et al. 2012. 'ZEB1 Drives Prometastatic Actin Cytoskeletal Remodeling by Downregulating MiR-34a Expression'. *The Journal of Clinical Investigation* 122 (9): 3170–83. https://doi.org/10.1172/JCI63608.

Amrutkar, Manoj, and Ivar P. Gladhaug. 2017. 'Pancreatic Cancer Chemoresistance to Gemcitabine'. *Cancers* 9 (11). https://doi.org/10.3390/cancers9110157.

Anczuków, Olga, Avi Z. Rosenberg, Martin Akerman, Shipra Das, Lixing Zhan, Rotem Karni, Senthil K. Muthuswamy, and Adrian R. Krainer. 2012. 'The Splicing Factor SRSF1 Regulates Apoptosis and Proliferation to Promote Mammary Epithelial Cell Transformation'. *Nature Structural & Molecular Biology* 19 (2): 220–28. https://doi.org/10.1038/nsmb.2207.

Aung, Kyaw L., Sandra E. Fischer, Robert E. Denroche, Gun-Ho Jang, Anna Dodd, Sean Creighton, Bernadette Southwood, et al. 2018. 'Genomics-Driven Precision Medicine for Advanced Pancreatic Cancer: Early Results from the COMPASS Trial'. *Clinical Cancer Research: An Official Journal of the American Association for Cancer Research* 24 (6): 1344–54. https://doi.org/10.1158/1078-0432.CCR-17-2994.

Bailey, Peter, David K. Chang, Katia Nones, Amber L. Johns, Ann-Marie Patch, Marie-Claude Gingras, David K. Miller, et al. 2016. 'Genomic Analyses Identify Molecular Subtypes of Pancreatic Cancer'. *Nature* 531 (7592): 47–52. https://doi.org/10.1038/nature16965.

Barriga, Francisco M., Elisa Montagni, Miyeko Mana, Maria Mendez-Lago, Xavier Hernando-Momblona, Marta Sevillano, Amy Guillaumet-Adkins, et al. 2017. 'Mex3a Marks a Slowly Dividing Subpopulation of Lgr5+ Intestinal Stem Cells'. *Cell Stem Cell* 20 (6): 801-816.e7. https://doi.org/10.1016/j.stem.2017.02.007.

Bielli, Pamela, Roberta Busà, Maria Paola Paronetto, and Claudio Sette. 2011a. 'The RNA-Binding Protein Sam68 Is a Multifunctional Player in Human Cancer'. *Endocrine-Related Cancer* 18 (4): R91–102. https://doi.org/10.1530/ERC-11-0041.

Bielli, Pamela, Valentina Panzeri, Rossano Lattanzio, Simona Mutascio, Marco Pieraccioli, Elisabetta Volpe, Vincenzo Pagliarulo, et al. 2018. 'The Splicing Factor PTBP1 Promotes Expression of Oncogenic Splice Variants and Predicts Poor Prognosis in Patients with Non-Muscle-Invasive Bladder Cancer'. *Clinical Cancer Research: An Official Journal of the American Association for Cancer Research* 24 (21): 5422–32. https://doi.org/10.1158/1078-0432.CCR-17-3850.

Bielli, Pamela, and Claudio Sette. 2017. 'Analysis of in Vivo Interaction between RNA Binding Proteins and Their RNA Targets by UV Cross-Linking and Immunoprecipitation (CLIP) Method'. *Bio-Protocol* 7 (10). https://doi.org/10.21769/BioProtoc.2274.

Bosetti, C., E. Lucenteforte, D. T. Silverman, G. Petersen, P. M. Bracci, B. T. Ji, E. Negri, et al. 2012. 'Cigarette Smoking and Pancreatic Cancer: An Analysis from the International Pancreatic Cancer Case-Control Consortium (Panc4)'. *Annals of Oncology: Official Journal of the European Society for Medical Oncology* 23 (7): 1880–88. https://doi.org/10.1093/annonc/mdr541.

Brabletz, Simone, and Thomas Brabletz. 2010. 'The ZEB/MiR-200 Feedback Loop--a Motor of Cellular Plasticity in Development and Cancer?' *EMBO Reports* 11 (9): 670–77. https://doi.org/10.1038/embor.2010.117.

Bradner, James E., Denes Hnisz, and Richard A. Young. 2017. 'Transcriptional Addiction in Cancer'. *Cell* 168 (4): 629–43. https://doi.org/10.1016/j.cell.2016.12.013.

Bray, Freddie, Jacques Ferlay, Isabelle Soerjomataram, Rebecca L. Siegel, Lindsey A. Torre, and Ahmedin Jemal. 2018. 'Global Cancer Statistics 2018: GLOBOCAN Estimates of Incidence and Mortality Worldwide for 36 Cancers in 185 Countries'. *CA: A Cancer Journal for Clinicians* 68 (6): 394–424. https://doi.org/10.3322/caac.21492.

Buchet-Poyau, Karine, Julien Courchet, Hervé Le Hir, Bertrand Séraphin, Jean-Yves Scoazec, Laurent Duret, Claire Domon-Dell, Jean-Noël Freund, and Marc Billaud. 2007. 'Identification and Characterization of Human Mex-3 Proteins, a Novel Family of Evolutionarily Conserved RNA-Binding Proteins Differentially Localized to Processing Bodies'. *Nucleic Acids Research* 35 (4): 1289–1300. https://doi.org/10.1093/nar/gkm016.

Caggiano, Cinzia, Marco Pieraccioli, Valentina Panzeri, Claudio Sette, and Pamela Bielli. 2019. 'C-MYC Empowers Transcription and Productive Splicing of the Oncogenic Splicing Factor Sam68 in Cancer'. *Nucleic Acids Research* 47 (12): 6160–71. https://doi.org/10.1093/nar/gkz344.

Calabretta, S., P. Bielli, I. Passacantilli, E. Pilozzi, V. Fendrich, G. Capurso, G. Delle Fave, and C. Sette. 2016. 'Modulation of PKM Alternative Splicing by PTBP1 Promotes Gemcitabine Resistance in Pancreatic Cancer Cells'. *Oncogene* 35 (16): 2031–39. https://doi.org/10.1038/onc.2015.270.

Caramel, Julie, Maud Ligier, and Alain Puisieux. 2018. 'Pleiotropic Roles for ZEB1 in Cancer'. *Cancer Research* 78 (1): 30–35. https://doi.org/10.1158/0008-5472.CAN-17-2476.

Chandana, Sreenivasa, Hani M. Babiker, and Daruka Mahadevan. 2019. 'Therapeutic Trends in Pancreatic Ductal Adenocarcinoma (PDAC)'. *Expert Opinion on Investigational Drugs* 28 (2): 161–77. https://doi.org/10.1080/13543784.2019.1557145.

Chung, Duk-Won D., Ricardo F. Frausto, Lydia B. Ann, Michelle S. Jang, and Anthony J. Aldave. 2014. 'Functional Impact of ZEB1 Mutations Associated with Posterior Polymorphous and Fuchs' Endothelial Corneal Dystrophies'. *Investigative Ophthalmology & Visual Science* 55 (10): 6159–66. https://doi.org/10.1167/iovs.14-15247.

Collesi, C., M. M. Santoro, G. Gaudino, and P. M. Comoglio. 1996. 'A Splicing Variant of the RON Transcript Induces Constitutive Tyrosine Kinase Activity and an Invasive Phenotype'. *Molecular and Cellular Biology* 16 (10): 5518–26. https://doi.org/10.1128/mcb.16.10.5518.

Cong, Lin, Qiaofei Liu, Ronghua Zhang, Ming Cui, Xiang Zhang, Xiang Gao, Junchao Guo, et al. 2018. 'Tumor Size Classification of the 8th Edition of TNM Staging System Is Superior to That of the 7th Edition in Predicting the Survival Outcome of Pancreatic Cancer Patients after Radical Resection and Adjuvant Chemotherapy'. *Scientific Reports* 8 (1): 10383. https://doi.org/10.1038/s41598-018-28193-4.

Conroy, Thierry, Françoise Desseigne, Marc Ychou, Olivier Bouché, Rosine Guimbaud, Yves Bécouarn, Antoine Adenis, et al. 2011. 'FOLFIRINOX versus Gemcitabine for Metastatic Pancreatic Cancer'. *The New England Journal of Medicine* 364 (19): 1817–25. https://doi.org/10.1056/NEJMoa1011923.

Dang, Chi V. 2012. 'MYC on the Path to Cancer'. *Cell* 149 (1): 22–35. https://doi.org/10.1016/j.cell.2012.03.003.

Das, Shipra, Olga Anczuków, Martin Akerman, and Adrian R. Krainer. 2012. 'Oncogenic Splicing Factor SRSF1 Is a Critical Transcriptional Target of MYC'. *Cell Reports* 1 (2): 110–17. https://doi.org/10.1016/j.celrep.2011.12.001.

David, Charles J., Mo Chen, Marcela Assanah, Peter Canoll, and James L. Manley. 2010. 'HnRNP Proteins Controlled by C-Myc Deregulate Pyruvate Kinase MRNA Splicing in Cancer'. *Nature* 463 (7279): 364–68. https://doi.org/10.1038/nature08697.

David, Charles J., and James L. Manley. 2010. 'Alternative Pre-MRNA Splicing Regulation in Cancer: Pathways and Programs Unhinged'. *Genes & Development* 24 (21): 2343–64. https://doi.org/10.1101/gad.1973010.

Dayton, Talya L., Tyler Jacks, and Matthew G. Vander Heiden. 2016. 'PKM2, Cancer Metabolism, and the Road Ahead'. *EMBO Reports* 17 (12): 1721–30. https://doi.org/10.15252/embr.201643300.

Decker, Carolyn J., and Roy Parker. 2012. 'P-Bodies and Stress Granules: Possible Roles in the Control of Translation and MRNA Degradation'. *Cold Spring Harbor Perspectives in Biology* 4 (9): a012286. https://doi.org/10.1101/cshperspect.a012286.

Di Leva, Gianpiero, Michela Garofalo, and Carlo M. Croce. 2014. 'MicroRNAs in Cancer'. *Annual Review of Pathology* 9: 287–314. https://doi.org/10.1146/annurev-pathol-012513-104715.

Diederichs, Sven, Lorenz Bartsch, Julia C. Berkmann, Karin Fröse, Jana Heitmann, Caroline Hoppe, Deetje Iggena, et al. 2016. 'The Dark Matter of the Cancer Genome: Aberrations in Regulatory Elements,

Untranslated Regions, Splice Sites, Non-Coding RNA and Synonymous Mutations'. *EMBO Molecular Medicine* 8 (5): 442–57. https://doi.org/10.15252/emmm.201506055.

Distler, M., D. Aust, J. Weitz, C. Pilarsky, and Robert Grützmann. 2014. 'Precursor Lesions for Sporadic Pancreatic Cancer: PanIN, IPMN, and MCN'. *BioMed Research International* 2014: 474905. https://doi.org/10.1155/2014/474905.

Dongre, Anushka, and Robert A. Weinberg. 2019. 'New Insights into the Mechanisms of Epithelial-Mesenchymal Transition and Implications for Cancer'. *Nature Reviews. Molecular Cell Biology* 20 (2): 69–84. https://doi.org/10.1038/s41580-018-0080-4.

Draper, B. W., C. C. Mello, B. Bowerman, J. Hardin, and J. R. Priess. 1996. 'MEX-3 Is a KH Domain Protein That Regulates Blastomere Identity in Early C. Elegans Embryos'. *Cell* 87 (2): 205–16. https://doi.org/10.1016/s0092-8674(00)81339-2.

Dubbury, Sara J., Paul L. Boutz, and Phillip A. Sharp. 2018. 'CDK12 Regulates DNA Repair Genes by Suppressing Intronic Polyadenylation'. *Nature* 564 (7734): 141–45. https://doi.org/10.1038/s41586-018-0758-y.

Dvinge, Heidi, Eunhee Kim, Omar Abdel-Wahab, and Robert K. Bradley. 2016. 'RNA Splicing Factors as Oncoproteins and Tumour Suppressors'. *Nature Reviews. Cancer* 16 (7): 413–30. https://doi.org/10.1038/nrc.2016.51.

Elkon, Ran, Alejandro P. Ugalde, and Reuven Agami. 2013. 'Alternative Cleavage and Polyadenylation: Extent, Regulation and Function'. *Nature Reviews. Genetics* 14 (7): 496–506. https://doi.org/10.1038/nrg3482.

Eswaran, Jeyanthy, Anelia Horvath, Sucheta Godbole, Sirigiri Divijendra Reddy, Prakriti Mudvari, Kazufumi Ohshiro, Dinesh Cyanam, et al. 2013. 'RNA Sequencing of Cancer Reveals Novel Splicing Alterations'. *Scientific Reports* 3: 1689. https://doi.org/10.1038/srep01689.

Eulalio, Ana, Isabelle Behm-Ansmant, and Elisa Izaurralde. 2007. 'P Bodies: At the Crossroads of Post-Transcriptional Pathways'. *Nature Reviews. Molecular Cell Biology* 8 (1): 9–22. https://doi.org/10.1038/nrm2080.

Garneau, Nicole L., Jeffrey Wilusz, and Carol J. Wilusz. 2007. 'The Highways and Byways of MRNA Decay'. *Nature Reviews. Molecular Cell Biology* 8 (2): 113–26. https://doi.org/10.1038/nrm2104.

Gerstberger, Stefanie, Markus Hafner, and Thomas Tuschl. 2014. 'A Census of Human RNA-Binding Proteins'. *Nature Reviews. Genetics* 15 (12): 829–45. https://doi.org/10.1038/nrg3813.

Grote, V. A., S. Rohrmann, A. Nieters, L. Dossus, A. Tjønneland, J. Halkjær, K. Overvad, et al. 2011. 'Diabetes Mellitus, Glycated Haemoglobin and C-Peptide Levels in Relation to Pancreatic Cancer Risk: A Study within the European Prospective Investigation into Cancer and Nutrition (EPIC) Cohort'. *Diabetologia* 54 (12): 3037–46. https://doi.org/10.1007/s00125-011-2316-0.

Gruber, Andreas J., and Mihaela Zavolan. 2019. 'Alternative Cleavage and Polyadenylation in Health and Disease'. *Nature Reviews. Genetics* 20 (10): 599–614. https://doi.org/10.1038/s41576-019-0145-z.

Hackeng, Wenzel M., Ralph H. Hruban, G. Johan A. Offerhaus, and Lodewijk A. A. Brosens. 2016. 'Surgical and Molecular Pathology of Pancreatic Neoplasms'. *Diagnostic Pathology* 11 (1): 47. https://doi.org/10.1186/s13000-016-0497-z.

Hentze, Matthias W., Alfredo Castello, Thomas Schwarzl, and Thomas Preiss. 2018. 'A Brave New World of RNA-Binding Proteins'. *Nature Reviews. Molecular Cell Biology* 19 (5): 327–41. https://doi.org/10.1038/nrm.2017.130.

Hessmann, E., G. Schneider, V. Ellenrieder, and J. T. Siveke. 2016. 'MYC in Pancreatic Cancer: Novel Mechanistic Insights and Their Translation into Therapeutic Strategies'. *Oncogene* 35 (13): 1609–18. https://doi.org/10.1038/onc.2015.216.

Hingorani, Sunil R., Lei Zheng, Andrea J. Bullock, Tara E. Seery, William P. Harris, Darren S. Sigal, Fadi Braiteh, et al. 2018. 'HALO 202: Randomized Phase II Study of PEGPH20 Plus Nab-Paclitaxel/Gemcitabine Versus Nab-Paclitaxel/Gemcitabine in Patients With Untreated, Metastatic Pancreatic Ductal Adenocarcinoma'. *Journal of Clinical Oncology: Official Journal of the American Society of Clinical Oncology* 36 (4): 359–66. https://doi.org/10.1200/JCO.2017.74.9564.

Hong, David S., Razelle Kurzrock, Yun Oh, Jennifer Wheler, Aung Naing, Les Brail, Sophie Callies, et al. 2011. 'A Phase 1 Dose Escalation, Pharmacokinetic, and Pharmacodynamic Evaluation of EIF-4E Antisense Oligonucleotide LY2275796 in Patients with Advanced Cancer'. *Clinical Cancer Research: An Official Journal of the American Association for Cancer Research* 17 (20): 6582–91. https://doi.org/10.1158/1078-0432.CCR-11-0430.

Hsu, Tiffany Y.-T., Lukas M. Simon, Nicholas J. Neill, Richard Marcotte, Azin Sayad, Christopher S. Bland, Gloria V. Echeverria, et al. 2015. 'The Spliceosome Is a Therapeutic Vulnerability in MYC-Driven Cancer'. *Nature* 525 (7569): 384–88. https://doi.org/10.1038/nature14985.

Hydbring, Per, Marcos Malumbres, and Piotr Sicinski. 2016. 'Non-Canonical Functions of Cell Cycle Cyclins and Cyclin-Dependent Kinases'. *Nature Reviews. Molecular Cell Biology* 17 (5): 280–92. https://doi.org/10.1038/nrm.2016.27.

Jemal, Ahmedin, Freddie Bray, Melissa M. Center, Jacques Ferlay, Elizabeth Ward, and David Forman. 2011. 'Global Cancer Statistics'. *CA: A Cancer Journal for Clinicians* 61 (2): 69–90. https://doi.org/10.3322/caac.20107.

Jiang, Hong, Xuemei Zhang, Jinhong Luo, Chunyan Dong, Junli Xue, Wei Wei, Jingde Chen, Jun Zhou, Yong Gao, and Changqing Yang. 2012. 'Knockdown of HMex-3A by Small RNA Interference Suppresses Cell Proliferation and Migration in Human Gastric Cancer Cells'. *Molecular Medicine Reports* 6 (3): 575–80. https://doi.org/10.3892/mmr.2012.943.

Kahles, André, Kjong-Van Lehmann, Nora C. Toussaint, Matthias Hüser, Stefan G. Stark, Timo Sachsenberg, Oliver Stegle, et al. 2018. 'Comprehensive Analysis of Alternative Splicing Across Tumors from 8,705 Patients'. *Cancer Cell* 34 (2): 211-224.e6. https://doi.org/10.1016/j.ccell.2018.07.001.

Kaida, Daisuke, Michael G. Berg, Ihab Younis, Mumtaz Kasim, Larry N. Singh, Lili Wan, and Gideon Dreyfuss. 2010. 'U1 SnRNP Protects Pre-MRNAs from Premature Cleavage and Polyadenylation'. *Nature* 468 (7324): 664–68. https://doi.org/10.1038/nature09479.

Kanda, Mitsuro, Hanno Matthaei, Jian Wu, Seung-Mo Hong, Jun Yu, Michael Borges, Ralph H. Hruban, et al. 2012. 'Presence of Somatic Mutations in Most Early-Stage Pancreatic Intraepithelial Neoplasia'. *Gastroenterology* 142 (4): 730-733.e9. https://doi.org/10.1053/j.gastro.2011.12.042.

Karni, Rotem, Elisa de Stanchina, Scott W. Lowe, Rahul Sinha, David Mu, and Adrian R. Krainer. 2007. 'The Gene Encoding the Splicing Factor SF2/ASF Is a Proto-Oncogene'. *Nature Structural & Molecular Biology* 14 (3): 185–93. https://doi.org/10.1038/nsmb1209.

Kim, Jee-Eun, Kyu Taek Lee, Jong Kyun Lee, Seung Woon Paik, Jong Chul Rhee, and Kyoo Wan Choi. 2004. 'Clinical Usefulness of Carbohydrate Antigen 19-9 as a Screening Test for Pancreatic Cancer in an Asymptomatic Population'. *Journal of Gastroenterology and Hepatology* 19 (2): 182–86.

Krech, R. L., and D. Walsh. 1991. 'Symptoms of Pancreatic Cancer'. *Journal of Pain and Symptom Management* 6 (6): 360–67.

Kristensen, L. S., T. B. Hansen, M. T. Venø, and J. Kjems. 2018. 'Circular RNAs in Cancer: Opportunities and Challenges in the Field'. *Oncogene* 37 (5): 555–65. https://doi.org/10.1038/onc.2017.361.

Kurosaki, Tatsuaki, and Lynne E. Maquat. 2016. 'Nonsense-Mediated MRNA Decay in Humans at a Glance'. *Journal of Cell Science* 129 (3): 461–67. https://doi.org/10.1242/jcs.181008.

Latouliere, Luisa de, Isabella Manni, Carla Iacobini, Giuseppe Pugliese, Gian Luca Grazi, Pasquale Perri, Paola Cappello, Franco Novelli, Stefano Menini, and Giulia Piaggio. 2016. 'A Bioluminescent Mouse Model of Proliferation to Highlight Early Stages of Pancreatic Cancer: A Suitable Tool for Preclinical Studies'. *Annals of Anatomy = Anatomischer Anzeiger: Official Organ of the Anatomische Gesellschaft* 207 (September): 2–8. https://doi.org/10.1016/j.aanat.2015.11.010.

Li, Bo, Triona Ni Chonghaile, Yue Fan, Stephen F. Madden, Rut Klinger, Aisling E. O'Connor, Louise Walsh, et al. 2017. 'Therapeutic Rationale to Target Highly Expressed CDK7 Conferring Poor Outcomes in Triple-Negative Breast Cancer'. *Cancer Research* 77 (14): 3834–45. https://doi.org/10.1158/0008-5472.CAN-16-2546.

Liang, Kaiwei, Xin Gao, Joshua M. Gilmore, Laurence Florens, Michael P. Washburn, Edwin Smith, and Ali Shilatifard. 2015a. 'Characterization of Human Cyclin-Dependent Kinase 12 (CDK12) and CDK13

Complexes in C-Terminal Domain Phosphorylation, Gene Transcription, and RNA Processing'. *Molecular and Cellular Biology* 35 (6): 928–38. https://doi.org/10.1128/MCB.01426-14.

———. 2015b. 'Characterization of Human Cyclin-Dependent Kinase 12 (CDK12) and CDK13 Complexes in C-Terminal Domain Phosphorylation, Gene Transcription, and RNA Processing'. *Molecular and Cellular Biology* 35 (6): 928–38. https://doi.org/10.1128/MCB.01426-14.

Llorian, Miriam, Schraga Schwartz, Tyson A. Clark, Dror Hollander, Lit-Yeen Tan, Rachel Spellman, Adele Gordon, et al. 2010. 'Position-Dependent Alternative Splicing Activity Revealed by Global Profiling of Alternative Splicing Events Regulated by PTB'. *Nature Structural & Molecular Biology* 17 (9): 1114–23. https://doi.org/10.1038/nsmb.1881.

Lu, Ping, Jing Geng, Lei Zhang, Yu Wang, Ningning Niu, Yuan Fang, Fang Liu, et al. 2019. 'THZ1 Reveals CDK7-Dependent Transcriptional Addictions in Pancreatic Cancer'. *Oncogene* 38 (20): 3932–45. https://doi.org/10.1038/s41388-019-0701-1.

Mayr, Christine, and David P. Bartel. 2009. 'Widespread Shortening of 3'UTRs by Alternative Cleavage and Polyadenylation Activates Oncogenes in Cancer Cells'. *Cell* 138 (4): 673–84. https://doi.org/10.1016/j.cell.2009.06.016.

McGuigan, Andrew, Paul Kelly, Richard C. Turkington, Claire Jones, Helen G. Coleman, and R. Stephen McCain. 2018. 'Pancreatic Cancer: A Review of Clinical Diagnosis, Epidemiology, Treatment and Outcomes'. *World Journal of Gastroenterology* 24 (43): 4846–61. https://doi.org/10.3748/wjg.v24.i43.4846.

Mercuri, Eugenio, Basil T. Darras, Claudia A. Chiriboga, John W. Day, Craig Campbell, Anne M. Connolly, Susan T. Iannaccone, et al. 2018. 'Nusinersen versus Sham Control in Later-Onset Spinal Muscular Atrophy'. *The New England Journal of Medicine* 378 (7): 625–35. https://doi.org/10.1056/NEJMoa1710504.

Michl, Patrick, and Thomas M. Gress. 2013. 'Current Concepts and Novel Targets in Advanced Pancreatic Cancer'. *Gut* 62 (2): 317–26. https://doi.org/10.1136/gutjnl-2012-303588.

Miller, Kimberly D., Rebecca L. Siegel, Chun Chieh Lin, Angela B. Mariotto, Joan L. Kramer, Julia H. Rowland, Kevin D. Stein, Rick Alteri, and Ahmedin Jemal. 2016. 'Cancer Treatment and Survivorship Statistics, 2016'. *CA: A Cancer Journal for Clinicians* 66 (4): 271–89. https://doi.org/10.3322/caac.21349.

Mohibi, Shakur, Xinbin Chen, and Jin Zhang. 2019. 'Cancer the'RBP'eutics-RNA-Binding Proteins as Therapeutic Targets for Cancer'. *Pharmacology & Therapeutics*, July, 107390. https://doi.org/10.1016/j.pharmthera.2019.07.001.

Morita, Yoshihiro, Macall Leslie, Hiroyasu Kameyama, David E. Volk, and Takemi Tanaka. 2018. 'Aptamer Therapeutics in Cancer: Current and Future'. *Cancers* 10 (3). https://doi.org/10.3390/cancers10030080.

Murphy, Janet E., Jennifer Y. Wo, David P. Ryan, Wenqing Jiang, Beow Y. Yeap, Lorraine C. Drapek, Lawrence S. Blaszkowsky, et al. 2018. 'Total Neoadjuvant Therapy With FOLFIRINOX Followed by Individualized Chemoradiotherapy for Borderline Resectable Pancreatic Adenocarcinoma: A Phase 2 Clinical Trial'. *JAMA Oncology* 4 (7): 963–69. https://doi.org/10.1001/jamaoncol.2018.0329.

Neoptolemos, John P., Jörg Kleeff, Patrick Michl, Eithne Costello, William Greenhalf, and Daniel H. Palmer. 2018. 'Therapeutic Developments in Pancreatic Cancer: Current and Future Perspectives'. *Nature Reviews. Gastroenterology & Hepatology* 15 (6): 333–48. https://doi.org/10.1038/s41575-018-0005-x.

Nowak, Dawid G., Jeanette Woolard, Elianna Mohamed Amin, Olga Konopatskaya, Moin A. Saleem, Amanda J. Churchill, Michael R. Ladomery, Steven J. Harper, and David O. Bates. 2008. 'Expression of Pro- and Anti-Angiogenic Isoforms of VEGF Is Differentially Regulated by Splicing and Growth Factors'. *Journal of Cell Science* 121 (Pt 20): 3487–95. https://doi.org/10.1242/jcs.016410.

Obeng, Esther A., Connor Stewart, and Omar Abdel-Wahab. 2019. 'Altered RNA Processing in Cancer Pathogenesis and Therapy'. *Cancer Discovery*, October. https://doi.org/10.1158/2159-8290.CD-19-0399.

Oken, M. M., R. H. Creech, D. C. Tormey, J. Horton, T. E. Davis, E. T. McFadden, and P. P. Carbone. 1982. 'Toxicity and Response Criteria of the Eastern Cooperative Oncology Group'. *American Journal of Clinical Oncology* 5 (6): 649–55.

Olive, Kenneth P., Michael A. Jacobetz, Christian J. Davidson, Aarthi Gopinathan, Dominick McIntyre, Davina Honess, Basetti Madhu, et al. 2009. 'Inhibition of Hedgehog Signaling Enhances Delivery of Chemotherapy in a Mouse Model of Pancreatic Cancer'. *Science (New York, N.Y.)* 324 (5933): 1457–61. https://doi.org/10.1126/science.1171362.

Olopade, O. I., M. O. Adeyanju, A. R. Safa, F. Hagos, R. Mick, C. B. Thompson, and W. M. Recant. 1997. 'Overexpression of BCL-x Protein in Primary Breast Cancer Is Associated with High Tumor Grade and Nodal Metastases'. *The Cancer Journal from Scientific American* 3 (4): 230–37.

Otto, Tobias, and Piotr Sicinski. 2017. 'Cell Cycle Proteins as Promising Targets in Cancer Therapy'. *Nature Reviews. Cancer* 17 (2): 93–115. https://doi.org/10.1038/nrc.2016.138.

Pagliarini, Vittoria, Chiara Naro, and Claudio Sette. 2015. 'Splicing Regulation: A Molecular Device to Enhance Cancer Cell Adaptation'. *BioMed Research International* 2015: 543067. https://doi.org/10.1155/2015/543067.

Paniccia, Alessandro, Justin Merkow, Barish H. Edil, and Yuwen Zhu. 2015. 'Immunotherapy for Pancreatic Ductal Adenocarcinoma: An Overview of Clinical Trials'. *Chinese Journal of Cancer Research = Chung-Kuo Yen Cheng Yen Chiu* 27 (4): 376–91. https://doi.org/10.3978/j.issn.1000-9604.2015.05.01.

Paronetto, Maria Paola, Ilaria Passacantilli, and Claudio Sette. 2016. 'Alternative Splicing and Cell Survival: From Tissue Homeostasis to Disease'. *Cell Death and Differentiation* 23 (12): 1919–29. https://doi.org/10.1038/cdd.2016.91.

Pereira, Bruno, Sofia Sousa, Rita Barros, Laura Carreto, Patrícia Oliveira, Carla Oliveira, Nicolas T. Chartier, et al. 2013. 'CDX2 Regulation by the RNA-Binding Protein MEX3A: Impact on Intestinal Differentiation and Stemness'. *Nucleic Acids Research* 41 (7): 3986–99. https://doi.org/10.1093/nar/gkt087.

Ponta, Helmut, Larry Sherman, and Peter A. Herrlich. 2003. 'CD44: From Adhesion Molecules to Signalling Regulators'. *Nature Reviews. Molecular Cell Biology* 4 (1): 33–45. https://doi.org/10.1038/nrm1004.

Poulikakos, Poulikos I., Yogindra Persaud, Manickam Janakiraman, Xiangju Kong, Charles Ng, Gatien Moriceau, Hubing Shi, et al. 2011. 'RAF Inhibitor Resistance Is Mediated by Dimerization of Aberrantly Spliced BRAF(V600E)'. *Nature* 480 (7377): 387–90. https://doi.org/10.1038/nature10662.

Raimondi, Sara, Albert B. Lowenfels, Antonio M. Morselli-Labate, Patrick Maisonneuve, and Raffaele Pezzilli. 2010. 'Pancreatic Cancer in Chronic Pancreatitis; Aetiology, Incidence, and Early Detection'. *Best Practice & Research. Clinical Gastroenterology* 24 (3): 349–58. https://doi.org/10.1016/j.bpg.2010.02.007.

Rawla, Prashanth, Tagore Sunkara, and Vinaya Gaduputi. 2019. 'Epidemiology of Pancreatic Cancer: Global Trends, Etiology and Risk Factors'. *World Journal of Oncology* 10 (1): 10–27. https://doi.org/10.14740/wjon1166.

Rhim, Andrew D., Paul E. Oberstein, Dafydd H. Thomas, Emily T. Mirek, Carmine F. Palermo, Stephen A. Sastra, Erin N. Dekleva, et al. 2014. 'Stromal Elements Act to Restrain, Rather than Support, Pancreatic Ductal Adenocarcinoma'. *Cancer Cell* 25 (6): 735–47. https://doi.org/10.1016/j.ccr.2014.04.021.

Rigo, Frank, Yimin Hua, Adrian R. Krainer, and C. Frank Bennett. 2012. 'Antisense-Based Therapy for the Treatment of Spinal Muscular Atrophy'. *The Journal of Cell Biology* 199 (1): 21–25. https://doi.org/10.1083/jcb.201207087.

Roberts, Nicholas J., Alexis L. Norris, Gloria M. Petersen, Melissa L. Bondy, Randall Brand, Steven Gallinger, Robert C. Kurtz, et al. 2016. 'Whole Genome Sequencing Defines the Genetic Heterogeneity of Familial Pancreatic Cancer'. *Cancer Discovery* 6 (2): 166–75. https://doi.org/10.1158/2159-8290.CD-15-0402.

Ryan, David P., Theodore S. Hong, and Nabeel Bardeesy. 2014. 'Pancreatic Adenocarcinoma'. *The New England Journal of Medicine* 371 (22): 2140–41. https://doi.org/10.1056/NEJMc1412266.

Saad, Anas M., Tarek Turk, Muneer J. Al-Husseini, and Omar Abdel-Rahman. 2018. 'Trends in Pancreatic Adenocarcinoma Incidence and Mortality in the United States in the Last Four Decades; a SEER-Based Study'. *BMC Cancer* 18 (1): 688. https://doi.org/10.1186/s12885-018-4610-4.

Samokhvalov, Andriy V., Jürgen Rehm, and Michael Roerecke. 2015. 'Alcohol Consumption as a Risk Factor for Acute and Chronic Pancreatitis: A Systematic Review and a Series of Meta-Analyses'. *EBioMedicine* 2 (12): 1996–2002. https://doi.org/10.1016/j.ebiom.2015.11.023.

Sánchez-Martínez, Concepción, María José Lallena, Sonia Gutiérrez Sanfeliciano, and Alfonso de Dios. 2019. 'Cyclin Dependent Kinase (CDK) Inhibitors as Anticancer Drugs: Recent Advances (2015-2019)'. *Bioorganic & Medicinal Chemistry Letters* 29 (20): 126637. https://doi.org/10.1016/j.bmcl.2019.126637.

Seidel, Judith A., Atsushi Otsuka, and Kenji Kabashima. 2018. 'Anti-PD-1 and Anti-CTLA-4 Therapies in Cancer: Mechanisms of Action, Efficacy, and Limitations'. *Frontiers in Oncology* 8: 86. https://doi.org/10.3389/fonc.2018.00086.

Seiler, Michael, Shouyong Peng, Anant A. Agrawal, James Palacino, Teng Teng, Ping Zhu, Peter G. Smith, Cancer Genome Atlas Research Network, Silvia Buonamici, and Lihua Yu. 2018. 'Somatic Mutational Landscape of Splicing Factor Genes and Their Functional Consequences across 33 Cancer Types'. *Cell Reports* 23 (1): 282-296.e4. https://doi.org/10.1016/j.celrep.2018.01.088.

Shi, Yigong. 2017. 'Mechanistic Insights into Precursor Messenger RNA Splicing by the Spliceosome'. *Nature Reviews. Molecular Cell Biology* 18 (11): 655–70. https://doi.org/10.1038/nrm.2017.86.

Silva, Inês P., and Georgina V. Long. 2017. 'Systemic Therapy in Advanced Melanoma: Integrating Targeted Therapy and Immunotherapy into Clinical Practice'. *Current Opinion in Oncology* 29 (6): 484–92. https://doi.org/10.1097/CCO.0000000000000405.

Soares, Kevin C., Lei Zheng, Barish Edil, and Elizabeth M. Jaffee. 2012. 'Vaccines for Pancreatic Cancer'. *Cancer Journal (Sudbury, Mass.)* 18 (6): 642–52. https://doi.org/10.1097/PPO.0b013e3182756903.

Stevens, R. J., A. W. Roddam, and V. Beral. 2007. 'Pancreatic Cancer in Type 1 and Young-Onset Diabetes: Systematic Review and Meta-Analysis'. *British Journal of Cancer* 96 (3): 507–9. https://doi.org/10.1038/sj.bjc.6603571.

Torres, Carolina, and Paul J. Grippo. 2018. 'Pancreatic Cancer Subtypes: A Roadmap for Precision Medicine'. *Annals of Medicine* 50 (4): 277–87. https://doi.org/10.1080/07853890.2018.1453168.

Trisciuoglio, Daniela, Maria Grazia Tupone, Marianna Desideri, Marta Di Martile, Chiara Gabellini, Simonetta Buglioni, Matteo Pallocca, Gabriele Alessandrini, Simona D'Aguanno, and Donatella Del Bufalo. 2017. 'BCL-XL Overexpression Promotes Tumor Progression-Associated Properties'. *Cell Death & Disease* 8 (12): 3216. https://doi.org/10.1038/s41419-017-0055-y.

Vaseva, Angelina V., Devon R. Blake, Thomas S. K. Gilbert, Serina Ng, Galen Hostetter, Salma H. Azam, Irem Ozkan-Dagliyan, et al. 2018. 'KRAS Suppression-Induced Degradation of MYC Is Antagonized by a MEK5-ERK5 Compensatory Mechanism'. *Cancer Cell* 34 (5): 807-822.e7. https://doi.org/10.1016/j.ccell.2018.10.001.

Von Hoff, Daniel D., Ramesh K. Ramanathan, Mitesh J. Borad, Daniel A. Laheru, Lon S. Smith, Tina E. Wood, Ronald L. Korn, et al. 2011. 'Gemcitabine plus Nab-Paclitaxel Is an Active Regimen in Patients with Advanced Pancreatic Cancer: A Phase I/II Trial'. *Journal of Clinical Oncology: Official Journal of the American Society of Clinical Oncology* 29 (34): 4548–54. https://doi.org/10.1200/JCO.2011.36.5742.

Wang, Jun, Laurent Dumartin, Andrea Mafficini, Pinar Ulug, Ajanthah Sangaralingam, Namaa Audi Alamiry, Tomasz P. Radon, et al. 2017. 'Splice Variants as Novel Targets in Pancreatic Ductal Adenocarcinoma'. *Scientific Reports* 7 (1): 2980. https://doi.org/10.1038/s41598-017-03354-z.

Wang, Ze-Lin, Bin Li, Yu-Xia Luo, Qiao Lin, Shu-Rong Liu, Xiao-Qin Zhang, Hui Zhou, Jian-Hua Yang, and Liang-Hu Qu. 2018. 'Comprehensive Genomic Characterization of RNA-Binding Proteins across Human Cancers'. *Cell Reports* 22 (1): 286–98. https://doi.org/10.1016/j.celrep.2017.12.035.

Wang, Zhiwei, Yiwei Li, Aamir Ahmad, Sanjeev Banerjee, Asfar S. Azmi, Dejuan Kong, and Fazlul H. Sarkar. 2011. 'Pancreatic Cancer: Understanding and Overcoming Chemoresistance'. *Nature Reviews. Gastroenterology & Hepatology* 8 (1): 27–33. https://doi.org/10.1038/nrgastro.2010.188.

Wang, Zhiwei, Yiwei Li, Dejuan Kong, Sanjeev Banerjee, Aamir Ahmad, Asfar Sohail Azmi, Shadan Ali, James L. Abbruzzese, Gary E. Gallick, and Fazlul H. Sarkar. 2009. 'Acquisition of Epithelial-Mesenchymal Transition Phenotype of Gemcitabine-Resistant Pancreatic Cancer Cells Is Linked with Activation of the Notch Signaling Pathway'. *Cancer Research* 69 (6): 2400–2407. https://doi.org/10.1158/0008-5472.CAN-08-4312.

Warburg, O. 1956. 'On the Origin of Cancer Cells'. *Science (New York, N.Y.)* 123 (3191): 309–14. https://doi.org/10.1126/science.123.3191.309.

Waters, Andrew M., and Channing J. Der. 2018. 'KRAS: The Critical Driver and Therapeutic Target for Pancreatic Cancer'. *Cold Spring Harbor Perspectives in Medicine* 8 (9). https://doi.org/10.1101/cshperspect.a031435.

Winter, Jordan M., Murray F. Brennan, Laura H. Tang, Michael I. D'Angelica, Ronald P. Dematteo, Yuman Fong, David S. Klimstra, William R. Jarnagin, and Peter J. Allen. 2012. 'Survival after Resection of Pancreatic Adenocarcinoma: Results from a Single Institution over Three Decades'. *Annals of Surgical Oncology* 19 (1): 169–75. https://doi.org/10.1245/s10434-011-1900-3.

Yin, Wei, and Mark Rogge. 2019. 'Targeting RNA: A Transformative Therapeutic Strategy'. *Clinical and Translational Science* 12 (2): 98–112. https://doi.org/10.1111/cts.12624.

Yoshida, Kenichi, Masashi Sanada, Yuichi Shiraishi, Daniel Nowak, Yasunobu Nagata, Ryo Yamamoto, Yusuke Sato, et al. 2011. 'Frequent Pathway Mutations of Splicing Machinery in Myelodysplasia'. *Nature* 478 (7367): 64–69. https://doi.org/10.1038/nature10496.

Zhang, Jian, and James L. Manley. 2013. 'Misregulation of Pre-MRNA Alternative Splicing in Cancer'. *Cancer Discovery* 3 (11): 1228–37. https://doi.org/10.1158/2159-8290.CD-13-0253.

Zhang, Yu, Lei Xu, Anqi Li, and Xiuzhen Han. 2019. 'The Roles of ZEB1 in Tumorigenic Progression and Epigenetic Modifications'. *Biomedicine & Pharmacotherapy = Biomedecine & Pharmacotherapie* 110 (February): 400–408. https://doi.org/10.1016/j.biopha.2018.11.112.